UNIVERSITY OF CAPE TOWN

FACULTY OF ENGINEERING AND THE BUILT ENVIRONMENT

Department of Civil Engineering

Service life extension of reinforced concrete structures using hydrophobic impregnation

Name: Haris Sohawon

Student Number: SHWHAR001

Supervisor: Professor Hans Beushausen

Date: 28th August 2018

A dissertation submitted to the Department of Civil Engineering, University of Cape Town, in partial fulfilment of the requirements for the degree of Master of Science in Civil Engineering.

Plagiarism declaration

1. I know that plagiarism is wrong. Plagiarism is to use another's work and pretend that it is one's own.

2. I have used the Harvard convention for citation and referencing. Each contribution to, and quotation in, this thesis from the work(s) of other people has been attributed, and has been cited and referenced.

3. This thesis is my own work.

4. I have not allowed, and will not allow, anyone to copy my work with the intention of passing it off as his or her own work.

5. This thesis/dissertation has been submitted to the Turnitin module (or equivalent similarity and originality checking software) and I confirm that my supervisor has seen my report and any concerns revealed by such have been resolved with my supervisor.

Signature: Signed by candidate

Date: 28th August 2018

Dedication

Dedicated to my family for the unconditional love and support.

Acknowledgements

The author would like to thank and acknowledge with gratitude the following persons who made significant contributions towards the completion of this thesis:

1. Professor Hans Beushausen, Department of Civil Engineering, University of Cape Town; for the continuous academic guidance, motivation, invaluable input and life lessons.

2. CoMSIRU directors; Emeritus Professor Mark Alexander and Professor Pilate Moyo, Department of Civil Engineering, University of Cape Town; for their suggestions, encouragement and critical evaluation.

3. Mr Michel Donadio, Market field development manager, Sika services AG Switzerland; for the technical support and input throughout this research.

4. Mr Wayne Smithers, Technical Manager and Mr Kevin Kimbrey, Regional Manager, Sika South Africa (Pty) Ltd, for the logistical support and input during this study.

5. Mr Steve Crosswell, Consultant, PPC Group Services; for the provision of cement for this research.

6. Mr Nooredien Hassen, Civil Engineering Concrete Laboratory Manager and Mr Tahir Mukaddam, Senior Technical Officer, University of Cape Town; for the logistical support and assistance in the laboratory.

7. The Civil Engineering Concrete Laboratory staff; Mr Chris Caesar, Mr Charles May, Mr Leonard Adams, Mr Charles Nicholas and Mr Elvino Witbooi; for the continuous help in the laboratory.

8. The Postgraduate students of CoMSIRU and other colleagues I have spent the past two years with for their friendship and support.

The author also acknowledges the financial and technical assistance of the following entities, throughout the duration of this study:

Abstract

Over the last few decades, the increasing premature deterioration of reinforced concrete structures, mainly due to rebar corrosion, has become a worldwide concern. This has been attributed to insufficient quality and quantity of cover concrete resulting from inadequate mix design and poor on-site workmanship respectively. Engineers also often lack understanding of concrete durability and prescribe insufficient cover depths relative to the exposure conditions. Concrete degradation has many financial and social implications on a larger scale. Direct costs relate to the repair and rehabilitation of existing structures to maintain serviceability while indirect costs include loss in productivity and reduced economic growth. With increasing demand for infrastructure and subsequent expansion of the built environment, there is greater need for concrete to withstand and perform in corrosive environments. Hence, designing for durability has gained significant importance amongst engineers and other stakeholders in the construction industry.

Furthermore, the appearance of cracks can be considered as an inevitable phenomenon in the design life of reinforced concrete structures, due to concrete being an inherently cracked material. The presence of cracks within the cover zone changes the dynamics of transport mechanisms and corrosion development. Cracks provide preferential ingress paths for deleterious species such as chlorides and this leads to a reduction in the time taken for reinforcement corrosion initiation and thus reduces the service life of the structure. Most service life models also consider concrete only in the uncracked state, leading to an overestimation of the actual performance and design life of reinforced concrete infrastructure.

Extensive research has been carried out to find means to promote the service life of reinforced concrete structures in aggressive environments. Hydrophobic (silane) impregnation represents a cost-effective way to increase the durability of concrete structures in cases where insufficient cover quality and depth have been achieved. The hydrophobic impregnation agent lines the internal capillary pore structure and provides a water-repellent surface without affecting the external appearance of the concrete. Thus, the risk of reinforcement corrosion and subsequent deterioration can be reduced as the ingress of water-dissolved aggressive species is minimised or prevented. The influence of silane impregnation on chloride ingress is well documented in literature and several experiments have been carried out over the last decades. However, there is limited work on the service life modelling of silane treated concrete. Hence, the purpose of this study was to investigate and quantify the influence of silane impregnation as a remedial measure for poor quality cover or insufficient cover depth in newly constructed structures and ultimately predict the time to corrosion initiation for specific cover depths and concrete types. The effectiveness of silane impregnation in cracked concrete was also studied.

Two w/b ratios (w/b = 0.45 and w/b = 0.60) and four binder types (CEM I 52.5N, Fly-ash (FA), Ground granulated Corex slag (GGCS) and CEM III/B 42.5N) were selected. Hence, a total of 8 main (normal) concrete mixes and 4 poor quality mixes were used. Poor quality concrete was produced by exposing the concrete specimens to relatively high temperature at early age. Cracked concrete was obtained by loading notched reinforced beams until the formation of cracks. Steel spacers were then placed in the notch and the beams were unloaded to create crack widths of 0.2 mm and 0.6 mm (below and above the commonly assumed crack width threshold of 0.4 mm).

Silane treatment was performed at a specimen age of 28 days by applying Sikagard®-706 Thixo at a consumption rate of 400 g/m^2.

Several experimental tests were performed on untreated and silane treated concrete. Compressive strength and Durability Index (DI) tests were carried out to characterise the concrete mixes. Accelerated carbonation and moisture profiling tests were undertaken to assess the influence of silane impregnation on concrete carbonation and relative humidity. Finally, uncracked and cracked (untreated and treated) concrete mixes were ponded in sodium chloride (NaCl) solution for 80 days, followed by chloride profiling. The data for the uncracked concrete was curve fitted using a solution to Fick's second law of diffusion. The regression parameters obtained (surface chloride concentration (C_s) and apparent chloride diffusion coefficient (D_a)) were then incorporated in a mathematical solution to Fick's second law to obtain suitable expressions that describe the penetration of chlorides with time for silane treated and untreated concrete mixes. Hence by determining the time taken for chloride concentration at the rebar level to reach the critical threshold (assumed to be 0.4% by mass of binder), the time to corrosion initiation of untreated and silane treated concrete was predicted for particular cover depths.

The results indicate that the silane penetration depth is highly dependent on the quality (porosity) and moisture content of the near surface zone as deeper penetration was recorded in the higher w/b ratio and poor-quality concrete mixes. Silane impregnation also reduced the capillary absorption and chloride conductivity for all the mixes. In terms of the bulk diffusion test, chloride ingress in the treated concrete mixes was suppressed and lower chloride surface concentration (C_s) and apparent chloride diffusion coefficient (D_a) were recorded. The influence of silane impregnation on carbonation was negligible in the w/b = 0.45 concrete mixes while a slight decrease in carbonation depth was observed in the w/b = 0.60 concrete mixes. The relative humidity of treated concrete (near the surface) initially increased relative to the untreated concrete. However, the difference in relative humidity between silane-treated and untreated concrete is reduced with time.

Higher chloride concentrations were measured in the cracked concrete at depths of 50-60 mm compared to the uncracked concrete. Greater chloride ingress was also recorded in the 0.6 mm crack width relative to the 0.2 mm crack width. For a particular crack width, chloride ingress in cracked concrete was influenced by the type of binder; a significant reduction in chloride content was recorded in the cracked slag (GGCS and CEM III/B) concrete mixes relative to the CEM I mix. The results also suggest that silane impregnation reduces chloride ingress in cracked concrete (up to a crack with of 0.6 mm) and consequently minimises the risk of premature reinforcement corrosion initiation, especially in slag concrete.

The service life prediction results emphasized the importance of adequate cover depths in the extreme marine exposure class (XS3) and highlighted the superior performance of slag concrete relative to CEM I concrete. A lower rate of chloride ingress was predicted in the silane treated concrete and consequently to achieve the same time to corrosion initiation, smaller cover depths are required. Alternatively, the results also show that the initiation period of rebar corrosion in structures with insufficient cover depth and quality can be effectively extended using silane impregnation.

Table of contents

List of figures

List of tables

Abbreviations and symbols

OPI Oxygen Permeability Index

WSI Water Sorptivity Index

CCI Chloride Conductivity Index

w/b Water to binder ratio

EPMA Electron Probe Microanalysis

FA Fly-ash

GGCS Ground Granulated Corex Slag

GGBS Ground Granulated Blastfurnace Slag

SANRAL South African National Road Agency Limited

SANS South African National Standards

GDP Gross Domestic Product

fib Fédération Internationale du Béton

1. Introduction

1.1 Background

Reinforced concrete, if properly designed and applied, can be considered as a durable and versatile composite material under normal service conditions. However, over the last few decades, premature deterioration and associated loss in serviceability of reinforced concrete structures has become a primary concern to engineers. The main factor contributing to such an increase in early degradation is a combination of poor quality and inadequate quantity of cover concrete, coupled with aggressive environmental conditions. For instance, the ingress of deleterious agents such as moisture, chloride ions and oxygen through a poor-quality and low concrete cover can potentially result in corrosion of the embedded steel reinforcement. Subsequent delamination and spalling of the concrete surrounding the affected site hence compromises the durability and performance of the structure (Bertolini *et al.,* 2013).

Considerable research has been undertaken to identify suitable solutions to avoid premature deterioration and extend the service life of reinforced concrete. Surface treatment represents a preventative measure to protect new and existing structures from environmental attack and reduce the risk of associated reinforcement corrosion. The aim of surface treatment is the reduction of the concrete cover's penetrability to aggressive substances. Hydrophobic impregnation (penetrant pore liner) is one type of surface treatment that has the ability to reduce the capillary absorption of water containing dissolved deleterious species (chlorides) and thus delay the initiation of rebar corrosion (Bertolini *et al.,* 2013; Dai *et al.,* 2010). The purpose of this study is to evaluate by how much the service life (time to corrosion initiation) of reinforced concrete can be extended using hydrophobic impregnation. This includes evaluating the performance of silane as a remedial measure to inadequate cover depths in aggressive environments. This research also intends to assess the effectiveness of silane impregnation in cracked and poor-quality concrete.

1.2 Problem statement and justification of research

A large number of existing structures have reached the end of their design and economic life but cannot be replaced due to financial and technical constraints and hence require life extension strategies (Alexander *et al.,* 2012). Every year, a significant amount of capital is invested by governments for repair and rehabilitation of reinforced concrete structures that are subject to environmental degradation. Repair is essential to extend the serviceability of infrastructure and thus the maintenance of existing structures represents technical and economic challenges on a larger scale. Moreover, rehabilitation costs of poorly designed or constructed concrete structures are generally higher than those of well-designed ones and hence result in inefficient investment (Guettala *et al.,* 2006).

Cover concrete represents the primary barrier against the ingress of aggressive agents towards the reinforcing steel and several design codes define cover depths according to particular environmental classes (Bertolini *et al.,* 2013). The thickness and quality of this zone is largely dependent on on-site quality control and curing conditions respectively (Christodoulou *et al.,* 2013). As the modern construction industry is under the perpetual constraints of time and money,

quality control is often neglected on site, resulting in poor execution and outcome of works. Hence, the design cover depth and quality are often not achieved due to improper placing, compaction and curing of in-situ concrete. Engineers that lack understanding of concrete durability can also prescribe insufficient cover depths or inappropriate binders relative to the environmental conditions. This increases the probability of premature deterioration of structures, which ultimately compromises durability and results in a reduction in service life. The potential use of surface treatments as a protective measure against early-age concrete deterioration is widely presented in literature but information about the extent of protection is limited (Burmeister, 2012). Hence, this study will help to gain more understanding on the use of hydrophobic impregnation as a method to improve the durability of reinforced concrete structures with low cover depth or low quality of cover.

As the properties of the cover concrete affect greatly the durability of reinforced concrete structures, the presence of cracks within that zone can potentially increase the ingress of harmful substances. Cracks provide favourable paths for the ingress of deleterious species. This results in shorter time to corrosion initiation, higher corrosion rates and further reduction in serviceability. Most service life prediction models consider concrete only in the uncracked state. Such idealised conditions may potentially overestimate actual performance (Kanjee *et al.*, 2012). In practice, cracks do occur frequently in concrete structures, particularly under the influence of load induced stresses. Transport mechanisms and corrosion development in cracked concrete may also be different compared to the uncracked state (Ballim *et al.*, 2009). Moreover, the performance of hydrophobic impregnation when applied to cracked concrete remains debatable (Wittman, 2008). Hence, further research needs to be conducted to better understand the influence of silane impregnation on the ingress of aggressive species in cracked concrete.

1.3 Aims and outcome

The main objective of this research is to quantify the service life extension possible using hydrophobic (silane) impregnation. The specific aims of this study are:

- To assess whether silane impregnation can be used as a remedial measure to problems of low cover or alternatively as a substitute to a portion of the design cover depth.
- To evaluate the relationship between w/b ratio and cement extenders on the performance of silane impregnation.
- To determine the effectiveness of silane impregnation in cracked and poor-quality concrete.
- To develop a suitable model that can predict the service life (time to corrosion initiation) of silane treated concrete structures for specific cover depths.

The anticipated outcome of this study is to successfully quantify the relationship between concrete cover depth and hydrophobic impregnation relative to the ingress of chlorides. This work will also provide more understanding on how intrinsic properties of concrete such as w/b ratio and binder type affect the performance of silane impregnation. Finally, it is expected that this research will be a source of future reference for further experimental work and will contribute to the knowledge

on hydrophobic impregnation as a solution to increase the service life (time to corrosion initiation) of reinforced concrete structures with insufficient cover quality and depth.

1.4 Scope and limitations

This research focuses on the use of hydrophobic impregnation (silane) as a preventive measure against the ingress of aggressive species (chloride ions), thereby quantifying by how much the expected service duration can be extended. In this research, the service life is considered as the time needed for corrosion initiation, i.e. the time needed for chloride concentrations to reach the assumed threshold value of 0.4% (by mass of binder) at the depth of the steel reinforcement. Hence, the propagation phase of rebar corrosion was not investigated. This study is further applicable to newly constructed structures; the repair of existing, already deteriorated structures was not considered explicitly. This work only considered silane impregnations; only one commercial silane (Sikagard®-706 Thixo) was used. Other types of surface treatments, such as surface coatings and pore blocking treatments were outside the scope of this research. The extent of experimental work was restricted by the availability of materials and time. Two main parameters (w/b ratio and binder type) were varied respectively to obtain 8 concrete mix designs. Poor quality and cracked concrete were created using the higher w/b ratio (w/b 0.60) to model the worst-case scenario, hence assessing the full protective potential of the hydrophobic impregnation. A deterministic approach (solution to Fick's second law of diffusion) was used to model the ingress of chlorides into untreated and silane treated concrete. It must be also noted that the results presented in this work are based on short term testing under laboratory (controlled) environmental conditions. Further long term and field data is needed to strengthen any conclusions made in this thesis.

1.5 Outline

The content of this thesis is split into eight main chapters; Chapter 1 – Introduction, Chapter 2 – Literature review, Chapter 3 – Methodology, Chapter 4 – Results and discussions, Chapter 5 – Service life modelling, Chapter 6 – Summary of results, Chapter 7 – Conclusions and Chapter 8 – Recommendations. Chapter 1 provides an overview of the research topic by outlining the background, problem statement, aims and limitations of this study. Chapter 2 presents a detailed literature review of the research topic and is further split into the following sub-sections; Transport mechanisms in uncracked and cracked concrete, concrete deterioration, carbonation of concrete, chloride ingress in concrete, concrete durability, service life design and hydrophobic impregnation and its influences on moisture content, carbonation, chloride ingress and cracks. Chapter 3 gives details on the experimental methods used to achieve the required objectives of this thesis; this includes a description of the materials, equipment and tests procedures followed. Chapter 4 provides an analysis and discussion of the results obtained from the experimental tests. Chapter 5 presents the prediction of chloride ingress by incorporating the experimental data presented in Chapter 4 in a model based on the error function solution to Fick's second law of diffusion. Chapter 6 gives a summary of the results from Chapter 4 and service life modelling outcome from Chapter 5. Chapter 7 provides the main conclusions that can be derived from the overall experimental results and service life modelling. Finally, Chapter 8 presents suggestions that can possibly improve the results of this study and future related work.

2. Literature review

This chapter provides a detailed literature review of the research topic and is divided into ten main sections. Section 2.1 and Section 2.2 outline transport mechanisms in uncracked and cracked concrete respectively. Section 2.3 discusses concrete deterioration and is followed by Section 2.4 and Section 2.5 which give details on the mechanism and consequence of carbonation and chloride ingress respectively. Section 2.6 presents the fundamentals of concrete durability while Section 2.7 gives an overview of concrete service life design and modelling. Section 2.8 gives an introduction to hydrophobic impregnation while Section 2.9 summarises the influence of water repellent treatment on moisture content, carbonation, chloride ingress and in cracks. Section 2.10 provides a summary of the literature review.

2.1 Transport mechanisms in uncracked concrete

The durability of concrete is largely influenced by processes that involve the ingress and movement of deleterious gases and ions (dissolved in water) through favourable paths in the pore structure. The service life of concrete is ultimately dependent on the rate or ease of movement of these aggressive species which is broadly termed as penetrability (Alexander *et al.*, 2010). For instance, deterioration mechanisms such as corrosion, alkali-silica reaction and carbonation are all related to the penetrability of concrete. The penetrability of concrete relative to a specific agent, for instance carbon dioxide, is a function of the complexity, degree of interconnectedness and moisture content of the capillary pore structure. The ease of ingress of substances in concrete is hence dependent on the quality of cement paste in the concrete cover and at the interface with aggregate particles (Richardson, 2002).

The mechanisms and respective material properties that govern the movement of fluids and ions through the pore structure of concrete are as follows (Alexander *et al.*, 2010):

- Capillary suction (sorptivity)
- Permeation (permeability)
- Diffusion (diffusivity)
- Migration (conductivity)

2.1.1 Capillary suction

Concrete, being inherently a porous material, has the tendency to absorb liquids due to capillary action. The latter is a function of the properties (surface tension, viscosity and density) of the liquid, the contact angle between the liquid and pore walls and the pore size. In concrete, the contact angle tends to be small because of molecular attraction between the liquid (water) and substrate (cement paste). In theory, capillary action increases as the pore dimensions decrease, while on the other hand, smaller pores can result in slower transport processes mainly due to friction. But in general, the higher the porosity, the greater the rate of absorption of liquids. This relationship forms the basis for sorptivity tests (Bertolini *et al.*, 2013). Sorptivity is calculated to quantify the uptake of liquids by capillary suction and is defined as the movement of the wetting front in a

dry or partially saturated porous medium. Sorptivity (S) is hence expressed as the mass of liquid (g) absorbed per specimen thickness (d) in time (t) (Alexander *et al.*, 2010).

$$S = \Delta \frac{M_t}{t^{0.5}} \left[\frac{d}{M_{sat} - M_0} \right] \quad \text{.....(2.1)}$$

where,

$\Delta M/t^{0.5}$ – slope of the straight line produced from a plot of mass of water (g) against square root of time ($\sqrt{s}$)

d – sample thickness (mm)

M_{sat} – saturated mass of concrete specimen (g)

M_o – dry mass of concrete specimen (g)

2.1.2 Permeation

Permeation refers to the movement of a fluid through the pore structure under the influence of an externally applied pressure, while the pores are filled with that particular fluid. Hence, permeability quantifies the ability of concrete to transfer fluids by permeation. Permeability is a function of the concrete microstructure, moisture conditions, and properties of the permeating fluid. The extent of permeation is critical in water-retaining structures where the transport of water through concrete must be limited (Ballim *et al.*, 2009). The main driving force for the permeation of liquids and gases through concrete is a pressure gradient. The flow of these gases and liquids through the pores is generally defined by Darcy's law (Alexander *et al.*, 2010).

- Water permeability coefficient

$$\frac{dq}{dt} = \frac{k.H.A}{L} \quad \text{.....(2.2)}$$

where,

dq/dt – flow (m^3/s)

k – coefficient of permeability (m/s)

H – represents the height of the column of water pressure difference across the sample ($\Delta P = H \cdot \delta \cdot g$, with δ = water density and g = acceleration due to gravity

A – cross sectional area of specimen (m^2)

L – thickness of specimen (m)

- Gas permeability coefficient

$$\frac{dq}{dt} = \frac{k_{gas}.A.(P_1^2 - P_2^2)}{2L.\mu.P_2} \quad \text{.....(2.3)}$$

where,

dq/dt – flow (m^3/s)

k_{gas} – gas permeability coefficient (m^2)

A – cross sectional area of specimen (m^2)

L – thickness of specimen (m)

P_1 – upstream pressure (Pa)

P_2 – downstream pressure (Pa)

μ – viscosity of the gas (Ns/m^2)

2.1.3 Diffusion

Diffusion is defined as the process whereby liquid, gas or ions move through a porous material, from a region of high concentration to a region of low concentration, under the influence of a concentration gradient. Gaseous diffusion occurs mainly in unsaturated concrete while ionic diffusion is prevalent under partially or fully saturated conditions and the latter represents the main transport mechanism for salts inside concrete. For instance, in the context of reinforcement corrosion, the transport of chlorides and oxygen to the embedded steel is governed by the diffusion process. The external surface salt concentration initially develops by the absorption process which is followed by diffusion towards lower concentration points within the concrete material. The diffusion rate is function of temperature, internal moisture content, and characteristics (diffusivity) of the particular species. The overall diffusion process is further affected by chemical interactions with the cement paste, the saturation conditions, defects such as voids or cracks and electrochemical effects due to stray currents and steel corrosion (Ballim *et al.*, 2009).

Gaseous and ionic diffusion in concrete can be modelled using Fick's first law of diffusion (for steady state diffusion). This law is used to define the rate of diffusion of ions or gas through a uniformly permeable material (Richardson, 2002).

$$J = -D_{eff}\frac{dC}{dx} \quad \text{.....(2.4)}$$

where,

J – mass transport rate (g/m^2s)

D_{eff} – effective diffusion coefficient (m^2/s)

dC/dx – concentration gradient ($g/m^3/m$)

C – concentration of fluid (g/m^3)

x – distance (m)

The negative sign in the formula indicates that the flux occurs along a negative concentration gradient.

However, diffusion seldom reaches stationary conditions in concrete structures and as a result, the modelling of ionic diffusion is best represented by Fick's second law of diffusion (non-steady state) (Bertolini *et al.*, 2013).

$$\frac{\partial C}{\partial t} = D\frac{\partial^2 C}{\partial x^2} \quad \text{(2.5)}$$

where,

D – diffusion coefficient (m^2/s)

t – time parameter (s)

C – concentration of fluid (g/m^3)

x – distance (m)

The boundary conditions for Equation 2.5 are as follows:

$C_x = 0$ at $t = 0$ and $0 < x < \infty$

$C_x = C_s$ at $x = 0$, and $0 < t < \infty$

where,

C_x – chloride concentration at depth x at time t (g/m^3)

C_s – surface chloride concentration (g/m^3)

2.1.4 Migration

Migration (also referred to as accelerated diffusion, electro-diffusion, or conduction) is the movement of ions in a solution under the influence of an electric field. The velocity of the ions is a function of the strength of the electric field, the charge and the hydrated size of the ions. The principles of migration in aqueous solutions can also be applied to concrete, due to ion movement in the pore solution. Similar to diffusion, the migration of ions in concrete is a function of the complexity, size, moisture content and interconnectedness of the pore system. The electrical resistivity of the concrete also plays a major role (Bertolini *et al.*, 2013). Migration is the most widely used transport mechanism in laboratory accelerated chloride conductivity tests which are based on the Nernst-Planck equation (Alexander *et al.*, 2010).

$$v = \left(D\frac{zF}{RT}\right)\left(\frac{dU}{dx}\right) \quad \text{(2.6)}$$

where,

v – velocity of the ionic species (m/s)

D – diffusion coefficient of the ionic species (m^2/s)

z – electrical charge (ionic valence) of diffusing ions

F – Faraday's constant (9.6548 x10^4 J/Vmol)

T – absolute temperature (K)

U – potential difference across the sample (V)

x – distance variable (m)

R – universal gas constant (8.314 J/molK)

It must be emphasized that in practice, the ingress and transport of aggressive species in concrete does not occur through a single but rather by a combination of different mechanisms. Figure 2-1 represents a structure located in a marine environment that is subject to wetting-drying cycles, seawater spray and periodic rainfall. Sea-water may penetrate the concrete through capillary suction or permeation when the external surface is wetted. If the evaporation rate exceeds the absorption rate, the ingress of oxygen together with the deposition and accumulation of salts by diffusion is promoted (Bertolini *et al.*, 2013).

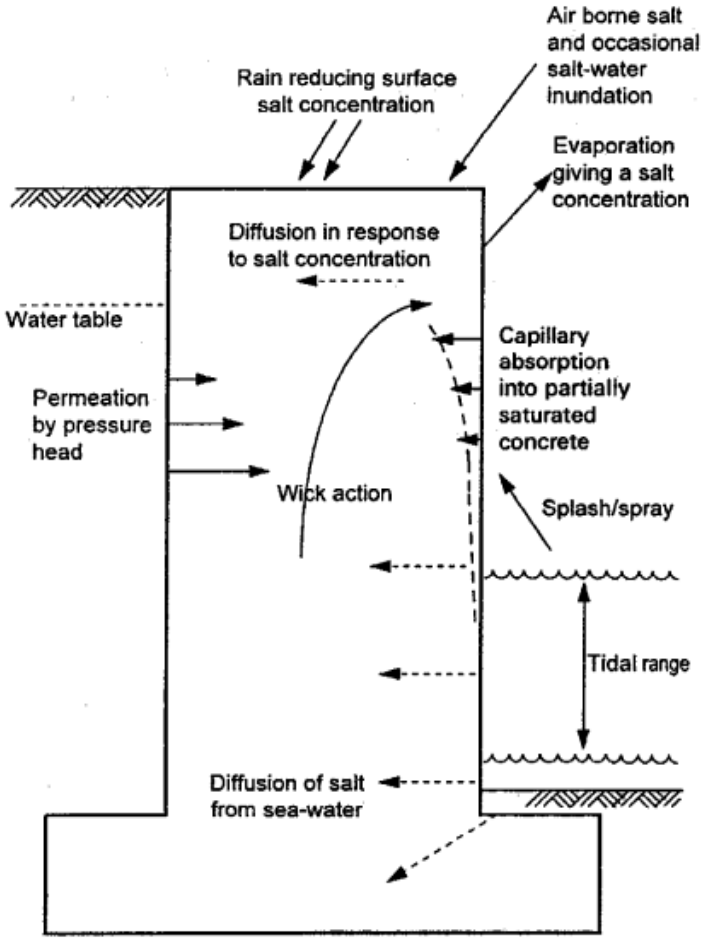

Figure 2-1: Transport mechanisms in a marine environment (Alexander *et al.*, 2013)

Hence, the study in isolation of a single transport process and concrete property for the ingress of particular species may not be a true representation of the actual situation. Research must aim at quantifying and modelling the movement of aggressive species (chlorides, sulphates, oxygen, carbon dioxide) through simultaneous but different transport mechanisms (Alexander *et al.*, 2010).

2.2 Transport mechanisms in cracked concrete

It is essential to understand the transport mechanisms in cracks as these provide short circuit routes to the embedded steel reinforcement. Excessive crack widths can potentially shorten the time to corrosion initiation, thereby reducing the overall serviceability of a structure. The transport properties of cracked concrete are a function of the crack properties (width, shape, tortuosity and orientation), concrete composition (interactions between the cement paste and penetrating species), cover depth and chemical composition of the pore solution (Pacheco & Polder, 2012; Gu *et al.*, 2015). As a fluid flows through a single crack, mass transfer can occur between the liquid and fracture surface (Figure 2-2), described by the following mechanisms; adsorption of ions from the liquid to the solid matrix, dissolution of the soluble phases from the solid matrix to the liquid and possible chemical reaction between the fluid and the internal crack surface. The physical processes (adsorption and dissolution) can be described through the advection-dispersion equation for mass transport as follows (Li, 2017).

$$\frac{\partial c_m}{\partial t} + m_{\rightarrow} = D_L \frac{\partial^2 c_m}{\partial x^2} - u \frac{\partial c_m}{\partial x} \quad \text{.....(2.7)}$$

where,

∂c_m – concentration of solute (ion or solvable phase) in the liquid solution (kg/m^3)

u – flow rate (m/s)

$m_{\rightarrow}$ – adsorption/dissolution rate of the ion/soluble phase (kg/m^{3}s)

D_L – diffusivity of the solute (m^2/s)

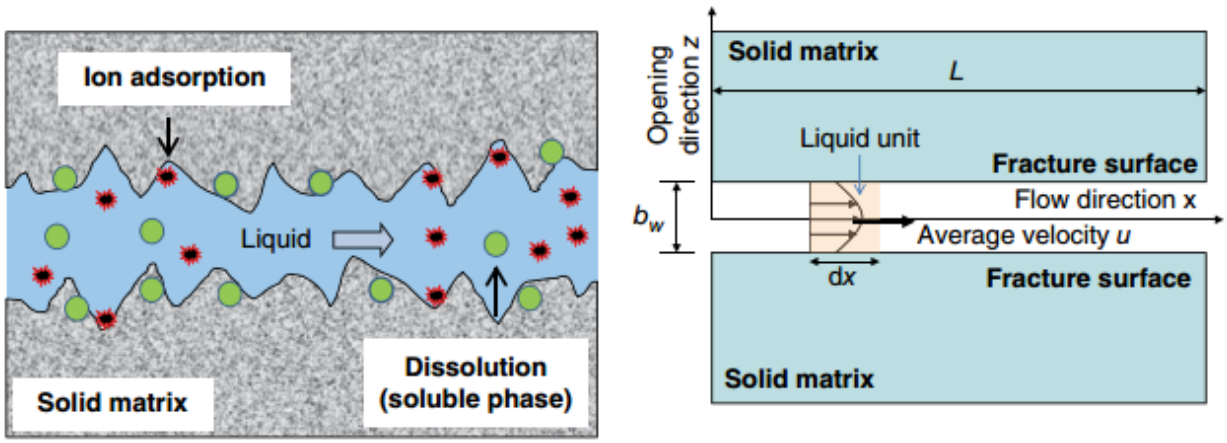

Figure 2-2: Mass transfer between a flowing liquid and the crack surface (left) and convection-dispersion modelling of mass transport (right) (Li, 2017)

2.3 Concrete deterioration

Concrete remains the most extensively used construction material due to its versatility, strength, durability and availability of its raw constituents. It forms the solid backbone of social and economic infrastructures essential for economic growth and advancement in countries. Well-designed

concrete can withstand exposure to damaging and challenging environments for a significant amount of time (Siddique *et al.,* 2011).

However, over the last few decades, there has been an increase in the premature deterioration of concrete infrastructure worldwide, linked mainly to reinforcement corrosion. The combinations of poor mix design, inadequate workmanship and highly aggressive environments are usually the conditions leading to the early degradation of concrete. The environments that promote deterioration are usually aqueous in nature, encompassing natural (soft-waters, sea-waters or ground waters), industrial and polluted environments. In such surroundings, concrete is subject to ion addition and exchange reactions that usually lead to the breakdown of the matrix microstructure and hence weakening of the material. The degradation rate varies according to the type of environment (acidic or mild) and the scale of damage is often a function of the concrete quality. With increasing demand for infrastructure and subsequent expansion of the built environment, there is greater need for concrete to withstand and perform in these aggressive environments. Significant amount of research has been conducted to better understand the causes of early degradation of concrete and develop durability design and specifications with the aim of increasing the service life of infrastructure. However, poor understanding of concrete durability and insufficient quality control on site still hinder sustainable construction. On a larger scale, concrete deterioration has many financial and social implications. Direct costs are related to the repair and rehabilitation of existing structures to maintain serviceability while indirect costs include loss in productivity and reduced gross domestic product (GDP) (Alexander *et al.,* 2013).

The following points are general principles that can be applied to the deterioration of concrete and hence used as guidelines to limit the extent of degradation (Ballim *et al.,* 2009):

- Deterioration is generally linked to the ingress and movement of aggressive species (liquids, gases and ions) through the pore structure of concrete. Hence, transport properties become important parameters that control the rate of deterioration.
- Practically all types of concrete deterioration occur in the presence of water in both the external environment and internal pore structure. Generally, concrete in dry environments shows a lower extent and rate of degradation relative to wet (humid) environments.
- The nature (characteristics) of the cement and supplementary cementitious materials used in the mix design has a significant influence on the resistance of the concrete to deterioration in particular environments.
- For most deterioration mechanisms, the rate and extent of damage can be considerably reduced through adequate workmanship (proper placing, compaction and curing), especially in the cover zone of the reinforced concrete element.

The degradation of concrete can arise due to defects (from physical, mechanical and chemical processes) or reinforcement corrosion (Figure 2-3). In practice, these processes may be interdependent and can occur simultaneously in the service life of reinforced concrete structures. Changes that occur in fresh concrete (within the first few hours after casting) such as plastic, settlement and thermal shrinkage are usually not considered as deterioration mechanisms, but must be prevented as they affect the long-term performance and durability of concrete. Concrete deterioration is

closely linked to reinforcement corrosion as the expansive products formed during the reactions generally lead to the cracking and spalling of surrounding concrete cover (Bertolini *et al.*, 2013).

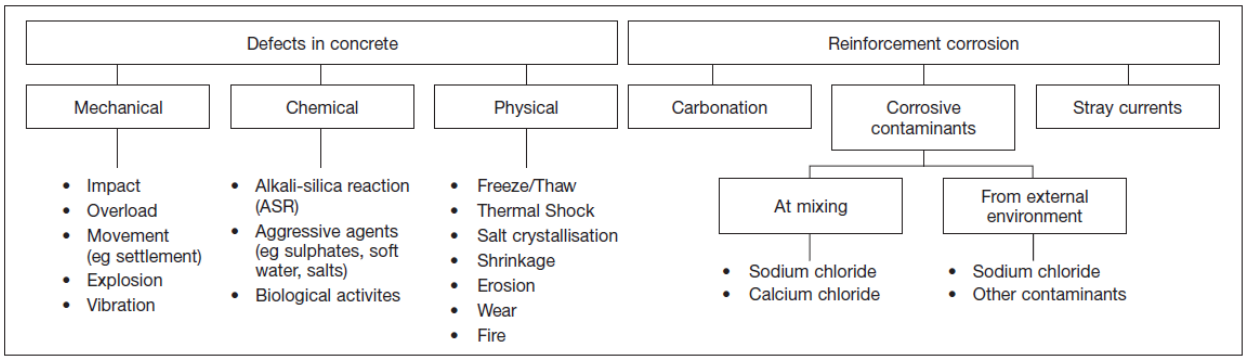

Figure 2-3: Causes of concrete deterioration (Alexander & Beushausen, 2009)

2.3.1 Reinforcement corrosion

The deterioration of concrete structures due to reinforcement corrosion can be modelled using a two-phase approach proposed by Tuutti (1982) – (Figure 2-4). The first phase (initiation) refers to the time taken for aggressive species (chlorides and carbon dioxide) from the surrounding environment to penetrate, move through the concrete cover and accumulate at the embedded steel in sufficient amount leading to the breakdown of the passivating layer, thereby initiating the corrosion process. The duration of this phase is dependent on the concrete quality, cover depth, exposure conditions and concentration limits for corrosion to start. Damage to the surrounding concrete is negligible at this stage. During the propagation phase, reinforcement corrosion occurs (in the presence of sufficient oxygen and water) which ultimately causes deterioration of the concrete. This period can be split into various phases, namely the onset of corrosion; the formation of expansive and voluminous corrosion products; cracking and delamination of the concrete cover and finally the failure of the structure (Ballim *et al.*, 2009). The corrosion rate, which is a function of temperature and humidity, determines the time taken to reach each of the stages mentioned (Bertolini *et al.*, 2013).

The consequences of reinforcement corrosion range from minor aesthetic cracking to severe structural damage that compromises the durability and performance of the structure (Figure 2-5). Corrosion is usually accompanied by rust stains on the external surface of the reinforced concrete member. Since the volumes of the corrosion reaction products (Fe_3O_4, $Fe(OH)_2$, $Fe(OH)_3$, and $Fe(OH)_3.3H_2O$) are 3-4 times greater than that of iron, tensile stresses are generated within the concrete cover. When these stresses exceed the tensile strength of the concrete, cracking occurs which can cause local spalling or complete delamination. Moreover, in the case of chloride induced corrosion, there is generally a reduction in cross section in localised areas along the rebar, thus compromising its inherent tensile strength and overall load bearing capacity of the reinforced concrete member. Finally, corrosion under particular conditions can lead to the brittle failure of high strength steel used in prestressed concrete (Bertolini *et al.*, 2013).

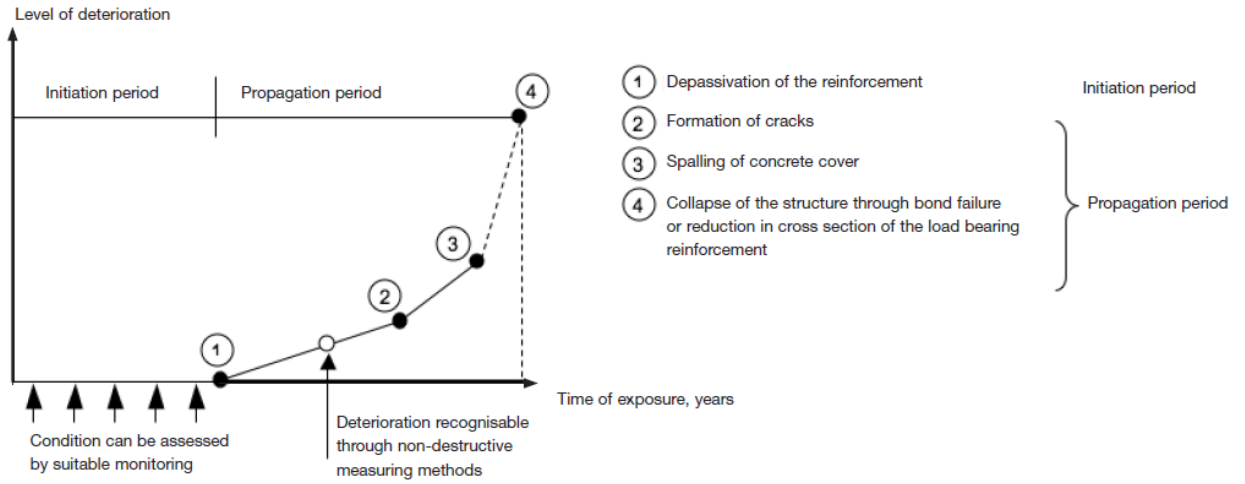

Figure 2-4: Two-phase model for deterioration due to reinforcement corrosion (Ballim *et al.*, 2009)

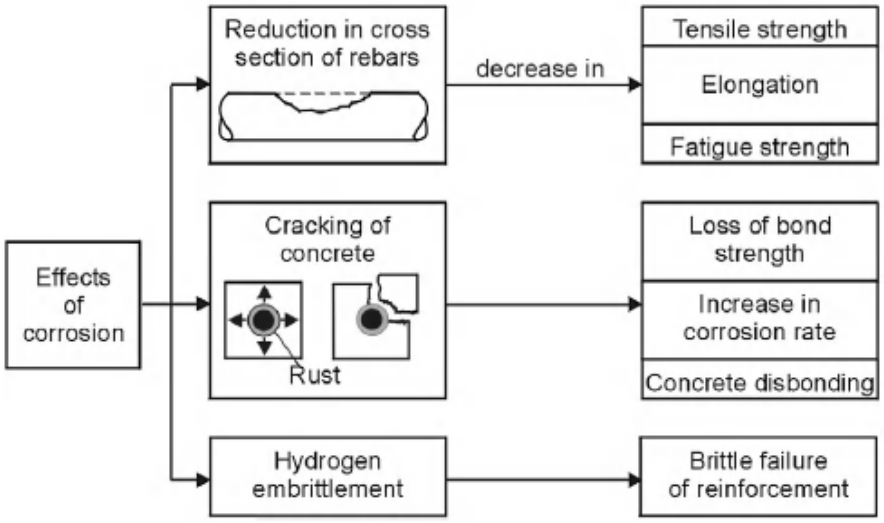

Figure 2-5: Consequences of reinforcement corrosion in concrete structures (Bertolini *et al.*, 2013)

Corrosion of reinforcement can be simplified into two main processes namely the anodic and cathodic reactions. The anodic process (Equation 2.8) involves the oxidation of iron atoms to ferrous ions when the protective layer at the surface of the reinforcement has been damaged. The cathodic process (Equation 2.9) consists of the reduction of oxygen from the surrounding air as it reacts with water to form hydroxyl ions. The distance between the anode and cathode can vary greatly depending on the location of damage on the concrete cover. The cathode and anode areas may also alternate along the length of a continuous reinforcing steel bar. Oxygen at the cathode contributes to the removal of electrons that were liberated from the oxidation of iron in the steel bar at the anode. The flux of ions and electrons respectively can be used to measure corrosion rate (Böhni, 2005).

Anodic reaction: $2Fe \rightarrow 2Fe^{2+} + 4e^{-}$……..……...……(2.8)

Cathodic reaction: $O_2 + 2H_2O + 4e^- \rightarrow 4OH^-$……..……..(2.9)

Overall reaction: $2Fe + 2H_2O + O_2 \rightarrow 2Fe(OH)_2$……..……..……..(2.10)

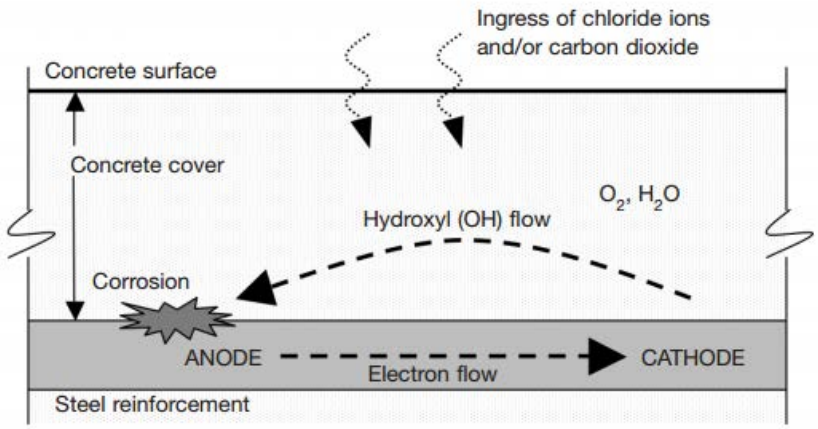

Figure 2-6: Mechanism of rebar corrosion (Alexander & Beushausen, 2009)

Table 2.1: Summary of conditions required for reinforcement corrosion (Böhni, 2005)

	Condition for corrosion of steel in concrete	Condition is fulfilled, if:
1	An anodic reaction is possible	The passive layer around the steel bar breaks down and depassivation of the steel occurs. This can be caused by carbonation of concrete or ingress of chloride ions into the concrete, reaching a critical level.
2	A cathodic reaction is possible	Oxygen as the driving force of the corrosion process is available at the interface of the reinforcement in a reasonable amount.
3	A flux of ions between the site of the anodic reaction and the site of the cathodic reaction is possible	The environment or electrolyte between the site of the anodic reaction and the site of the cathodic reaction conducts well.
4	A flux of electrons is possible	There is a metallic connection between the sites of the anodic and cathodic reactions. For monolithic reinforced concrete structures, this condition is usually fulfilled.

Reinforcing steel in concrete is protected against corrosion mainly due to the alkaline environment (pH 13) resulting from the cement hydration reactions. This allows the formation of a protective layer (consisting of thermodynamically stable compounds of iron) around the steel that prevents the anodic dissolution of the iron. As long as this few nanometres thick passive layer is sustained, corrosion will not occur. However, poor quality concrete may allow carbon dioxide in the air or chloride ions from the surrounding environment to penetrate sufficiently deep through the pores and react with calcium hydroxide present. This reaction eventually leads to a reduction in pH of the concrete that causes the protective layer around the steel to dissolve. Hence, the steel reinforcement becomes vulnerable to corrosion. The presence of moisture is usually required to sustain the corrosion reaction (Stuart, 2013; Bertolini *et al.*, 2013).

2.4 Carbonation of concrete

2.4.1 Mechanism

The carbonation of concrete is a result of chemical reactions between the alkaline components of the cement paste (NaOH, KOH, $Ca(OH)_2$ and calcium-silicate hydrates) and atmospheric carbon dioxide (CO_2). These reactions occur only in the presence of a certain amount of water and generally cause the pH of the concrete to decrease from 12.5 to values between 9 and 6. However, the pH stays at the value of saturated $Ca(OH)_2$ solution, around 12.5, as long as not all $Ca(OH)_2$ has reacted. Hence, the concentration of $Ca(OH)_2$ present is a significant factor that ultimately determines the carbonation resistance of concrete (Böhni, 2005). During carbonation, the following reactions may occur (Hunkeler, 1994):

- Uptake of CO_2 in the pore water (formation of carbonic acid)

$$CO_2 + H_2O \rightarrow 2H^+ + CO_3^{2-} \quad (2.11)$$

- Dissolution of alkaline constituents of the pore water

$$NaOH \rightarrow Na^+ + OH^- \quad (2.12)$$

$$KOH \rightarrow K^+ + OH^- \quad (2.13)$$

$$Ca(OH)_2 \rightarrow Ca^+ + 2OH^- \quad (2.14)$$

- Full reaction releases water

$$2NaOH + H_2O + CO_2 \rightarrow Na_2CO_3 + 2H_2O \quad (2.15)$$

$$2KOH + H_2O + CO_2 \rightarrow K_2CO_3 + 2H_2O \quad (2.16)$$

$$Ca(OH)_2 + H_2O + CO_2 \rightarrow CaCO_3 + 2H_2O \quad (2.17)$$

Since the solubilities of Na_2CO_3 and K_2CO_3 are higher than that of $CaCO_3$, they remain dissolved in the pore water, whereas $CaCO_3$ is deposited. With further carbonation reaction, the carbonates react, if there is sufficient CO_2 and water available, to form soluble hydrogen carbonate (HCO_3^-, bicarbonate). This causes further decrease in overall pH (Böhni, 2005).

$$Na_2CO_3 + H_2O + CO_2 \rightarrow 2NaHCO_3 \quad (2.18)$$

$$K_2CO_3 + H_2O + CO_2 \rightarrow 2KHCO_3 \quad (2.19)$$

$$CaCO_3 + H_2O + CO_2 \rightarrow Ca(HCO_3)_2 \quad (2.20)$$

The final pH resulting from the complete carbonation reaction hence depends on the following parameters (Hunkeler, 1994):

- Alkali content of the cement (Na_2O, K_2O)

- Degree of hydration of the cement
- Moisture content of concrete
- Partial pressure of CO_2
- Temperature

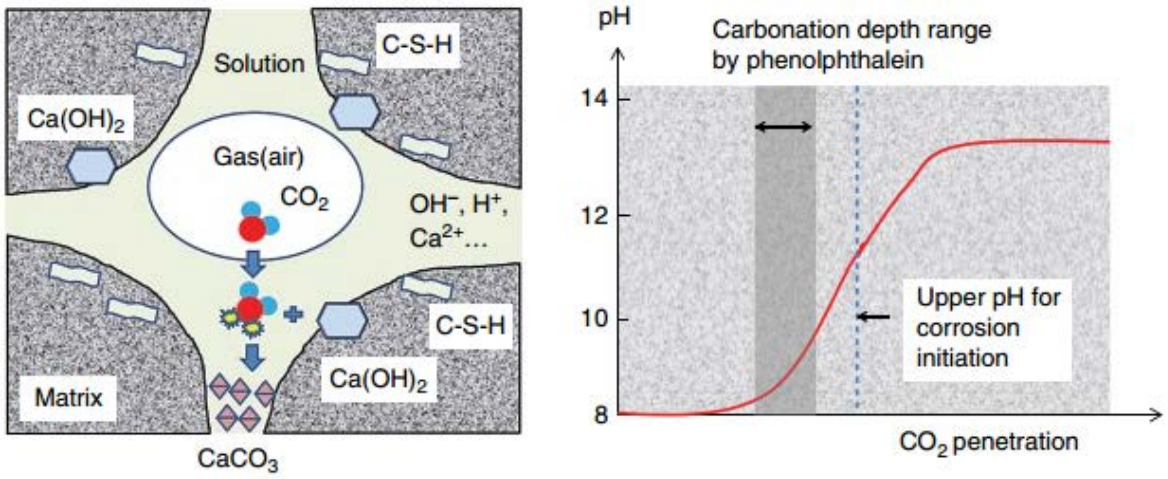

Figure 2-7: Mechanism of carbonation at pore level (left) and change in pH due to carbonation (right) (Li, 2017)

The carbonation reaction is typically initiated on the external surface of concrete and propagates with time, resulting in a low pH front. The test for carbonation depth involves spraying an alcoholic solution of phenolphthalein on the extracted concrete sample. The surfaces where the pH is greater than 9 (basic environment) usually show a pink coloration whereas carbonated concrete surfaces remain colourless. The rate of carbonation decreases exponentially with time and can be modelled by Equation 2.21 (Bertolini *et al.*, 2013).

$$d = K\sqrt{t} \quad \text{(2.21)}$$

where,

d – depth of carbonation (mm)

t – time (years)

K – carbonation coefficient (mm/year$^{1/2}$) which takes into account the diffusion coefficient (D), the CO_2 concentration at the concrete surface and the quantity of alkaline components to be consumed (assuming they remain constant over time).

2.4.2 Carbonation induced corrosion

Carbonation induced corrosion typically involves multiple pitting along the reinforcement. The anodic and cathodic sites are adjacent to each other (microcell corrosion). Environmental conditions favourable for the carbonation reaction (50 to 65 % relative humidity), are usually too dry to promote rapid steel corrosion which usually requires humidity levels above 80%. However, structures exposed to external environmental conditions such as rain may be vulnerable to carbonation

induced corrosion as the moisture content of the concrete cover may vary. Carbonation rates generally increase with higher carbon dioxide concentration and w/b ratios. For the same w/b ratio, the incorporation of fly-ash and slag reduces the carbonation resistance of concrete (due to lower calcium hydroxide content) (Alexander *et al.*, 2012; Bertolini *et al.*, 2013).

2.5 Chloride ingress in concrete

2.5.1 Mechanism

Chlorides may be introduced in fresh concrete through the use of contaminated mix constituents such as sea-dredged sand and contaminated water. Chlorides from sea-water and deicing salts may also penetrate hardened concrete through capillary suction and diffusion (Bertolini *et al.*, 2013).

When saturated concrete is exposed to sodium chloride solution, the difference in ionic strength between the external and pore solution initiates the movement of ions. Chlorides move into the concrete pore water while alkalis and hydroxides start to leach out. This process, termed as diffusion, involves several ion interactions that lead to a charge equilibrium. The flux of one category of ion is influenced by the flux of other ions due to the interaction of their respective electric fields. The concrete pore system in the as built structure is not fully saturated with water (moisture flow can occur through the pore structure). This moisture flow varies in both magnitude and direction and can lead to the convection of ions in and out of the concrete over time. When the concrete is too dry, moisture flow is too low to carry ions and may result in the buildup of ions in certain locations. Significant interaction (termed as 'binding') can also occur between the ions and cement paste matrix during the movement of ions within the pore system. This interaction, which depends primarily on the type and amount of binder and temperature, can delay the penetration of additional chloride ions (Luping *et al.*, 2012; Bijen, 2003).

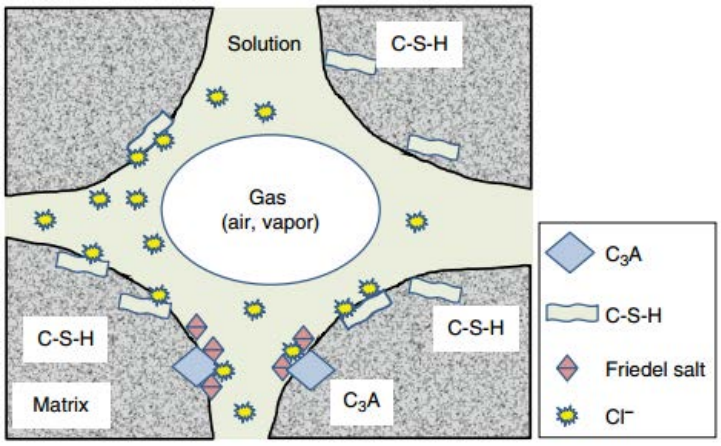

Figure 2-8: Transport of chlorides through the pore structure by different mechanisms (Li, 2017)

In practice, chloride penetration is an overall complex process. For instance, in a splash and spray environment, the concrete surface is exposed to continuous wetting and evaporation (drying) cycles. This zone is typically referred to as the convection zone (Δx) where water containing dissolved chlorides moves in and out (Figure 2-9). This prevents the development of a clear diffusion

mechanism. Beyond the convection zone, diffusion is the main transport mechanism (Sarja, 2006; Ballim *et al.*, 2009).

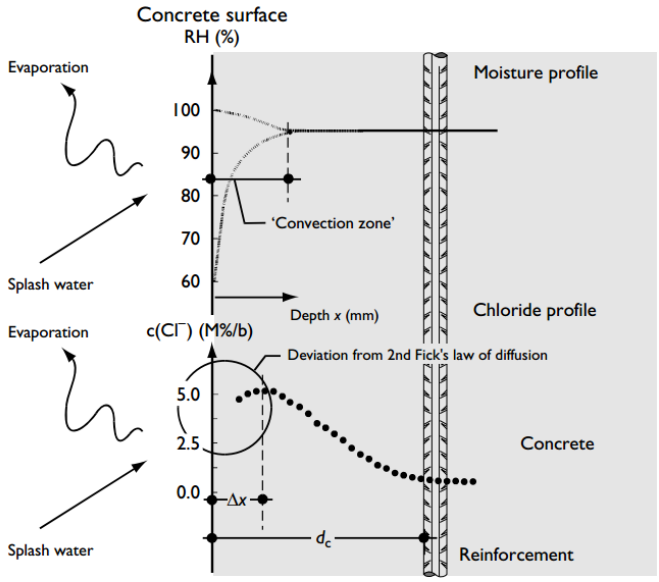

Figure 2-9: Typical moisture and chloride profiles for the splash zone (Sarja, 2006)

Chloride ingress is significantly affected by the exposure conditions. Figure 2-10 shows the chloride penetration contours for concrete in a marine environment. Highest chloride surface concentrations are obtained at relatively high elevation. This can be attributed to cyclic wetting and drying at this location (splash/spray zone) that causes accumulation of salts. At lower elevation (tidal zone), the concrete is relatively wetter and transport of chlorides occurs deeper. In the permanently submerged part, equilibrium between free and bound chlorides and moderately fast transport to the inner parts (steady-state diffusion) governs the total chloride content (Bertolini *et al.*, 2013).

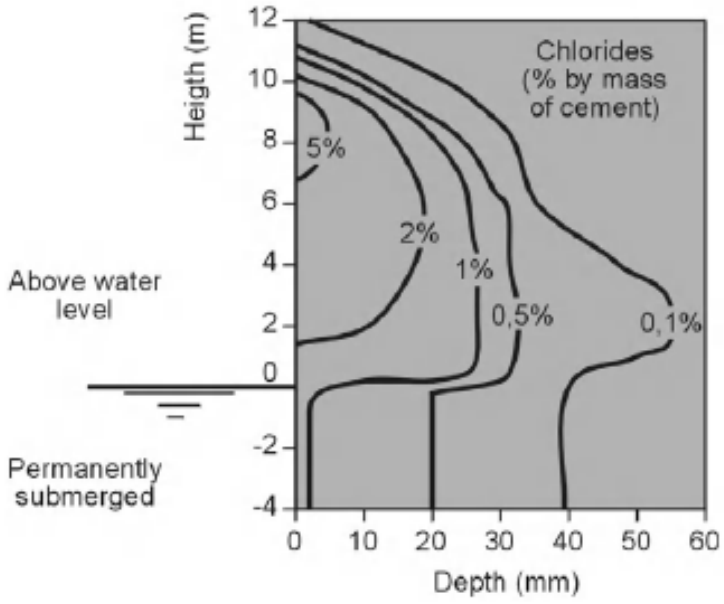

Figure 2-10: Typical chloride penetration contours as a function of height above sea-water (Bertolini *et al.*, 2013)

2.5.2 Chloride ingress modelling

A chloride ingress model for concrete typically predicts the chloride profile C(x,t) after a certain period of time (t) and hence the chloride concentration C at the depth of the steel rebar. The output of this model is normally evaluated against a 'chloride threshold level' (Luping *et al.*, 2012). This threshold value is known as the critical chloride concentration (C_{cr}) at the reinforcement depth that leads to the loss of the protective gamma-ferric (passive) oxide layer. This critical chloride content is a function of several interlinked factors such as pore solution chemistry, properties of the steel-concrete interface, amount of oxygen available and electrochemical potential of the steel reinforcement. For example, relatively low chloride content is required for corrosion initiation in structures exposed to the atmosphere. In the case of fully immersed (saturated) structures, relatively higher chloride content is needed to initiate corrosion due to the lack of oxygen and this results in lower reinforcement corrosion potential (Bertolini *et al.*, 2013, Richardson, 2002).

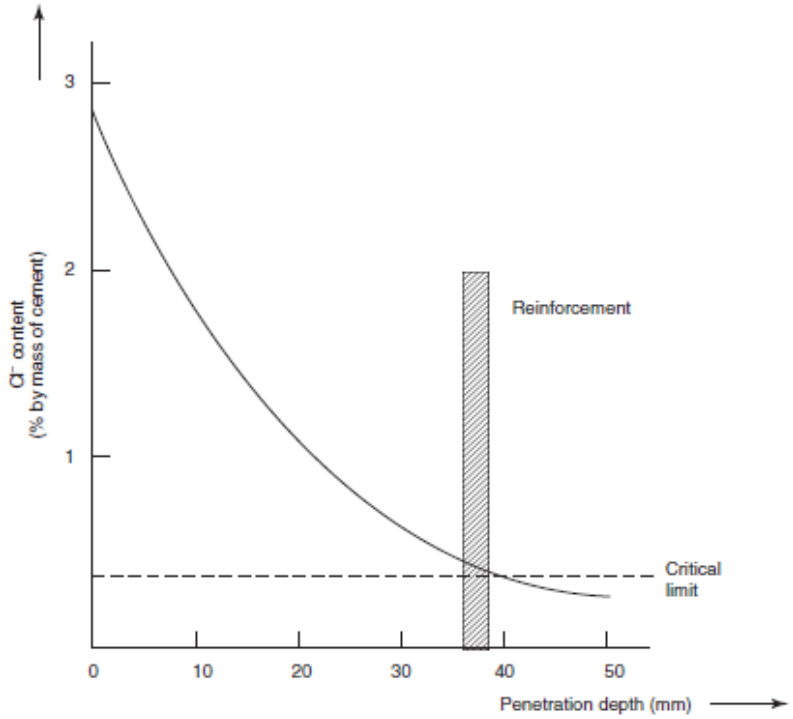

Figure 2-11: Comparison of critical chloride concentration (C_{cr}) to predicted chloride profile (Bijen, 2003)

There are generally two types of chloride ingress models; mechanistic (physical) and empirical models. Mechanistic models aim at describing physical and electrochemical processes using independently acquired input data, with no further manipulation such as curve fitting. Fick's first law of diffusion forms the basis of the simplest physical models for chloride penetration. These models consider mass balances and the relationship between chlorides and pore water (transport and binding). Field exposure data is utilised to affirm the predictions of the models. If insufficient correlation is obtained between the measurements and the model's output, further data must be acquired to improve the accuracy of the model. The main limitations of this type of model are that a significant amount of input data (that is often not readily available) is required for calibration and several boundary conditions (linked to the material and environment) need to be defined. Due to these

complexities, physical models are not suitable for practical applications and are mostly used as research tools (Luping *et al.*, 2012).

On the other hand, empirical models are typically established on a solution of Fick's second law of diffusion and aim at fitting experimental data into mathematical functions that describe the transport of chlorides through concrete. For example, the data obtained from chloride profiles taken on structures can be manipulated (curve fitted) to obtain regression parameters (chloride surface concentration and apparent diffusion coefficient) that can be subsequently used to predict chloride profiles at the required age. Although empirical models offer a relatively simple solution to chloride penetration, they require high quality and long-term data to avoid underestimating or overestimating chloride content. This includes understanding and integrating the variation of the chloride diffusion coefficient and surface concentration with time (Luping *et al.*, 2012; Poulsen & Mejlbro, 2010).

Chloride ingress models are based on several fundamental assumptions, which are summarised in the following sections.

2.5.2.1 Mass balance equations

The mass balance equation for chloride ions can be described in various ways, depending on whether diffusion and binding are expressed as separate terms. The basic equation shows the overall quantity of chlorides per unit volume. The chloride flux (J_{Cl}) varies along various locations in the concrete. The difference in chloride flux in and out a tiny slice of concrete of thickness dx will alter the overall quantity of chlorides (C_{tot}) within that slice (Figure 2-12). The change in total chloride content per unit time is equal to the difference in chloride flux to and from the slice, divided by the thickness of the slice (Luping *et al.*, 2012). Hence, the mass equilibrium equation is described as follows:

$$\frac{\partial C}{\partial t} = \frac{\partial c_t}{\partial t} = -\frac{\partial JCl}{\partial x} \quad \text{.....(2.22)}$$

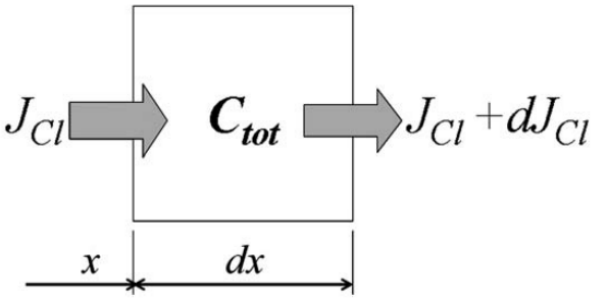

Figure 2-12: Schematic of mass balance equation for chlorides (Luping *et al.*, 2012)

The chloride content (c_t) represents the concentration per unit volume of concrete (not in terms of pore volume) and flux (J_{Cl}) is expressed per unit area of concrete. The negative sign implies that the chloride content will decrease if ∂J_{Cl} is positive. However, when describing chloride ingress, ∂J_{Cl} is negative and the chloride content will increase with time (Luping *et al.*, 2012).

The variation in total chloride quantity can also be expressed as a change in free chloride (c) (dissolved in the pore water) and bound chloride (c_b) such that balance is maintained between free and bound chlorides. Chloride flux in the pore solution will first cause a change in free chloride ion concentration (c), followed by an instantaneous change in bound chloride (c_b) due to the high chloride binding rate (Luping *et al.*, 2012). Hence, the mass balance equation can be expressed as follows:

$$\frac{\partial C}{\partial t} = \frac{\partial c}{\partial t} + \frac{\partial c_b}{\partial t} = -\frac{\partial JCl}{\partial x} \quad \text{.....(2.23)}$$

2.5.2.2 Flux explanations

Chloride flux (q_{Cl}) resulting from pure diffusion of chlorides (of concentration C) dissolved in liquid water has been conventionally explained by Fick's first law.

$$q_{Cl} = -D\frac{\partial C}{\partial x} \quad \text{.....(2.24)}$$

It must be emphasized here that the diffusion coefficient (D) in Fick's first law of diffusion is not a material property and is a function of the conditions. Thus, it cannot be estimated from simple diffusion tests.

It is now widely accepted that Fick's first law of diffusion represents an oversimplified description of chloride transport. The influences of the electric potential field ϕ (due to other ions) and potential difference (used in migration tests) need to be considered in the flux equation. Hence, flux can be expressed by the Nernst-Planck equation (Luping *et al.*, 2012).

$$q_{Cl} = -D_i\left(\frac{\partial c_i}{\partial x} + c_i\frac{\partial ln\gamma_i}{\partial x} + \frac{z_i F}{RT}c_i\frac{\partial \emptyset}{\partial x}\right) \quad \text{.....(2.25)}$$

The flux of chloride ions is influenced by other ions present, and therefore the results of tests used to determine the diffusion coefficient of chlorides (D_i) will be affected by the diffusion coefficient of other ions. A formation factor (which considers the restrictivity and tortuosity of the pore structure) then must be applied to define the flux of all ions (Luping *et al.*, 2012).

2.5.2.3 Interaction/Binding

A certain degree of interaction occurs between chlorides and hydration products (especially aluminates) as the former move through the cement matrix. This interaction (termed as binding) restricts the movement of chloride ions and consequently reduces the concentration of free chlorides in the pore water. Thus, the diffusion process is slowed down. The binding capacity is a function of the concentration of free chloride ions, cement type, w/b ratio and pH. The (non-linear) correlation between free and bound chlorides is usually described using a binding isotherm (Figure 2-13) (Gardner, 2006; Böhni, 2005).

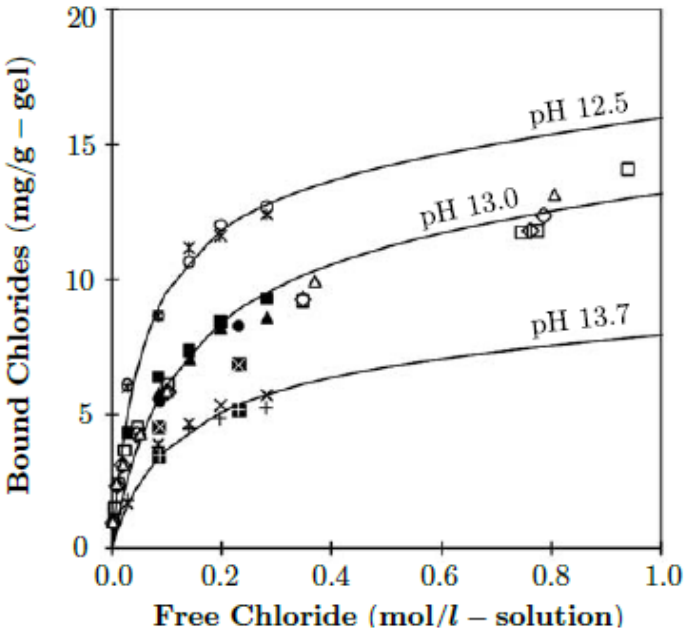

Figure 2-13: Typical binding isotherm describing the connection between bound and free chlorides (Tang & Nilsson, 1993)

2.5.3 Chloride ingress models based on Fick's second law of diffusion

As chloride diffusion occurs into concrete, a change in chloride ion content (C) occurs at any time (t) at every point (x) of the concrete (non-steady state diffusion). Assuming one-dimensional diffusion, a gradient of chloride concentration C exists along the x-axis. Hence, using this concept, chloride ingress can be modelled for various situations. For instance, considering an element (of cross-section dA = 1) that is parallel to the chloride diffusion into a semi-infinite volume of concrete (Figure 2-14). The volume (dV) between two consecutive points at a distance (dx) is 1.dx = dx. The flux of chlorides is described as the amount of chloride ions that diffuse into this volume (dV) of concrete, per unit time (dt). Similarly, the amount of chloride diffusing out from the volume dV is defined as the flux at x + dx. Hence, there is a change in flux along the x-axis into the concrete (Poulsen & Mejlbro, 2010). The increase in chloride within the volume dV during time (dt = 1) can be represented as follows:

$$\frac{\partial C}{\partial t}dx = F - \left\{F + \frac{\partial F}{\partial x}dx\right\} = -\frac{\partial F}{\partial x}dx \quad \text{.....(2.26)}$$

or,

$$\frac{\partial C}{\partial t} = -\frac{\partial F}{\partial x} \quad \text{.....(2.27)}$$

Equation 2.27, also called the mass balance equation, describes Fick's second law of diffusion which states that the change in chloride concentration per unit time (in an infinitesimal volume) is equal to the change of flux per unit length (Poulsen & Mejlbro, 2010).

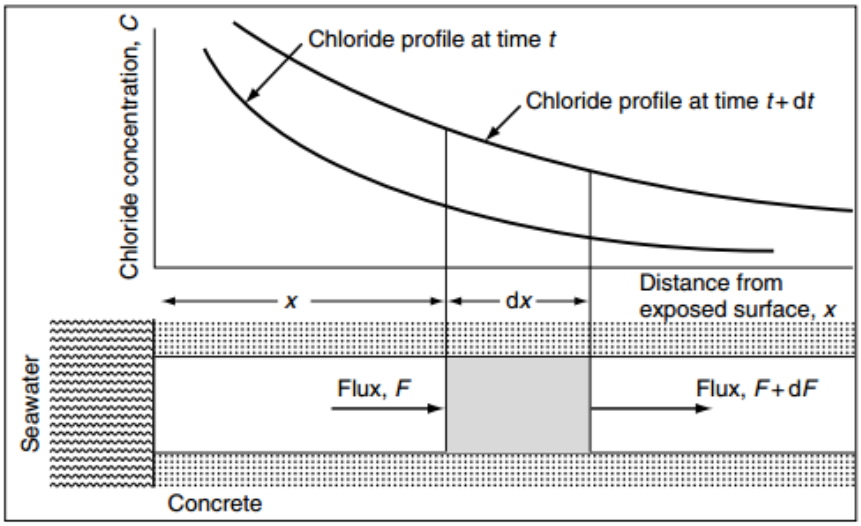

Figure 2-14: Fick's second law of diffusion – The change in chloride ion content per unit time is equal to the change in flux per unit length (Poulsen & Mejlbro, 2010)

Substituting Equation 2.24 into Equation 2.27, the following expression can be obtained:

$$\frac{\partial C}{\partial t} = -\frac{\partial}{\partial x}\left\{-D\frac{\partial C}{\partial x}\right\} = D\frac{\partial^2 C}{\partial x^2} \quad \text{.....(2.28)}$$

The boundary conditions for Equation 2.28 are as follows (Ballim *et al.*, 2009):

$C_x = 0$ at $t = 0$ and $0 < x < \infty$

$C_x = C_s$ at $x = 0$ and $0 < t < \infty$

The simplest mathematical solution to Fick's second law (Equation 2.29), whereby the surface chloride concentration (C_s) and chloride diffusion coefficient (D_a) are considered constant, is known as the Crank's error function solution (also called Gauss error function). The approach is also only valid for semi-infinite conditions and a linear binding isotherm. As chloride analysis considers the total soluble chloride concentration, the use of the error function solution is physically incorrect. However, from an engineering perspective, it provides a reasonable and convenient estimate of the chloride content (Sarja, 2006).

$$C(x,t) = C_i + (C_s - C_i).erf\left(1 - \frac{x}{2\sqrt{(t - t_{exp}).D_{app}}}\right) \quad \text{.....(2.29)}$$

where,

C(x,t) – chloride concentration at depth x at age t

C_i – initial chloride background level (g/m^3)

C_s – surface chloride content (g/m^3)

D_{app} – apparent chloride diffusion coefficient (m^2/s)

t_{exp} – time until first exposure to chlorides (s)

t – concrete age (s)

erf – error function

The error function (erf) is defined as:

$$erf\ x = \emptyset\left(\sqrt{2x}\right) = \frac{2}{\sqrt{\pi}}\int_0^x e^{-t^2}dt = \frac{2}{\sqrt{\pi}}\left(x - \frac{x^3}{1!\,3} + \frac{x^5}{2!\,5} + \cdots + \frac{(-1)^n x^{2n+1}}{n!\,(2n+1)}\right) \text{.....(2.30)}$$

where, n = 0,1,2…

Hence, this solution can be utilised to mathematically explain the chloride profiles obtained from either structures in the field or non-steady state laboratory tests. In laboratory (immersion) tests, cylindrical or cubic specimens are coated with epoxy resin on the sides except the top surface, and submerged in sodium chloride solution for a certain period. After exposure, chloride profiling is performed by extracting slices off the specimen at regular intervals. These slices are then milled into fine powder, dissolved in nitric acid and titrated with silver nitrate solution together with a suitable indicator (Sarja, 2006). Hence, the chloride ion content is determined at specific depths. The experimental data is plotted and curve fitted to Equation 2.29 as shown in Figure 2-15.

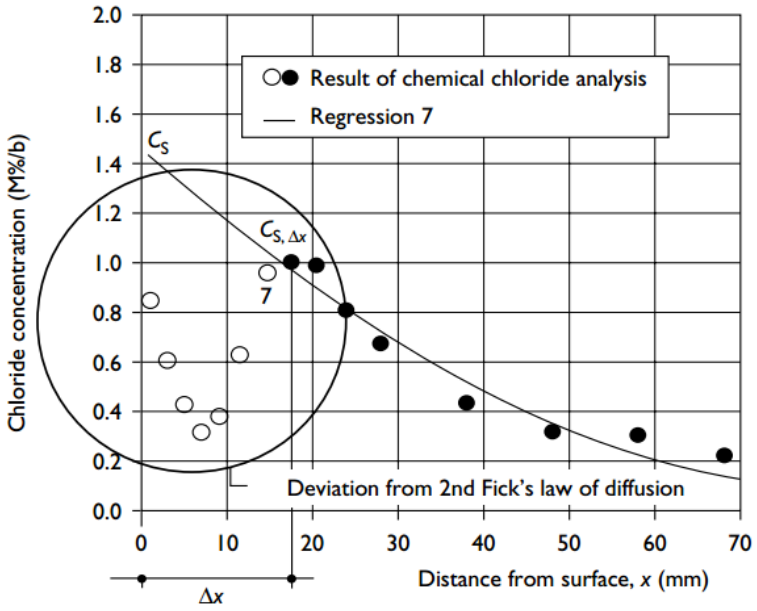

Figure 2-15: Typical measured chloride profile for concrete in the marine splash zone and subsequent curve fitting (neglecting data points in the convection zone) (Sarja, 2006)

The result of this procedure yields the best fitting pair of chloride diffusion coefficient and surface concentration. In the case of actual structures, cores are usually taken and analysed in a similar way. The (effective) diffusion coefficient obtained can hence be applied to define the rate of chloride ingress and thus predict long term chloride penetration in existing and new reinforced concrete structures (Bertolini *et al.*, 2013). It must be noted that to successfully describe the penetration of chlorides in existing structures, the data points for the convection zone are usually neglected in the curve fitting process (Sarja, 2006).

The chloride penetration profile (Figure 2-15) shows the distribution of chloride content (usually expressed as % of binder) against the depth (measured from the concrete surface). Since a sample with infinitely small thickness cannot be extracted, the surface chloride concentration (C_s) is calculated by extrapolation of the profile to the depth (x = 0). The surface concentration obtained is hence not the real concentration at that time, but rather a regression parameter. In practice, the surface chloride concentration (C_s) is time dependent and varies according to environmental conditions. C_s may reach a stationary value for a period which is short relative to the lifespan of the structure (leading to the common assumption that C_s is constant). However, it must be emphasized that in cases where external chloride levels are relatively low, the maximum surface chloride concentration may be reached after a longer period. The chloride profile usually converges towards the initial chloride concentration (C_i) with increasing distance from the surface. As the initial chloride content is based from the experimental data, it is crucial to collect enough data points near the tail of the chloride profile to obtain a reasonable estimate. Alternatively, the initial chloride concentration can be assumed to be negligible. The chloride profile can be also used to determine the depth of the convection zone (Δx) (Sarja, 2006).

In practice, the chloride diffusion coefficient (rate of chloride penetration) decreases with aging concrete. This is mainly attributed to ongoing hydration of the cementitious material (especially in blended cements) that reduces the capillary porosity over time. The time dependent diffusion coefficient D(t) (that considers the reduction in chloride diffusivity with time) can be described by Equation 2.31 (Van der Wegen *et al.*, 2012; Ballim *et al.*, 2009).

$$D(t) = D_0 \left(\frac{t_0}{t}\right)^n \quad \text{.....(2.31)}$$

where,

D_0 – diffusion coefficient at a reference time t_0 (for example 28 days)

n – aging coefficient (reduction factor)

The aging coefficient ($0<n<1$) is a function of the rate of hydration, extent of drying (type of environment) and type of binder.

2.5.4 Chloride induced corrosion

Chloride induced corrosion is considered as a significant deterioration mechanism responsible for the loss in serviceability of reinforced concrete structures. When sufficient chlorides reach the surface of the embedded reinforcement, the corrosion process is initiated by the localised breakdown of the passive gamma ferric oxide layer. A decline in pH of the pore water occurs as the solubility of calcium hydroxide ($Ca(OH)_2$) is reduced. The moisture content and electrical conductivity of the concrete are also increased (Böhni, 2005). Chlorides in concrete can be either dissolved in the pore solution (free) or chemically and physically bound to cement hydrate particles. It is generally agreed that only free chlorides are responsible for corrosion initiation. The mechanisms of chloride attack are as follows (Poursaee, 2016):

- Ingress of chloride ions into the oxide film through pores or defects in the passive layer.

- Adsorption of chloride ions on the metal surface which are in competition with dissolved oxygen or hydroxyl ions. Chloride ions compete with hydroxyl ions for ferrous ions produced by corrosion reaction, leading to the formation of soluble complex of ion chloride that diffuse away from the anode thereby destroying the protective gamma ferric layer and allowing corrosion to proceed.

Chloride induced corrosion is generally indicated by localised pitting of the reinforcement and high corrosion rates. The areas that are no longer protected by the passive iron oxide layer act as anodes (active zones) relative to the surrounding passive areas where cathodic reactions involve the reduction of oxygen. The overall reactions lead to the local loss in cross section of the steel rebar, cracking and spalling of the surrounding concrete cover which has structural and durability implications (Bertolini *et al.*, 2013).

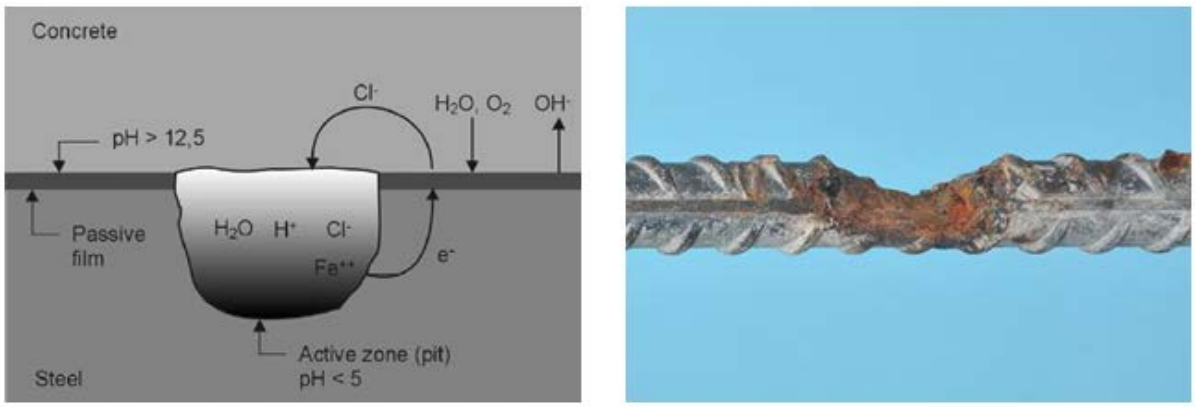

Figure 2-16: Mechanism of chloride induced corrosion (Bertolini, 2008)

2.6 Concrete durability

Sustainability has become a major issue in the modern construction industry. This requires the frugal use of finite resources to invest in new infrastructure while reducing the negative impacts on the society, economy and environment. Hence, designing for durability has become a necessity for engineers who must make use of concrete with adequate specifications to achieve satisfactory performance over the service life of structures. There needs to be a balance in mix designs as over-specification results in inefficient investment and waste of resources while under-specification leads to the premature deterioration of infrastructure and subsequent financial and economic problems on a larger scale (Richardson, 2002). Durability and service life prediction have gained significant importance in the recent years mainly due to structures under performing in particular environments. The poor durability of these concrete structures hence adds weight to construction and maintenance budgets worldwide (Beushausen & Luco, 2016). Durability is defined as “the ability of a structure or component to resist the design environment over a particular design life, without excessive loss in serviceability or need for major repairs”. Therefore, durability can be related to material performance rather than considered as an intrinsic material property of concrete. This is attributed to the fact that a specific concrete may be durable or suitable in a particular environment only. Durability can hence be described as the deterioration of material quality over the design life of the structure in a given environment (Ballim *et al.*, 2009).

Conventional durability design methods focus on prescribing limiting values for certain mix design parameters such as water to binder ratio (w/b), cement content and compressive strength. However, the issue remains that these selected parameters do not give a true representation of the concrete's resistance to the ingress of chlorides and permeation of carbon dioxide respectively. This is because the prescriptive method neglects the influence of other factors such as binder and aggregate type. Moreover, the impact of on-site practice during the commissioning process is ignored and this can potentially result in large discrepancies in quality between the proposed design and the as built structure. Concrete strength alone does not give a true indication of the durability of a structure and therefore cannot be used as a sole basis when designing for durability. On the other hand, performance-based approaches involve the measurement of certain material properties that are relevant to the deterioration mechanisms under specific exposure classes. This method of designing for durability includes testing concrete extracted from the as built structure and this accounts for material composition, on site practices and environmental conditions. Hence, relative to prescriptive (deemed to satisfy) concepts, performance-based approaches provide a sound basis for durability prediction and service life design. Most test methods used in performance-based approaches quantify the ingress potential of deleterious species relative to the quantity and quality of the cover concrete (Beushausen & Luco, 2016).

2.6.1 Factors affecting durability of concrete

Concrete durability can be represented as the relationship between concrete as a system and the surrounding environment (Figure 2-17), as durability assessments require the consideration of both. The concrete system consists of intrinsic and extrinsic factors that affect the resistance of concrete to deterioration while environmental factors relate to the degree of aggressiveness and exposure levels that the concrete is subject to (Ballim *et al.*, 2009).

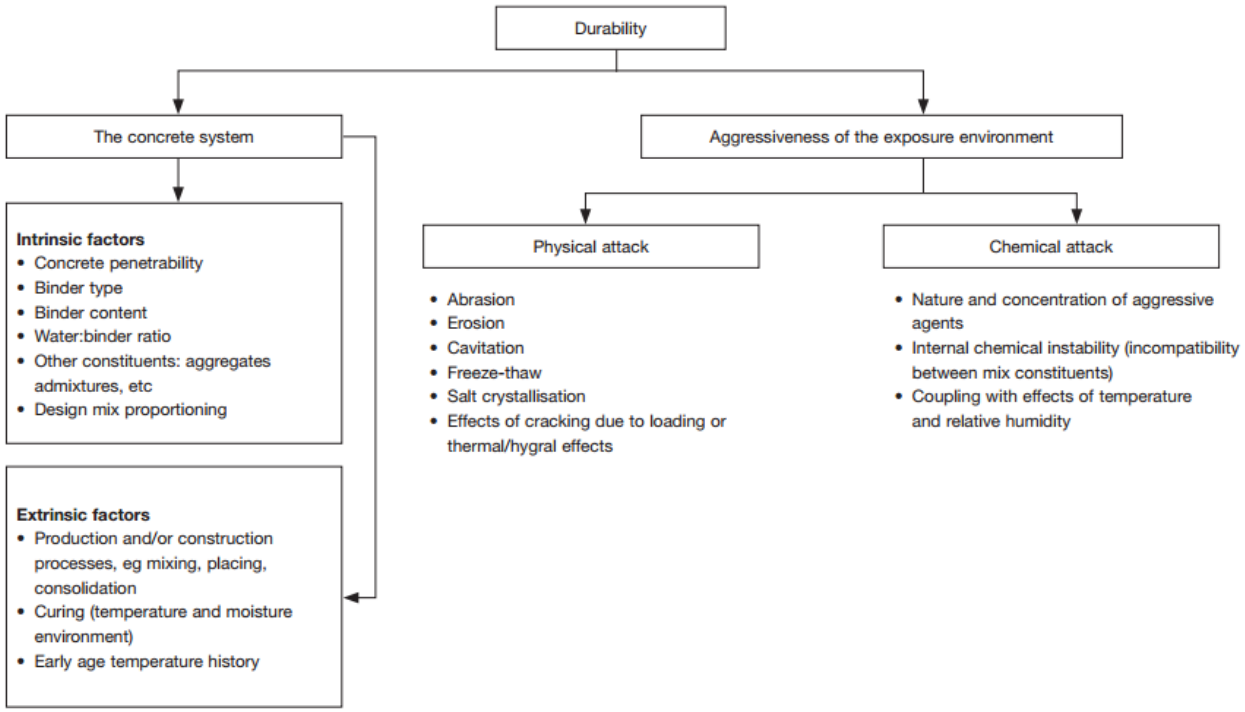

Figure 2-17: Concrete and environmental factors influencing durability (Ballim *et al.*, 2009)

2.6.1.1 Conditions of aggressiveness

The durability and performance of concrete structures is significantly affected by the aggressiveness level of the environment. Hence, it is fundamental to include this factor in the durability assessment of concrete structures. The aggressiveness of the environment can be split into physical and chemical attacks respectively. Important parameters relating to the environment include temperature, humidity, nature and concentration of deleterious agents, which are described as exposure classes in various standards. It is often noticed that the prevailing environmental conditions can be described using more than one exposure class. It must be also emphasized that these environmental parameters can vary across the different parts of the structure or fluctuate between different regions in a country on a larger scale (Beushausen & Luco, 2016).

Class	Description
XS1	Exposed to airborne salt but not in direct contact with seawater
XS2a	Permanently submerged
XS2b	XS2a + exposed to abrasion (heavy seas and pounding waves)
XS3a	Tidal, splash and spray zones
XS3b	XS3a + exposed to abrasion

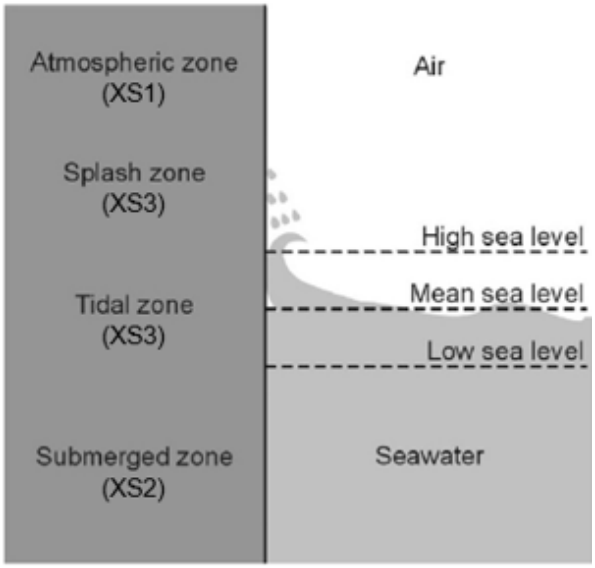

Figure 2-18: Marine environmental classes (EN 206, 2013; Beushausen & Luco, 2016; Bertolini *et al.*, 2013)

The environment is considered not aggressive if the humidity levels are below a certain threshold. For instance, the risks of carbonation and chloride induced corrosion become negligible below relative atmospheric humidities of about 70% and 50% respectively. The environment is also considered non-aggressive if the concrete is maintained under conditions of full saturation with water. In these conditions corrosion is limited, even in the presence of chlorides, due to the inability of sufficient oxygen to reach the surface of the reinforcement (Bertolini *et al.*, 2013). Marine environments are generally aggressive to reinforced concrete structures due to potential chloride induced corrosion and subsequent premature deterioration. The severity of chloride induced corrosion is the highest in the tidal and splash/spray zones due to the associated wetting and drying cycles. Highest chloride content is found at heights where salt water is supplied at regular time intervals with intermittent surface wetting and drying. Based on long term performance tests and local experience, the EN classes for the marine environment have been modified to suit the South African context (Figure 2-18) (Beushausen & Luco, 2016).

2.6.1.2 Concrete quality

The ability of a structure to resist deterioration is also a function of several properties which are generally termed as quality of concrete (Bertolini *et al.*, 2013). These include:

- Water to cement ratio (w/c)
- Cement type and content
- Mixing, placing, compaction and curing
- Cracking on microscopic and macroscopic scales
- Other aspects such as air content

Concrete quality is hence dependent on the composition of concrete and workmanship applied during construction phase.

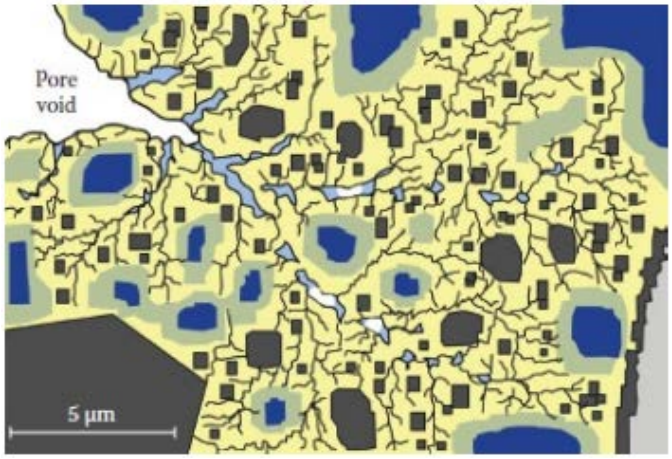

Figure 2-19: Schematic of cement matrix after setting (Liu, 2017)

2.6.1.3 Cover thickness

Failure to achieve the design cover is one of the major reasons for the premature deterioration of reinforced concrete structures. Since the protective potential of concrete is approximately related to the square of the cover, the performance of concrete structures is highly sensitive to the cover thickness and the achievement of sufficient cover generally yields more benefits than controlling any other parameters. Both the prescriptive and performance durability design approaches recommend minimum cover depths according to relevant environmental exposures, but the latter also makes allowance for varying mix composition and construction site practices (Alexander *et al.*, 2013).

An increase in cover thickness generally promotes the effectiveness of this zone by increasing protection against the ingress of deleterious species towards the embedded reinforcement. Hence, the time to corrosion initiation can be potentially extended, depending on the quality of concrete and cause of corrosion. Figure 2-21 highlights the importance of cover thickness in relation to the time to rebar corrosion initiation; reducing the nominal cover by half results in a significant reduction in the service life of reinforced concrete.

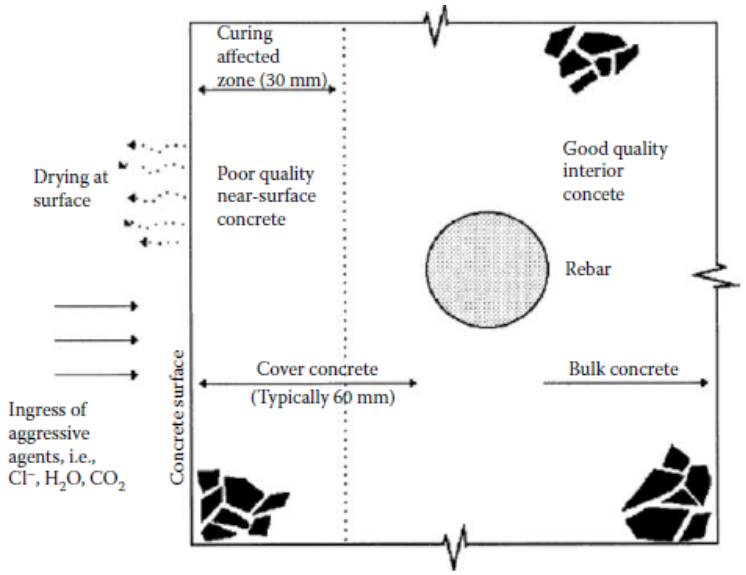

Figure 2-20: Protection of embedded reinforcement by concrete cover (Alexander *et al.*, 2017)

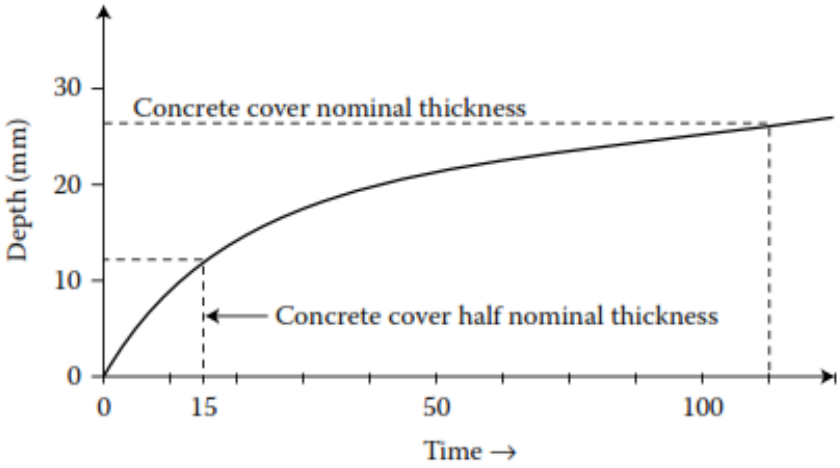

Figure 2-21: Reduction of the time to corrosion initiation due to local reduction in concrete cover (Alexander *et al.*, 2017)

It is theoretically feasible to increase the concrete cover to maintain sufficient durability in case of increasing environment severity. However, in practice cover levels cannot be increased beyond certain limits (70-90 mm) due to mechanical and structural constraints (Bertolini *et al.*, 2013).

2.6.1.4 Cracks

The appearance of cracks can be considered as an inevitable phenomenon in the design life of reinforced concrete structures due to the typical low tensile strength of concrete. The effects of cracks may range from trivial aesthetic discomfort to catastrophic failures of structures. Cracks vary in frequency and size and can form at the time of construction (plastic shrinkage and settlement cracks), during the operational phase (structural and drying shrinkage cracks) or at a later age (corrosion related cracks). Shrinkage related cracks occur either at regular intervals or as surface map cracks, structural cracks occur mostly at locations of high stress concentration while

cracks resulting from reinforcement corrosion typically run parallel to the reinforcement (Figure 2-22) (Bertolini *et al.*, 2013).

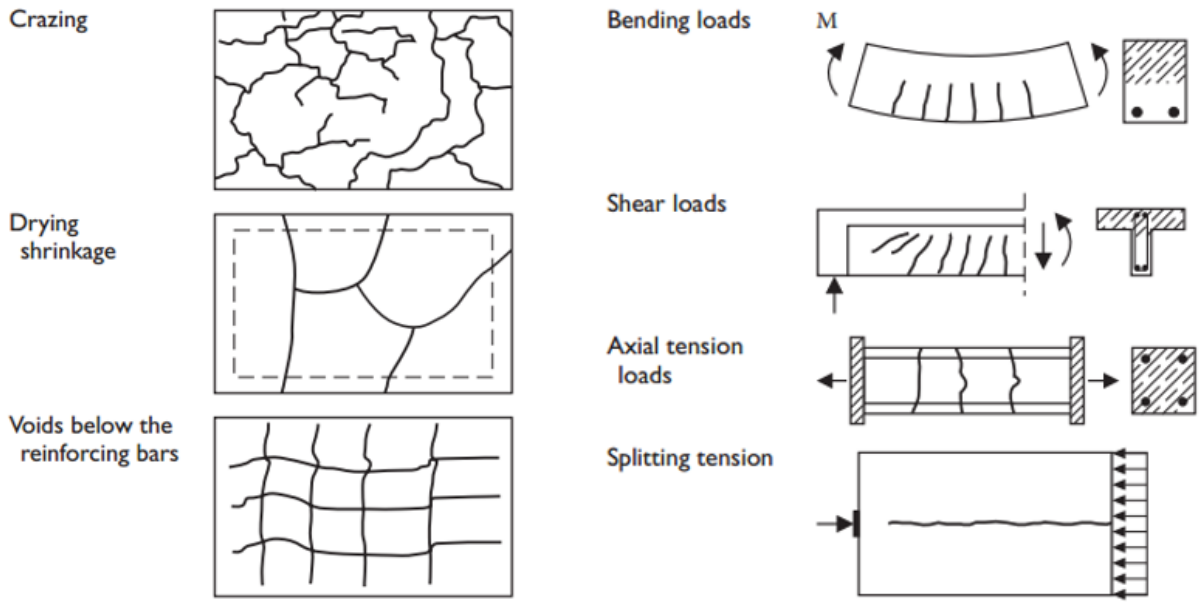

Figure 2-22: Cracks due to concrete properties (left) and external loading (right) (Raupach, 2014)

Dormant and narrow cracks may also be subject to autogenous (self) healing under favourable conditions (Richardson, 2002). This refers to the ability of cementitious materials to heal and close cracks in concrete. The sealing of cracks can hence reduce penetrability and foster the durability of the affected concrete. Self-healing of concrete can be attributed to various physical, chemical and mechanical processes (Figure 2-23) namely (Alexander *et al.*, 2010):

(i) Precipitation of calcium carbonate crystals
(ii) Blocking of flow paths by impurities or concrete particles (debris) from the crack surface.
(iii) Hydration of unreacted cement
(iv) Expansion of hydrated cementitious matrix in the crack flanks

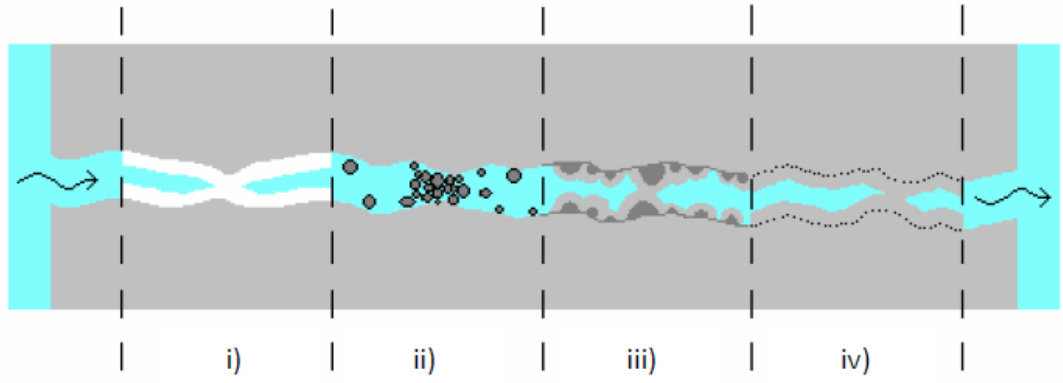

Figure 2-23: Potential mechanisms contributing to self-healing of concrete (Hua, 2010)

This self-healing behaviour is dependent on several factors such as the presence of water pressure, crack width and crack stability. However, the degree of self-healing in a cracked concrete specimen is found to be extremely reliant on the crack width. Smaller cracks are expected to heal faster and more efficiently than larger ones. For instance, in certain situations where there is a small crack width, the cracks may heal entirely. Hence, self-healing can potentially increase the durability and improve safety of damaged infrastructure. Nonetheless, this is a rare phenomenon in most normal concrete materials due to their brittle nature and larger crack widths. A crack width smaller than 50 µm is suggested for the self-healing process to occur efficiently as microcracks require less filling materials to connect the crack edges (Hua, 2010).

Cracks generally have a greater negative impact on the durability of a concrete structure than on its load bearing capacity. For instance, cracks provide localised and favourable ingress paths for deleterious agents such as moisture and chlorides in marine environments which can shorten the initiation time for corrosion (Figure 2-24). The detrimental effects of these cracks are a function of several parameters including width, frequency, orientation, depth and the nature (dormant or active). Allowable crack sizes are usually provided in structural design codes together with equations for calculating maximum crack widths. However, the accuracy of these formulae remains debatable due to the complex interactions between the intrinsic concrete properties (penetrability and thickness of cover) and external environmental conditions (Bertolini *et al.*, 2013).

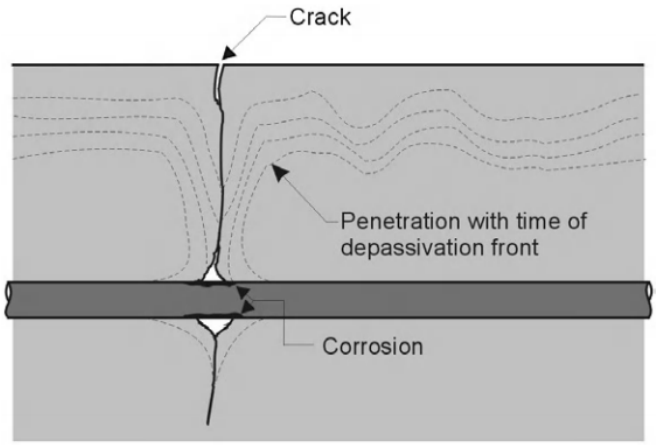

Figure 2-24: Penetration with time of the depassivation front (due to carbonation or chloride ingress) in cracked concrete (Bertolini *et al.*, 2013)

A crack opening of 0.4 mm is usually taken as the limiting crack width, below which the corrosion rate is expected to be similar to that of uncracked concrete (Alexander *et al.*, 2010). Modest crack widths (0.3-0.4 mm) generally result in low corrosion rates after initiation and chemical processes within the cement paste together with the formation of corrosion products can potentially seal the crack near the reinforcement and restore the protective oxide film. However, repassivation may be hindered by the following conditions (Bertolini *et al.*, 2013):

- Poor quality concrete and low cover thickness,
- Active cracks (due to the presence of varying loads),
- Presence of depassivating agents such as carbon dioxide and chlorides,

- When water flows through the crack (reduces local alkalinity and removes corrosion products).

Otieno et al (2010) investigated the influence of crack width (0.7 mm, 0.4 mm and incipient – very fine cracks), water to binder ratio (w/b 0.40 and 0.55), binder type (100% CEM I and 50/50 OPC/Corex slag) and crack reopening on the corrosion rate in cracked concrete. Incipient cracks were produced by loading reinforced beams until the crack was visible with hand-held lens, followed by unloading. The author concluded that corrosion rate was reduced with a lower water to binder ratio, inclusion of slag and smaller crack widths. Crack reopening increased corrosion rates, especially in actively corroding specimens. The author also found out that concrete with incipient cracks have significant corrosion rates compared to uncracked concrete, especially in the case of a high water to binder ratio, CEM I (low resistivity) mix. These results contradict the common assumption of 0.4 mm as a limiting crack width and further supports the idea that each concrete mix has a unique crack width threshold.

2.7 Service life design

The design service life is defined as the period over which a structure remains serviceable and performs satisfactorily its intended purpose without the need for major repairs (Li, 2017). Table 2.2 summarises the typical design life specified in codes for various concrete structures that form part of the social and economic infrastructures.

Table 2.2: Design life specified for various concrete structures (adapted from Li, 2017)

Structure	Classification	Service life (years)
Building	Temporary	1-5
	Industrial buildings	30
	Residential buildings	50
	Monumental buildings	>100
Bridge	Small to medium bridges, viaducts over normal urban roads	30-50
	Highway bridges	75
	Large bridges, large-scale viaduct, urban light rail transit, viaduct over express roads	100
	Highway and railway bridges	120
Port	Open piled jetties, mooring and berthing	15-30
	Reclamation, shore protection, breakwaters, gravity quay walls	50
	National or regional port, flood defence, coastal management infrastructure	100
Tunnel	Road tunnels	150
Nuclear energy	Structures for nuclear power plants	30-40
	Radioactive waste containers	>300

The service life of concrete structures can be quantified using particular models that predict the time to cracking or unacceptable level of damage, for a specific environment. These models are usually developed using laboratory and on site data which are required for calibration. Service life models may include several input parameters such as material properties, mix designs, durability

indicators, environmental conditions and protective measures such as corrosion inhibitors and surface coatings (Beushausen & Luco, 2016). Two different approaches may be considered for service life prediction (Ballim *et al.*, 2009):

- Firstly, concrete (made with a certain mix design) may be placed within a particular environment, and the data collected is then used to estimate the ingress of deleterious agents (carbon dioxide/chloride ions) in similar concrete placed in a comparable environment.
- Secondly, if the ingress depth (mm) of certain aggressive species (chlorides/carbon dioxide) is known for a particular concrete at a specific time (t), the time to corrosion can be determined, whereby the extent of damage on the structure can be addressed through repair (as a protective measure).

Most service life models are developed based on uncracked concrete properties and this leads to an overestimation of the actual serviceability of the structure. Aforementioned, cracks do occur in practice and they affect the transport mechanisms by providing preferential ingress paths for aggressive agents within the concrete cover. Literature specifically indicates a substantial increase in diffusivity and higher corrosion rates due to the presence of cracks. The quantification of the crack influences is generally not a straightforward process but can be achieved through a combination of experiments and numerical simulations on cracked concrete in order to develop correction factors as a function of the crack properties (type, width and frequency). These adjustment factors would then be applied to penetrability test results to obtain more realistic values (Beushausen & Luco, 2016).

2.7.1 *fib* Model Code

The *fib* model code for service life design considers a design method which aims at avoiding or minimising deterioration due to environmental actions. This approach is similar to the current methodology used to design for loading and thus makes use of appropriate models that quantify the loading (environmental actions) and the resistance (concrete resistance against deterioration due to the particular environmental actions). Four different design levels are available (Ballim *et al.*, 2009), as discussed in the following sections.

2.7.1.1 Full probabilistic design approach

The full probabilistic method is typically used for exceptional structures and require probabilistic models that are sufficiently validated to provide representative and realistic results. The parameters used in the models and their associated uncertainties are quantifiable by means of physical tests and statistical models. The design engineer can hence select the required reliability against failure and assess the durability of the structure by considering the environmental influences and material resistance. One of the major drawbacks of full probabilistic design is that it is a time-consuming approach and requires a certain level of expertise, specific knowledge and a large amount of in-situ data (Ballim *et al.*, 2009; Beushausen & Luco, 2016).

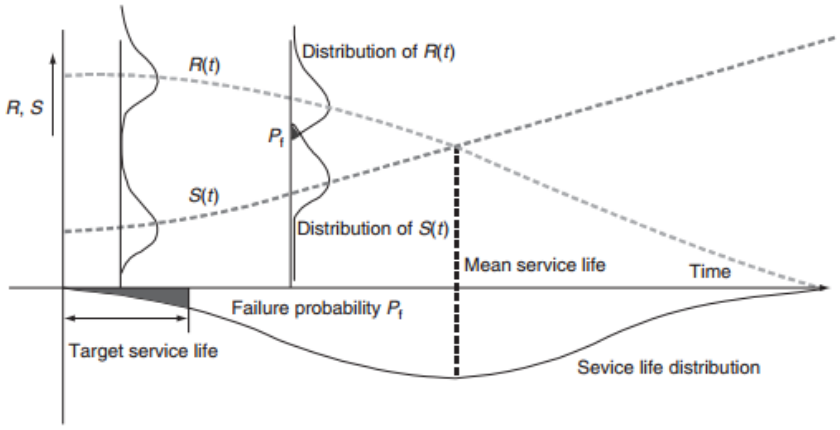

Figure 2-25: Illustration of probabilistic design approaches (Soutsos, 2010)

2.7.1.2 Semi-probabilistic approach (partial safety factor design)

The semi-probabilistic approach represents a simplification of the full probabilistic approach as the probabilistic nature of the problem (variability of load and material resistance) is expressed through partial safety factors. These safety factors are usually calibrated against a large number of experiments and similar models to the full probabilistic method are used (Ballim *et al.*, 2009; Beushausen & Luco, 2016).

2.7.1.3 Deemed to satisfy rules

The deem to satisfy approach is similar to durability specifications provided in most recent standards and codes. The specifications may include material and product selection, dimensions, and construction procedures) that vary according to particular environmental classes. If these limiting conditions are met, then the structure is expected to resist the design environment for the specified period. The *fib* deem to satisfy method, unlike traditional service life design rules, is intended to be calibrated against the full probabilistic approach.

2.7.1.4 Avoidance of deterioration

This approach aims at avoiding the deterioration of reinforced concrete through the use of durable materials (stainless steel/non-reactive aggregates) or the implementation of protection systems such as coatings and impregnations.

2.7.2 Durability Index approach (South Africa)

The South African (performance based) Durability Index approach is based on material indexing. This involves characterising the near surface zone through Durability Index (DI) tests and hence quantifying the resistance of the concrete against the transport of deleterious agents that are responsible for the initiation and propagation of reinforcement corrosion. Three laboratory tests, namely the Oxygen Permeability Index (OPI), Water Sorptivity Index (WSI) and Chloride Conductivity Index (CCI) tests, were developed to provide relatively quick experimental results using either in situ or laboratory concrete. The tests (described in Section 3.4.2) are typically conducted at early age (28 days) and hence can be used for quality control purposes as the Durability Indexes

are sensitive to material processing and construction techniques (placing, compaction and quality of curing) (Alexander *et al.*, 2017; Alexander *et al.*, 2008).

Table 2.3: Suggested criteria to classify durability of concrete using Index values (adapted from Alexander *et al.*, 2017)

Durability class	Oxygen Permeability Index (OPI/Log-scale)	Water Sorptivity Index (WSI/mmhr$^{-0.5}$)	Chloride Conductivity Index (CCI/mScm^{-1})
Excellent	>10	< 6	< 0.75
Good	9.5 – 10	6 – 10	0.75 – 1.50
Poor	9.0 – 9.5	10 – 15	1.50 – 2.50
Very poor	< 9.0	> 15	> 2.50

Research has shown that the early age (28 day) Oxygen Permeability Index (OPI) and Chloride Conductivity Index (CCI) can be related to long term carbonation and chloride diffusion respectively, for a wide range of concretes. Hence, these Durability Indexes provide a sound basis for durability design and service life prediction (Beushausen & Luco, 2016; Alexander *et al.*, 2017).

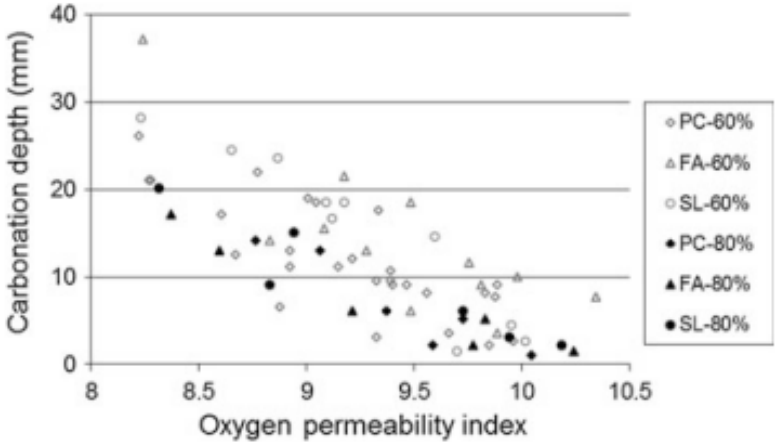

Figure 2-26: Correlation between carbonation depth (mm) and Oxygen Permeability Index (log-scale) (Mackechnie & Alexander, 2002; Salvoldi *et al.*, 2015)

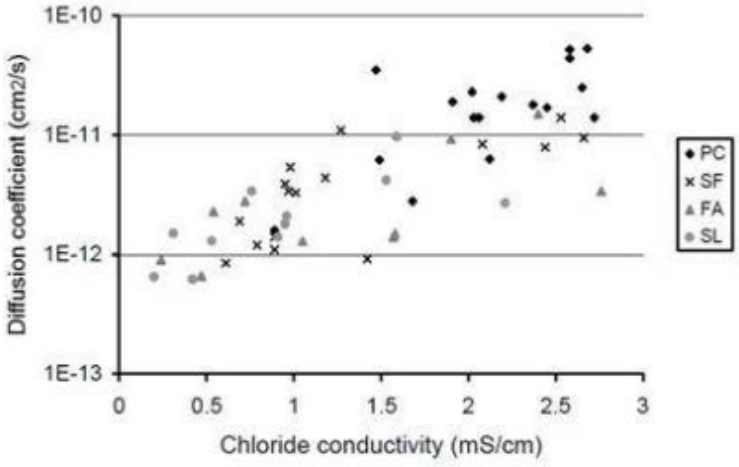

Figure 2-27: Correlation between chloride diffusion coefficient (cm^2/s) and Chloride Conductivity Index (mS/cm) (Mackechnie, 2001)

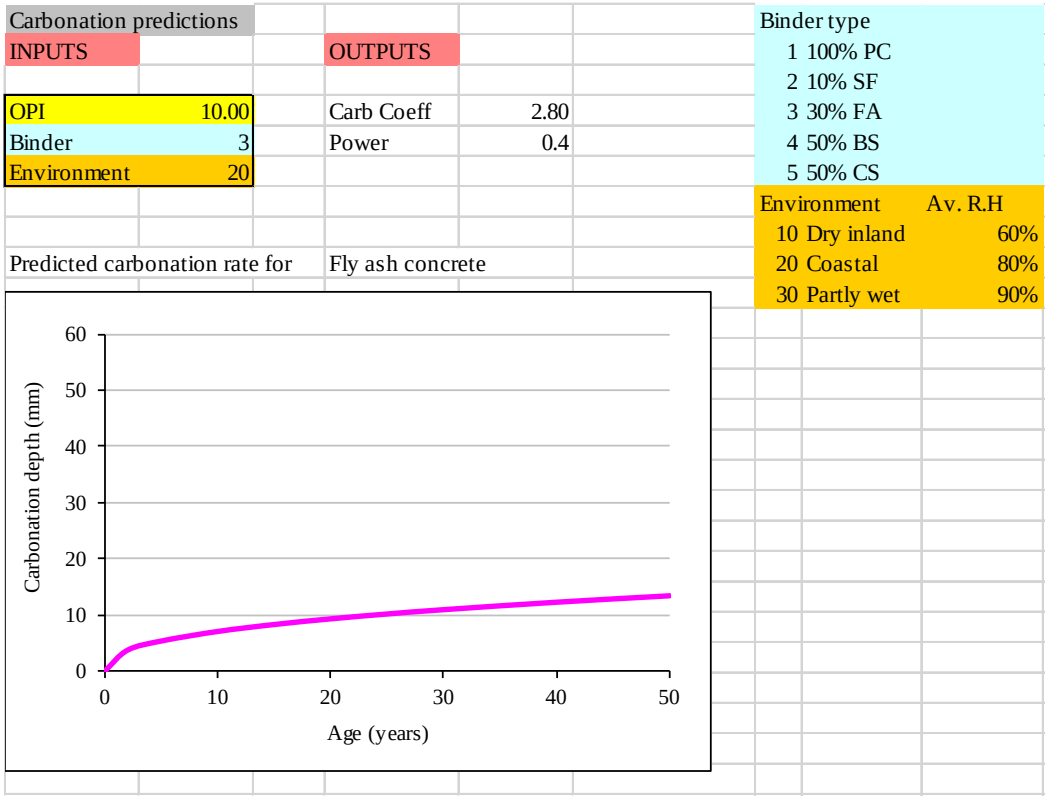

Figure 2-28: Example of carbonation depth prediction using Oxygen Permeability Index (OPI) value, binder type and environmental exposure conditions

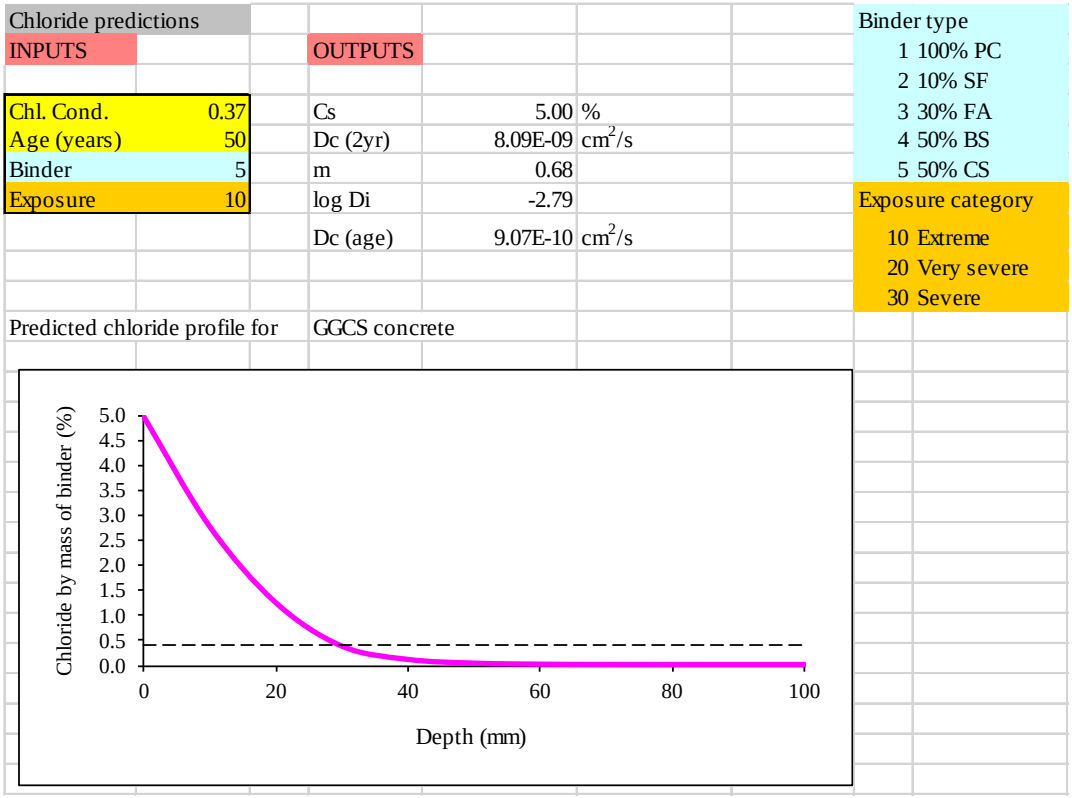

Figure 2-29: Example of chloride ingress prediction based on Chloride Conductivity Index (CCI) value, age at testing, binder type and exposure conditions

The South African service life prediction models link OPI values to mean carbonation depth development for typical South African environmental conditions such as dry inland (60% RH), coastal (80% RH) and partly wet (90% RH). Similarly, CCI values are used in this model to predict chloride ingress for extreme (structures exposed directly to sea-water with heavy wave action/abrasion), very severe (structure exposed directly to sea water under sheltered conditions with little wave action) and severe (structure in a sheltered location within 1 km of the shore) conditions. The model inputs hence consist of a Durability Index values (OPI/CCI), the binder type, age of concrete (for CCI test) and environmental class. (Beushausen & Luco, 2016) Figure 2-28 and Figure 2-29 show the MS EXCEL-based tools for carbonation and chloride ingress prediction respectively.

Two approaches can be used to specify Durability Index values; the deem-to-satisfy approach and rigorous approach. The deemed to satisfy approach imitates structural design codes and recommends OPI and CCI values for a particular cover level, environmental condition and design life. If these limiting OPI or CCI values are met before and after construction, then the structure is estimated to meet durability requirements for the specified cover, exposure class and design life. On other hand, the rigorous approach involves the use of relevant service life prediction models and is typically used for durability critical structures. The latter approach provides greater flexibility as it allows the tailoring of Durability Index values for a particular situation, rather than the use of pre-determined conditions (Alexander *et al.*, 2017; Alexander & Beushausen, 2008).

SANRAL (South African National Road Agency Limited) makes use of a blend (hybrid) of performance and prescriptive approaches to concrete durability and thus specifies limiting Oxygen Permeability Index (OPI/log-scale), Water Sorptivity Index (WSI/mmhr$^{-0.5}$) and Chloride Conductivity Index (CCI/mScm^{-1}) values for specific cover depths, binder blends and exposure classes. The environmental classes defined by SANRAL are similar to the ones in BS EN 206 (2013) and Eurocode 2 (2002) durability design standards while the binder blends are based on common ones used in South Africa. The microenvironments described by SANRAL with respect to carbonation and chloride induced corrosion are provided in Appendix J.

With this hybrid approach, the concrete mix is optimised by the material (concrete) supplier to meet the durability requirements prior to construction and in some instances some economy can be achieved relative to the prescriptive mix. The contractor subsequently has the obligation to apply the necessary on site workmanship (placing, compaction, curing and finishing) to make sure that the limiting Durability Index values are met. The quality of the in-situ concrete is also verified in this process. This two level approach allows the responsibility of producing durable concrete to be shared amongst the mix producer and contractor (Alexander, 2016; Alexander *et al.*, 2017).

Table 2.4 and Table 2.5 provide limiting Durability Index values (OPI and CCI) used by SANRAL for a service life of 100 years. These tables indicate that there is a trade-off between material quality (oxygen permeability/chloride conductivity) and concrete cover. The use of higher quality concrete (represented by greater OPI and lower CCI values) allows a reduction in cover depth (mm) and vice versa.

Table 2.4: Limiting Durability Index values with respect to carbonation induced corrosion (adapted from SANRAL Table 6000/1, 2009)

		In situ Durability Index values for various cover depths and exposure classes (100 year service life)				
Microenviron-ment designation	Recommended minimum cover (mm)	Cover depth (mm)	OPI (log scale)		Sorptivity (mm/hr$^{0.5}$)	
			Recommended value	Minimum value	Recommended value	Maximum value
XC1a	40	40	N/A	N/A	10.0	12.0
XC1b	40	40	9.20	9.00	10.0	12.0
		50	9.00	9.00	10.0	12.0
		60	n/a	n/a	n/a	n/a
XC2	40	40	9.40	9.00	10.0	12.0
		50	9.10	9.00	10.0	12.0
		60*	9.00	9.00	10.0	12.0
		70*	n/a	n/a	n/a	n/a
XC3	40	40	9.40	9.00	10.0	11.0
		50	9.10	9.00	10.0	11.0
		60*	9.00	9.00	10.0	11.0
		70*	n/a	n/a	n/a	n/a
XC4	45	40	9.60	9.20	10.0	10.0
		50	9.30	9.00	10.0	10.0
		60*	9.10	9.00	10.0	10.0
		70*	9.00	9.00	10.0	10.0

*These cover depths should be avoided to limit crack widths

Table 2.5: Limiting Durability Index values with respect to chloride induced corrosion (adapted from SANRAL Table 6000/1, 2009)

		In situ Durability Index values for various cover depths and exposure classes (100 year service life)				
Microenvironment designation	Recommended minimum cover (mm)	Cover depth (mm)	Chloride Conductivity (mS/cm)		Sorptivity (mm/hr$^{0.5}$)	
			70:30 CEM I:FA	50:50 CEM I:GGCS	Recom-mended value	Maximum value
XS1	50	40	1.50	2.10	10.0	12.0
		50	2.10	2.80	10.0	12.0
		60	2.60	3.40	10.0	12.0
XS2a	50	40	1.00	1.40	10.0	11.0
		60	1.40	2.00	10.0	11.0
		60	1.80	2.50	10.0	11.0
XS2b	60 (Mandatory)	60	1.45	2.00	10.0	11.0
XS3a	50	40	0.65	1.00	10.0	10.0
		50	1.10	1.45	10.0	10.0
		60	1.45	2.00	10.0	10.0
XS3b	60 (Mandatory)	60	1.10	1.55	10.0	10.0

In the event that the specified cover and Durability Index values are not met, a reduction in payment is applicable. Table 2.6 shows the criteria used by SANRAL to adjust payment with reference to a major freeway infrastructure project. The limiting OPI value and cover depth according to the specifications were 9.70 and 40 mm respectively (Nganga *et al.*, 2013).

Table 2.6: Reduced payment criteria based on limiting DI values (Adapted from Alexander *et al.*, 2017)

	Oxygen Permeability Index		Concrete cover (40 mm)	
	OPI (log scale)	**Percentage payment**	**Overall cover (mm)**	**Percentage payment**
Full acceptance	> 9.70	100%	$\geq$ 85% < (100$\pm$15)%	100%
Conditional acceptance*	> 8.75 $\leq$ 9.70	80%	< 85% $\geq$ 75%	85%
Conditional acceptance**	-	-	< 75%	70%
Rejection	< 8.75	Not applicable	< 65%	Not applicable

*with reduced payment
**with remedial measures approved by Engineer; and reduced payment

2.8 Hydrophobic impregnation

Hydrophobic impregnations are products that are usually applied on the surface of a concrete substrate (as an invisible film) to reduce the uptake of water and dissolved aggressive species. The hydrophobic agent is typically dissolved in a solvent (water or alcohol) and applied by spraying or brushing, depending on its viscosity. The applied material dries with the evaporation of the solvent and is transported into the pore structure through capillary action. Creamy hydrophobic treatments have longer drying time relative to liquid systems and this usually results in superior penetration efficiency, and thus higher protective potential. The main advantage of hydrophobic treatment is that the latter provides a water-repellent surface without affecting the appearance of the concrete and does not hinder the movement of water vapour in and out of the concrete (Raupach, 2014; Meier & Wittman, 2011).

Figure 2-30: Silane based cream (left) and liquid (right) (Sika, 2016)

2.8.1 Fundamentals and mechanism of hydrophobic impregnation

Aforementioned, liquid water is rapidly transported in non-saturated pores by capillary action, and the rate of absorption is a function of the surface tension, the density and viscosity of the liquid, contact angle between the liquid and pore walls, and the pore size opening. In normal (untreated) concrete, the contact angle (θ) is low (< 90°) because of molecular attraction between the cement paste and water (hydrophilic behaviour). The drop of water will typically spread flat on the surface followed by capillary rise in the pore structure, resulting in the suction of water.

As the silane molecules cover the capillary walls, they become devoid of ionic electrical charges (Figure 2-31) and polar molecules such as water are no longer attracted to the concrete surface. The overall interaction between water and concrete is reduced and water molecules are excluded, creating a contact angle greater than 90° and water droplets (held together by internal hydrogen bonds) are formed on the treated surface (Figure 2-32) (Tepfers, 2009).

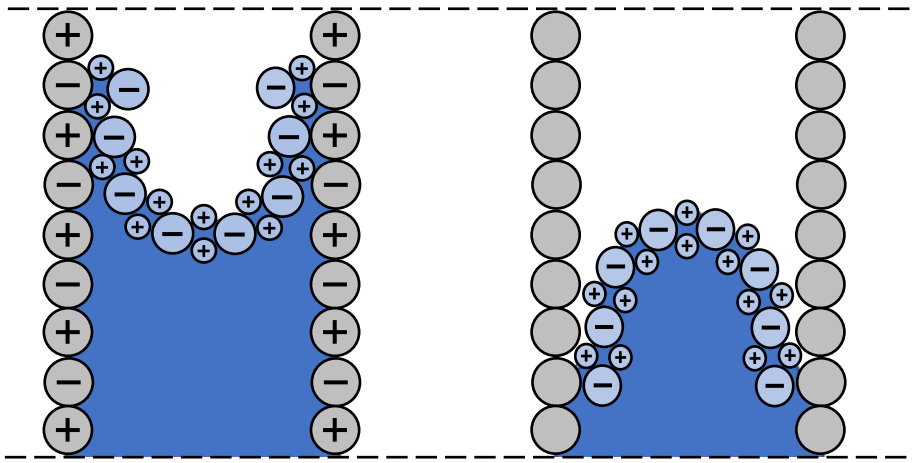

(a) (b)

Figure 2-31: Intrusion of water in a hydrophilic capillary (a) and hydrophobic capillary (b) (adapted from Tepfers, 2009)

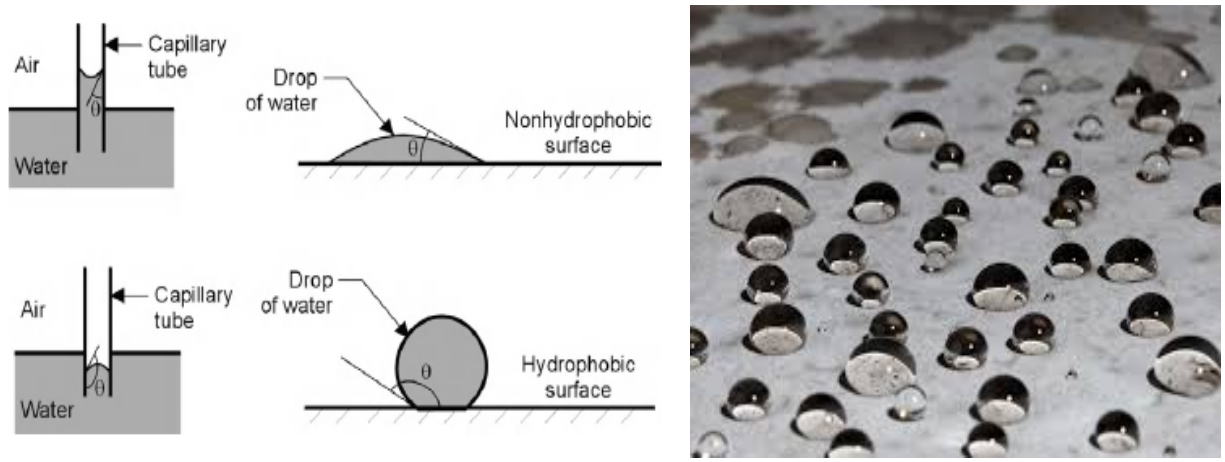

Figure 2-32: Interaction between water and concrete surface for untreated and treated surfaces (Bertolini *et al.*, 2013; Sika, 2015)

Silane, siloxane (Figure 2-33) or a mixture of these two components are typically used as hydrophobic impregnation products. Silane molecules are relatively smaller (1×10^{-6} – 1.5×10^{-6} mm diameter) relative to siloxane molecules (1.5×10^{-6} – 7.5×10^{-6} mm diameter) and hence, in general greater penetration depth is obtained with the use of pure silane products. However, a smaller molecular size correlates to higher volatility (Pan *et al.*, 2017). Pure silane is hence mostly used in gel consistency as this enables the application of thick layers of water repellent product on vertical surfaces without slumping or sagging (Liu, 2017; Sika 2016).

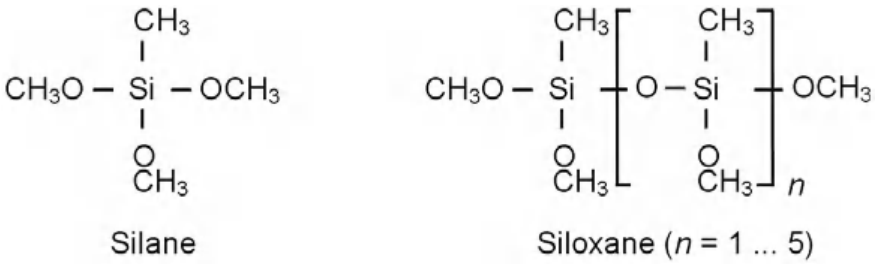

Figure 2-33: Silane and siloxane molecular structures (Bertolini *et al.*, 2013)

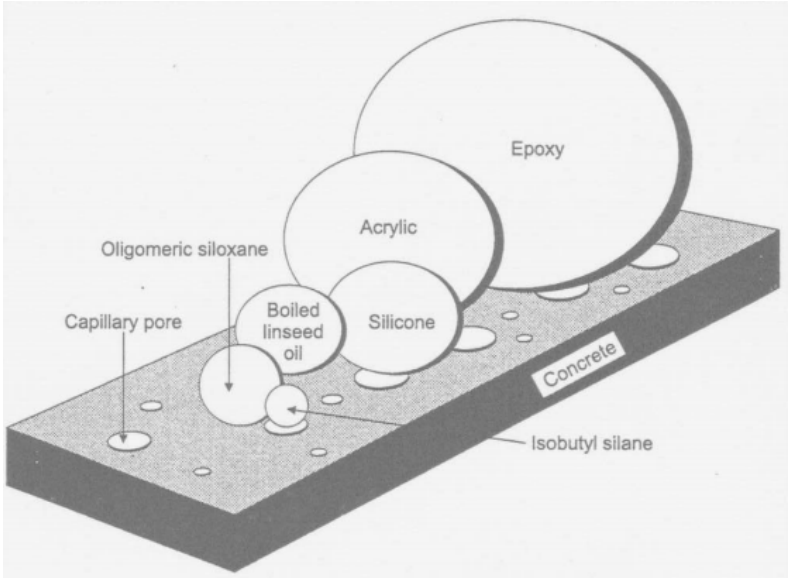

Figure 2-34: Molecular size of various hydrophobic agents, including silane and siloxane relative to capillary pore diameter (Moriconi *et al.*, 2002)

Silane or siloxane molecules possess a specific organic alkyl group and several alkoxy groups. The molecular structure of the alkyl group influences the water repelling properties of silane and siloxane. An alkyl group with higher molecular weight (iso-butyl and n-octyl) provides greater hydrophobicity relative to a lower molecular weight alkyl group (methyl and ethyl) (Pan *et al.*, 2017).

In contrast, the alkoxy groups (such as ethoxy and methoxy) govern the penetration depth of silane and siloxanes (Pan *et al.*, 2017). Alkoxy groups can react with moisture present in the pore structure to form silicone resin which bonds the hydrophobic layer to the concrete substrate (Figure 2-35). The first step involves the hydrolysis of silane molecules (alkoxy groups) to form unstable silanol molecules. These silanol molecules undergo further condensation reaction to form silicone resin that effectively joins the hydrophobic film to the cementitious substrate through hydrogen bonds. This reaction is catalysed by the alkalinity of the concrete. These alkoxy groups can also react with other silane molecules through a polymerisation process. These chemical reactions are generally dependent on the temperature, moisture content and pH value of the pore solution. Following the bonding reaction of the alkoxy groups with the concrete substrate, the alkyl group extends outwards relative to the pore surfaces (Figure 2-36) (Pan *et al.*, 2017; Bertolini *et al.*, 2013, Meier & Wittman, 2011).

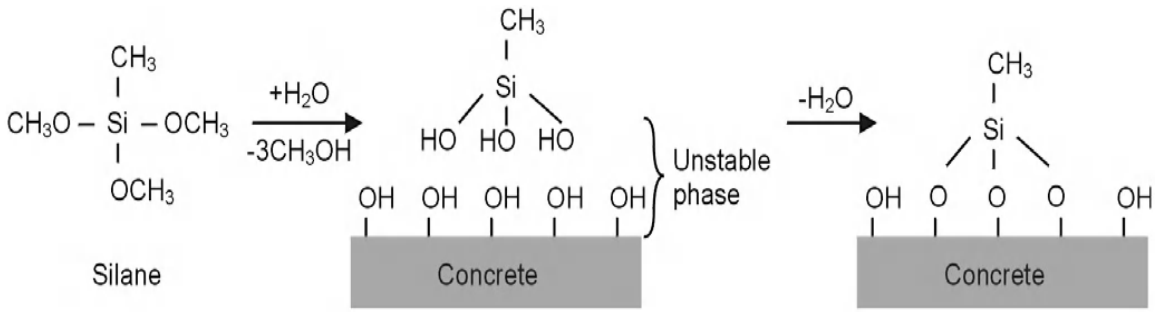

Figure 2-35: Reaction between (methyl-methoxy) silane and concrete substrate (Bertolini *et al.*, 2013)

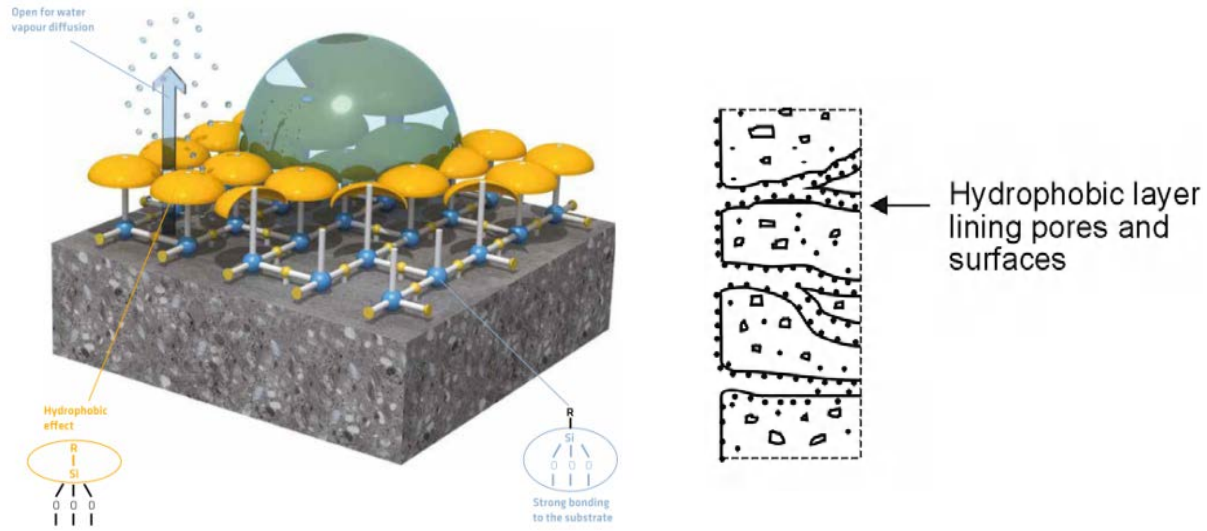

Figure 2-36: Illustration of hydrophobic action (Sika, 2015; Bertolini *et al.*, 2013)

2.8.2 Factors affecting the performance of hydrophobic impregnation

The performance of water repellent treatment is often assessed or characterised by the extent to which the treated concrete can reduce the capillary absorption of water and dissolved salts. The performance itself depends on three factors namely (Meier & Wittman, 2011):

- Type of water repellent agent,
- Penetration depth,
- Quantity of water repellent agent in the near surface zone.

The type of water repellent (silane/siloxane gel, cream or liquid) must be carefully selected according to the application location in order to obtain effective results. The penetration depth is a function of several parameters:

- Age, quality of concrete (w/b ratio, cement type, curing etc) and contact time

Water repellent agents are typically applied at least one month after construction. As the water repellent product enters the concrete pore structure mainly through capillary suction, the porosity of the cement paste plays a major role in determining the penetration depth. As the w/b ratio is

increased, the concrete becomes less dense and pore spaces and the average pore sizes increase, resulting in a greater penetration potential of the water repellent agent. Higher penetration depth can also be obtained by increasing the contact time between the silane product and the concrete surface. In this case, gels or creams are useful as they provide the surface with adequate silane for relatively longer time periods (Meier & Wittman, 2011, Selander, 2010).

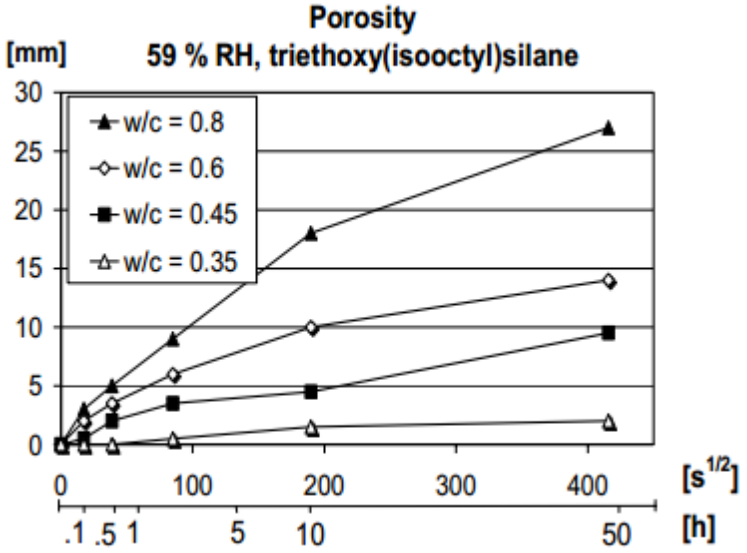

Figure 2-37: Influence of water to cement ratio and contact time on silane penetration depth (Selander, 2010)

- Moisture content in the near surface zone

The penetration depth of the water repellent product also depends on the humidity levels inside the concrete, particularly near the surface. A higher moisture content reduces capillary suction as a large proportion of the pores are filled with water. Hence the extent to which silanes enter the concrete is reduced, resulting in a decrease in penetration depth. From Figure 2-38, it is clear that fully saturated concrete (100% RH) cannot be treated with silane impregnation, as the penetration depth is negligible under these conditions (Meier & Wittman, 2011; Selander, 2010).

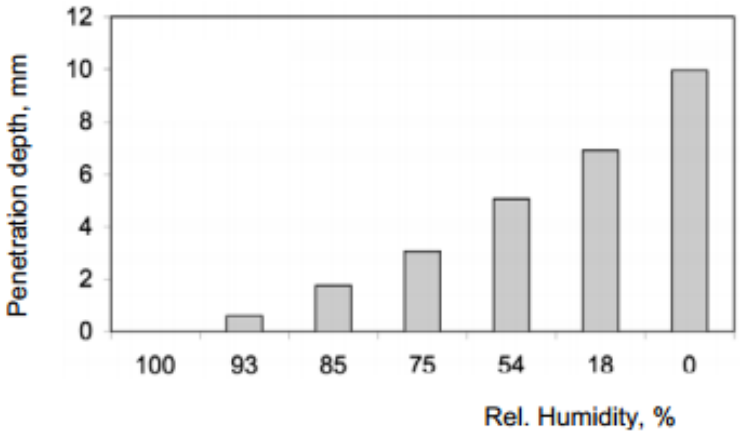

Figure 2-38: Effect of relative humidity on the silane penetration depth (Meier & Wittman, 2011)

- Type of application (liquid, paste cream or gel) and amount of product used

The application method has a significant influence on the penetration depth of the water repellent agent. For instance, deep impregnation (increased contact time) using silane gel results in a superior penetration depth relative to surface impregnation with liquid silane. A higher application amount (g/m^2) also generally increases the penetration depth (Meier & Wittman, 2011).

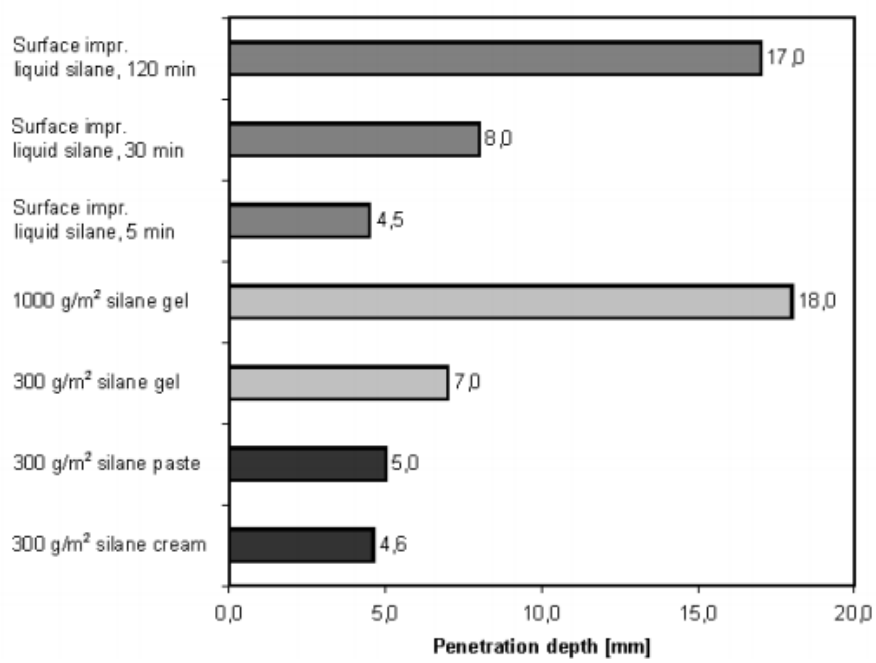

Figure 2-39: Penetration depth as a function of the application method, amount of product used and contact time (Meier & Wittman, 2011)

2.8.3 Classes of water repellent treatment

Water repellent treatment can be classified into three categories, according to the performance required (Table 2.7). As the effectiveness of the treatment increases from C1 to C3, the required minimum penetration depth increases accordingly.

Table 2.7: Classes of water repellent treatment (adapted from Meier & Wittman, 2011)

Classes	Require-ments	Performance	Objectives of application	Required minimum penetration depth (mm)
C1	Surface treat-ment	Keep the surface uni-formly dry; Reduction of capillary absorption of an inter-face before placing a coating	Reduction of biocolonisation; Pre-treatment of substrates; Appearance of concrete facades; Anti-graffiti systems.	2
C2	Water repel-lent treatment	Reduction in capillary water absorption	Increase frost resistance; Reduction of chloride penetra-tion; Reduction of electrical conduc-tivity of near surface zone.	4

C3	Deep water repellent treatment	Long-term reduction of absorption of water and salt solutions	Reduction in chloride penetration in marine environment; Protection from aggressive water and sulphate containing water; Improvement of frost resistance.	6

2.8.4 Durability of hydrophobic impregnation

The effectiveness of hydrophobic impregnation can decrease in the long term, especially in the case of insufficient penetration depth and aggressive environmental conditions. Literature suggests that protection against water ingress is still possible after 10-15 years (Tepfers, 2008, Selander, 2010; Christodoulou *et al.,* 2013; Liu, 2017). The performance of hydrophobic impregnation is mainly affected by ultraviolet (UV) radiation, thermal shocks and abrasion which can lead to the breakdown of the molecular structure of silanes with time. Carbonation of concrete can also reduce the thickness of the hydrophobic layer (Antons *et al.*, 2015). Hence, it is important to achieve sufficient penetration depth (Table 2.7). The hydrophobic material should also withstand the alkalinity of the concrete pore solution (Polder *et al.*, 2001; Büttner & Raupach, 2008).

Once a structure has been treated, it is recommended to implement a maintenance program to make sure that the protective measure remains effective throughout the intended service life. This would involve regular on-site visual inspections (every 5 years) to assess the residual silane penetration depth and resistance to capillary absorption. In the case of reduced effectiveness, the water repellent product should be reapplied (Meier & Wittmann, 2011; Freitag & Bruce, 2010; Lucquiaud *et al.,* 2014).

2.9 Influence of hydrophobic impregnation

2.9.1 Moisture content

Since hydrophobic impregnation only lines the internal pore structure, the exchange of water vapour between the concrete and external environment is not compromised. This allows the concrete to “breathe” and generally lowers the overall internal humidity levels with time, especially under wetting and drying conditions (Bertolini *et al.*, 2013). Lower moisture content is expected in treated concrete that is exposed to rain relative to non-hydrophobised concrete, as the former does not absorb water during rain but loses water in dry periods due to evaporation (Polder *et al.*, 2000).

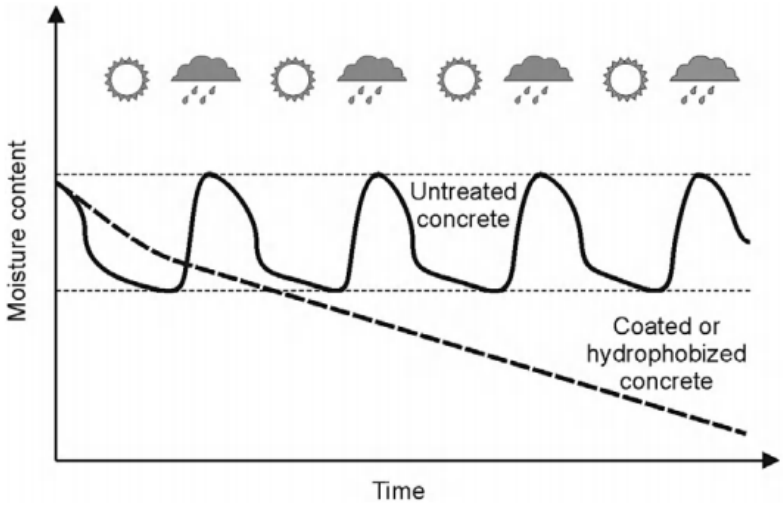

Figure 2-40: Reduction in moisture content of treated (hydrophobised) concrete substrate (Bertolini *et al.*, 2013)

2.9.2 Carbonation

The effect of hydrophobic impregnation on the carbonation rate generally depends on the humidity levels inside the concrete and external environmental or testing conditions (Selander, 2010). For instance, higher carbonation rate in treated concrete can be explained by the fact that the hydrophobic agent prevents the ingress of water and therefore makes the concrete drier with time. This allows a higher diffusion rate of carbon dioxide, resulting in greater carbonation depth with time (Schueremans *et al.*, 2008; Freitag & Bruce, 2010). On the other hand, a reduction in carbonation depth due to water repellent treatment can be attributed to the lowered moisture content within the impregnated layer. As less water is available for the neutralisation reaction between carbon dioxide gas and calcium hydroxide, the carbonation rate is reduced (Selander, 2010; Zhang *et al.*, 2017).

Table 2.8 summarises the conclusions drawn by several researchers who investigated the influence of silane (hydrophobic) impregnation on the carbonation depth.

Table 2.8: Summary of the influence of hydrophobic impregnation on carbonation

Authors	Concrete type	Pre-conditioning	Exposure conditions	Conclusions
Polder *et al.*, 2000	CEM I and CEM III/B (w/b 0.50)	- Air cured for 28 days at 20°C and 65% RH - Silane treatment at 28 days and stored at 20°C and 65% RH for further 4 weeks	Outdoor (inland) environment for 5 years	No significant influence of silane treatment on carbonation depth. The cement type had a greater effect on the carbonation depth.
Schueremans *et al.*, 2008	Quay wall constructed in 1993 (Zeebrugge harbour)	- First silane treatment after demoulding. - Second application of silane after 7 days.	Outdoor (coastal) environment for 12 years	Higher carbonation depth in silane treated concrete

Zhang *et al*., 2017	Ordinary Portland cement (w/b 0.50)	- Demoulded after 1 day - Cured until age of 14 days at 20°C and 95% RH. Then stored at 20°C and 60% RH for 7 more days. - Silane treatment at 21 days and stored for 7 further days at 60% RH	Accelerated carbonation for 7, 28 and 72 days CO_2: 20 ± 2% RH: 70% Temp: 20 ± 3°C	Treated concrete recorded smaller carbonation depth relative to the untreated concrete

2.9.3 Chloride ingress and service life prediction

One of the major applications of hydrophobic treatment is in the service life extension of reinforced concrete structures that are exposed to aggressive (marine) environments. Numerous studies have shown that the use of silane impregnation modifies the surface of concrete and reduces the capillary absorption of water and dissolved deleterious agents such as chlorides. Hence, in a marine environment, the rate of ingress of chloride ions is reduced compared to untreated concrete. This provides a low cost and effective way to promote the serviceability of the concrete structure by reducing the risk (prolonging the initiation) of chloride-induced corrosion (Figure 2-41) (Dai *et al.*, 2010; Meier & Wittman, 2011; Moriconi *et al.*, 2002). Water repellent treatment is applied as standard on all new concrete bridge decks in countries such as the Netherlands and United Kingdom (Polder *et al.*, 2000; Dyer, 2014).

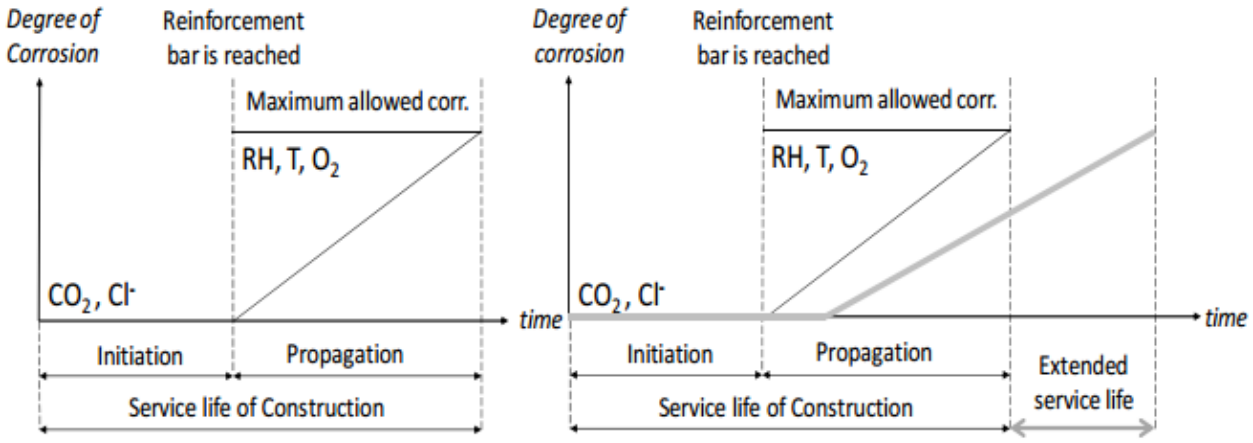

Figure 2-41: Service life extension as a result of water repellent treatment (Selander, 2010)

The influence of silane impregnation on chloride ingress is well documented in literature and several experiments have been carried out over the last decades. However, there is limited work on the service life prediction of silane treated concrete. The following gives a summary of the work from selected authors.

Zhang et al., 2017

Zhang et al (2017) studied the influence of silane impregnation on the durability properties of cement based materials. One mix design (ordinary Portland cement, w/b 0.50) was used. Cube specimens (100 x 100 x 100 mm) were cast, demoulded after one day and placed in a curing room (20 ± 2°C temperature and 95% RH) until the age of 28 days. The specimens were then stored at 60% RH for 7 additional days, followed by the application of three different types of water repellent agent (Table 2.9).

Table 2.9: Water repellent agents used (adapted from Zhang *et al.*, 2017)

	Type	Amount used (g/m^2)	Note
Reference	-	-	Untreated
L1	Liquid silane	470	Surface absorption
C400	Silane cream	400	Surface brushing
G400	Silane gel	400	Surface brushing

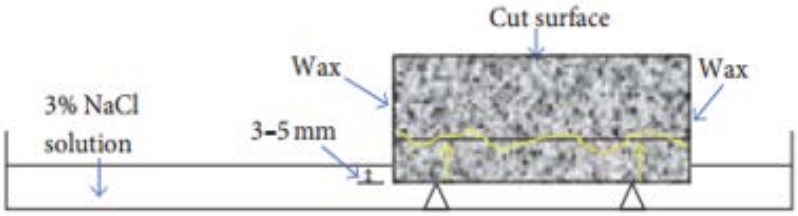

Figure 2-42: Illustration of chloride penetration test setup (Zhang *et al.*, 2017)

After silane treatment, the cubes were left at 60% RH for a further 7 days to allow sufficient polymerisation reactions. The sides of the treated and control (untreated) specimens were coated with wax and then put into contact with a 3% sodium chloride (NaCl) solution for 28 days (Figure 2-42). Chloride profiling was then performed using the ion selective electrode method.

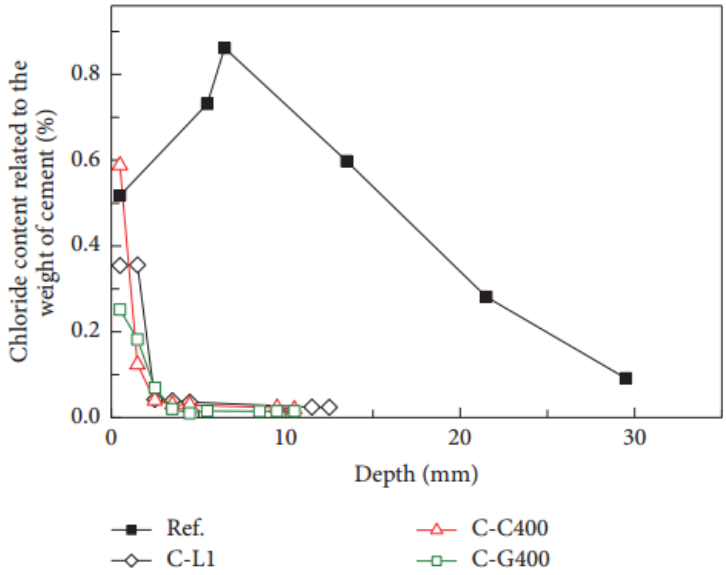

Figure 2-43: Chloride profiles for untreated and treated concrete after 28 days in contact with 3% NaCl (Zhang *et al.*, 2017)

According to Figure 2-43, there was deeper chloride penetration in the untreated concrete relative to the silane treated concrete. The author explained that since water repellent treatment reduces capillary action, the uptake of chloride solution is reduced and subsequent diffusion is also slowed down. The small amount of chlorides detected in the first 3 mm of the treated concrete was attributed to open big pores close to the surface and overall surface roughness (Zhang *et al.*, 2017).

Tanaka et al., 2015

Tanaka et al (2015) investigated chloride ingress in silane impregnated concrete and subsequently attempted to predict the chloride ion penetration with time. In this study, only one type of concrete (ordinary Portland cement, w/b 0.50) was used. Concrete cubes (100x100x100 mm) were cast, seal cured for 7 days and conditioned at 20°C and 60% RH until the age of 28 days. Four types of water repellent products (Table 2.10) were then applied with a brush and the specimens were left in an environmental room at 20°C and 65% RH until the age of 56 days. The treated and control samples were then immersed in 10% by mass sodium chloride (NaCl) solution for 71 days.

Table 2.10: Silane water repellent products (Tanaka *et al.*, 2015)

Type	Bases	Active ingredient concentration (% by mass)	Volume of application (g/m^2)
Type A	Alkyl alkoxysilanes and reactive siloxane	80	200
Type B	Alkyl alkoxysilanes and siloxane	>90	200
Type C	Alkyl alkoxysilanes	>98	220
Type D	Poly-alkyl alkoxysiloxane	10	200

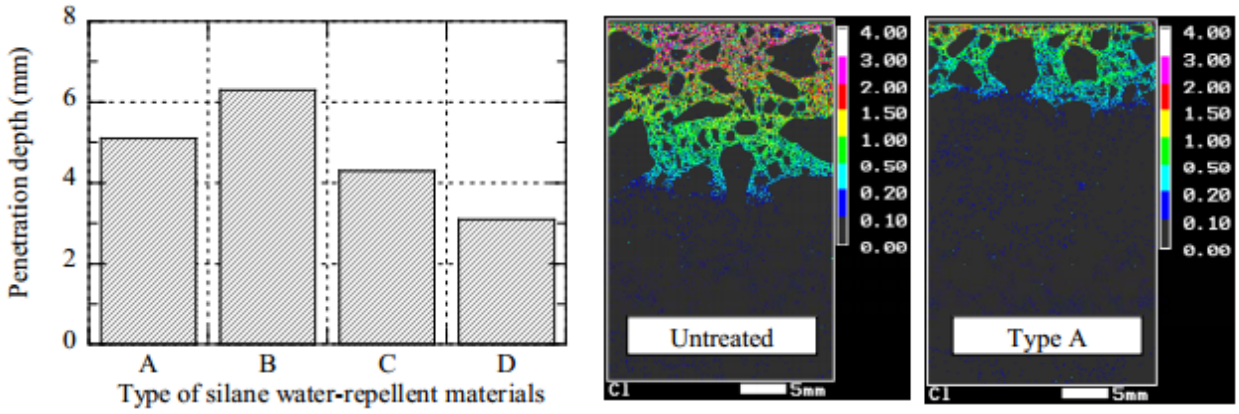

(a) (b)

Figure 2-44: Silane impregnation depth (a) and chloride ion penetration profile (b) (Tanaka *et al.*, 2015)

The penetration depths of the water repellent products were measured 56 days after treatment and the results are shown in Figure 2-44 (a). Higher penetration depth of the silane impregnation was obtained with increasing active ingredient content. Chloride ion profiles were obtained by performing electron probe microanalysis (EPMA). Relative to the untreated samples, chloride ingress was significantly reduced in treated concrete. Chloride ion penetration depth was approximately 20 mm in the control concrete and 10 mm in concrete treated with type C. The surface chloride

concentration was also reduced in the treated concrete and better performance was achieved with increasing concentration of active ingredient (Figure 2-45).

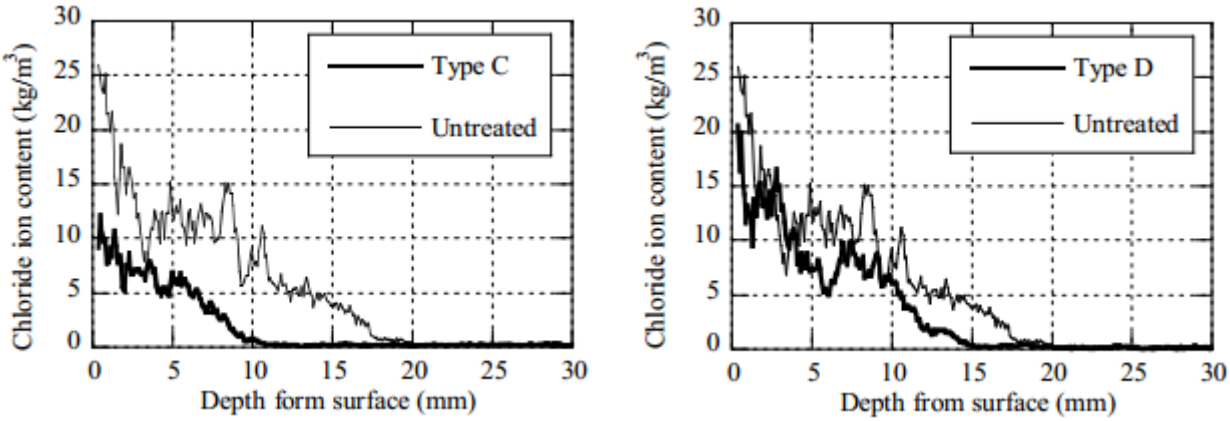

Figure 2-45: Chloride penetration profile for type C and type D water repellent products (Tanaka *et al.*, 2015)

The chloride penetration model used to calculate the surface chloride content (C_0) and apparent diffusion coefficient (D_a) was based on a modified solution to Fick's second law of diffusion. The silane treated concrete was considered as a two-layer material with two separate diffusion coefficient; D_s (within the impregnated layer) and D_c (the unaffected concrete) as shown in Figure 2-46.

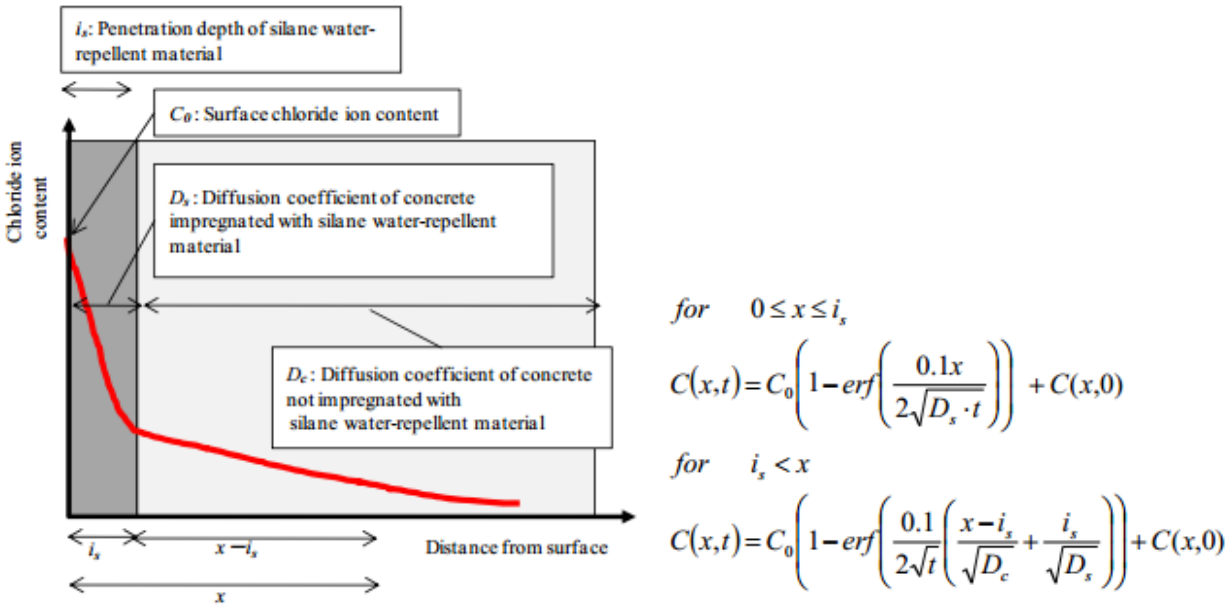

Figure 2-46: Chloride ion penetration model of silane treated concrete (Tanaka *et al.*, 2015)

Hence two equations (Figure 2-46) were developed with boundary conditions ($0 \le x \le i_s$) and ($x > i_s$), where;

i_s – silane penetration depth (cm),

x – distance from the surface (cm)

C(x,t) – chloride ion content at depth x from the surface (kg/m^3)

C(x,0) – initial chloride content (kg/m^3)

C_0 – surface chloride ion content (kg/m^3)

t – time (years)

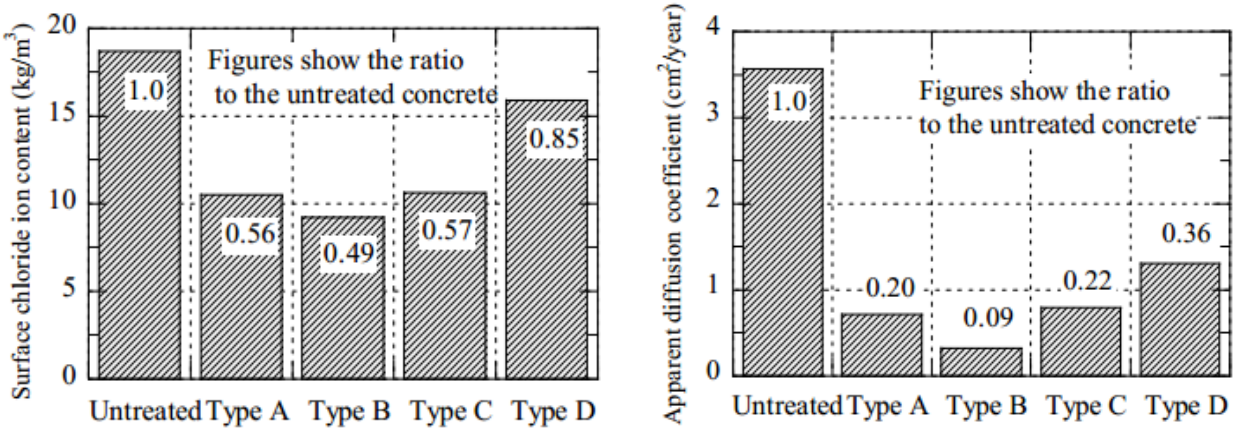

Figure 2-47: Surface chloride concentration (a) – (kg/m^3) and apparent chloride diffusion coefficient (b) – (cm^2/year) results (Tanaka *et al.*, 2015)

The data points within the impregnated layer were fitted to the equation valid for ($0 \leq x \leq i_s$) to obtain the regression parameters (surface chloride ion content and apparent chloride diffusion coefficient). From Figure 2-47, it is clear that the surface chloride concentration and apparent diffusion coefficient is reduced by 40-50% and 80-90% respectively for the concrete treated with high concentration silanes (type A, B and C).

In order to predict chloride penetration with time, the surface chloride ion concentration for the untreated concrete was set to 4.5 kg/m^3, which is the surface chloride ion content 0.1 km from the coastline (as specified by the Japanese standards). Using the results from the curve fitting in Figure 2-47 (a), the surface chloride ion content for the silane treated concrete was calculated as a multiple of 4.5 kg/m^3. The apparent chloride diffusion coefficient for untreated and treated concrete were set as in Figure 2-47 (b), the initial chloride content was considered to be negligible (0 kg/m^3) and the cover depth was set to 50 mm (Tanaka *et al.*, 2015).

From Figure 2-48, by setting the critical chloride ion content to (1.2 kg/m^3 ≈ 0.38% of binder content), the service lives of untreated and treated (type B) concrete was about 3 years and 20 years respectively (Tanaka *et al.*, 2015). It must be noted here that the time dependent reduction of the apparent chloride diffusion coefficient (Ballim *et al.*, 2009; Costa & Appleton, 1999) was not considered in the calculations and therefore the service life extension through the use of silane impregnation is potentially underestimated.

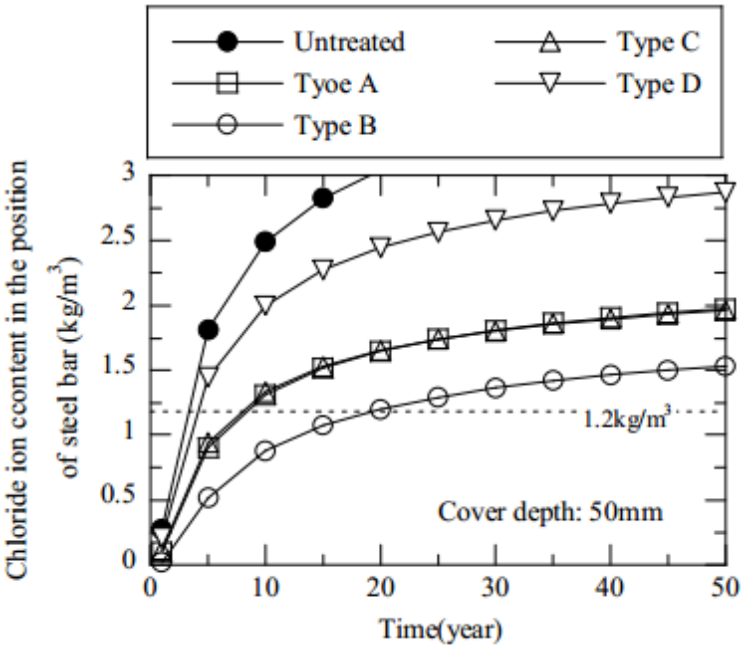

Figure 2-48: Chloride ion prediction results (at a depth of 50 mm) for silane treated and untreated concrete (Tanaka *et al.*, 2015)

Medeiros et al., 2016

Medeiros et al (2016) investigated the service life extension of concrete using surface treatments, including a silane product. The concrete mix was made using Brazilian Portland cement (CPI II E-32) which is equivalent to a slag modified Portland cement with a w/b ratio of 0.52. The concrete specimens (100 mm diameter cylinders) were cured at 23°C and 100% RH for 91 days to obtain a high degree of hydration. The cylinders were then cut into 50 mm thick slices that were left to dry under laboratory conditions (25°C and 70 $\pm$ 4% RH) for 7 days. The water repellent product (silane/siloxane) was then applied on one of the surface of the slices. The specimens were then vacuum saturated with de-aerated water for 24 hours. After a further 7 days, the 50 mm thick slices were placed in a migration cell (consisting of two cells filled with 3% NaCl solution and 0.3 N NaOH solution respectively) as shown in Figure 2-49. 30 V was then applied for 30 hours across the migration cell.

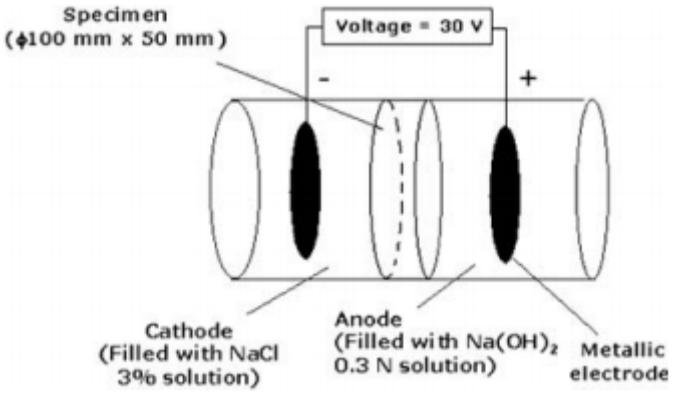

Figure 2-49: Migration test setup (Medeiros, 2008)

After the test, the specimens were fractured in the direction of the chloride flux and an aqueous solution of silver nitrate (0.1 M $AgNO_3$) was sprayed on the exposed surfaces. The chloride penetration depth was determined by measuring the distance over which silver chloride (AgCl) precipitate formed. Hence, the diffusion coefficient (D/m^2s^{-1}) was calculated using Equation 2.32 which is based on a mathematical model developed by Luping and Nilsson (1992) for non-steady state chloride migration (Medeiros *et al.*, 2016). The calculated chloride diffusion coefficients are shown Table 2.11 (only the results for the water repellent products will be discussed).

$$D = \frac{RT}{zFE} \cdot \frac{x_d - ax_d^b}{t} \quad \text{.....(2.32)}$$

where,

D – chloride diffusion coefficient (m^2/s)

R – gas constant (8.31 J/molK)

T – temperature (298 K)

z – ion valence (-1 for chloride)

F – Faraday constant (96.5 J/Vmol)

E – electric field (-600 V/m)

x_d – chloride penetration depth (m)

t – test time (s)

a/b – constants (a = 1.061, b = 0.589)

Table 2.11: Chloride diffusion coefficients (adapted from Medeiros *et al.*, 2016)

	Chloride diffusion coefficient (m^2/s)
Reference	3.52E-12
Water repellent	3.06E-12
Acrylic + water repellent	1.17E-12

A mathematical solution to Fick's second law (Equation 2.33) was then used to predict the service life of the untreated and treated concrete samples.

$$\frac{C_{cl} - C_0}{C_s - C_0} = 1 - erf\left(\frac{x}{2\sqrt{D_{eff}t}}\right) \quad \text{.....(2.33)}$$

where,

C_{cl} – chloride content (%) at depth x at time t

C_s – chloride surface concentration (%)

C_0 – initial chloride content in the concrete (%)

x – depth at which chloride content is equal to C_{cl} (m)

D_{eff} – effective chloride diffusion coefficient (m^2/s)

t – time (s)

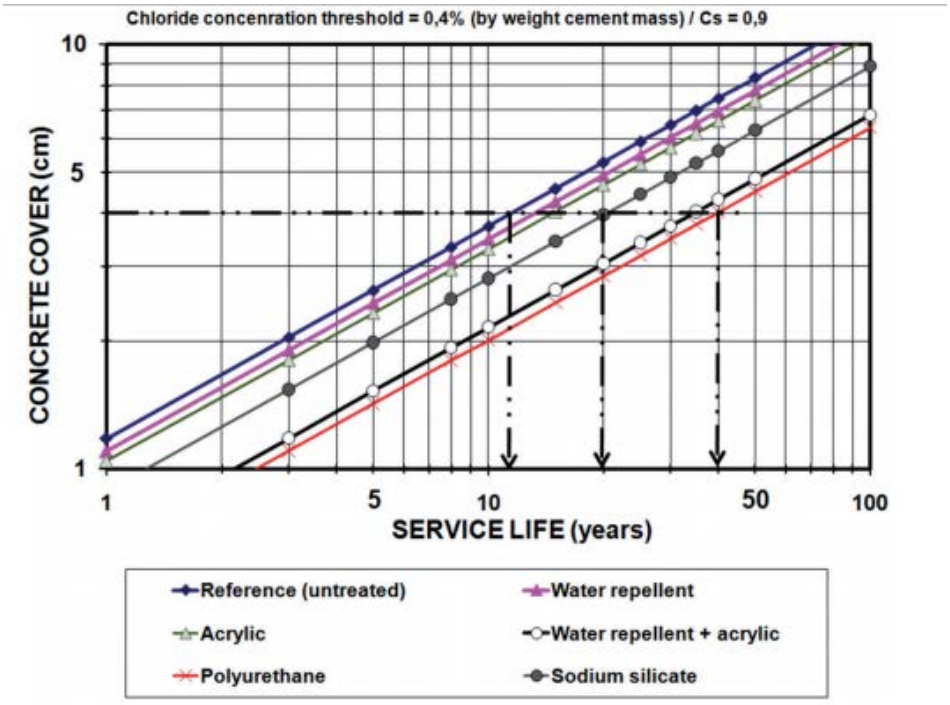

Figure 2-50: Estimated service life of the untreated and treated concrete (Medeiros, 2016)

Hence by assuming zero initial chloride content (C_0 = 0%), setting the chloride surface concentration to 0.9% (concrete with w/b 0.48 to 0.68 subject to salt spray), and fixing the chloride concentration (C_{Cl}) at depth x to the critical chloride content (C_{cr} = 0.4%), the service life (t) of the untreated and treated concrete samples was calculated. For each cover depth (x/m), the equivalent service life was determined, as shown in Figure 2-50. The results indicate that for a cover of 40 mm, the service life of reinforced concrete can be extended by 15% and 77% through the application of a water repellent product (silane/siloxane) and a combination of water repellent/acrylic products respectively.

2.9.4 Cracks

From a durability point of view, the presence of cracks is detrimental to the service life of reinforced concrete structures. Cracks provide preferential paths for deleterious agents (carbon dioxide or chlorides) that ultimately can shorten the initiation time to reinforcement corrosion if the required conditions are met. The influence of hydrophobic impregnation on the penetration of chlorides in cracked concrete remains debatable and further studies under realistic conditions are required (Wittman, 2008; Dai *et al.*, 2010). The following sections present a summary of the work from selected authors.

Dai et al., 2010

Dai et al (2010) investigated the effectiveness of water repellent treatment as a chloride barrier in cracked concrete. For the experiments, one type of concrete (Portland cement – w/b 0.68) was

used with a 28-day compressive strength of 34 MPa. Reinforced concrete prisms (150 x 100 x 100 mm) were cast and cracks were introduced (using a splitting test) before and after the application of the silane impregnation to model two possible real-life scenarios in reinforced concrete structures. An average crack width of 0.15 mm was aimed which, according to the author, represents a realistic crack width under normal service conditions. The water repellent product (silane based gel) was applied at a consumption rate of 904 g/m^2 on two sides of each prism while the remaining surfaces were sealed with epoxy resin. Then, the prisms (cracked – untreated and treated) were exposed to a cyclic wetting (4 hours) and drying (8 hours) period using sea-water showers in an outdoor environment for 1 year. After this chloride exposure, the prisms were analysed through an electron probe microscopy analysis (EPMA) to accurately measure the chloride penetration in the cracked (untreated and treated) specimens.

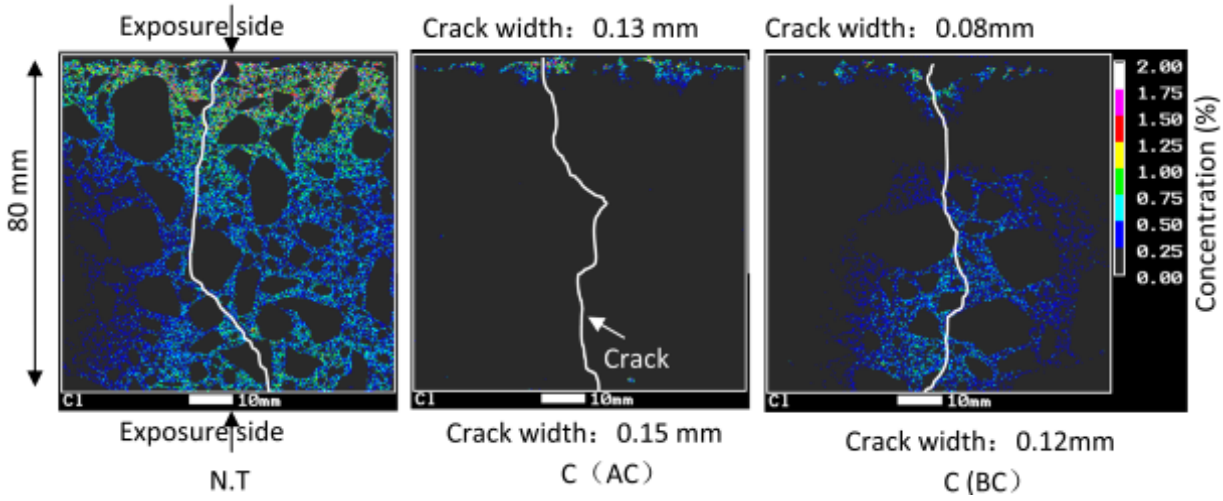

Figure 2-51: Chloride penetration results (N.T – Non-treated, AC – Treated after crack, BC – Treated before crack) (Dai *et al.*, 2010)

From Figure 2-51, it can be observed that chlorides penetrate rapidly and deeper into the cracked and untreated concrete as the cracks were instantly filled with salt solution. The chloride concentration decreased as the distance from the exposure surfaces increased. The chlorides penetrated up to 8 mm in the silane treated concrete (after the formation of cracks). On the other hand, chlorides penetrated up to 17 mm and 70 mm (from the two exposure surfaces) in the prisms that were treated before the formation of cracks. Hence, author concluded that hydrophobic impregnation was most effective in reducing chloride penetration in cracked concrete, assuming the crack is stable, the crack width is smaller than 0.13 mm and that water-repellent treatment is performed after the formation of cracks (Dai *et al.*, 2010).

Wittman et al., 2008

Wittman et al (2008) studied the effectiveness of silane impregnation to prevent chloride penetration in cracked concrete. One type of concrete (Portland cement – w/b 0.50) was used in this study. Reinforced concrete prisms (100 x 100 x 300 mm) were cast, demoulded after 2 days and cured in a humid chamber (20°C temperature and >90% relative humidity) for 28 days. Then all the specimens were oven dried at 50°C for 3 days. After this drying period, the prisms were removed from

the oven, allowed to cool in a desiccator and coated with wax on four sides, leaving the top (finished) and bottom surfaces open. These prisms were then loaded under the three-point bending test and cracks (0.1 mm, 0.2 mm and 0.4 mm in width) were induced. Water repellent treatment was performed by placing the cracked (bottom) surface in contact with liquid silane for 1 hour (deep impregnation). Hence, three groups of cracked samples were prepared in total; untreated, treated before introduction of cracks, and treated after induction of cracks. The cracked samples (untreated/treated) were then placed in contact with a 3% sodium chloride (NaCl) solution for 28 days. The arrangement was similar to the one used to determine the capillary suction of porous materials. After exposure to the salt solution, two-dimensional chloride profiling was performed by cutting slices through the bottom of the prism and horizontally through the crack surface (Figure 2-52).

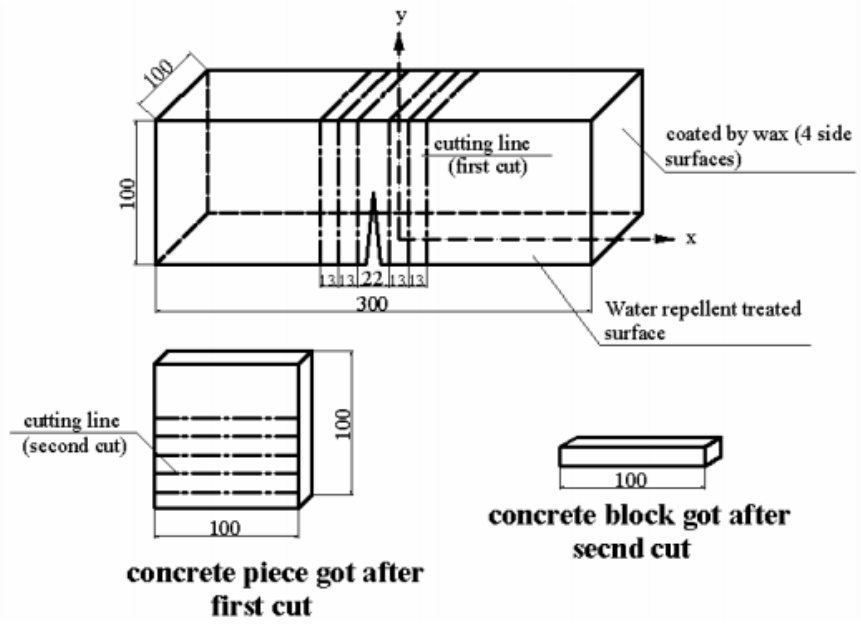

Figure 2-52: Illustration of cutting sequence for chloride profiling (Wittman *et al.*, 2008)

According to Figure 2-53, considering the untreated (a) cracked concrete, it can be noted that there is a significant increase in chloride content near the crack opening, and higher crack widths correlated to greater ingress of chlorides. This was attributed to the rapid transport of chloride solution in cracks. At 30-40 mm (horizontal) distance from the crack opening, the chloride profile is similar to that of uncracked concrete. Considering the concrete that was treated and subsequently cracked (b), it can be noted that chloride ingress is reduced for all crack widths. However, the effectiveness of the water repellent treatment decreases with a larger crack width; higher chloride penetration depth and greater horizontal diffusion was observed as the crack size was increased from 0.1 to 0.4 mm. Comparing the results of the concrete that was treated after the introduction of cracks (c) with the untreated cracked concrete (a), there is a significant reduction in chloride ingress, with no penetration in the concrete with a 0.1 mm crack width. The results hence suggest that water repellent treatment provides superior reduction in chloride ingress when the product is applied after the formation of cracks (Wittman *et al.*, 2008).

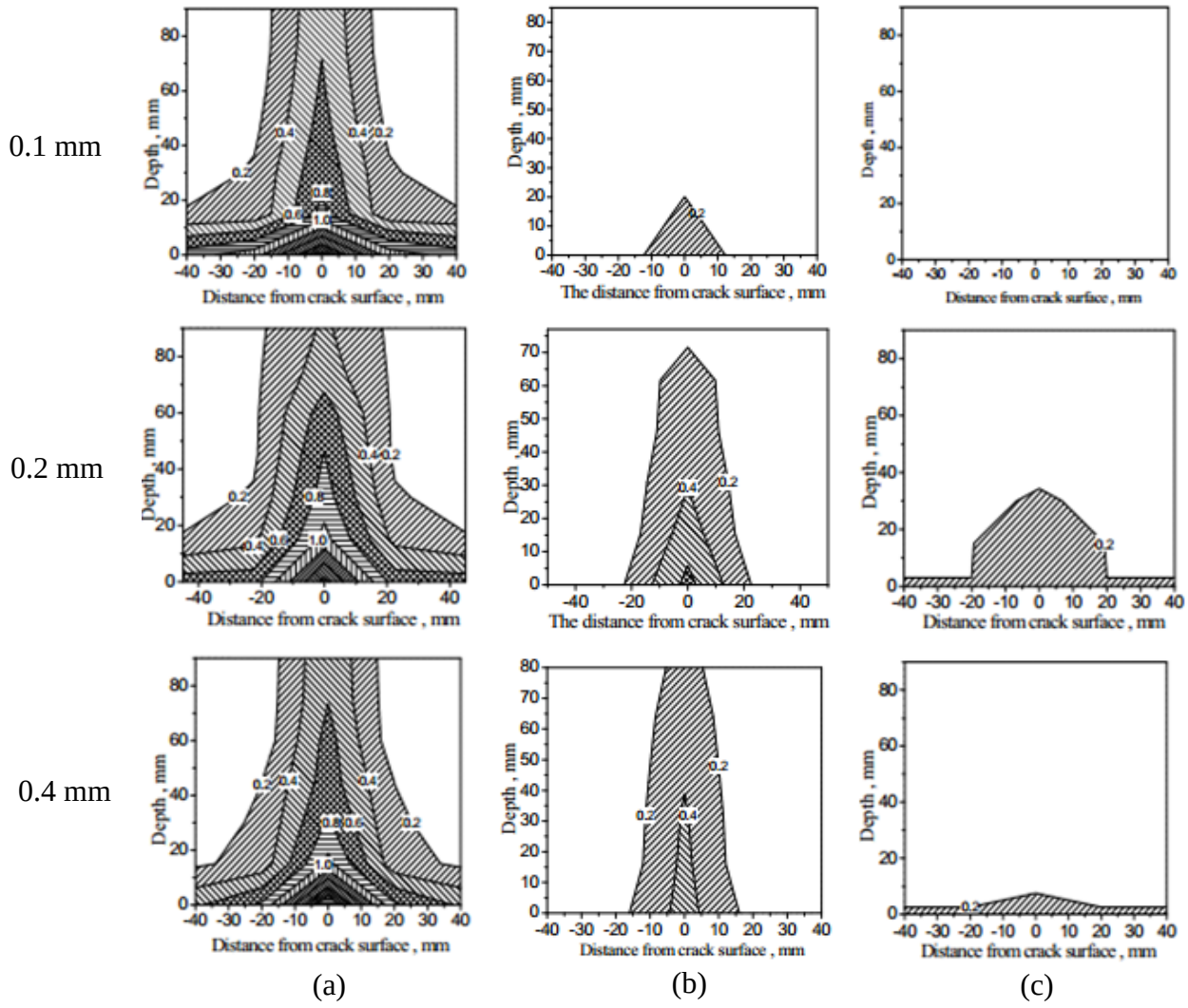

Figure 2-53: Contour diagrams showing chloride penetration in cracked concrete; untreated (a), treated before cracking (b), treated after cracking (c) (Wittman *et al.*, 2008)

2.10 Summary

This chapter discussed the transport properties of uncracked and cracked concrete, concrete deterioration (including mechanisms of reinforcement corrosion), concrete durability, service life design and hydrophobic impregnation. The durability of reinforced concrete structures is related to the rate of movement of aggressive substances across the concrete microstructure through various and often simultaneous transport mechanisms (capillary absorption, permeation, diffusion and migration). The overall transport processes in cracked concrete also need to be considered as cracks provide preferential ingress paths for deleterious agents and hence can shorten the time to reinforcement corrosion initiation (Alexander *et al.*, 2010). Transport mechanisms in cracked concrete (adsorption and dissolution) are a function of the concrete quality (w/b, binder type, penetrability), crack properties (width, shape, tortuosity and orientation) and cover depth (Pacheco & Polder, 2012; Gu *et al.*, 2015; Li, 2017).

Concrete deterioration, mainly due to rebar corrosion, has several implications on larger scale. Direct costs include the repair and rehabilitation of affected structures to maintain serviceability while indirect costs relate to losses in productivity and slower economic growth. The increase in premature deterioration of newly constructed infrastructure is often linked to insufficient cover depth and quality resulting from a lack of understanding of concrete durability, improper mix designs and inadequate attention to quality control on site (Alexander *et al.*, 2013).

The consequences of reinforcement corrosion range from minor aesthetic cracking to severe structural damage that compromises the durability and performance of the infrastructure. Rebar corrosion is initiated through two major mechanisms; carbonation and chloride ingress. The former relates to the diffusion of carbon dioxide gas from the environment into the concrete and reaction with the alkaline constituents of concrete. Chloride ingress in concrete depends on the exposure conditions, but typically chlorides initially enter through capillary absorption followed by diffusion. Chlorides, when present in sufficient concentration, reduce the solubility of calcium hydroxide. Hence, both mechanisms of carbonation and chloride ingress result in a reduction in the concrete pH followed by the breakdown of the passivating layer around the embedded steel rebar, thereby initiating reinforcement corrosion (Bertolini *et al.*, 2013; Li, 2017).

A chloride ingress model for concrete typically predicts the chloride profile after a certain amount of time and hence the chloride concentration at the depth of the steel rebar. The output of this model is normally evaluated against a 'chloride threshold level'. This threshold value is known as the critical chloride concentration (C_{cr}) at the reinforcement depth that leads to the loss of the protective gamma-ferric (passive) oxide layer. This critical chloride content is a function of several interlinked factors such as pore solution chemistry, properties of the steel-concrete interface, amount of oxygen available and electrochemical potential of the steel reinforcement. Hence, each concrete mix has a unique chloride threshold. A model based on the error function solution to Fick's second law of diffusion is often used to predict the service life of reinforced concrete. While it is based on several simplified assumptions, it remains one of the most widely used methods as it provides a reasonable estimate from an engineering point of view. The time dependence of the apparent chloride diffusion coefficient (D_a) and surface chloride concentrations (C_s) must be considered to have realistic predictions (Bertolini *et al.*, 2013, Sarja, 2006).

The durability of concrete has become a major concern in the modern construction industry with the expansion of the social and economic infrastructure and the need for structures to last longer in aggressive environments. Concrete durability is a function of several factors including the level of aggressiveness of the environment, concrete quality, cover thickness, and the presence of cracks. A performance-based approach, relative to the conventional prescriptive approach offers greater control and flexibility over the durability design of concrete structures as it accounts for the variances of the concrete composition, on site workmanship and environmental exposure classes. Hence, performance-based approaches provide a platform for service life design and prediction. The South African (performance based) Durability Index approach is based on material indexing. This involves characterising the near surface zone through Durability Index tests and hence quantifying the resistance of the concrete against the transport of deleterious agents that are responsible for the initiation and propagation of reinforcement corrosion. Three laboratory tests,

namely the Oxygen Permeability Index (OPI), Water Sorptivity Index (WSI) and Chloride Conductivity Index (CCI) tests, provide relatively quick experimental results using either in situ or laboratory concrete. Research has shown that the early age (28 day) Oxygen Permeability Index (OPI) and Chloride Conductivity Index (CCI) can be related to long term carbonation and chloride diffusion respectively, for a wide range of concretes. Hence, these Durability Indexes provide a sound basis for durability design and service life prediction (Alexander *et al.*, 2017; Alexander & Beushausen, 2008).

Extensive research has been undertaken to find ways to improve the durability of concrete structures. Surface treatments are products that are typically applied on concrete with the primary aim of reducing the cover's penetrability to deleterious agents. Hydrophobic (silane) impregnation is one type of surface treatment that can supress capillary absorption of liquids. Practically all types of concrete deterioration occur in the presence of water in both the external environment and internal pore structure. Generally, concrete in dry environments shows a lower extent and rate of degradation relative to wet (humid) environments. Hence, the use of hydrophobic (silane) impregnation allows a reduction in ingress of water dissolved aggressive species (chlorides), leading to an extension in the time taken for rebar corrosion initiation and effectively extending the service life of reinforced concrete (Bertolini *et al.*, 2013; Alexander & Beushausen, 2009; Dai *et al.*, 2010). It must be noted that the effectiveness of silane impregnation can decrease with time due to UV radiation, thermal shocks, abrasion and carbonation (Polder *et al.*, 2001; Antons *et al.*, 2015). Hence, regular maintenance (reapplication of the water repellent product) is needed to ensure that the protective measure is sustained (Meier & Wittmann, 2011; Lucquiaud *et al.*, 2014).

Water repellent treatment is applied as standard on all new concrete bridge decks in countries such as the Netherlands and United Kingdom (Polder *et al.*, 2000; Dyer, 2014). However, there is insufficient quantification of the extent of protection; the effect of silane impregnation on chloride ingress is well documented in literature and several experiments have been carried out over the last decades but there is limited work on the service life prediction of silane treated concrete. The work presented in literature often make use of a single w/b and binder type and neglect the time dependence of the chloride diffusion coefficient (D_a) in the service life modelling which leads to underestimation of the service life extension possible. The influence of hydrophobic impregnation in cracks remains debatable especially in the case of larger crack widths (> 0.4 mm) and the combined influence of the concrete composition (binder type) and silane impregnation needs to be investigated further.

3. Methodology

This section describes the research approach taken to achieve the required objectives of this thesis. Further details of the resources in terms of materials and equipment used to perform the experimental tests are provided. Details on the test conditions and procedures followed are also summarised.

3.1 Overview

The methodology of this research is summarised in Figure 3-1. The experimental approach starts with the consideration of certain parameters that were varied to achieve a range of concrete mixes. Two w/b ratios (w/b of 0.45 and 0.60) and four binder types were selected (CEM I 52.5N, Fly-ash (FA), Ground granulated corex slag (GGCS) and CEM III/B 42.5N). Hence a total of 8 main mixes were used, as described in Section 3.2. The normal concrete specimens were demoulded 24 hours after casting and subsequently wrapped in plastic sheeting and placed in an environmental room (23 $\pm$ 2°C temperature and 63 $\pm$ 2% relative humidity). After reaching an age of 7 days, the plastic sheeting was removed and the specimens were allowed to air-cure under the aforementioned controlled environmental conditions until the age of 56 days.

Poor quality concrete was produced by exposing the concrete specimens to relatively high temperature at early age, as described in Section 3.3. Cracked concrete was obtained by loading notched reinforced beams until the formation of cracks. Steel spacers were then placed in the notch and the beams were unloaded to create crack widths of 0.2 mm and 0.6 mm (below and above the commonly assumed crack width threshold of 0.4 mm (Alexander *et al.,* 2010)). Silane treatment was performed at the age of 28 days by applying Sikagard®-706 Thixo at a consumption rate of 400 g/m^2. Table 3.1 shows a summary of the tests performed on the untreated and silane treated concrete specimens.

Table 3.1: Summary of experimental tests

Type of test		Reasons for carrying out test	Test standard
Compressive strength		To characterise the concrete mixes	SANS 5863 (2006)
Durability Index	Cut surfaces (OPI, WSI, CCI)		SANS 3001-CO3-2 (2015) UCT DI Manual (2017) SANS 3001-CO3-3 (2015)
	Uncut surfaces (WSI, CCI)	To investigate the effect of silane impregnation on capillary absorption and chloride conductivity	UCT DI Manual (2017) SANS 3001-CO3-3 (2015)
Accelerated carbonation		To assess the influence of silane treatment on carbonation	*fib* bulletin 34 (2006)
Bulk diffusion	Uncracked concrete	To obtain the chloride surface concentrations (C_s) and apparent chloride diffusion coefficients (D_a)	ASTM C1556 (2004) ASTM C1152 (2012)
	Cracked concrete	To investigate the influence of silane impregnation in cracked concrete	
Moisture profiling		To evaluate the influence of silane treatment on the relative humidity in the concrete	Parrott (1988)

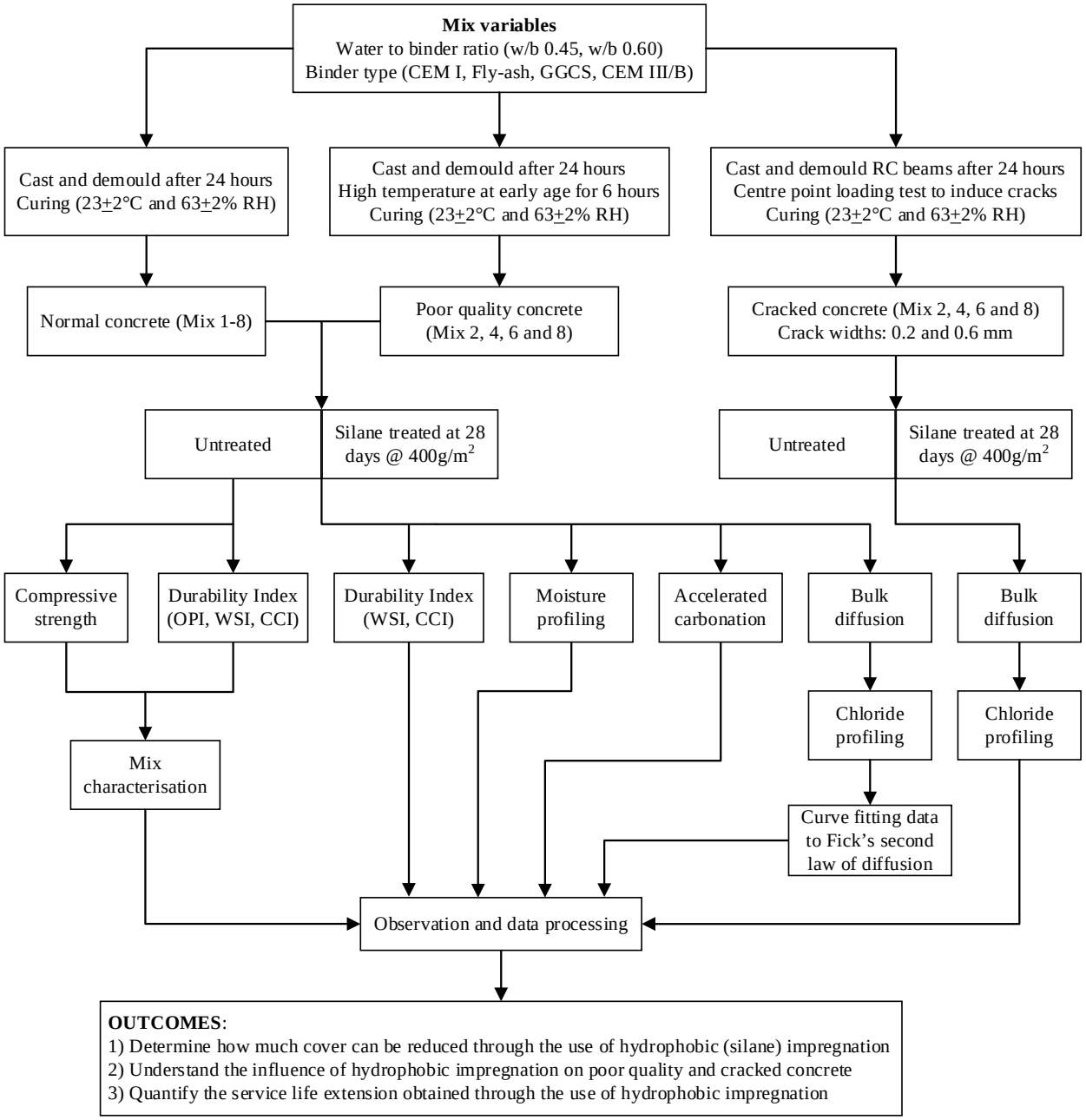

Figure 3-1: Summary of experimental approach

3.2 Mix design

The mix design was performed according to the Cement and Concrete Institute (C&CI) volumetric mix design method (Alexander & Beushausen, 2009). This method consists of calculating the mass of the mix constituents with the requirement that the total volume should add up to the total volume of concrete. Trial mixes were performed prior to casting of the specimens to determine the water content and the workability was assessed by the slump test in accordance with SANS 5862-1 (2006). Superplasticizer (Chryso premia- 310) was added in increments of 5 mL (to a 40 litre mix) using a syringe until the required workability was achieved. A slump range of 60-100 mm was chosen which corresponds to the workability for general concrete construction.

Table 3.2: Mix design (materials in [kg/m^3])

	Mix 1 (Control)	Mix 2 (Control)	Mix 3	Mix 4	Mix 5	Mix 6	Mix 7	Mix 8
Material (kg/m^3)	**100% CEM I 52.5N**	**100% CEM I 52.5N**	**30% FA**	**30% FA**	**50% GGCS**	**50% GGCS**	**100 % CEM III/B 42.5N**	**100% CEM III/B 42.5N**
W/b ratio (w/b)	**0.45**	**0.60**	**0.45**	**0.60**	**0.45**	**0.60**	**0.45**	**0.60**
Cement (CEM III/B 42.5N)	-	-	-	-	-	-	411	308
Cement (CEM I 52.5N)	411	308	288	216	206	154	-	-
Extender (Fly-ash)	-	-	123	93	-	-	-	-
Extender (GGCS)	-	-	-	-	206	154	-	-
Fine aggregate (Crusher sand)	426	472	406	457	419	467	413	463
Fine aggregate (Dune sand)	426	472	406	457	419	467	413	463
Coarse aggregate (19-mm Greywacke)	1040	1040	1040	1040	1040	1040	1040	1040
Water	185	185	185	185	185	185	185	185
Total binder (kg/m^3)	411	308	411	308	411	308	411	308
Fly-ash content (%)	-	-	**30**	**30**	-	-	-	-
GGCS content (%)	-	-	-	-	**50**	**50**	-	-
Slump (mm)	70	60	90	65	75	60	70	70

3.2.1 Mix variables

A total of 8 main concrete mixes were used in this study (Table 3.2) with the addition of 4 poor quality mixes manufactured in accordance with Section 3.3.3. Two mix parameters were varied to evaluate the performance of the hydrophobic impregnation:

- W/b ratio (w/b 0.45 and w/b 0.60)

W/b ratio has a major influence on the strength and penetrability of concrete (Alexander, 2016). A w/b 0.45 was utilised as it is the maximum prescribed for the XS3 exposure class by BS EN206 (2013). A higher w/b 0.60 was used to model more conventional mix designs.

- Cement extenders (Fly-ash and GGCS)

Supplementary cementitious materials have a major impact on the penetrability of hardened concrete (Thomas, 2013). Hence, fly-ash and ground granulated Corex slag were used at typical replacement levels of 30% and 50% respectively.

3.2.2 Cement

For this study, two cement types were used; Locally produced CEM I 52.5N from Riebeek West PPC factory Western Cape Province South Africa and CEM III/B 42.5N manufactured by ENCI from Europe (Netherlands). CEM III/B 42.5N, containing 66-80% Ground granulated Blastfurnace slag (GGBS), was included to make this research internationally relevant. The common composition of these cements is given in Table 3.3, based on previous research.

Table 3.3: Typical oxide analysis of CEM I 52.5N and CEM III/B 42.5N (adapted from Kanjee *et al.*, 2012; ENCI, 2015)

(%) Composition	CaO	Al_2O_3	SiO_2	Fe_2O_3	MgO	K_2O	SO_3	Na_2O
CEM I 52.5N	65.80	4.00	21.10	3.35	0.87	0.70	2.30	0.10
CEM III/B 42.5N	45.0	11.0	29.0	1.0	-	-	2.86	0.66

3.2.3 Extenders

Fly-ash (Class F) and ground granulated Corex slag (GGCS) used for this research were obtained locally from the Lethabo plant in Gauteng and the Saldanha Bay steel plant in the Western Cape respectively. The composition of these cement extenders is provided in Table 3.4.

Table 3.4: Typical oxide analysis of fly-ash and GGCS (Alexander *et al.*, 2012)

(%)	CaO	Al_2O_3	SiO_2	Fe_2O_3	MgO	K_2O	TiO_2	Na_2O	Mn_2O_3	MnO	P_2O_5	SO_3
Fly-ash	5.85	30.0	54.6	2.75	1.91	0.76	1.74	0.60	0.02	-	0.85	0.30
GGCS	37.2	16.0	30.8	0.87	13.7	0.35	0.51	0.12	-	0.09	-	3.19

3.2.4 Fine aggregate

A 50/50 blend of Philippi dune sand and greywacke crusher sand was used as fine aggregate. Philippi dune sand was used as the rounded shape and smooth surface texture of the grains could potentially contribute to better workability (Alexander & Beushausen, 2009). However, a portion of the natural (dune) sand was replaced with crusher sand to compensate for the lack of particle size passing the 150 and 75 µm sieve sizes. Crusher sand typically has a uniform grading, good particle shape and adequate dust content. Consequently, bleeding and segregation of the concrete mixes was minimised. All the sands used in this study were oven-dried for 24 hours at 80°C and allowed to cool for atleast 4 hours prior to use. A sieve analysis of the dune and crusher sands were carried out in accordance with SANS 201 (2008). Figure 3-2 shows the grading chart for the 50/50 blend of Philippi dune and crusher sands. The individual grading curves for the dune sand and crusher sand can be found in Appendix K.

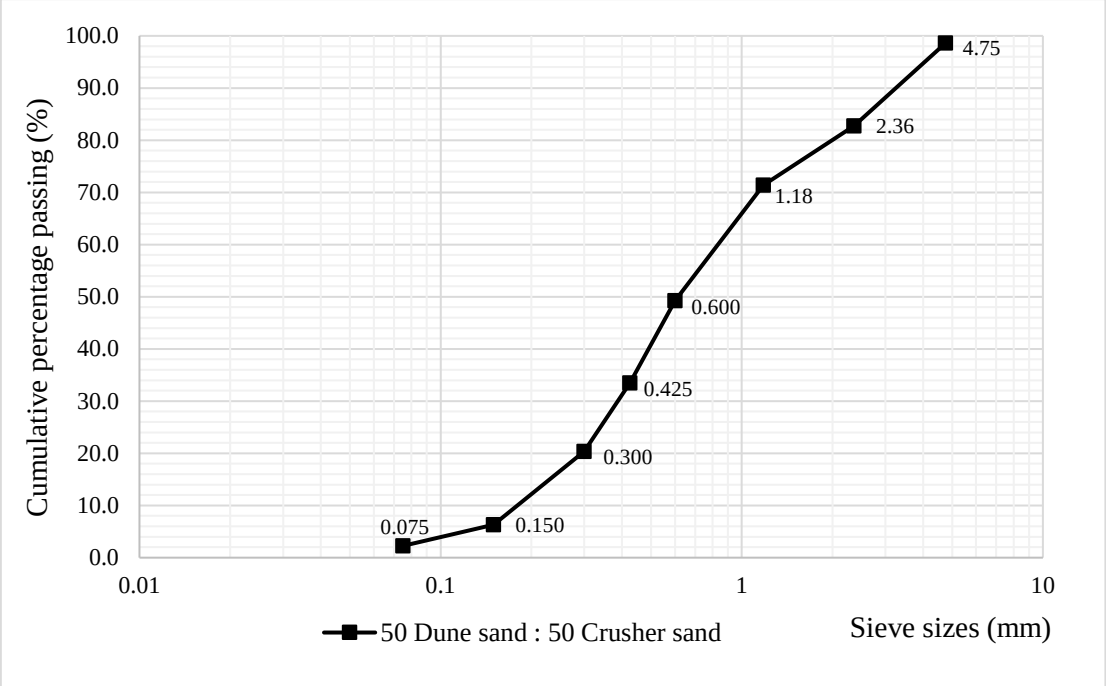

Figure 3-2: Grading curve (50 Dune sand: 50 Crusher sand), F.M = 3.4

3.2.5 Coarse aggregate

19 mm Greywacke stone was used as coarse aggregate. This rock, known as the Malmesbury Shale in the Western Cape, originates from thermal metamorphism of argillaceous rocks as a result of the intrusion of plutons of the Cape Granite (Alexander & Beushausen, 2009). The sieve analysis was performed in accordance with SANS 201 (2008) and the grading curve is provided in Figure 3-3.

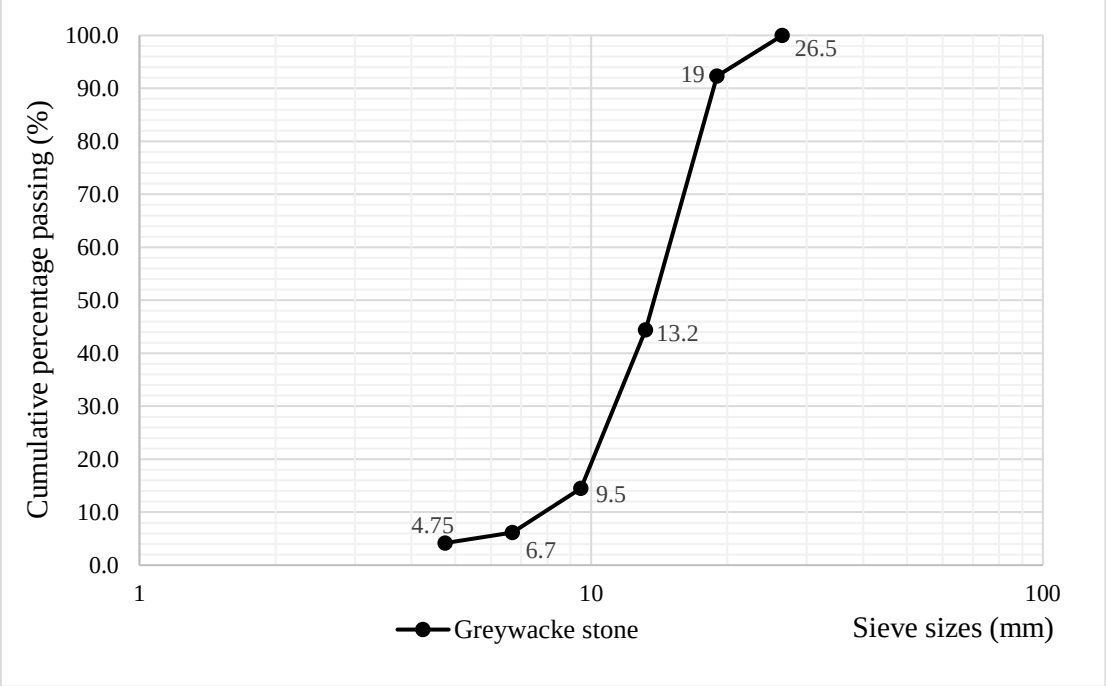

Figure 3-3: Grading curve (greywacke stone)

3.3 Specimen preparations

3.3.1 Casting

The various mixes (Mix 1-Mix 8) were cast using appropriate moulds. Reasonably cohesive concrete mixes were obtained after the addition of the required amount of superplasticizer, with no visible segregation and hence on overall, satisfactory rheological properties were achieved. The measured slump values are shown in Table 3.2. Compaction was performed using a vibrating table for 30 seconds. The moulds were then covered with polythene sheets for 24 hours.

3.3.2 Curing

All the (normal) concrete specimens used for Durability Index, carbonation, bulk diffusion and relative humidity tests were demoulded after 24 hours, placed in an environmental room (maintained at a temperature of 23 $\pm$ 2°C and relative humidity of 63 $\pm$ 2%) and wrapped in plastic sheets for an additional 6 days (until reaching an age of 7 days). After this period, the plastic sheets were removed and the specimens were air cured in the environmental room until the day of testing. This curing regime was used to model on site curing for newly constructed structures. All the strength specimens were demoulded after 24 hours and cured in a water bath at 23 $\pm$ 2°C until the testing date.

Figure 3-4: Curing method: plastic sheeting

3.3.3 Poor quality concrete

Poor quality versions of Mix 2, Mix 4, Mix 6 and Mix 8 were obtained by subjecting the respective (strength and durability) concrete specimens to different elevated temperatures (Table 3.5) at early age (after demoulding) for 6 hours. A similar method was used by Burmeister (2012). The lower quality of the mixes was confirmed through the Durability Index tests results' (Section 4.2). Higher (80°C) and lower (30°C) temperatures were used with Mix 2 and Mix 8 respectively as poor-quality concrete was not obtained at 50°C. After that, the specimens were placed in an environmental room (maintained at a temperature of 23 $\pm$ 2°C and relative humidity of 63 $\pm$ 2%) until the day of testing.

Table 3.5: Temperatures used to produce poor quality concrete

Mix number	w/b	Composition	Temperature (°C)
2	0.60	100% CEM I	80
4	0.60	70% CEM I/30% FA	50
6	0.60	50% CEM I/50% GGCS	50
8	0.60	100% CEM III/B	30

3.3.4 Induction of cracks

Cracked concrete specimens were manufactured as follows:

- 120 mm x 130 mm x 380 mm reinforced concrete beams were cast with Y10 mild steel bars placed at 40 mm cover. A 1 mm thick and 12 mm deep PVC strip was placed at the centre of the beam mould prior to casting. After demoulding, a notch was created which allowed the crack to propagate at midspan, when the beams were loaded.

Figure 3-5: Beam mould (left) and test specimen (right)

- The reinforced concrete beams were subject to the centre-point loading (three-point bending) test, and the beams were positioned such that the reinforcement carried the tensile force generated. This method also provided a realistic generation of cracks. The beams were loaded until a crack was formed and propagated sufficiently. 1.2 mm and 1.6 mm thick steel spacers were then inserted in the 1 mm notch such that after unloading, crack widths of 0.2 mm and 0.6 mm were obtained.

Figure 3-6: Induction of cracks on reinforced concrete beams

- The beams were then cut to 120 mm x 120 mm x 130 mm prisms. 12 mm of concrete was removed from the top to expose the crack opening (Figure 3-7).

Figure 3-7: Before and after removal of top concrete layer

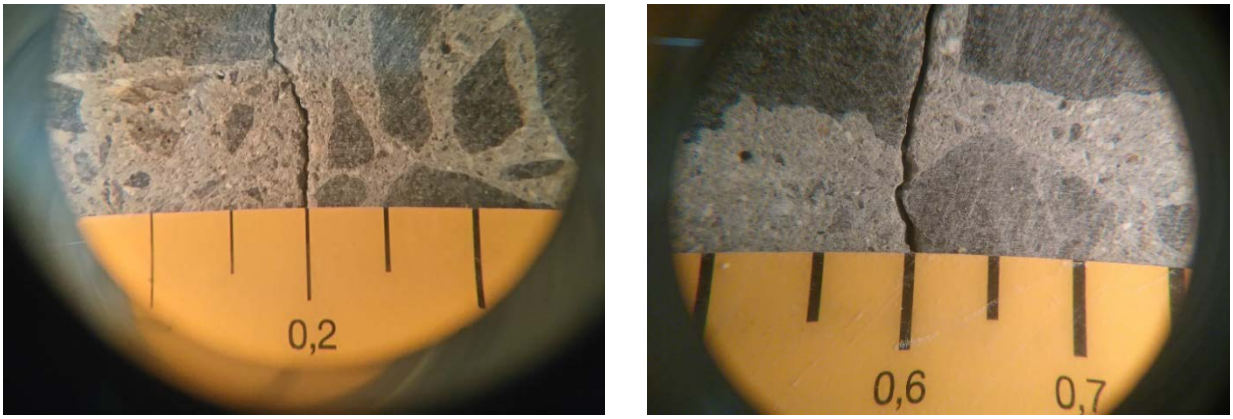

Figure 3-8: Crack widths obtained (0.2 mm and 0.6 mm)

3.3.5 Silane treatment

After 28 days, the surfaces of the concrete specimens were roughened using sand paper to remove any impurities and release oil. Sikagard®-706 Thixo (a silane based water repellent impregnation cream) was then applied at a consumption rate of 400 g/m^2 using a brush. Sikagard®-706 Thixo is a solvent free water repellent product with about 80% (silane) active ingredient (Sika, 2016). The treated specimens were then placed in an environmental room (maintained at a temperature of 23 $\pm$ 2°C and relative humidity of 63 $\pm$ 2%) until the age of 56 days.

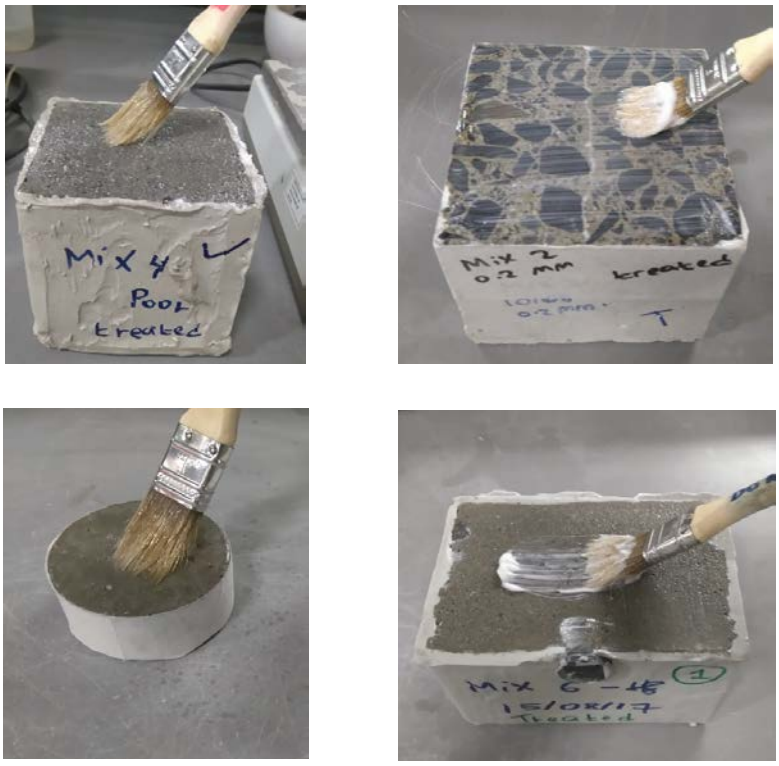

Figure 3-9: Silane treatment

3.4 Experimental tests

3.4.1 Compressive strength

Compressive strength tests were carried out on three 100 mm x 100 mm x 100 mm cubes of each mix. These tests were carried out to determine compressive strength and hence characterize each mix. Furthermore, in order to monitor strength development, the test was performed at ages of 3, 7 and 28 days respectively. The test procedure was in accordance with SANS 5863 (2006) and the cubes were cured in a water basin at 23 $\pm$ 2°C.

3.4.2 Durability Index

Cores were extracted from 56-day cured concrete cubes (100 mm). Four specimens were used per test and each consisted of a 70 $\pm$ 2 mm diameter concrete disc with a thickness of 30 $\pm$ 2 mm, cored and cut in accordance with standard procedures for the preparation of test specimens for concrete Durability Index testing (SANS 3001-CO3-1). The specimens were oven dried at 50°C for seven days prior to testing.

Each of the Durability Indexes is related to transport mechanisms (gaseous diffusion, absorption and ionic diffusion respectively), which are linked to the reinforcement corrosion mechanism (Ballim *et al.,* 2009). Hence these tests allowed the characterisation of the concrete with respect to durability requirements. Water Sorptivity Index (WSI) and Chloride Conductivity Index (CCI) tests were also carried out on uncut (formwork) surfaces to evaluate the influence of silane impregnation on the transport properties (capillary suction and conductivity) respectively (Figure 3-10).

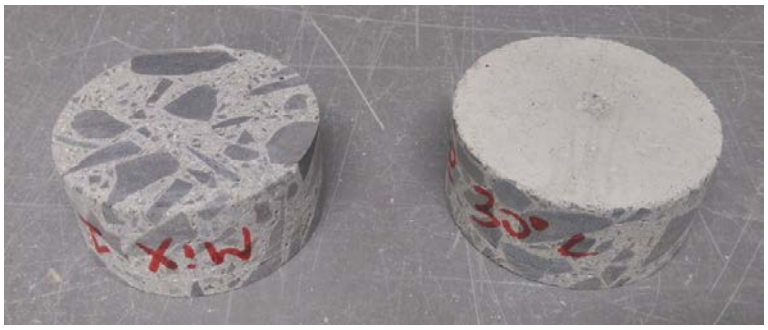

Figure 3-10: Durability Index test specimens (discs) – cut (left) and uncut (right)

3.4.2.1 Oxygen Permeability Index (OPI)

The OPI test involved measuring the pressure decay of oxygen through the 30-mm thick and 70 mm diameter concrete discs. OPI values were calculated as the negative log of the coefficient of permeability (k/ms^{-1}) (Owens, 2013). The test was performed in accordance with SANS 3001-CO3-2 (2015).

The OPI test evaluates the overall micro and macrostructure of the outer surface of the cast concrete and is predominantly sensitive to macro-voids and cracks which provide short-circuit routes for the permeating gas. Hence, this test is useful to assess the extent of compaction, presence of bleed voids and channels and the degree of interconnectedness of the pore structure (Salvoldi *et al.*, 2015).

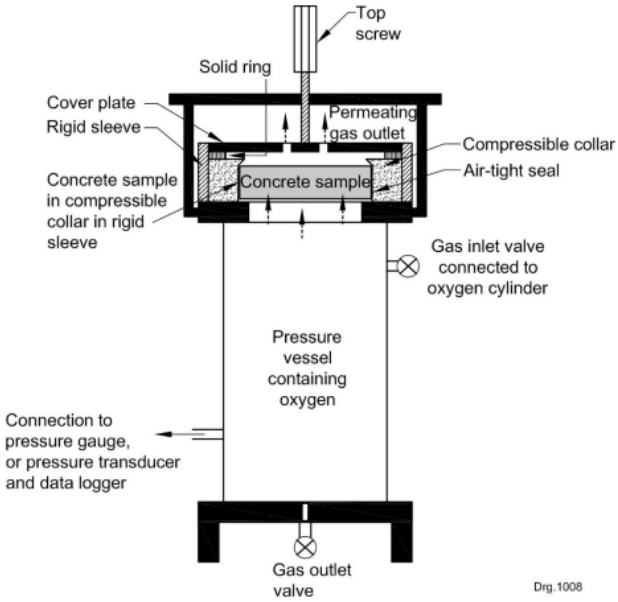

Figure 3-11: Oxygen Permeability Index (OPI) test setup (UCT, 2017)

3.4.2.2 Water Sorptivity Index (WSI)

The WSI test was performed by measuring the rate of absorption of calcium hydroxide solution through dry concrete discs under capillary action regulated by their porosity. The outer edges of concrete discs were sealed with tape to promote one-way movement of the liquid. The concrete specimens were then placed, test face down, in a few millimetres of calcium hydroxide solution

and their masses were recorded at specific time intervals. Hence, the rate of absorption was calculated in mm/hr$^{0.5}$. The porosity was calculated by subtracting the dry mass from the saturated mass of the concrete discs. This test was carried out in accordance with the DI test manual (UCT, 2017).

The WSI test is very sensitive to the micro-structural properties of the near-surface region of concrete and consequently gives an indication of the quality and efficiency of curing (Beushausen & Luco, 2016).

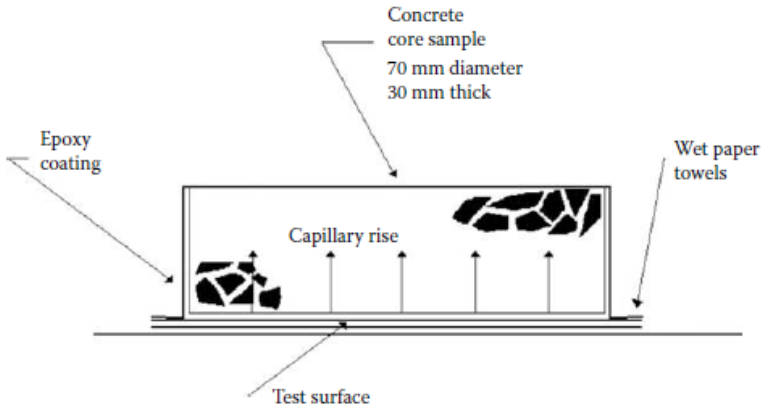

Figure 3-12: Water Sorptivity Index (WSI) test setup (Alexander *et al.*, 2017)

3.4.2.3 Chloride Conductivity Index (CCI)

The CCI test is a chloride migration test which involves applying a potential difference of 10V across the 70 mm diameter and 30 mm thick concrete discs placed in a 5M NaCl solution. These concrete discs were oven dried at 50°C and vacuum saturated with NaCl solution prior to the test. The chloride conductivity was calculated by measuring the current flowing through the sample and was given as mS/cm (milli-Siemens per centimetre) (Owens, 2013). The test was carried out in accordance with SANS 3001-CO3-3 (2015).

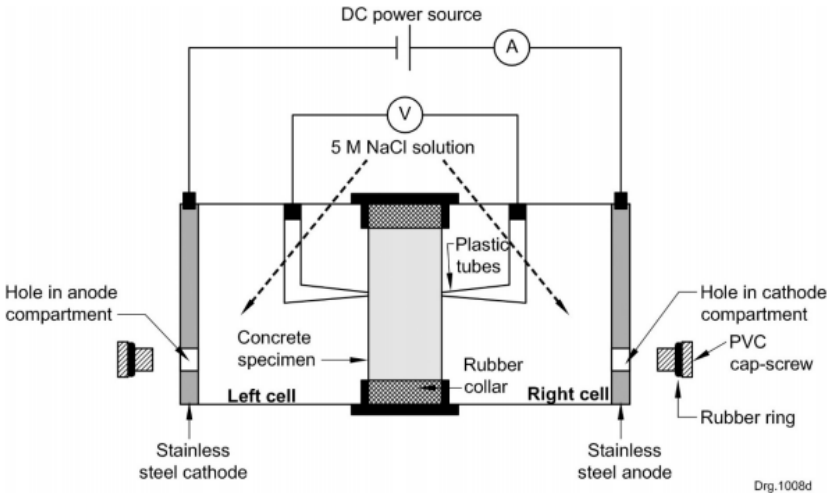

Figure 3-13: Chloride Conductivity Index (CCI) test setup (Alexander *et al.*, 2017)

Transport processes of chlorides entering concrete are intricate, involving diffusion, capillary suction, hydrostatic pressure, convection and migration in addition to physical and chemical binding.

The CCI test gives an indication of the chloride ingress potential though the pore structure of the concrete. Therefore, this test method is utilised for performance-based design and quality control of concrete structures exposed to the marine environment (Beushausen & Luco, 2016).

3.4.3 Penetration depth

The hydrophobic impregnation depth was measured 4 weeks after treatment. The indirect tensile splitting test was performed on silane treated 100 mm x 100 mm x 100 mm concrete cubes and water was sprayed on the internal surface. The hydrophobised part of concrete repelled any water while the untreated part showed darker coloration, due to water absorption. A Vernier caliper was used to take the measurements. The average of six measurements was taken as the penetration depth.

Figure 3-14: Hydrophobic impregnation depth measurement

3.4.4 Accelerated carbonation

Accelerated carbonation tests were performed on two 100 mm x 100 mm x 100 mm concrete cubes per mix at the age of 56 days. All the sides of these specimens, except two opposite exposure surfaces, were coated with epoxy resin, to ensure unidirectional carbon dioxide ingress. The coated samples were then placed in a carbonation chamber (maintained at a temperature of 20 $\pm$ 2°C, relative humidity of 65 $\pm$ 5% and carbon dioxide concentration of 2 $\pm$ 0.1%) for 16 weeks. The exposure conditions were according to the *fib bulletin 34: Model code for service life design* (Schiessl *et al.*, 2006). After this exposure period, the specimens were removed from the chamber and phenolphthalein solution was applied on freshly cut surfaces. These slices were left for 24 hours in an environmentally controlled room (maintained at a temperature of 23 $\pm$ 2°C and relative humidity of 53 $\pm$ 2%) and thereafter the carbonation depth was measured using a Vernier caliper. A total of 8 measurements was taken.

3.4.5 Bulk diffusion

Bulk diffusion tests were carried out in accordance with ASTM C1556 (2004), starting at a sample age of 56 days. Three 100 mm x 100 mm x 100 mm cube specimens were used per mix. All the sides, except the exposure surface, were coated with Sikadur® 32N (epoxy resin) to ensure unidirectional chloride ingress. The samples were then immersed in 165g/L sodium chloride solution

at 10 ± 5 mm head for 80 days. A similar test setup was used in the work of Donadio et al (2014). It must be noted that hydrophobic impregnation is not efficient under hydrostatic pressure (Medeiros *et al.*, 2008). However, a pressure head of 10 ± 5 mm was considered negligible. The test was carried out in a controlled environment (at a temperature of 23 ± 2°C and relative humidity of 53 ± 2%).

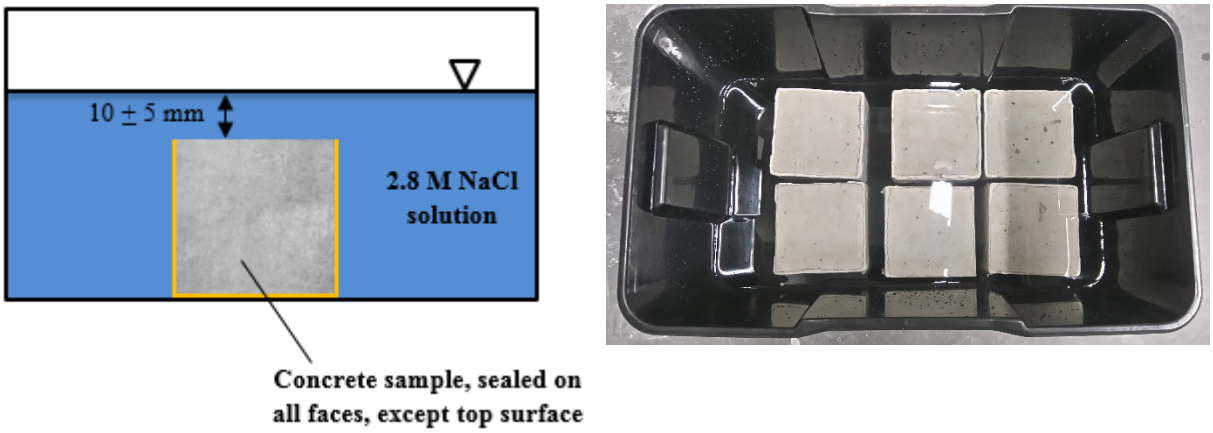

Figure 3-15: Bulk diffusion test setup (uncracked concrete)

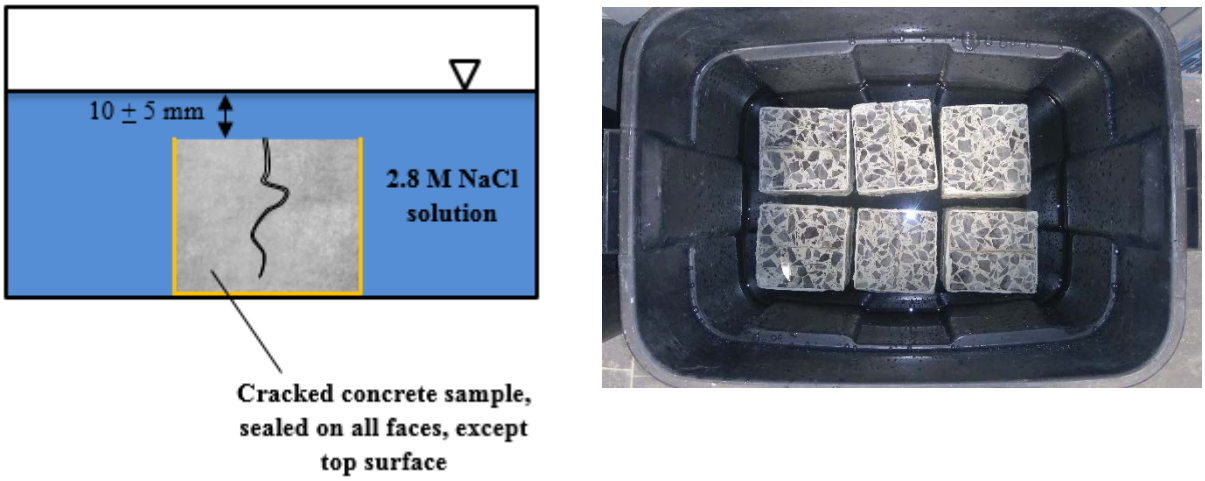

Figure 3-16: Bulk diffusion test setup (cracked concrete)

After this exposure period, the specimens were removed from the salt solution. The test specimens (uncracked/cracked) were first cut perpendicular to the exposure surface, atleast 30 mm from the edge to avoid edge effects and disturbances from the coating. Figure 3-17 shows how far from the crack (15 mm) the test specimen was cut for chloride profiling. Then the sample was sliced parallel to the exposure surface in suitable increments. The increments used for chloride profiling are described in Table 3.6 and Table 3.7. Smaller increments were used for slag concretes with w/b 0.45 due to the high chloride binding capacity of the extender and reduced porosity. Greater increments were used for the w/b 0.60 mixes as deeper chloride ingress was expected in higher w/b ratio mixes. These slices were pulverized and milled into approximately 10 g powder samples and placed in air tight resealable plastic bags. A potentiometric titrator was then used to determine the acid soluble chloride ion content, in accordance with ASTM C1152 (2012).

Table 3.6: Increments (mm) used for chloride profiling (uncracked concrete)

w/b 0.45				w/b 0.60			
100% CEM I	30% Fly-ash	50% GGCS	100% CEM III/B	100% CEM I	30% Fly-ash	50% GGCS	100% CEM III/B
0-2		0-1		0-5			
2-4		1-2		5-10			
4-6		2-3		10-15			
6-8		3-4		15-20			
8-10		4-5		20-25			
10-15		5-6		25-30			
15-20		6-8		30-35			
20-25		8-10		35-40			
25-30		10-15		-			
-		15-20		-			

Table 3.7: Increments (mm) used for chloride profiling (cracked concrete)

w/b 0.60			
100% CEM I	30% Fly-ash	50% GGCS	100% CEM III/B
0-10		0-5	
10-20		5-10	
20-30		10-15	
30-40		15-20	
40-50		20-25	
50-60		25-30	
-		30-35	
-		35-40	
-		40-45	
-		45-50	
-		50-60	

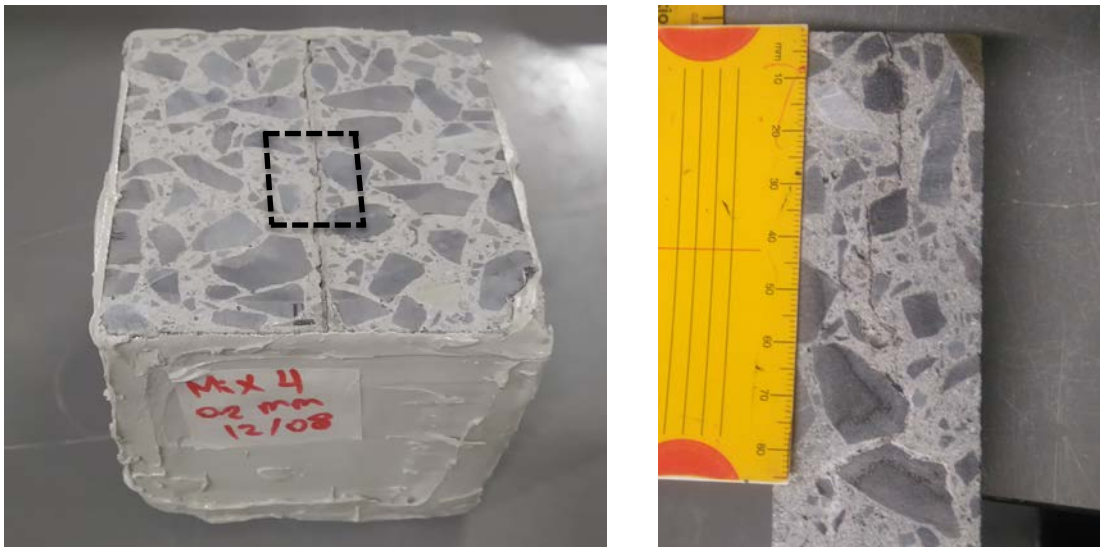

Figure 3-17: Chloride profiling method (cracked concrete)

3.4.6 Moisture profiling

The moisture profiling method was adapted from the work of Parrott (1988). Four 100 mm x 100 mm x 150 mm concrete prisms were cast for Mix 2, Mix 4 and Mix 6 using specially designed moulds that contained three removable steel pins (7 mm diameter and 80 mm long) and PVC collars. Once the concrete was demoulded and the steel pins removed, 7-mm diameter and 80 mm long cavities were obtained. These cavities were then sealed with a silicon button (with a small slit in the middle) and a hollow PVC cap (Figure 3-18).

(a) (b)

Figure 3-18: Moisture profile test mould (a) and specimen (b)

All the specimens were then placed in an environmental room (maintained at a temperature of 23 ± 2°C and relative humidity of 63 ± 2%) and wrapped in plastic sheets for 7 days. After that, all the sides of the specimen were coated with Sikadur® 32N epoxy resin, except the drying (top) surface to ensure unidirectional moisture movement. After 28 days, two of the four specimens were treated with Sikagard®-706 Thixo hydrophobic impregnation (Section 3.3.5). Relative humidity measurements were taken at various depths (4 mm, 50 mm, and 80 mm) relative to the exposure surface using a 5 mm-diameter humidity probe that was connected to a digital hygrometer as shown in Figure 3-19. An initial measurement was taken 24 hours after silane treatment and subsequently after 16 weeks.

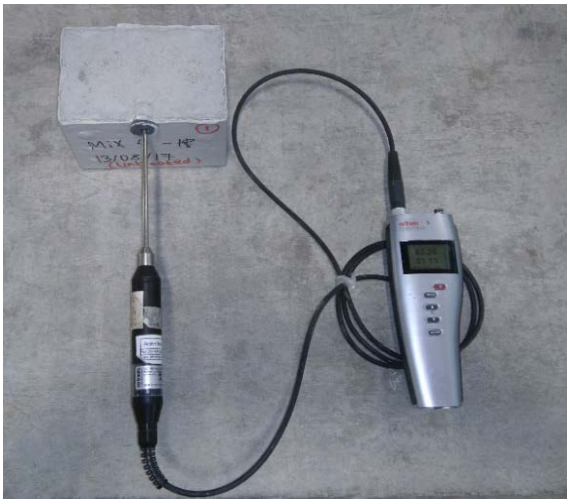

Figure 3-19: Relative humidity measurement setup

3.5 Closure

This Chapter described the experimental methods (materials, test procedures) used to achieve the aims of this thesis. Two water to binder rations (w/b 0.45, w/b 0.60) and four binder types (CEM I 52.5N, FA, GGCS, CEM III/B 42.5N) were chosen to obtain 8 main concrete mixes. The main concrete mixes were cured so as to mimic on site curing (demoulded after 24 hours, placed in an environmental room at 23 $\pm$ 2ºC and 63 $\pm$ 2% RH, wrapped in plastic sheeting until the age of 7 days and then air cured until the age of 56 days. One of the objectives of this work was to evaluate the effectiveness of hydrophobic (silane) impregnation as a remedial measure for poor quality cover concrete. Hence, in addition to these 8 main concrete mixes, 4 poor-quality concrete mixes were manufactured by exposing the concrete (strength and durability) specimens to elevated temperature at early age (after demoulding). Cracked concrete (0.2 and 0.6 mm widths) was made by loading notched reinforced concrete beams, inserting steel spacers in the notch followed by unloading. Hydrophobic (silane) impregnation was performed at an age of 28 days, using Sikagard®-706 Thixo at a consumption rate of 400 g/m^2, according to the manufacturer's product guidelines. The silane penetration depth was measured after 4 more weeks.

Compressive strength and Durability Index (DI) tests were performed to characterise the concrete mixes. Durability Index (WSI and CCI) tests were also carried out on uncut (formwork) surfaces to assess the influence of hydrophobic (silane) impregnation on the transport properties (sorptivity and conductivity) of the concrete mixes. Finally accelerated carbonation and bulk diffusion tests were conducted to evaluate the effect of silane impregnation on the concrete's resistance to carbonation and chloride ingress respectively. The data obtained from the bulk diffusion test was thereafter used in the service life modelling of untreated/treated concrete (Chapter 5). Moisture profiling was performed to evaluate the influence of silane impregnation on the relative humidity in the concrete.

4. Results and discussions

This chapter analyses and discusses the results obtained from experimental testing as described in Chapter 3. The compressive strength, Durability Index, accelerated carbonation, bulk diffusion and moisture profiling test results are provided in the following sections.

4.1 Compressive strength

Compressive strength tests were performed using three 100 mm cubes (as described in Section 3.4.1. The test was carried out at 3, 7 and 28 days to characterise the concrete mixes and monitor strength development. Section 4.1.1 and 4.1.2 present the compressive strength test results for the main and poor-quality mixes respectively.

4.1.1 Main mixes

The compressive strength was calculated by dividing the maximum uniaxial force with the cross-sectional area of the cube specimen. The compressive strength test results for the main mixes are displayed in Figure 4-1. The detailed results for each cube specimen are provided in Appendix A.

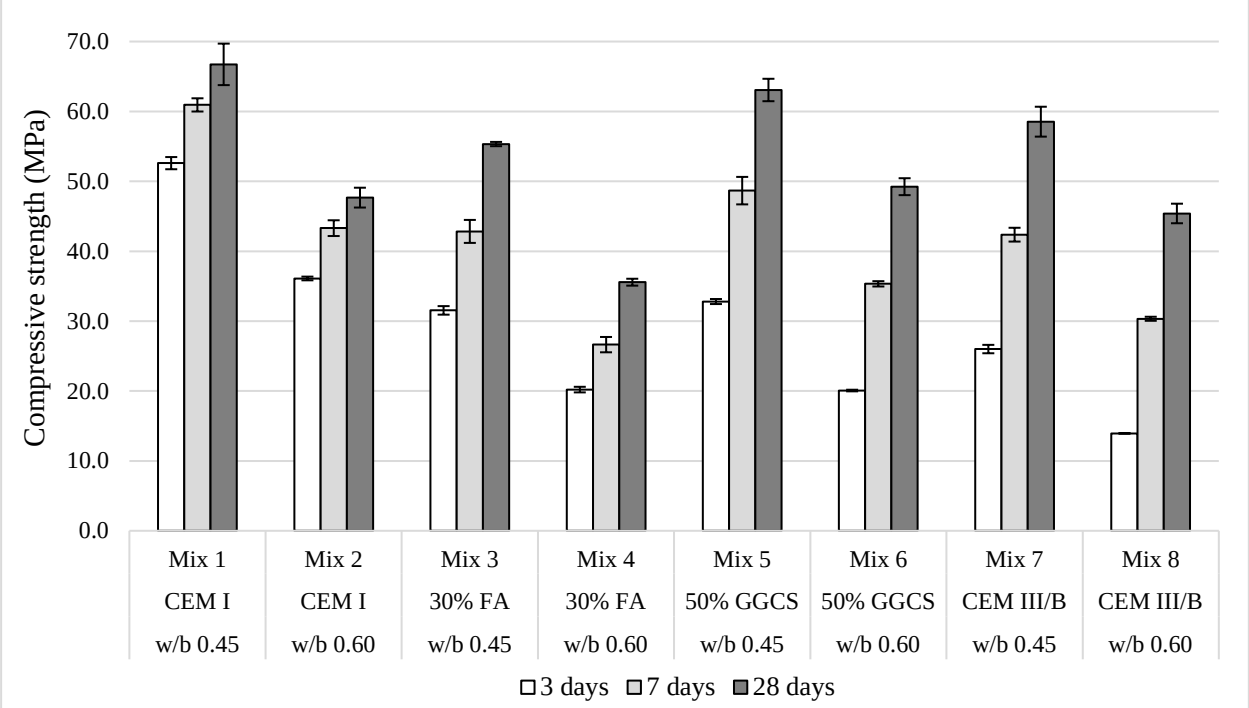

Figure 4-1: Compressive strength test results (main mixes) (error bars indicate STDV)

As expected, the compressive strength of the mixes increased with a reduction in w/b ratio and increasing age. Lower w/b ratio concrete mixes have a less porous and stronger cement paste matrix and a more refined microstructure, particularly at the interfacial transition zone (ITZ) between the paste and aggregate, which is the weak link partially governing the compressive strength of concrete. Extended curing promotes the hydration reaction, leading to an increase in compressive strength with age (Alexander & Beushausen, 2009).

For the same w/b ratio, relative to the CEM I mixes (Mix 1 and Mix 2), the inclusion of fly-ash generally decreased the compressive strength of the concrete at all ages. This can be attributed to the slower pozzolanic reactions and significantly lower calcium content that does not contribute to strength development at early age (Siddique *et al.*, 2011). The GGCS mixes (Mix 5 and Mix 6) displayed a lower compressive strength at early age but similar 28-day compressive strength relative to the CEM I mixes (Mix 1 and Mix 2). Corex slag concrete is known to display more rapid strength development after 3 days relative to other slag concretes (Alexander *et al.*, 2003). The CEM III/B mixes (Mix 7 and Mix 8) showed a decrease in compressive strength at early age relative to the CEM I mixes (Mix 1 and Mix 2). However, this difference in compressive strength was less apparent at 28 days. Slags react relatively slower than Portland cement to form the same hydration products, calcium silicates (C-S-H) leading to a reduction in early strength development. The strength approaches that of plain cement concrete and can be slightly higher at later ages (Nawy, 2008; Ramezanianpour, 2014). It must be noted that CEM I 52.5N and CEM III/B 42.5N were used for Mix 1/Mix 2 and Mix 7/Mix 8 respectively. Higher cement classes generally produce concrete with higher strength due to finer clinker content (greater rate of hydration).

4.1.2 Poor quality mixes

The compressive strength test results for the poor-quality mixes are displayed in Figure 4-2. The results of the control mixes (Mix 2, Mix 4, Mix 6, and Mix 8) are repeated here for the sake of comparison. The detailed results for each cube specimen are provided in Appendix A.

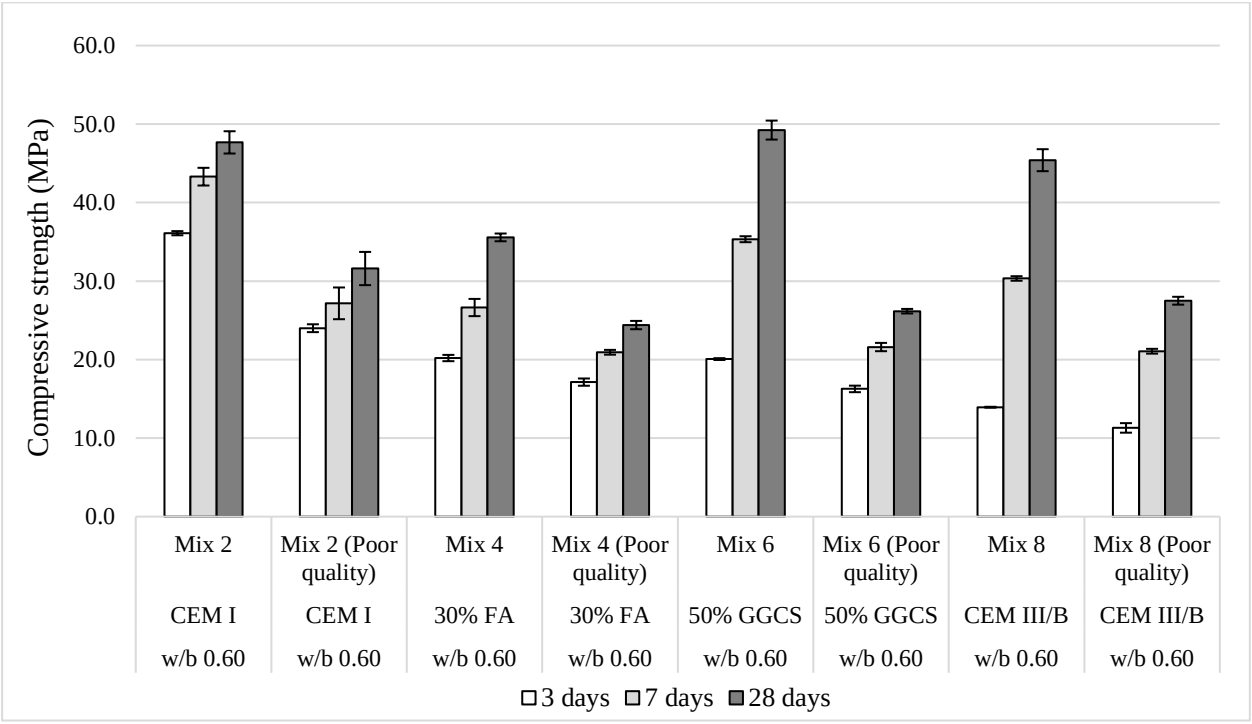

Figure 4-2: Compressive strength test results (poor quality mixes) (error bars indicate STDV)

According to Figure 4-2, it is evident that, at all ages, the poor-quality mixes display lower compressive strength relative to their respective control mixes. Since the concrete was subjected to

high temperatures at early age, the moisture content in the capillaries was reduced. Hence, cementing (hydration) reactions were slowed down, leading to a reduction in strength development. The lower compressive strength of Portland cement concrete (Mix 2 poor) at elevated temperatures (80°C) could potentially also be attributed to the poor distribution of rapidly forming hydration products which contributed to a porous microstructure. It must be noted that Mix 2 poor achieved the highest strength among the poor-quality mixes because cement extenders such as fly-ash, GGCS and GGBS react slower relative to Portland cement and hence affect the strength to a greater extent (Alexander & Beushausen, 2009; Mehta *et al.*, 2006; Thomas, 2013; Siddique *et al.*, 2011).

4.2 Durability Index

Durability Index (DI) tests were performed on cut surfaces (for mix characterisation) and uncut surfaces (to assess the influence of silane impregnation on transport properties such as capillary water absorption and chloride conductivity).

4.2.1 Cut surfaces

4.2.1.1 Oxygen Permeability Index (OPI)

The OPI test results (for mix characterisation purposes) are shown in Figure 4-3. The test was carried out as explained in Section 3.4.2.1. The detailed results are provided in Appendix B.

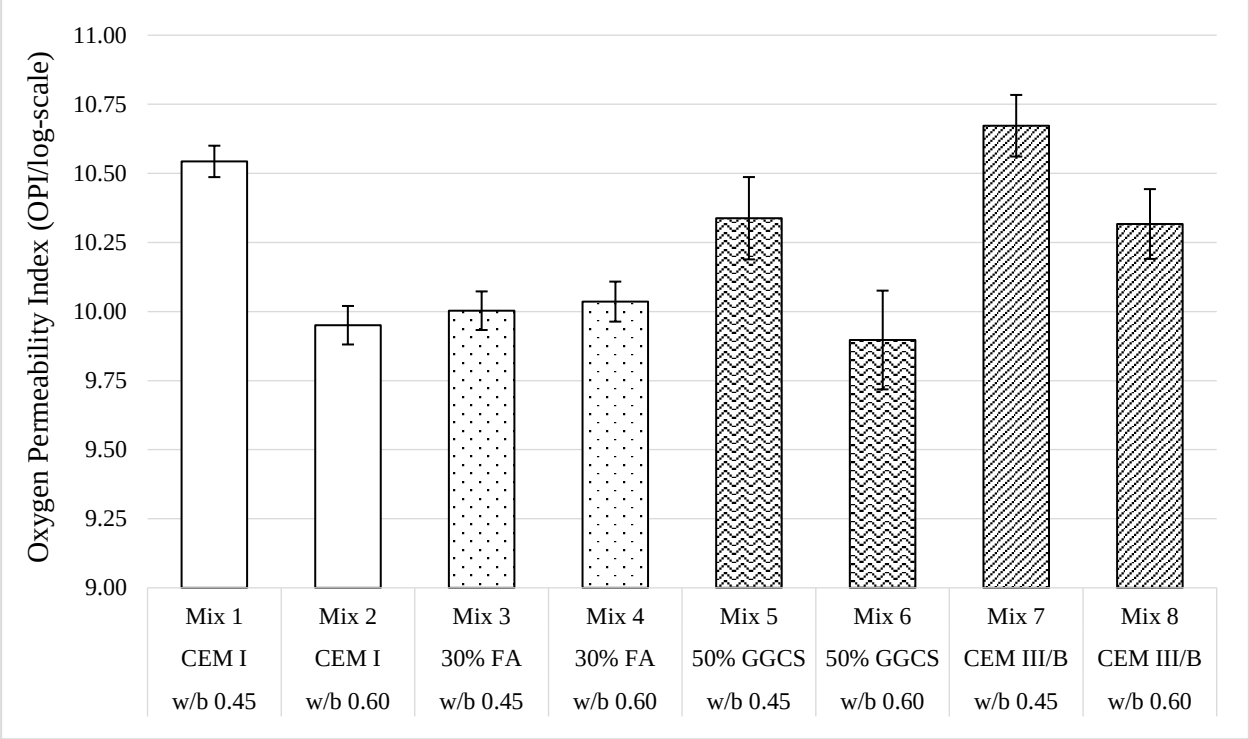

Figure 4-3: Oxygen Permeability Index (OPI) test results (main mixes) (error bars indicate STDV)

Common OPI values for South African concretes range from 8.5 to 10.5, a higher value indicating higher impermeability and thus a concrete of potentially higher quality (Alexander & Beushausen,

2009). From Figure 4-3, it can be noted that, except for the fly-ash mixes (Mix 3 and Mix 4), the OPI values decreased with an increase in w/b ratio. This can be attributed to a more porous cement paste matrix which is more permeable to pressurised gas. Similar results can be found in literature (Alexander & Beushausen, 2009) and previous works (Salvoldi *et al.*, 2015; Kanjee, 2015).

Comparing the w/b 0.45 mixes, except for Mix 3, the overlapping of the error bars suggests similar results between Mix 1, Mix 5 and Mix 7. The lower OPI value of Mix 3 can be explained by the slower pozzolanic reactions of concrete containing fly-ash that result in more permeable concrete at early ages. (Thomas, 2013; Nawy, 2008) Comparing the w/b 0.60 mixes, similar OPI values were recorded between Mix 2, Mix 4 and Mix 6. It must be noted that Mix 8 (100% CEM III/B) displayed a higher OPI value relative to Mix 2 (100% CEM I). This can be explained by the fact that the use of GGBS contribute to pore size refinement and the production of a denser concrete microstructure with lower permeability (Siddique *et al.*, 2011).

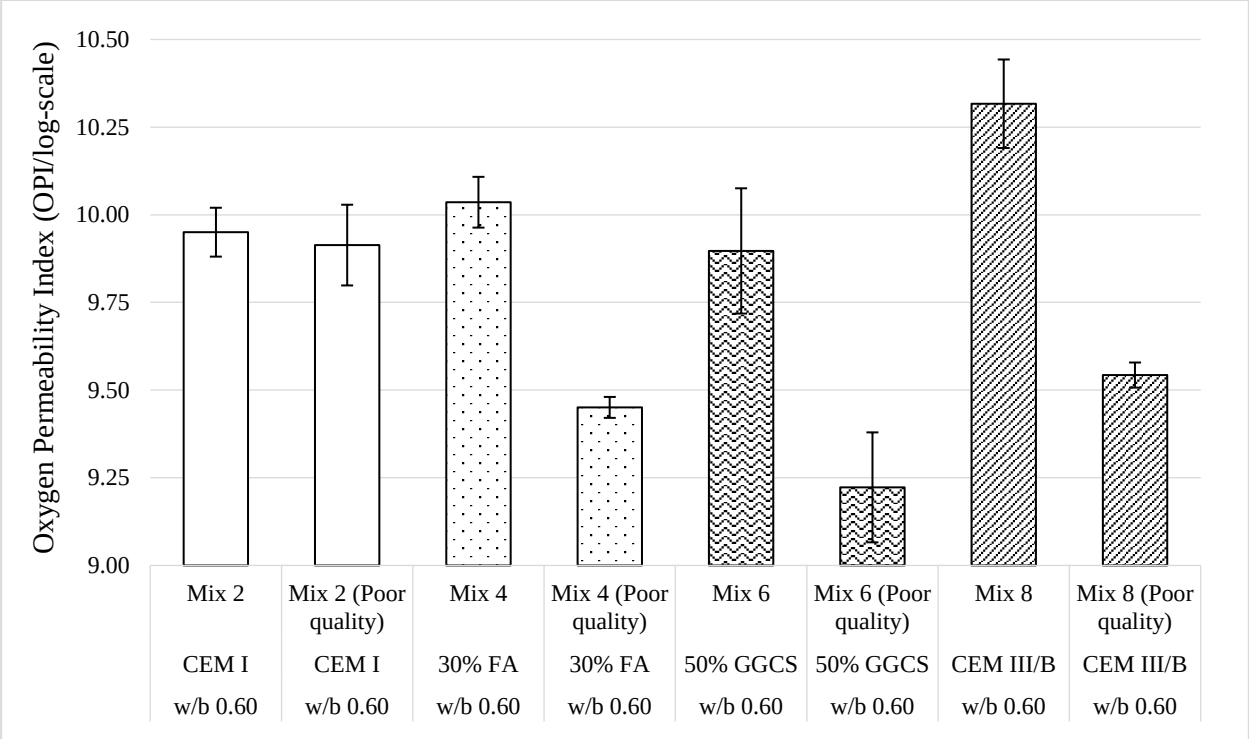

Figure 4-4: Oxygen Permeability Index (OPI) test results (poor quality mixes) (error bars indicate STDV)

From Figure 4-4, it must be noted that, except for Mix 2 poor, OPI values near or below 9.50 were recorded, suggesting that poor quality mixes (in terms of permeability) were successfully obtained under laboratory conditions. Since the concrete was subjected to elevated temperatures at early age, the moisture content in the capillaries was reduced, leading to a reduction in the hydration reactions. This resulted in a significant loss in concrete quality and the resistance to the ingress of chemical species was reduced.

4.2.1.2 Water Sorptivity Index (WSI)

The Water Sorptivity Index test results (for mix characterisation) are presented in Figure 4-5 and Figure 4-7. The test was performed as described in Section 3.4.2.2. The detailed results are provided in Appendix B.

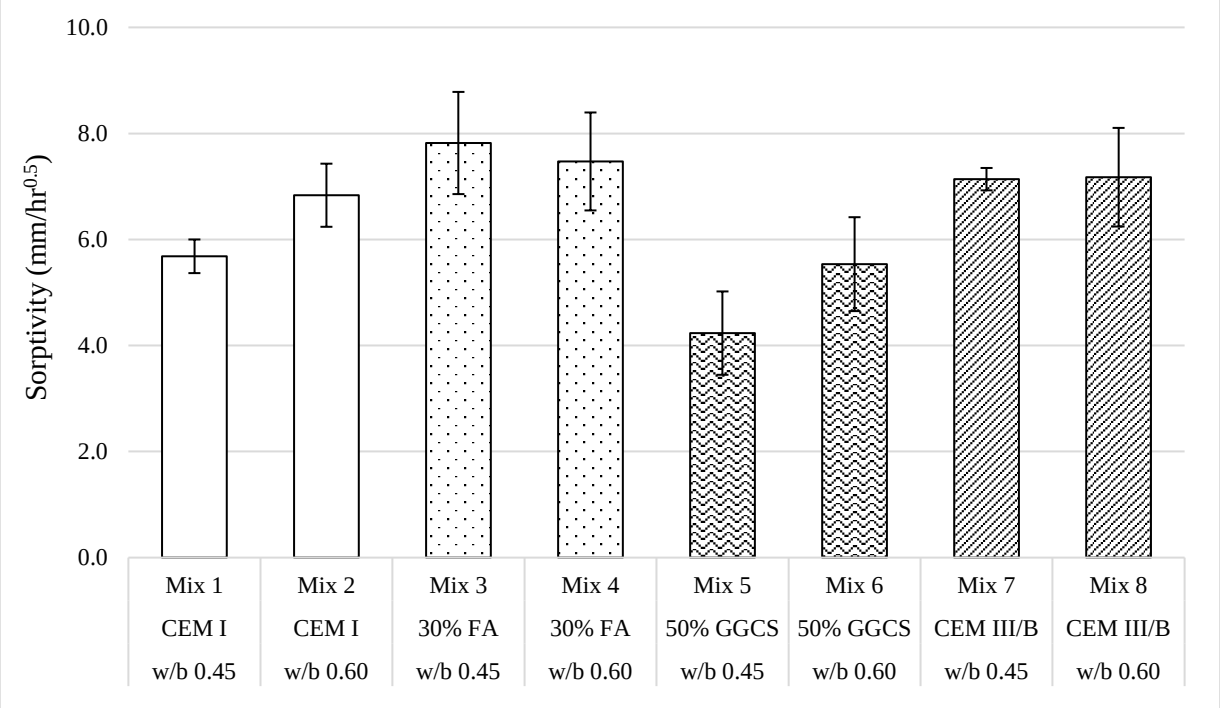

Figure 4-5: Water Sorptivity Index (WSI) test results (main mixes) (error bars indicate STDV)

Typical WSI values for good quality concrete range from 6-10 mm/hr$^{0.5}$ (Alexander *et al.*, 2017), and from Figure 4-5, the overall results suggest that the concrete mixes will have adequate resistance to the capillary absorption of liquids. The effect of changing w/b ratio is reflected in the CEM I-based mixes (Mix 1 and Mix 2). A higher w/b ratio increased the sorptivity of the mix and this can be explained by the increase in porosity within the paste microstructure (Alexander & Beushausen, 2009).

Comparing the w/b 0.60 mixes (Mix 2, Mix 4, Mix 6 and Mix 8), the overlapping of the error bars suggests similar results between the sorptivity results. The influence of binder type was more noticeable in the w/b 0.45 mixes; the sorptivity of the concrete mix increased with the inclusion of fly-ash (Mix 3) and use of CEM III/B (Mix 7) while the replacement of CEM I with GGCS (Mix 5) reduced sorptivity. The higher sorptivity of Mix 3 and Mix 7 can be explained by the slower pozzolanic reactions of fly-ash that results in a more permeable concrete at early ages and the slower cementing reaction rates of CEM III/B (80% GGBS/20% PC) relative to CEM I (close to 100% PC) respectively (Thomas, 2013; Nawy, 2008). The reduction in sorptivity in Mix 5 may be attributed to superior (enhanced) reactivity of Corex slag relative to other slags that improves the durability properties of concrete (Alexander *et al.*, 2003). The porosity test results for the main mixes (for mix characterisation) are presented in Figure 4-6. The detailed results are provided in Appendix B.

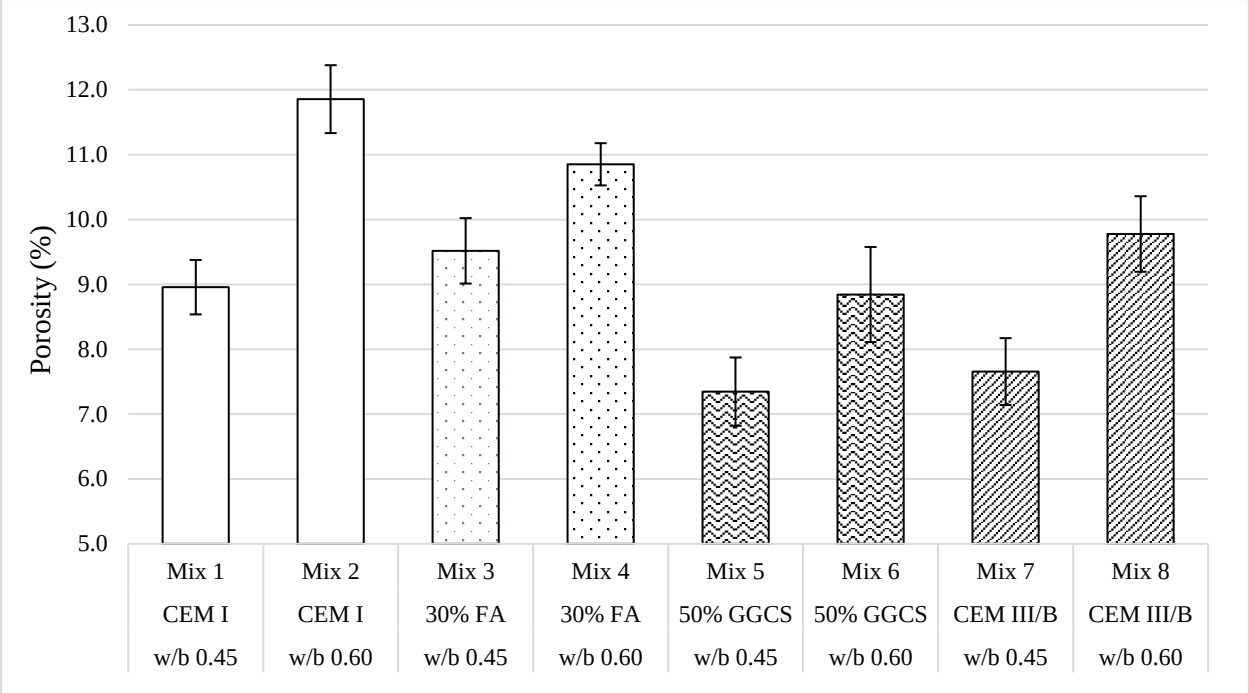

Figure 4-6: Porosity test results (main mixes) (error bars indicate STDV)

From Figure 4-6, as expected, there is a clear influence of water to binder ratio (w/b) on the porosity of the concrete mixes; an increase in w/b lead to higher porosity. This result is well documented in literature (Mehta *et al.*, 2006; Alexander & Beushausen, 2009; Mindess *et al.*, 2003; Soutsos, 2010). As the hydration process occurs, the void (water filled) space in between cement particles is gradually filled with hydration products. However, in higher w/b ratio mixes, the cement grains are further apart, and the extent to which hydration products can fill up the space is limited. This results in greater capillary voids (porosity) after hydration.

Comparing the w/b 0.45 mixes, Mix 3 shows similar porosity to Mix 1 (as indicated by the overlapping error bars). On the other hand, Mix 5 and Mix 7 displayed lower porosity relative to Mix 1. For the w/b 0.60 mixes, the use of blended cements (Mix 4, Mix 6 and Mix 8) resulted in a decrease in capillary porosity compared to Mix 2. These results can be explained by the fact that the use of supplementary cementitious materials such as FA, GGCS and GGBS tend to refine the concrete pore structure over time (Soutsos, 2010). The moderately small, glassy texture and spherical shape allow low calcium (Class F) fly-ash particles to act as fillers while GGCS and GGBS react with calcium hydroxide to form extra hydrated calcium silica hydrates in the paste. These reactions lead to the densification of the concrete microstructure and a reduction in porosity (Ramezanianpour, 2014; Siddique *et al.*, 2011).

The WSI test results for the poor-quality mixes are shown in Figure 4-7. The detailed results are provided in Appendix B. From the results, except for Mix 2 poor, all the poor-quality mixes show an increase in sorptivity to values greater than 10 mm/hr$^{0.5}$ relative to their respective control mixes. This can be attributed to the fact that the concrete was subject to high temperature at early age. As the moisture content was reduced, cementing (hydration) reactions were slowed down, leading to the creation of a relatively more porous microstructure and consequently a reduction in concrete quality (Alexander & Beushausen, 2009; Soutsos, 2010).

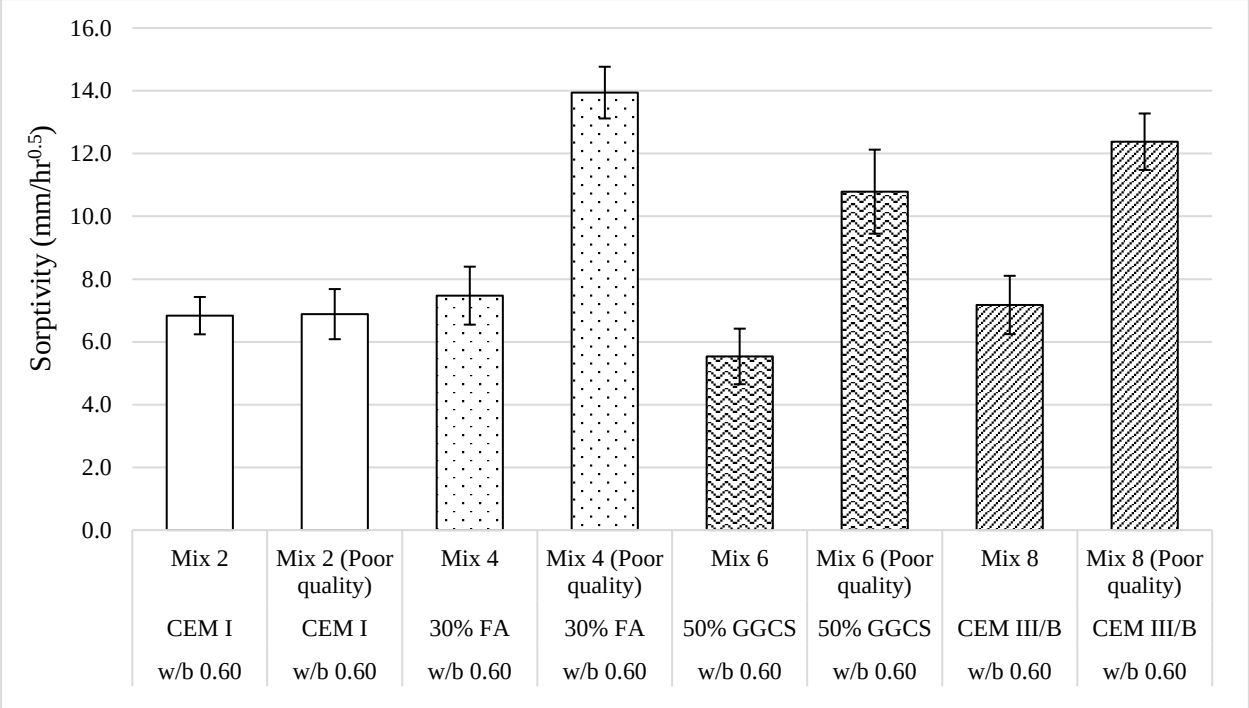

Figure 4-7: Water Sorptivity Index (WSI) test results (poor quality mixes) (error bars indicate STDV)

The porosity test results for the poor-quality mixes are shown in Figure 4-8. Apart from Mix 2 poor, all the poor-quality mixes display an increase in porosity. This can be attributed to the insufficient curing (slower hydration reactions) that lead to the development of a relatively more porous cement paste matrix (Alexander & Beushausen, 2009; Poursaee, 2016).

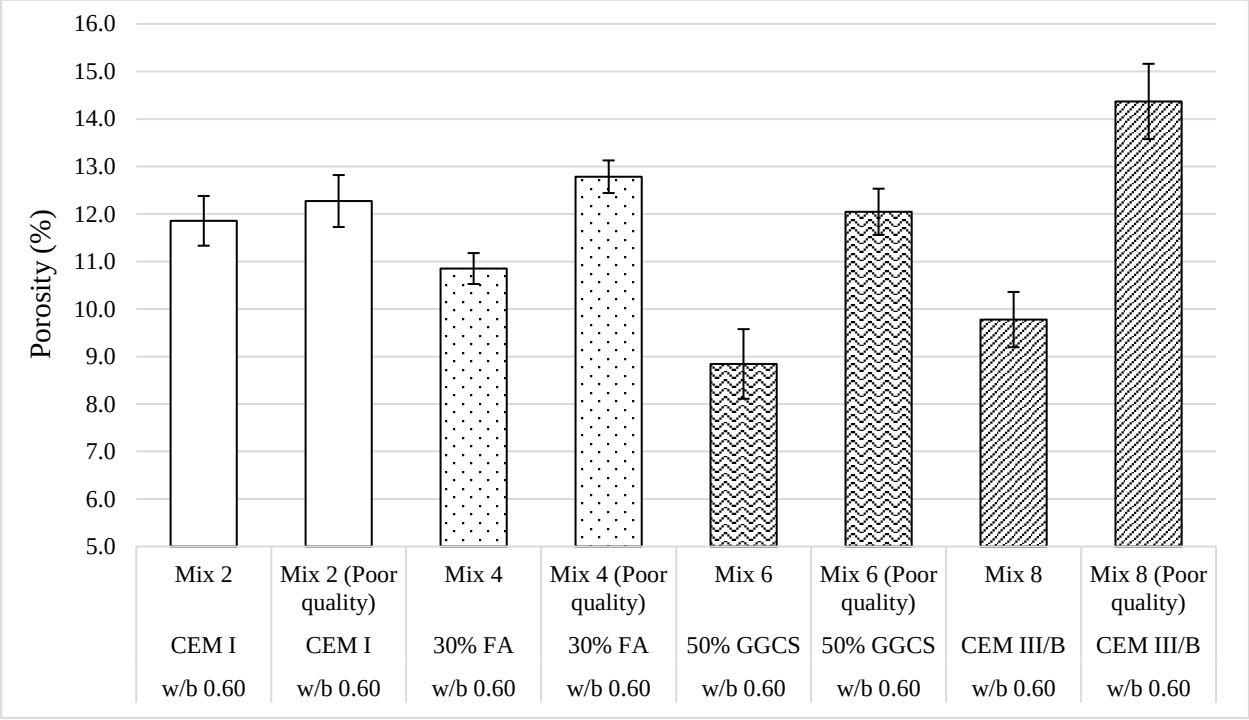

Figure 4-8: Porosity test results (poor quality mixes) (error bars indicate STDV)

4.2.1.3 Chloride Conductivity Index (CCI)

The Chloride Conductivity Index (CCI) test results (for mix characterisation) are summarised in Figure 4-9 and Figure 4-10. The test was performed as described in Section 3.4.2.3. The detailed results for individual specimens are provided in Appendix B. From the results, there is a clear influence of w/b ratio on the CCI values; as the w/b ratio is increased, the CCI values increased accordingly. This observation is due to the increase in porosity of the cement paste matrix which allows greater migration of chloride ions (Alexander & Beushausen, 2009). A higher w/b ratio also correlates to a larger number of interconnections between the pores which act as channels of flow in the cement paste (Mehta *et al.*, 2006).

As expected, for the same w/b ratio, the inclusion of GGCS and GGBS reduced the CCI values significantly. These supplementary cementitious materials increase the resistivity of concrete and hence reduce the movement of chloride ions within the pore structure under an externally applied potential difference. Furthermore, GGCS and GGBS can react with calcium hydroxide to form extra hydrated calcium silica hydrates in the cement paste matrix. These reactions lead to the densification of the concrete microstructure and a reduction in porosity which overall reduce the penetrability to chloride ions. The fly-ash mixes (Mix 3 and Mix 4) recorded similar CCI values relative to the CEM I mixes (Mix 1 and Mix 2) (Ramezanianpour, 2014; Siddique *et al.*, 2011).

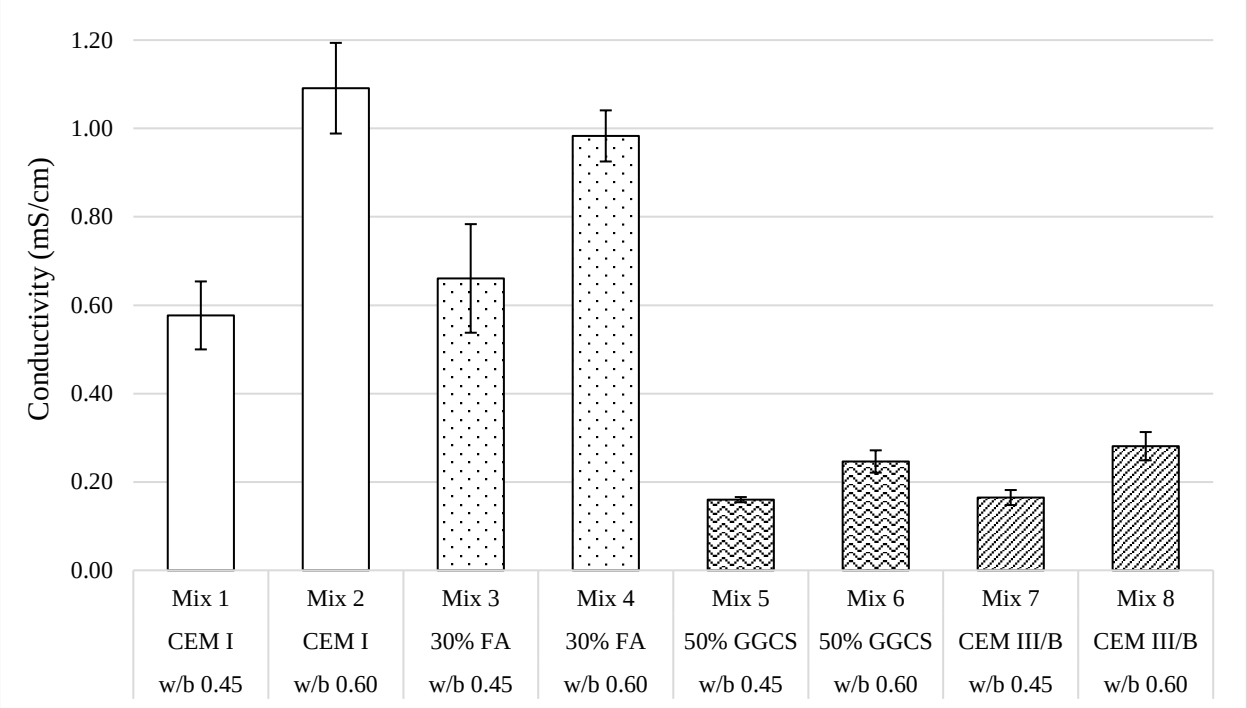

Figure 4-9: Chloride Conductivity Index (CCI) test results (main mixes) (error bars indicate STDV)

The CCI test results for the poor-quality mixes are shown in Figure 4-10. The detailed results are provided in Appendix B. Relative to the respective control mixes, all the poor-quality mixes show an increase in chloride conductivity. Values greater than 1.50 mS/cm in Mix 2 poor and Mix 4 poor suggest that these mixes will have poor resistance to chloride ingress (Alexander *et al.*, 2017). It must be emphasized that despite the high porosity of Mix 6 poor and Mix 8 poor, the chemical

resistance of these slag concretes to chloride ions still contribute to a reduction in CCI values relative to Mix 2 poor and Mix 4 poor.

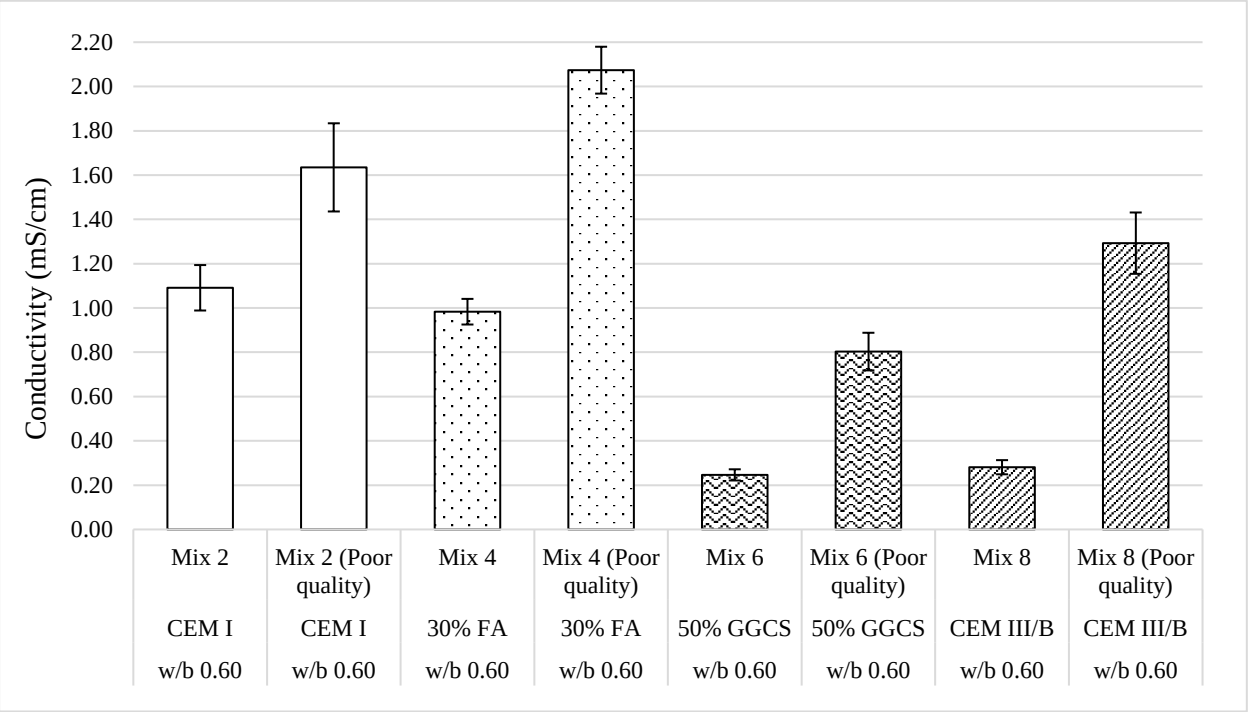

Figure 4-10: Chloride Conductivity Index (CCI) test results (poor-quality mixes) (error bars indicate STDV)

4.2.2 Uncut surfaces

Water Sorptivity Index (WSI) and Chloride Conductivity Index (CCI) tests were also performed on uncut concrete discs to evaluate the influence of silane (hydrophobic) impregnation on the transport properties (sorptivity and conductivity) of the concrete mixes. It must be noted that these Durability Index tests are not designed to test concrete treated with silane impregnation and these tests were carried out for comparison purposes only.

4.2.2.1 Water Sorptivity Index (WSI)

The WSI test results for the main mixes and poor-quality mixes are summarised in Figure 4-11 and Figure 4-12 respectively. The detailed results are provided in Appendix B. For all the mixes, the treated concrete shows a significant reduction in sorptivity, as expected. As discussed in Section 2.8, hydrophobic (silane) impregnation chemically modifies the near surface zone of concrete and reduces the capillary uptake of water (Raupach, 2014; Liu, 2017). Similar observations were made in previous research that studied the effect of hydrophobic impregnation on capillary suction of water in concrete (Gerdes & Wittmann, 2001; Medeiros & Helene, 2008; Zhang *et al.*, 2017). The results also suggest that the durability properties of poor quality concrete can be substantially improved through hydrophobic impregnation. However, it must be emphasized that the resistance to capillary absorption is increased only within the impregnated layer and the rest of the concrete is still characterised as poor quality.

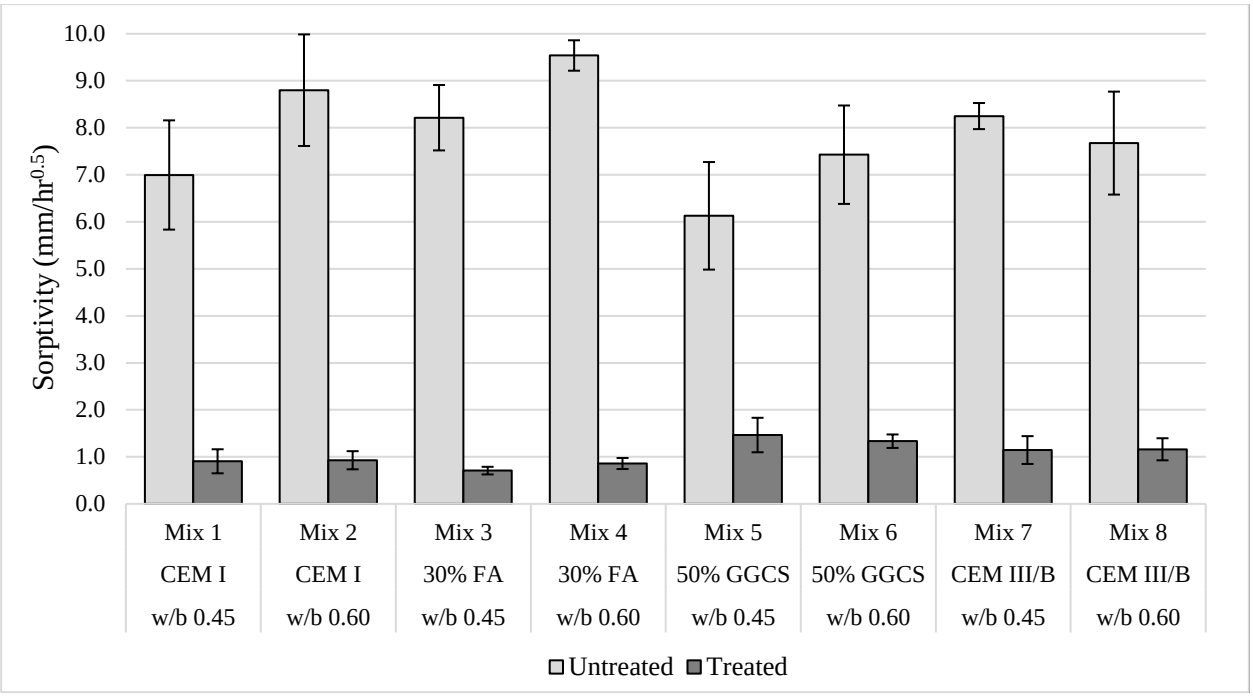

Figure 4-11: Water Sorptivity Index (WSI) test results (untreated vs treated – main mixes) (error bars indicate STDV)

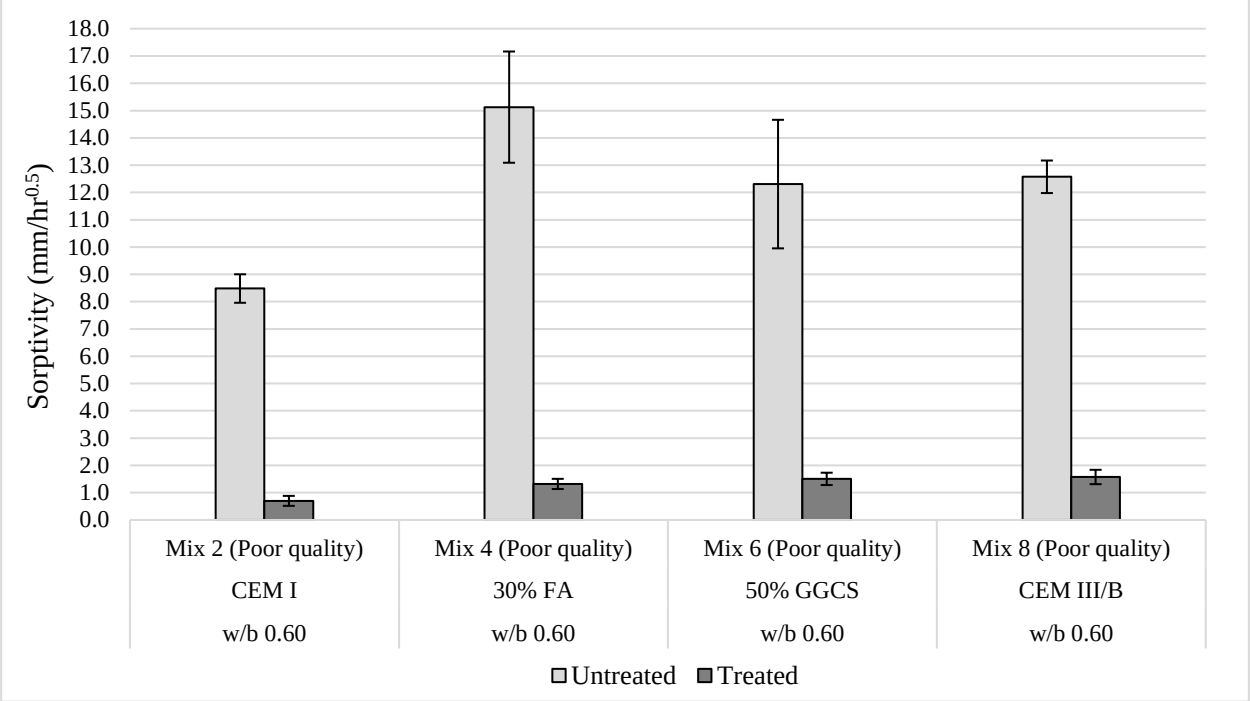

Figure 4-12: Water Sorptivity Index (WSI) test results (untreated vs treated – poor quality mixes) (error bars indicate STDV)

4.2.2.2 Chloride Conductivity Index (CCI)

The CCI test results for the main mixes and poor-quality mixes are summarised in Figure 4-13 and Figure 4-14 respectively. The detailed results are provided in Appendix B. According to the results, the CCI values are reduced for treated concrete and the effect is more pronounced in the

CEM I mixes (Mix 1/Mix 2), FA mixes (Mix 3/Mix 4) and poor-quality mixes (Mix 2 poor, Mix 4 poor, Mix 6 poor and Mix 8 poor). Similar results were obtained in previous works which investigated the effect of hydrophobic impregnation on chloride migration (Medeiros & Helene, 2008; Medeiros *et al.*, 2016), although the researchers made use of different test methods.

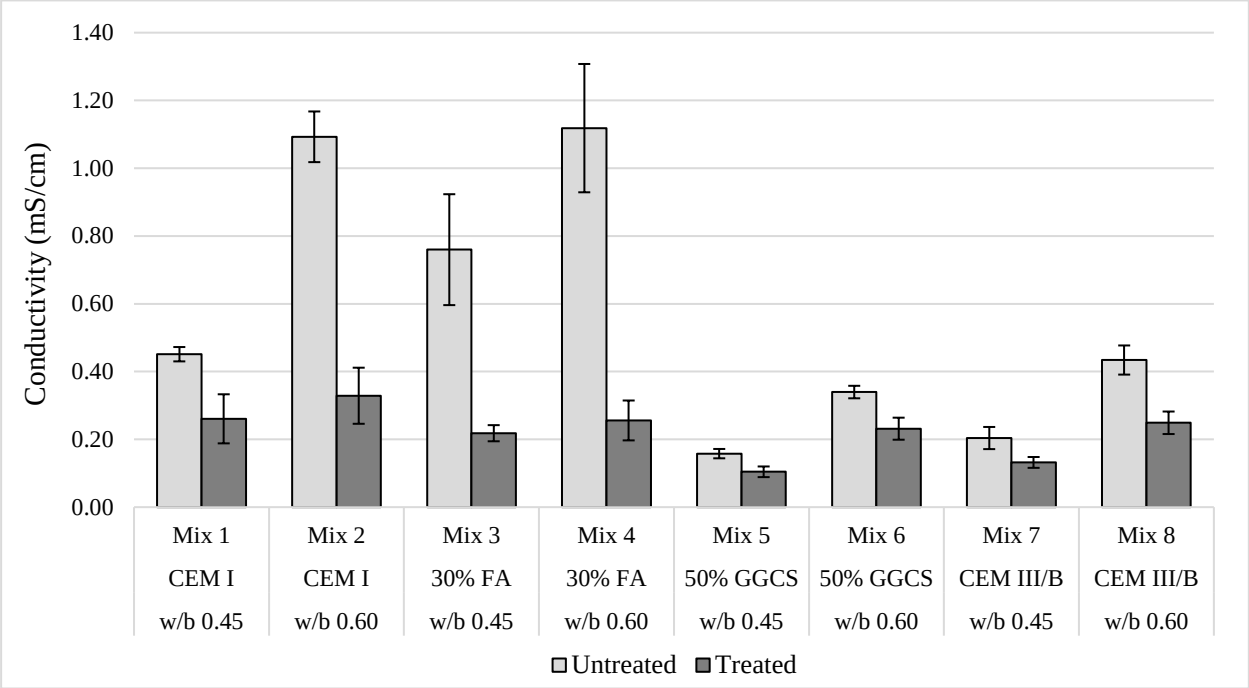

Figure 4-13: Chloride Conductivity Index (CCI) test results (untreated vs treated – main mixes) (error bars indicate STDV)

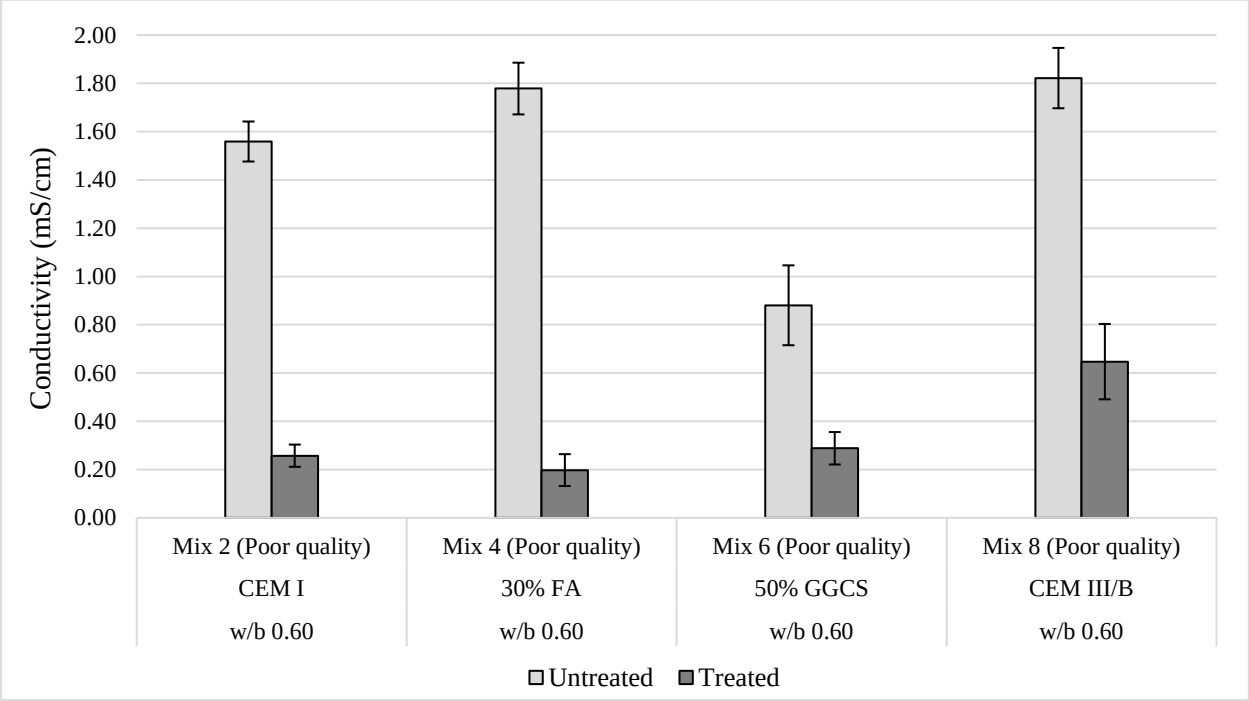

Figure 4-14: Chloride Conductivity Index (CCI) test results (untreated vs treated – poor quality mixes) (error bars indicate STDV)

The lower CCI values can be explained by the lower saturation of the treated concrete; Chloride migration requires a continuous moisture path. (Li, 2017; Poursaee, 2016; Zhang, 2017)

4.3 Penetration depth

The silane penetration depth test results for the main and poor-quality mixes are summarised in Figure 4-15 and Figure 4-16 respectively. The detailed results are provided in Appendix C.

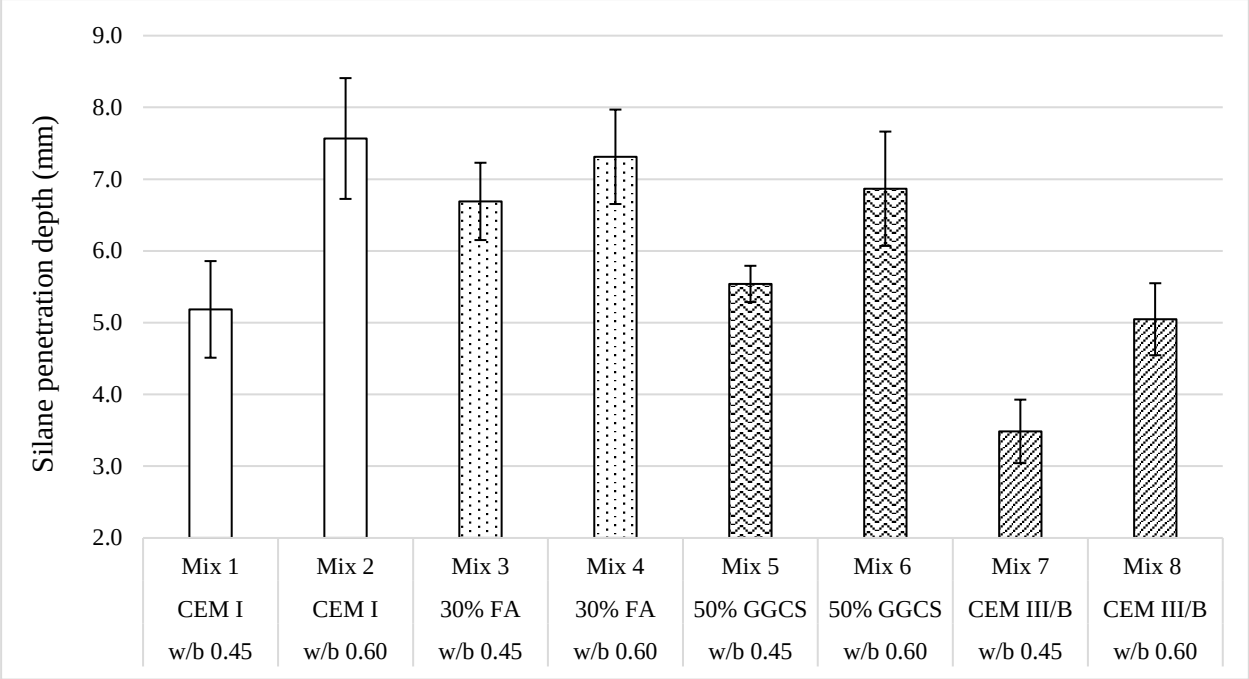

Figure 4-15: Silane penetration depth test results (main mixes) (error bars indicate STDV)

From Figure 4-15, an increase in w/b ratio correlated to a deeper penetration depth. This can be attributed to higher capillary porosity of the cement paste matrix which allows greater penetration of the water repellent product. Similar observations were made in previous research by Bofeldt & Nyman (2002), Johansson (2006) and Meier & Wittman (2011). The effect of binder type for the w/b 0.60 mixes was unclear due to the overlapping of error bars but for the w/b 0.45 mixes, the inclusion of FA and GGBS (CEM III/B) increased and reduced the penetration depth respectively. Fly-ash usually increases the porosity of concrete at early age due to slower pozzolanic reactions that do not contribute to matrix densification while GGBS reduces capillary porosity by forming additional hydrated calcium silica hydrates in the cement paste matrix (Ramezanianpour, 2014, Thomas, 2013).

According to Figure 4-16, except for Mix 2 poor, the penetration depth of the silane is greater in poor quality concrete. This can be related to the more porous cement paste microstructure that enables the product to penetrate deeper into the concrete. It must be also noted that the concrete was subject to high temperature at early age and the moisture content in the capillary pores was reduced compared to the control mixes. As the water repellent agent enters the pore system primarily by capillary suction, a higher penetration depth is generally expected in less saturated (drier) concrete (Selander, 2010; Meier & Wittman, 2011).

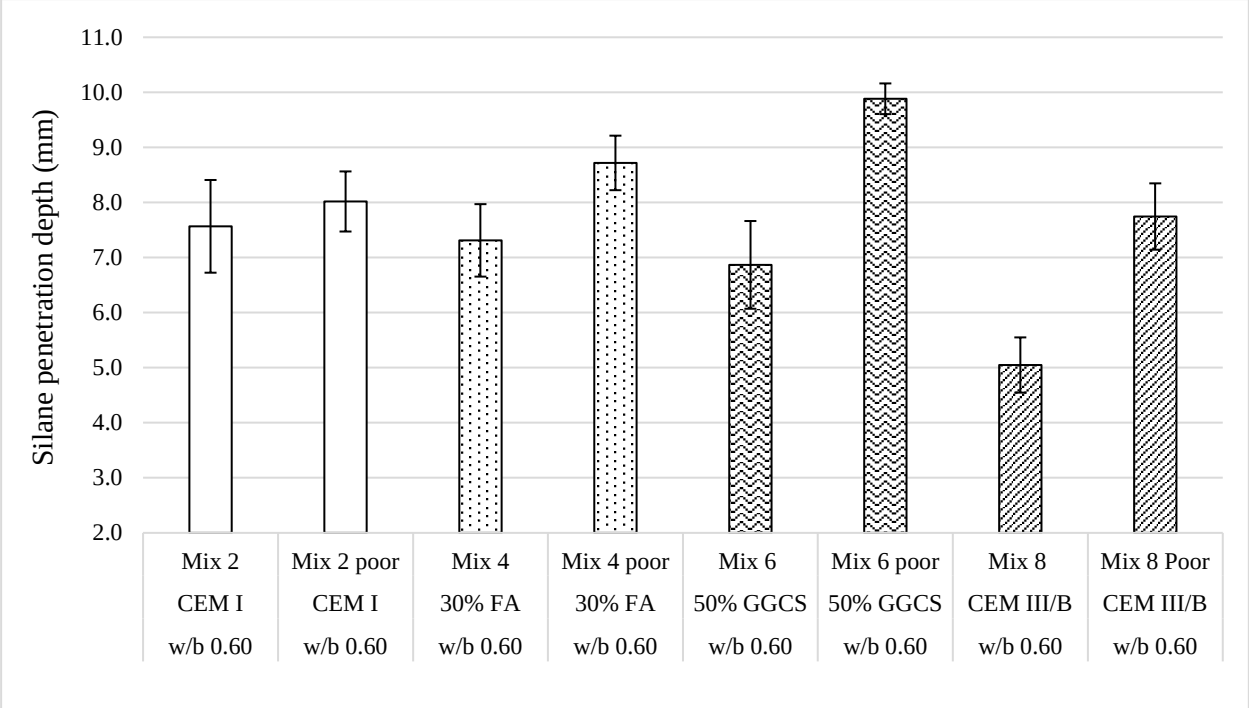

Figure 4-16: Silane penetration depth test results (poor-quality mixes) (error bars indicate STDV)

From Figure 4-17, as expected, the porosity of the concrete mixes was related to the silane penetration depth. A reasonable linear correlation value (R^2 = 0.60) was obtained. The correlation to the Water Sorptivity Index (Figure 4-18) was unexpectedly low (R^2 = 0.37), as the water repellent product enters concrete mainly through capillary action (Meier & Wittman, 2011).

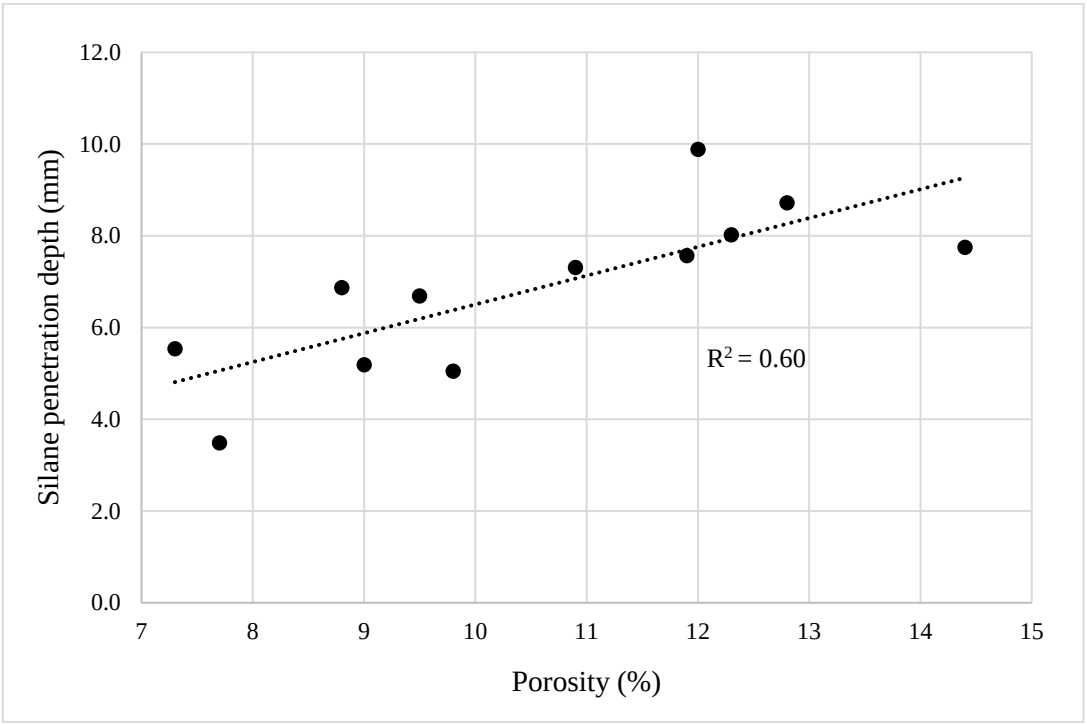

Figure 4-17: Correlation between silane penetration depth (mm) and porosity (%)

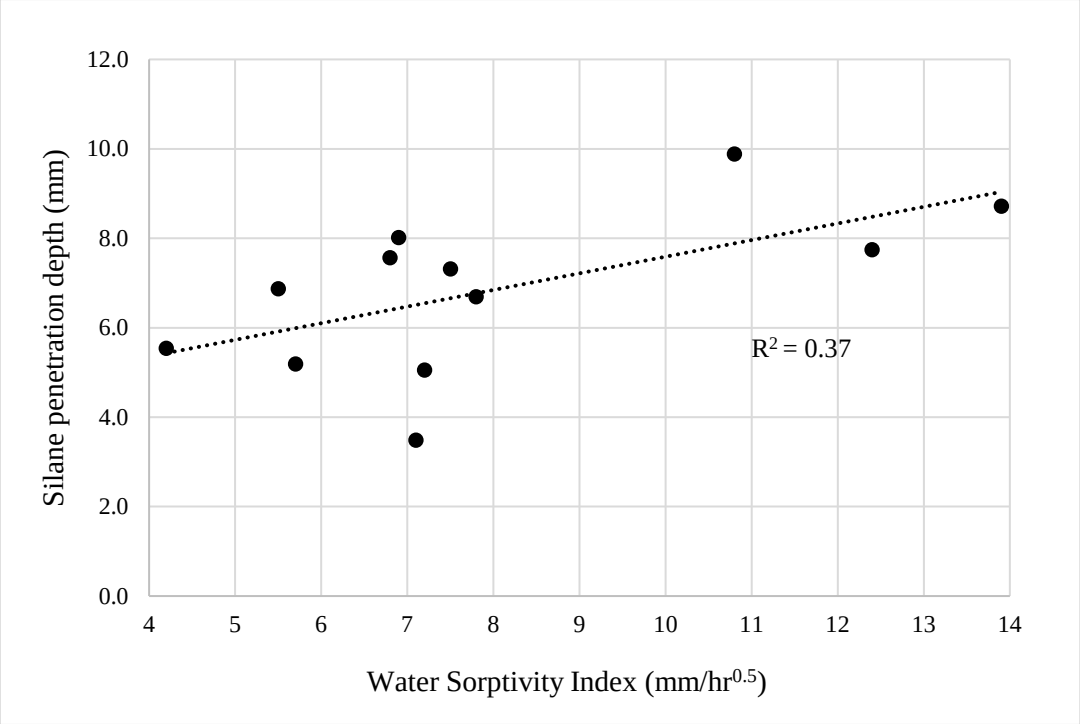

Figure 4-18: Correlation between silane penetration depth (mm) and WSI (mm/hr$^{0.5}$)

From the experimental results, the silane penetration depth (measured at an age of 56 days) was also observed to be related to the Oxygen Permeability Index (tested at 56 days). The penetration depth of the water repellent product increased with lower OPI values (Figure 4-19). A good positive linear correlation (R^2 = 0.90) was observed between the silane penetration depth and Oxygen Permeability Index, suggesting a useful relationship between the independent variable (silane penetration depth/mm) and dependent variable (Oxygen Permeability Index/log-scale).

The OPI test evaluates the overall micro and macrostructure of the outer surface of the cast concrete and is predominantly sensitive to macro-voids and cracks which provide short-circuit routes for the permeating gas. Hence, this test is useful to assess the extent of compaction, presence of bleed voids and channels and the degree of interconnectedness of the pore structure (Salvoldi *et al.*, 2015). Since the silane penetration depth is a function of the quality of the concrete (Meier & Wittman, 2011), the OPI test provides a good estimate of the silane penetration depth potential in concrete mixes. However, it must be emphasized that in this study the number of mixes was limited to 12 and therefore the linear correlation value (R^2) is potentially overestimated.

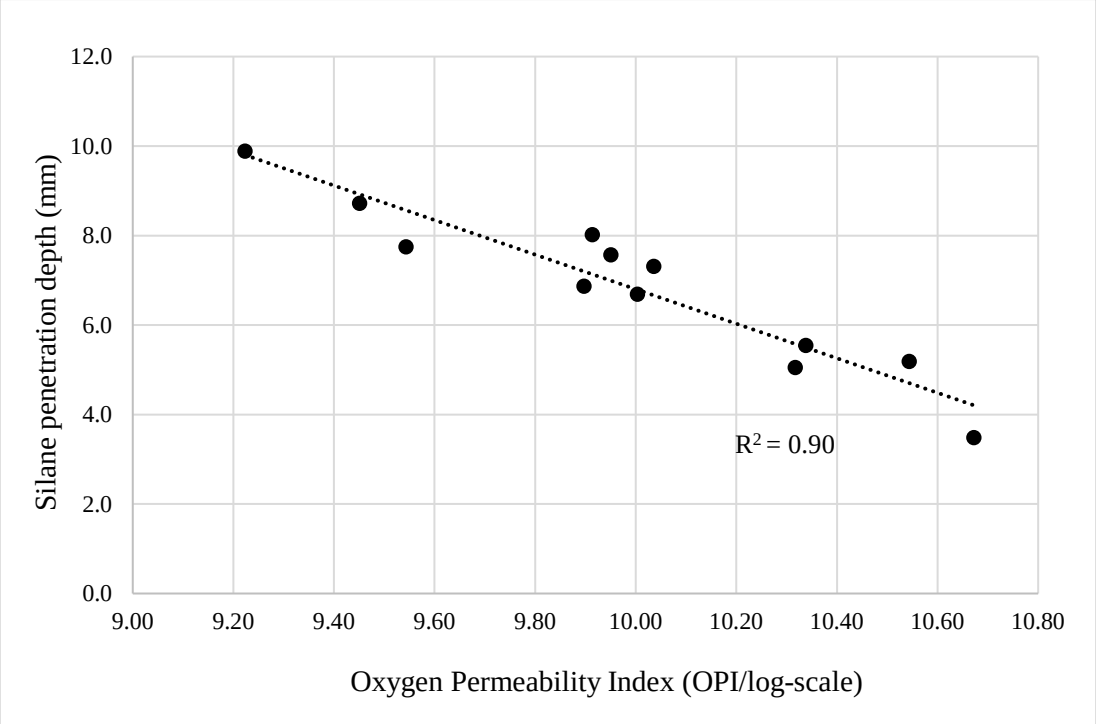

Figure 4-19: Correlation between silane penetration depth (mm) and OPI (log-scale)

4.4 Accelerated carbonation

The accelerated carbonation test results for the main mixes and poor-quality mixes are shown in Figure 4-20 and Figure 4-21 respectively. The detailed results are provided in Appendix D. According to Figure 4-20, comparing the untreated mixes, the carbonation depth increases with higher w/b ratio and the addition of supplementary cementitious materials (fly-ash, GGCS and GGBS). An increase in w/b ratio correlates to a weaker and more porous cement paste matrix with higher interconnectivity in the pore structure which allows higher diffusion of carbon dioxide gas. Similar results can be found in literature (Alexander & Beushausen, 2009) and previous studies (Salvoldi *et al.*, 2015; Kanjee, 2015).

The incorporation of cement extenders causes higher carbonation due to a reduction in calcium hydroxide (carbonatable material) content. For instance, fly-ash, being a pozzolan, reacts slowly with calcium hydroxide liberated during the hydration of Portland cement. Slag is characterised as a latent hydraulic binder which requires activation by lime to produce calcium silicates (C-S-H). Hence, the reactions of these supplementary materials decrease the calcium hydroxide content in the pore solution and reduce the resistance of the concrete to carbonation (Nawy, 2008; Soutsos, 2010, Thomas, 2013).

According to Figure 4-21, comparing the untreated mixes, higher carbonation depth is obtained in the poor-quality mixes. This can be explained by the insufficient curing (slower hydration reactions) that produced a relatively more porous cement paste microstructure. Furthermore, the pores in the poor-quality concrete are drier compared to their respective control mixes, and this allows higher diffusion rate of carbon dioxide. Hence, higher carbonation rates are expected (Alexander & Beushausen, 2009; Thomas, 2013; Poursaee, 2016).

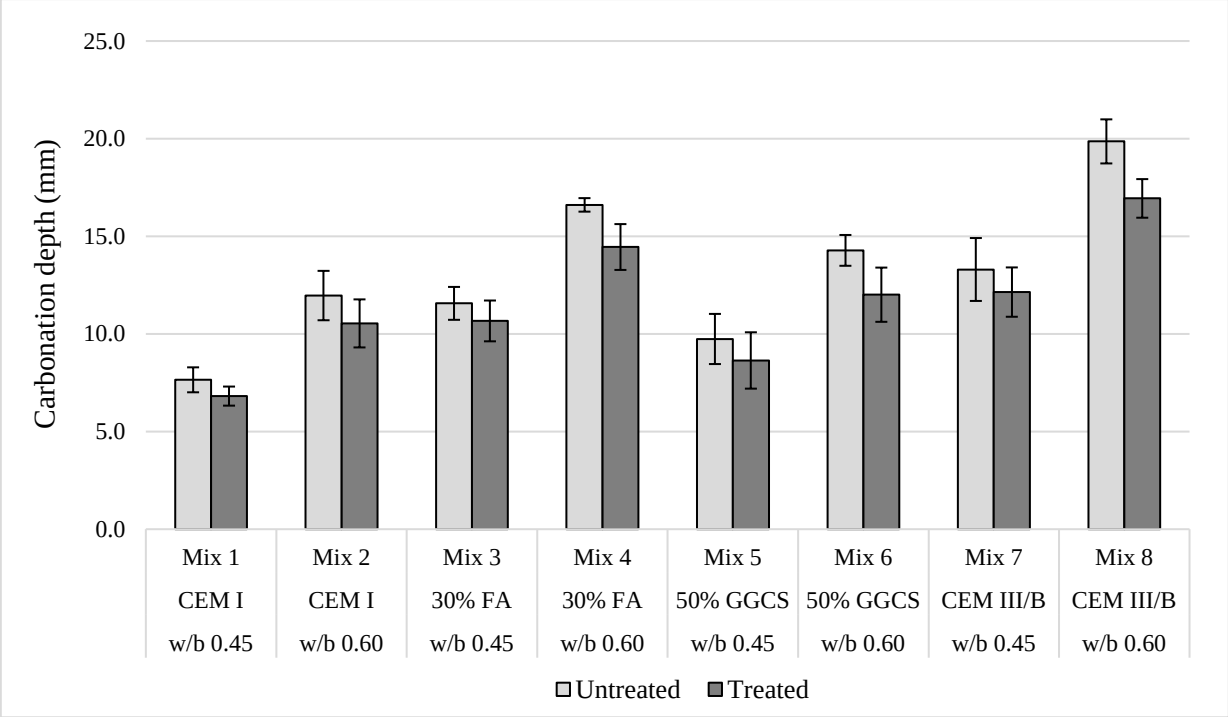

Figure 4-20: Accelerated carbonation test results (main mixes – 16 weeks) (error bars indicate STDV)

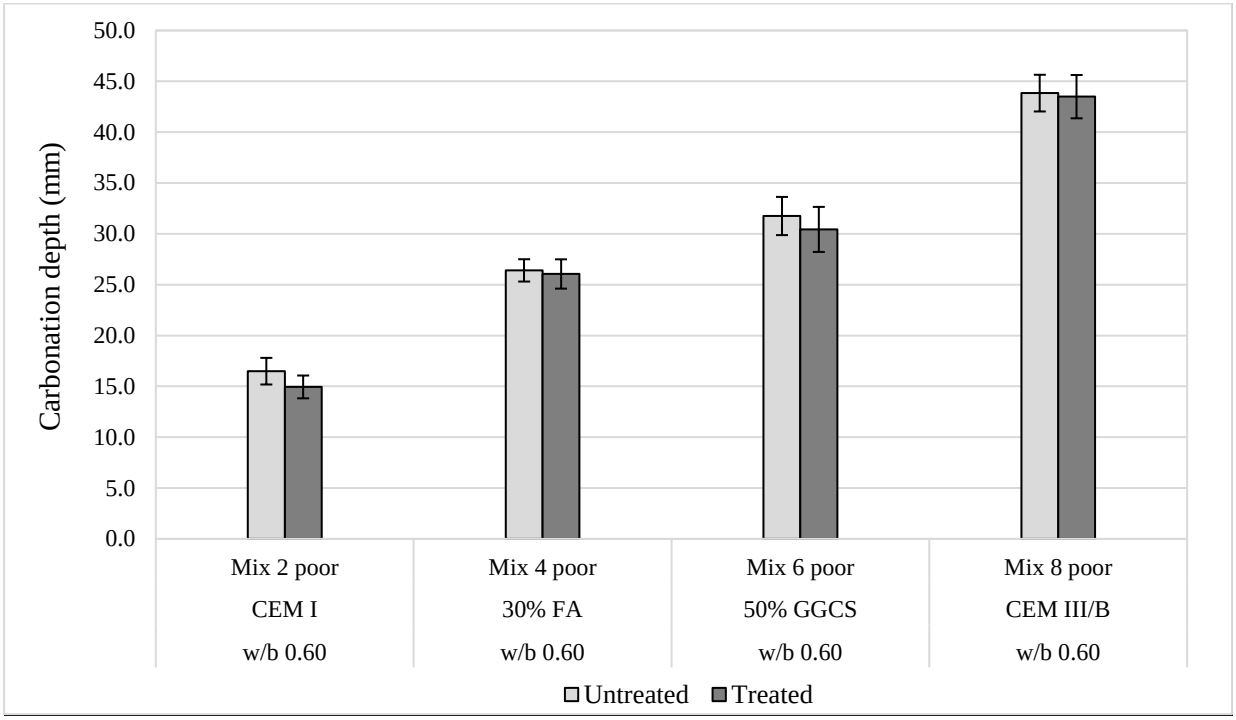

Figure 4-21: Accelerated carbonation test results (poor quality mixes – 16 weeks) (error bars indicate STDV)

Comparing the untreated and treated mixes, it can be noted that the silane impregnation does not have significant impact on the carbonation depth, especially in lower w/b ratio mixes (w/b 0.45) and poor-quality mixes. However, except for Mix 2, there is reduction in carbonation depth in the

w/b 0.60 mixes (Mix 4, Mix 6 and Mix 8). Similar results were obtained in research by Zhang *et al* (2017) and Jiesheng *et al* (2017). Aforementioned, the influence of hydrophobic impregnation on the carbonation rate is a function of the humidity levels inside the concrete and external environmental or testing conditions (Selander, 2010). From the moisture profiling results (Section 4.6), the silane treated concrete shows higher relative humidity (near the surface) compared to the untreated concrete. As the diffusion of carbon dioxide is slower with higher relative humidity in the pores, lower carbonation depth was obtained in silane treated concrete. The effect was more apparent in the w/b 0.60 mixes possibly due to higher silane penetration depth.

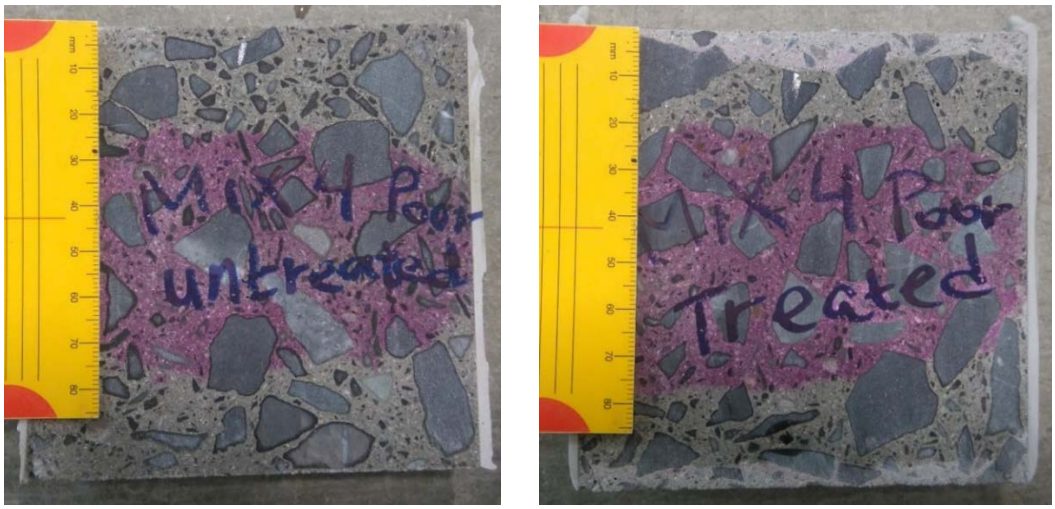

Figure 4-22: Accelerated carbonation test results (Mix 4 poor)

Figure 4-22 shows the accelerated carbonation test result for one of the mixes (Mix 4 poor). It can be noted that the carbonation front proceeds ahead of the silane impregnation depth.

4.5 Bulk diffusion

The chloride bulk diffusion test results for the uncracked and cracked concrete are discussed in Section 4.5.1 and 4.5.2 respectively. The test was conducted as described in Section 3.4.5.

4.5.1 Uncracked concrete

The chloride profiling and curve fitting data is provided in Appendix E and Appendix G respectively. Figure 4-23 and Figure 4-24 show the surface chloride concentrations (obtained by curve fitting the data points to a solution of Fick's second law of diffusion) for the main and poor-quality mixes respectively after 80 days of ponding. Comparing the untreated main mixes, except for Mix 1-4, a higher w/b ratio correlated to an increase in chloride content in the near surface zone. This observation is due to the increase in porosity of the cement paste matrix which allows greater penetration of chloride ions (Alexander & Beushausen, 2009). The influence of binder type was unclear due to the overlapping of the error bars. From Figure 4-24, it can be noted that the poor-quality versions of Mix 2, Mix 4, Mix 6 and Mix 8 show lower surface chloride concentration. This is because the significantly higher diffusion coefficient (D_a) of these mixes allows chloride ions to diffuse deeper inside the concrete, thus reducing the chloride content at the surface (Zhang *et al.*, 1998).

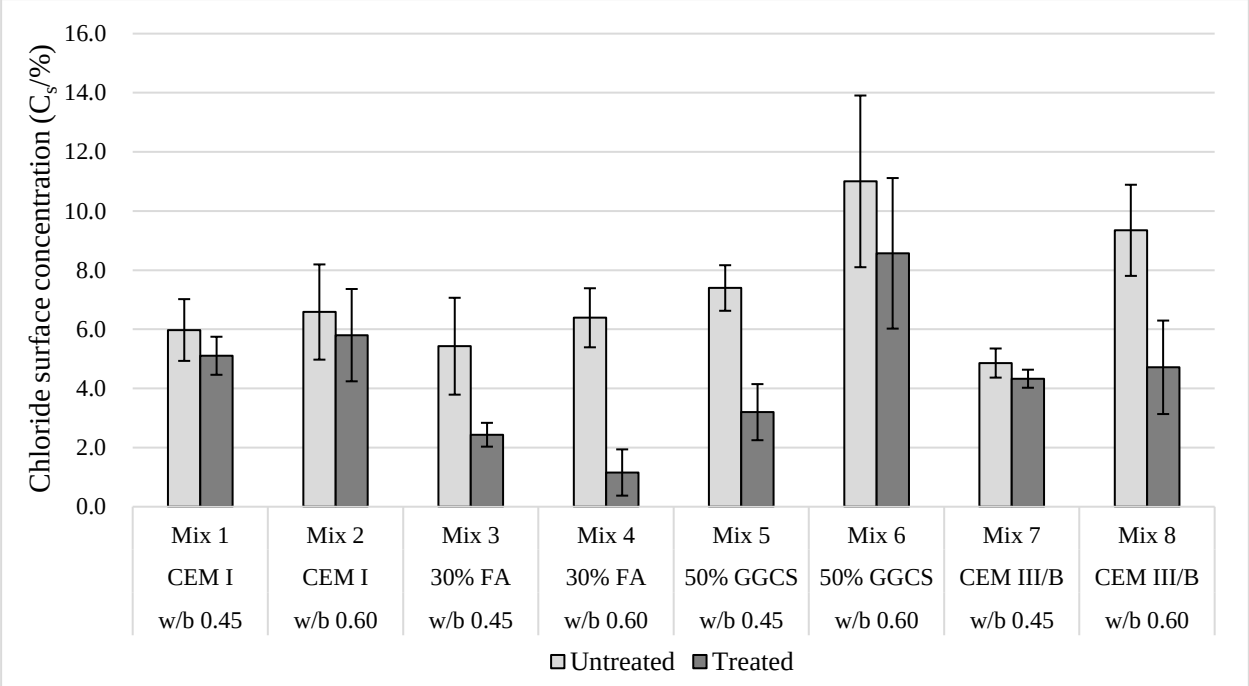

Figure 4-23: Surface chloride concentration results (C_s/% by mass of binder) – main mixes (error bars indicate STDV)

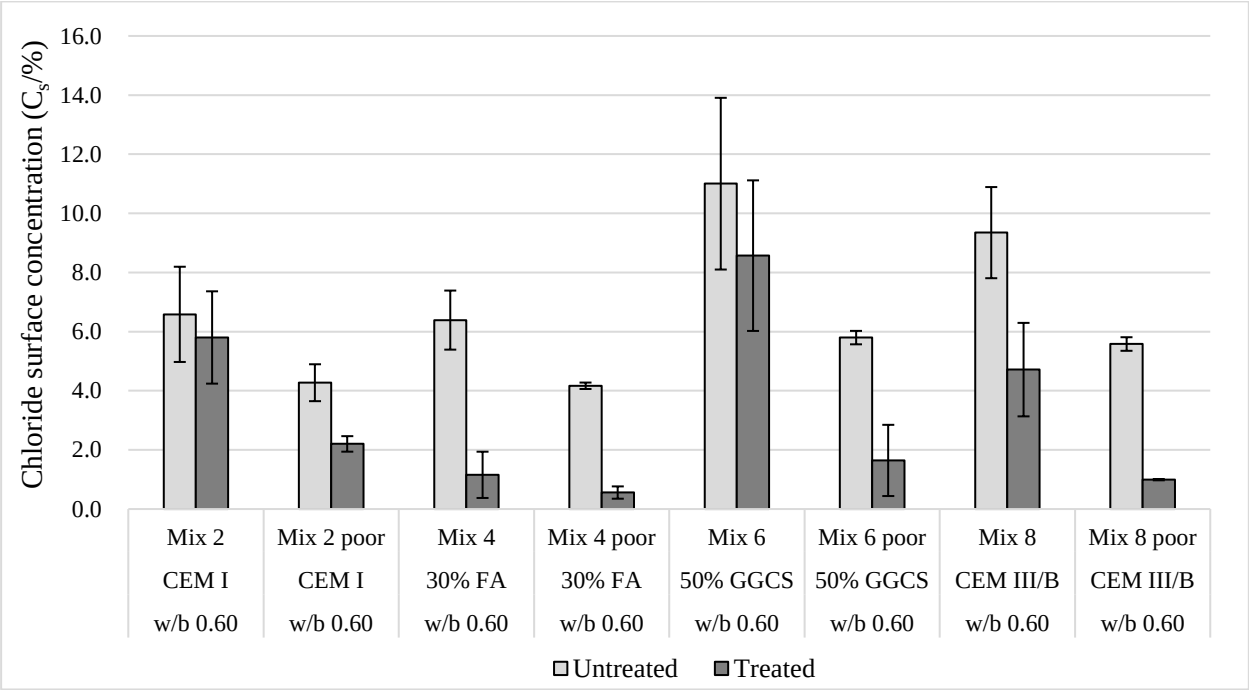

Figure 4-24: Surface chloride concentration (C_s/% by mass of binder) – poor quality mixes (error bars indicate STDV)

The general trend indicates that treated concrete shows a lower surface concentration relative to untreated concrete. As discussed in Section 2.8.1, silane impregnation chemically modifies the near surface of concrete and decreases the capillary absorption of water and any dissolved deleterious agents, for instance chlorides. Hence, the surface chloride concentration was reduced in the treated concrete. Similar observations were made in previous research by Tanaka et al (2015),

Zhang et al (2017), and Jiesheng et al (2017). It must be noted however that the reduction in surface chloride concentration is negligible in the CEM I mixes (Mix 1 and Mix 2) and some slag mixes (Mix 6 and Mix 7). The poor-quality treated mixes generally showed better performance, compared to untreated mixes, and this can be attributed to the higher penetration depth of the water repellent product in these mixes as discussed in Section 4.3.

Figure 4-25 and Figure 4-26 show the apparent chloride diffusion coefficients (obtained by curve fitting the chloride profiling data points to a solution to Fick's second law of diffusion) for the main and poor-quality mixes respectively.

Note: A (negative) log scale was used to improve the visibility of the results. Hence a higher number indicates lower apparent chloride diffusion coefficient.

From Figure 4-25, comparing the untreated mixes, it can be noted that a reduction in w/b ratio and the inclusion of slag reduced the apparent chloride diffusion coefficient. A smaller w/b ratio correlates to a reduction in porosity of the cement paste matrix which slows down the diffusion of chloride ions (Alexander & Beushausen, 2009). A lower w/b ratio also reduces the interconnections between the pores which otherwise act as channels of flow in the cement paste (Mehta *et al.*, 2006).

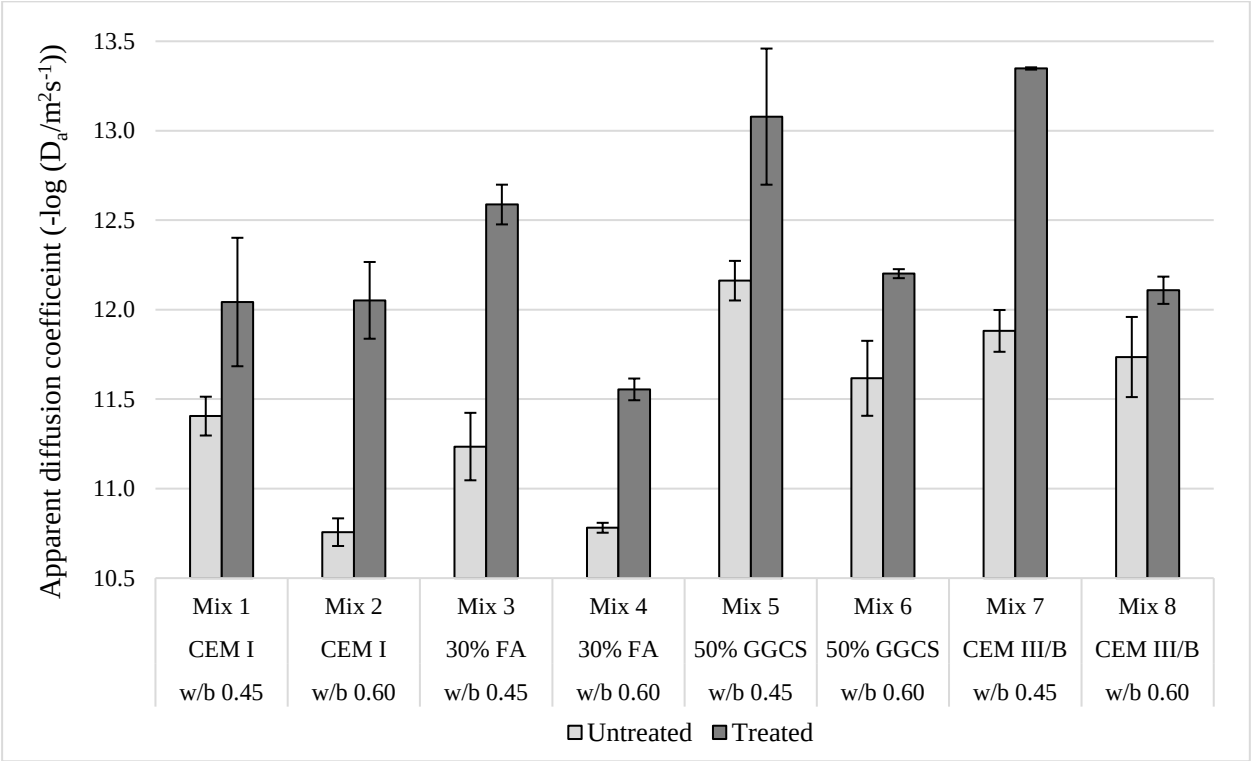

Figure 4-25: Apparent chloride diffusion coefficient results (-log D_a/m^2s^{-1}) – main mixes (error bars indicate STDV)

Slag in concrete can bind chlorides and hence reduce the chloride ion concentration within the pore solution. Furthermore, GGCS and GGBS can react with calcium hydroxide to form extra hydrated calcium silica hydrates in the cement paste matrix. These reactions lead to the densifica-

tion of the concrete microstructure and a reduction in porosity which overall reduce the penetrability to chloride ions (Ramezanianpour, 2014; Siddique *et al.*, 2011). The fly-ash mixes (Mix 3 and Mix 4) showed similar apparent chloride diffusion coefficients relative to the CEM I mixes (Mix 1 and Mix 2) and this can be explained by the slower pozzolanic reactions that increase the penetrability of concrete at relatively early age (Thomas, 2013).

According to Figure 4-26, comparing the untreated mixes, higher diffusion coefficients were obtained in the poor-quality mixes. This can be attributed to insufficient curing (slower hydration reactions) that produced a relatively more porous cement paste microstructure. Furthermore, the pores in the poor-quality concrete were drier compared to their respective control mixes, and this allowed higher penetration and diffusion rate of chlorides (Alexander & Beushausen, 2009; Poursaee, 2016). It must be noted that an apparent diffusion (D_a) of 1.42E-08 m^2/s (8.0 on log-scale) for Mix 4 poor (untreated) is unrealistic in practice.

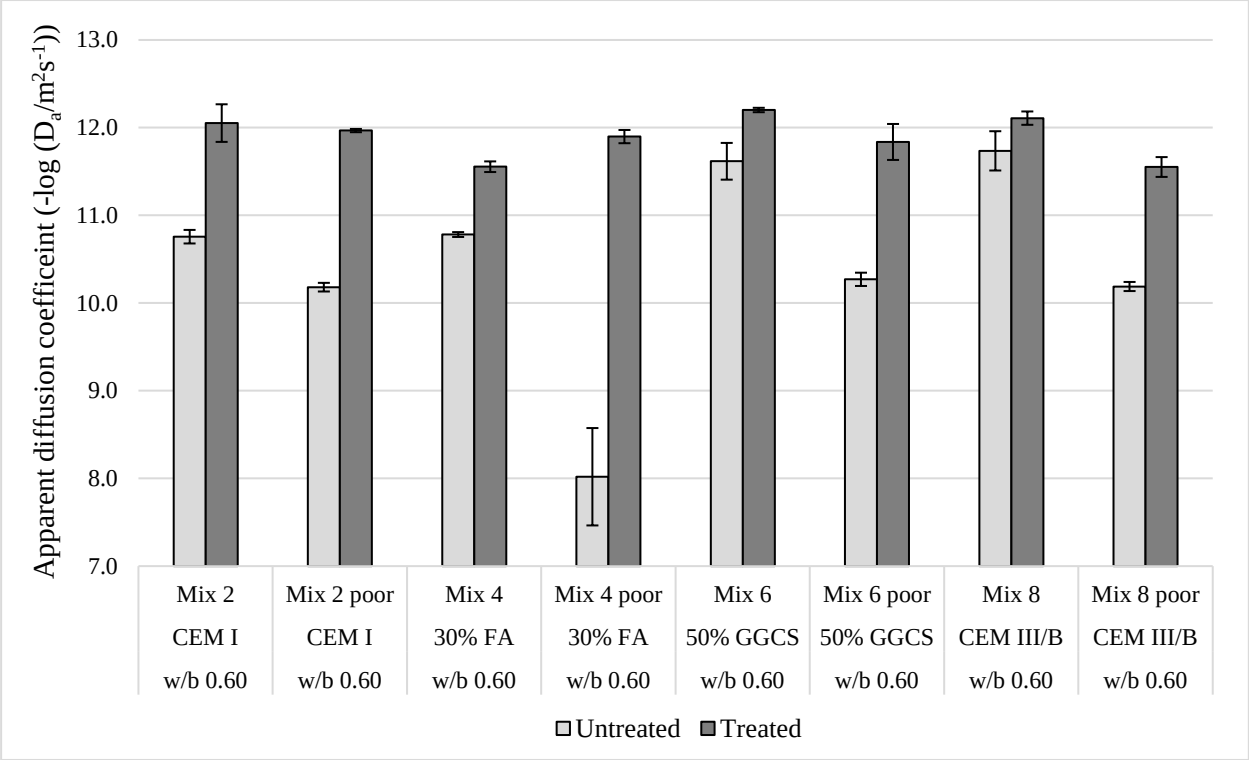

Figure 4-26: Apparent chloride diffusion coefficient results (-log D_a/m^2s^{-1}) – poor quality mixes (error bars indicate STDV)

Furthermore, from Figure 4-25 and Figure 4-26, the silane treated concrete showed substantially lower apparent chloride diffusion coefficients relative to the untreated concrete. Firstly, as the chloride penetration and content is reduced within the near surface zone, the supply of chloride ions that can diffuse deeper into the concrete is smaller. Secondly, the diffusion of chlorides is significantly slowed down in silane impregnated (treated) concrete as the capillary pores are less saturated compared to untreated concrete (Li, 2017; Poursaee, 2016). Similar observations were made in previous works by Zhang et al (2017) and Tanaka et al (2015). From Table 4.1, it can be

noted that the reduction in apparent chloride diffusion coefficients is generally higher in the w/b 0.45 and poor-quality mixes relative to the w/b 0.60 and control mixes respectively.

Table 4.1: Summarised apparent diffusion coefficients (D_a/m^2s^{-1})

			Untreated	Treated	Reduction in D_a (m^2/s)
Mix no	**Composition**	**w/b**	**D_a (m^2/s)**	**D_a (m^2/s)**	**%**
Mix 1	100% CEM I	0.45	4.02E-12	1.09E-12	73
Mix 2	100% CEM I	0.60	1.77E-11	9.66E-13	95
Mix 2 poor	100% CEM I	0.60	6.62E-11	1.08E-12	98
Mix 3	70% CEM I/30% FA	0.45	6.16E-12	2.64E-13	96
Mix 4	70% CEM I/30% FA	0.60	1.66E-11	2.81E-12	83
Mix 4 poor	70% CEM I/30% FA	0.60	1.42E-08	1.28E-12	100
Mix 5	50% CEM I/50% GGCS	0.45	7.03E-13	1.03E-13	85
Mix 6	50% CEM I/50% GGCS	0.60	2.63E-12	6.30E-13	76
Mix 6 poor	50% CEM I/50% GGCS	0.60	5.42E-11	1.57E-12	97
Mix 7	100% CEM III/B	0.45	1.35E-12	4.49E-14	97
Mix 8	100% CEM III/B	0.60	1.99E-12	7.86E-13	61
Mix 8 poor	100% CEM III/B	0.60	6.51E-11	2.87E-12	96

From the experimental results, the apparent chloride diffusion coefficient (D_a/m^2s^{-1}) of the un-treated main mixes (Mix 1-8) was observed to be related to their respective Chloride Conductivity Index ($CCI/mScm^{-1}$). The apparent chloride diffusion coefficient (D_a) increased with higher CCI values (Figure 4-27). A good positive linear correlation ($R^2 = 0.92$) was recorded, suggesting a strong connection between the independent variable (apparent chloride diffusion coefficient/D_a) and dependent variable (Chloride Conductivity Index/CCI). The correlation between the apparent chloride diffusion coefficient (D_a/m^2s^{-1}) and CCI (mS/cm) for the treated concrete mixes was less favourable ($R^2 = 0.55$).

It must be noted that the two test methods for chloride ingress; bulk diffusion and CCI test, involve different mechanisms of diffusion and migration respectively. However, as both chloride diffusion and migration depend on the overall complexity (size, tortuosity and interconnectivity) of the capillary pore structure (Alexander *et al.*, 2010; Richardson, 2002), reasonable correlation can be obtained between the two transport mechanisms. Hence, the CCI test can be used as a rational measure of the resistance of the concrete to chloride penetration. This result is extensively documented in literature (Alexander *et al.*, 2008, Alexander *et al.*, 2017 and Beushausen & Luco, 2016) and similar observations were made in previous works (Mackechnie, 2001; Kanjee, 2015).

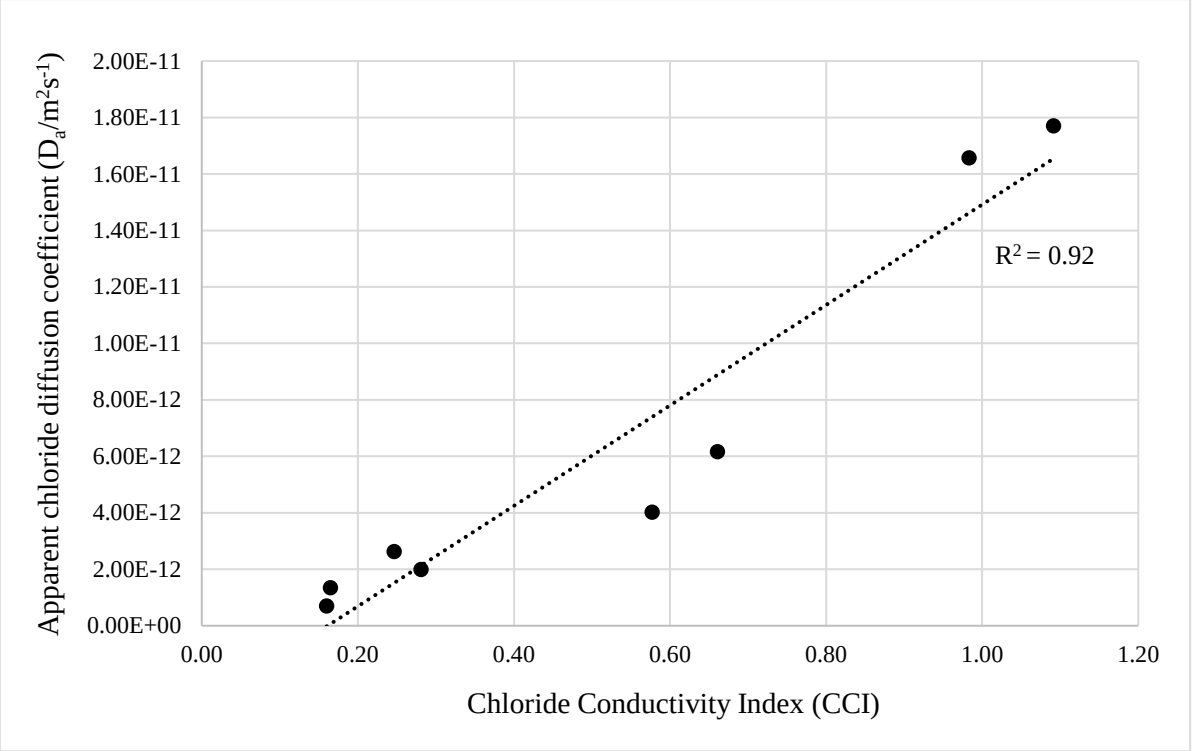

Figure 4-27: Correlation between apparent chloride diffusion coefficient (D_a/m^{2}s^{-1}) and Chloride Conductivity Index (CCI/mScm^{-1}) for untreated concrete (Mix 1-8)

4.5.2 Cracked concrete

Figure 4-28 to Figure 4-31 show the chloride profiling results for the cracked concrete mixes (Mix 2, Mix 4, Mix 6 and Mix 8 respectively). The detailed results are provided in Appendix F. The curves for the uncracked concrete mixes were included for comparison purposes. It must be emphasized that the bulk diffusion test on the cracked concrete was performed using a higher concentration (16.5%) sodium chloride (NaCl) solution whereas sea-water has an average chloride concentration of 3.5% (Alexander, 2016).

Considering the untreated cracked concrete, it can be noted that the chloride concentration (% by mass of binder) tends to decrease with increasing depth (mm) for both crack widths of 0.2 and 0.6 mm. This can be attributed to the gradual decrease in the crack width with increasing depth. The chloride content in the first 5 mm (near the surface) is higher in the 0.6 mm cracks due to a wider crack opening. Furthermore, compared to the uncracked concrete, the chloride content remains significantly higher up to depths of 50-60 mm. This is because the crack allows the salt solution to penetrate deep inside the concrete and the increased surface area in contact with the salt solution allows greater amount of chlorides to diffuse locally into the concrete through the internal crack surface (Kanjee, 2015). It can also be noted that the chloride concentration near the surface (0-5 mm) is lower in the cracked concrete compared to the uncracked concrete. This was attributed to the use of cut surfaces for the cracked concrete which reduces the build-up of chlorides on the surface (Section 3.3.4).

From Figure 4-28 and Figure 4-29, the cracked (untreated) versions of Mix 2 (100% CEM I) and Mix 4 (30% FA) showed similar results in terms of chloride ingress and this can be explained

by the slower pozzolanic reactions of fly-ash that do not contribute to pore size refinement at early ages (Thomas, 2013). Comparing Figure 4-30 and Figure 4-31 to Figure 4-28, cracked (untreated) versions of Mix 6 (50% GGCS) and Mix 8 (100% CEM III/B) displayed better chloride ingress resistance relative to Mix 2 (100% CEM I) and this was characterised by a significant reduction in chloride concentration with depth for both 0.2 and 0.6 mm crack widths.

As mentioned in Section 2.2, the transport mechanisms in cracked concrete are dependent on the crack properties (width, shape, tortuosity and orientation), concrete composition (mainly the interactions between the cement paste components and the penetrating species) and pore solution chemistry (Pacheco & Polder, 2012; Gu *et al.,* 2015). As the salt solution fills the crack, components of the slag in the concrete can bind a proportion of the chlorides and hence reduce chloride ion ingress through the internal crack surface. Furthermore, GGCS and GGBS react with calcium hydroxide to form extra hydrated calcium silica hydrates in the cement paste matrix. These reactions lead to the densification of the cement paste matrix and a reduction in porosity which overall reduce the penetrability to chloride ions (Ramezanianpour, 2014; Siddique *et al.,* 2011).

Considering the treated cracked concrete, it can be noted that the chloride concentration initially decreases with increasing depth, followed by a gradual increase. Hence it can be interpreted that the silane impregnation is effective up to the maximum penetration depth only. Another explanation could be that hydrophobic impregnation is not a water proofing measure and hence is not effective under hydrostatic pressures (Medeiros *et al.,* 2008). The treated cracked concrete samples were kept under 10 $\pm$ 5 mm salt solution from the surface, but as the cracks allows salt solution to penetrate deeper into the concrete, the effective ponding head was higher. It can be also noted that the near surface chloride concentration is lower in the treated 0.6 mm compared to the treated 0.2 mm crack width mixes (opposite results were obtained for the cracked untreated mixes). Nonetheless, by scaling the measured chloride content at depths of 50-60 mm (typical concrete cover in the marine environment) by the ratio (3.5/16.5) and assuming a chloride threshold of 0.4% by mass of binder, it can be noted that the treated cracked concrete shows lower risk of reinforcement corrosion initiation relative to the untreated cracked concrete mixes.

Dai et al (2010) showed that hydrophobic impregnation could suppress chloride ingress in cracked (Portland cement, w/b 0.68) concrete with an average crack width of 0.15 mm, under cyclic sea water wetting and drying cycles. The results of this thesis suggest that chloride ingress is reduced in treated cracked concrete (up to a crack width of 0.6 mm). In general, the treated cracked slag concrete showed better performance relative to the treated cracked CEM I and FA mixes. Better results were obtained with the slag concretes (Mix 6 and Mix 8) possibly due to the higher chloride binding capacity of the supplementary cementitious materials (GGCS and GGBS respectively).

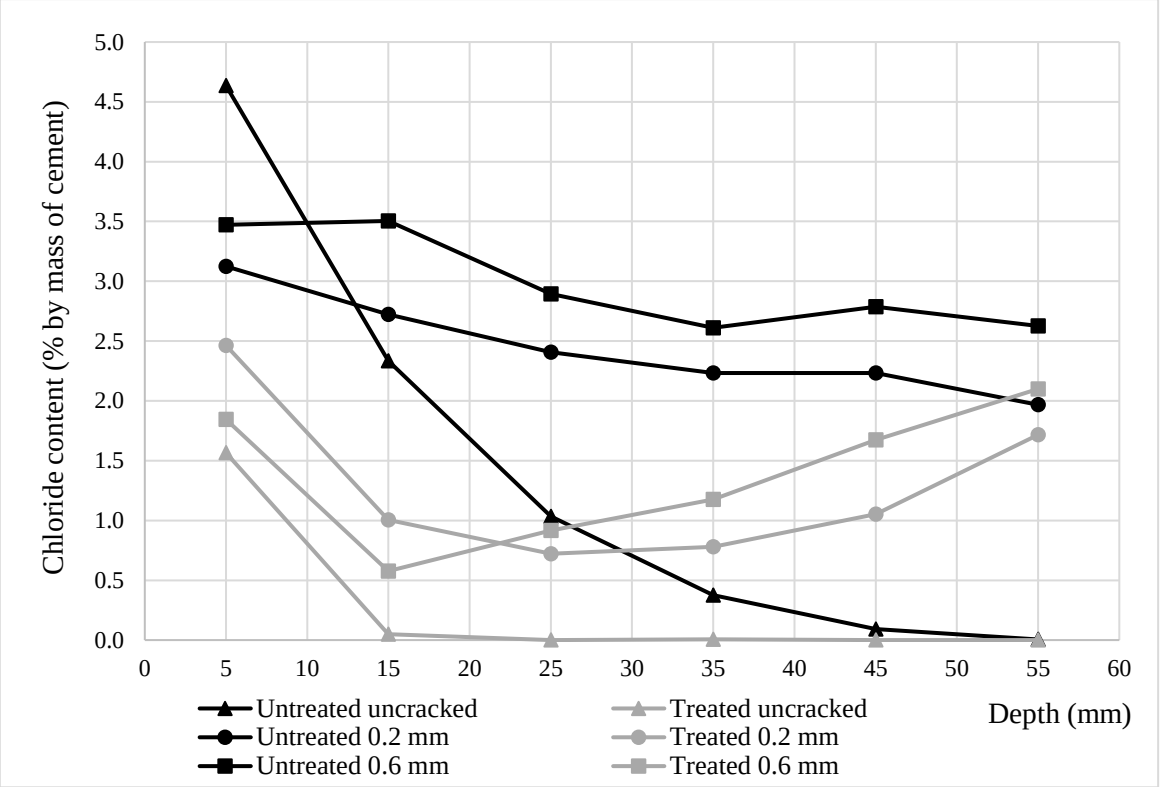

Figure 4-28: Chloride profiles for Mix 2 (100% CEM I) - uncracked vs cracked concrete

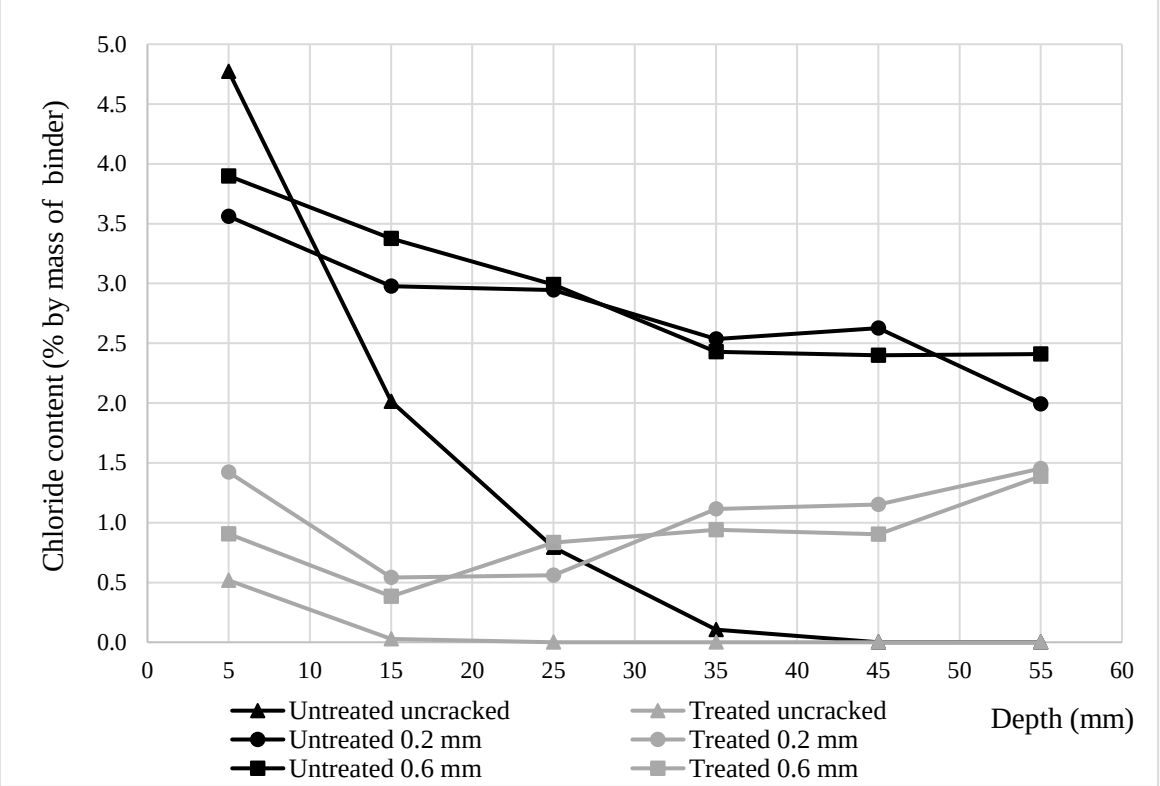

Figure 4-29: Chloride profiles for Mix 4 (30% Fly-ash) – uncracked vs cracked concrete

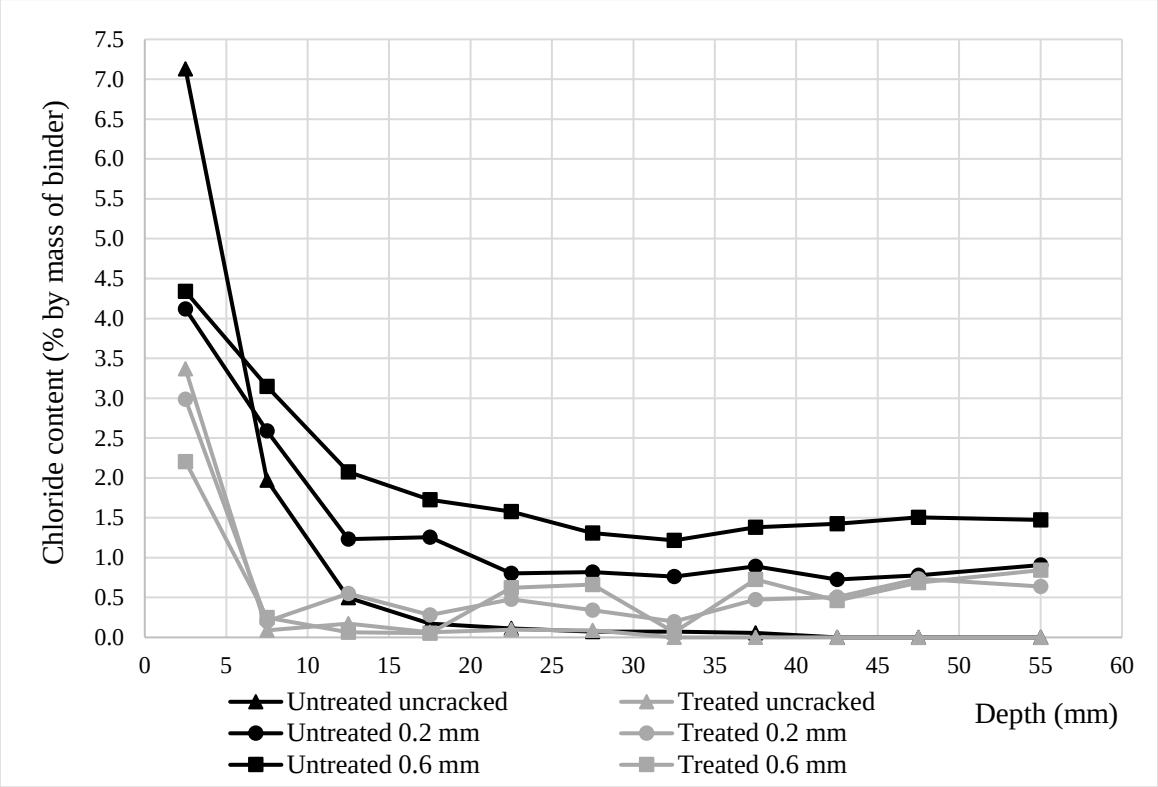

Figure 4-30: Chloride profiles for Mix 6 (50% GGCS) – uncracked vs cracked concrete

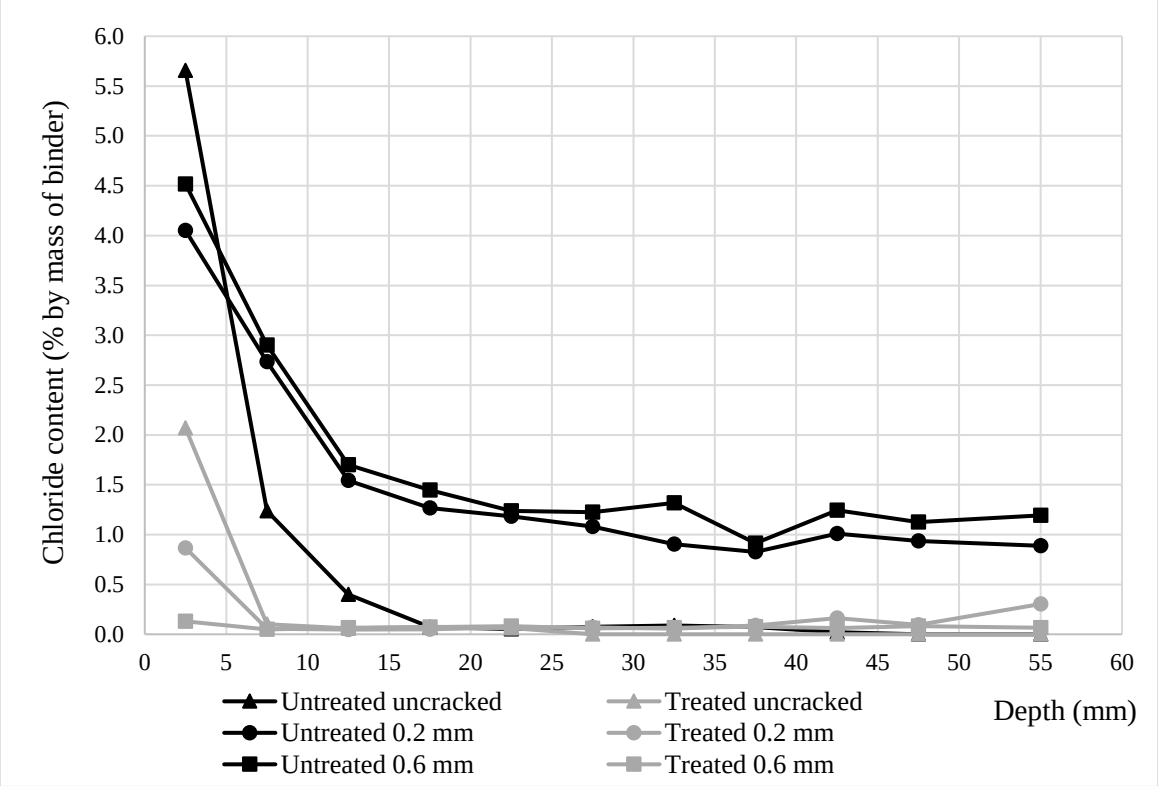

Figure 4-31: Chloride profiles for Mix 8 (CEM III/B) – uncracked vs cracked concrete

4.6 Moisture profiling

The moisture profiles measured 1 day after silane treatment and after 16 weeks at 63 ± 2% RH for the untreated and treated concrete mixes (Mix 2, Mix 4 and Mix 6) are shown in Figure 4-32 and Figure 4-33 respectively. The detailed results are provided in Appendix H.

From Figure 4-32, it can be noted that the relative humidity of the near surface zone is significantly increased soon after silane treatment. This result can be related to the condensation reactions that occur when the silane molecules react with the concrete substrate to form silicon resin. Water is released during this process which increases the relative humidity (Pan *et al.*, 2017). Figure 4-33 shows that higher relative humidity is still observed after 16 weeks but the difference in relative humidity (near the surface) between silane treated and untreated concrete is reduced with time. This can be attributed to the fact that hydrophobic impregnation only lines the internal pore structure with silane molecules and hence does not hinder the movement of water vapour in and out of the concrete (Bertolini *et al.*, 2013). The small difference between untreated and treated concrete after 16 weeks could be also due to measuring inaccuracy.

The main limitation of these results is that the concrete has not been allowed to dry out significantly before the application of the silane. The relative humidity measurements hence represent the sealed in moisture content that is redistributed with time as the concrete surface dries out. It must be noted that in practice if the specimens are subject to rain and sun (intermittent wetting and drying cycles), the moisture content in the treated concrete would be lowered relative to the untreated concrete as the former does not absorb water during wetting but loses water in dry periods by evaporation (Polder, 2000).

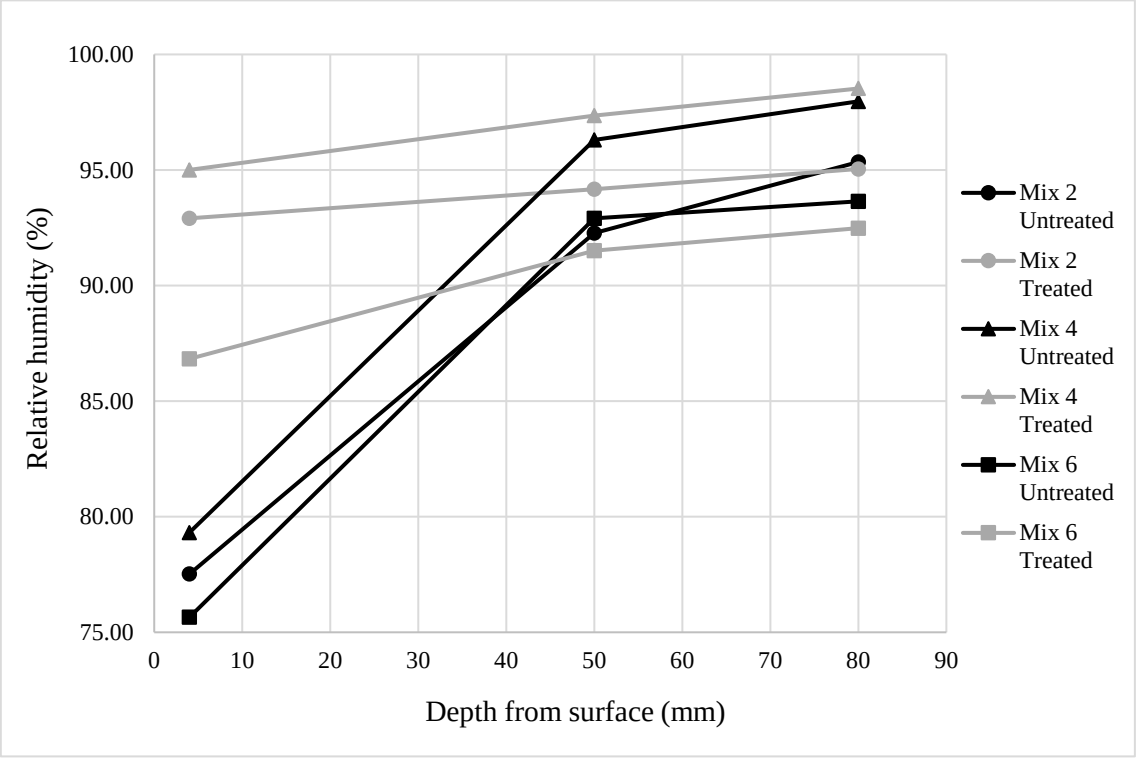

Figure 4-32: Moisture profile 1 day after silane treatment

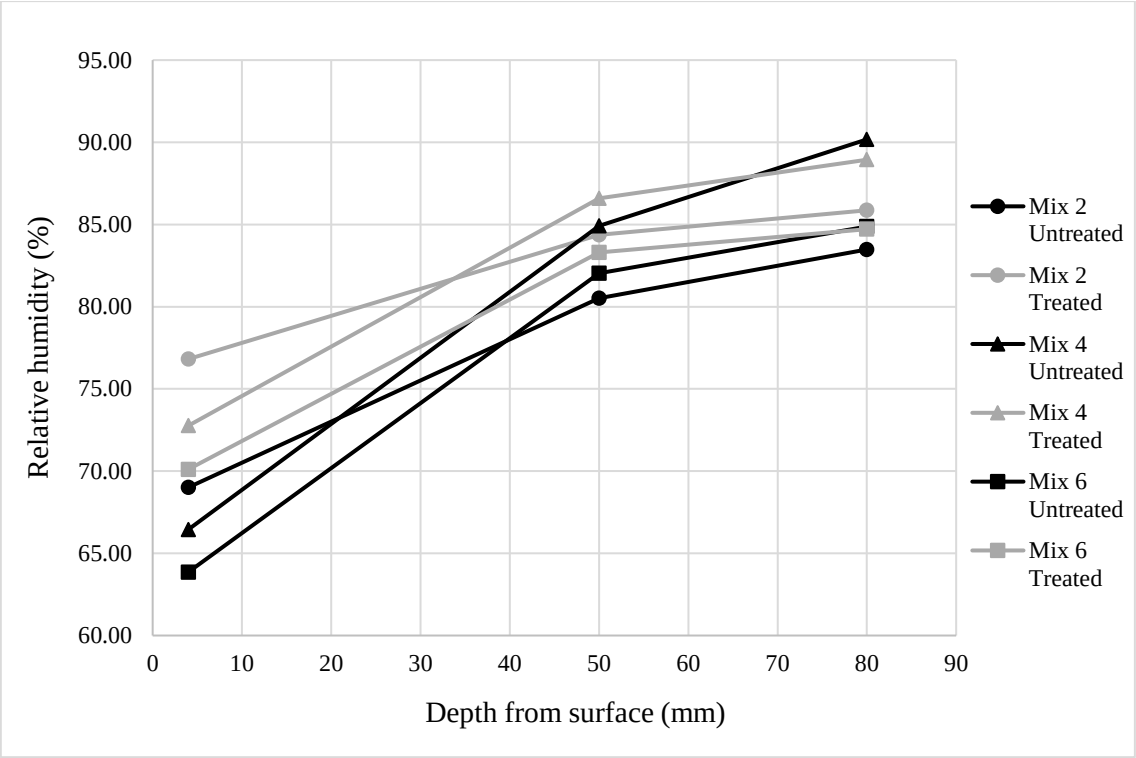

Figure 4-33: Moisture profiles after 16 weeks at 63 ± 2% RH

5. Service life modelling

This Chapter presents the prediction of chloride ingress using a simplified model based on Fick's second law of diffusion. The regression parameters (surface chloride concentration (C_s) and apparent chloride diffusion coefficient (D_a)) obtained from the experimental data presented in Chapter 4, were incorporated into a mathematical solution to Fick's second law to obtain suitable expressions that describe the penetration of chlorides with time for silane treated and untreated concrete mixes. Hence, by determining the time taken for chloride concentrations at the rebar level to reach a critical threshold (assumed to be 0.4% by mass of binder), the service life (time to corrosion initiation) of untreated and silane treated concrete was evaluated for specific cover depths.

5.1 Limitations

Fick's second law of diffusion cannot be applied without constraints and several factors must be considered to obtain a reasonably realistic service life prediction:

- Models based on Fick's second law describe the rate of chloride ingress based on the assumption that non-stationary diffusion is the main transport mechanism. However, in practice, the transport processes vary according to the exposure zones. For instance, except for fully submerged structures, chlorides initially enter concrete by capillary suction followed by ionic diffusion (Bertolini *et al.*, 2013; Alexander & Beushausen, 2009; Richardson, 2002).
- The error function solution of Fick's second law is valid only for a constant chloride surface concentration (C_s) (Sarja, 2006; Richardson, 2002). In practice, the surface chloride concentration increases due to accumulation of chlorides, especially under wetting and drying cycles. However, the chloride surface concentration usually reaches a constant value within a period which is relatively short compared to the design service life of the structure (Costa & Appleton, 1999; Sarja, 2006). Hence, the maximum chloride surface concentrations were used in the service life prediction as discussed in Section 5.2.
- The error function solution of Fick's second law is also only valid for a constant apparent chloride diffusion coefficient (D_a) (Sarja, 2006; Richardson, 2002). However, the chloride diffusion coefficient decreases with aging concrete due to continuous hydration of the cementitious components (especially in blended cements) that reduces the capillary porosity over time and due to on-going binding of chlorides (Van der Wegen *et al.*, 2012; Ballim *et al.*, 2009; Costa & Appleton, 1999). Hence, the time dependence of the apparent chloride diffusion coefficient (D_a) was considered (Section 5.3).
- The ingress of chlorides is also affected by the binding capacity of the hydration products and other influencing factors. As a result, the diffusion coefficient is considered as an apparent value. Moreover, throughout the chloride analysis, only the total acid soluble chloride content is measured, thereby neglecting the binding of chlorides (Soutsos, 2010; Sarja, 2006; Bertolini *et al.*, 2013).

It must be emphasized that despite all the limitations of using a solution to Fick's second law to model chloride ingress, the approach remains one of the most convenient ways to describe the transport of chlorides into concrete and provides a reasonable estimate from an engineering standpoint (Soutsos, 2010; Sarja, 2006).

5.2 Surface chloride concentration (C_s)

5.2.1 Untreated concrete

The chloride surface concentration used in the service life prediction was obtained from literature (Mackechnie, 2001; Polder *et al.*, 2014). This data was measured from local (South African) and international (Netherlands) marine concrete structures and field exposed specimens. From Table 5.1, it can be noted that the chloride surface concentration (C_s) is mainly a function of the concrete composition and exposure conditions. Compared to Portland cement concrete, higher surface concentrations are observed for fly-ash and slag concrete due to their higher chloride binding capacity which increases their ability to hold chloride ions (Mackechnie, 2001).

Higher values of C_s are expected in the tidal/splash zone where the intermittent wetting and drying of sea-water causes accumulation of salts and hence increases the chloride content on the concrete near surface. The lower surface concentration in the atmospheric zone can be explained by the equilibrium that is established between the deposition of wind-borne chlorides and rainfall which increase and decrease chloride content on the surface respectively (Mackechnie, 2001; Bertolini *et al.*, 2013).

Table 5.1: Chloride surface concentrations (% by mass of binder) – adapted from (Mackechnie, 2001; Polder *et al.*, 2014*)

Concrete type	Tidal/splash zone (XS3)	Atmospheric zone (XS1)
CEM I	4.0	2.0
CEM I with 30% FA	5.0	2.5
CEM I with 50% GGCS	6.0	3.0
CEM III/B (70% GGBS)*	5.0	2.5

Hence, for each untreated concrete mix (Mix 1-8), the appropriate surface chloride concentration (% by mass of binder) was selected from Table 5.1 and inserted into a mathematical solution to Fick's second law of diffusion (Section 5.5).

5.2.2 Treated concrete

Table 5.2 shows the chloride surface concentrations obtained through extrapolation of the best fit curve of the data obtained during the short-term laboratory exposure (Section 4.5.1/Appendix G). The chloride surface concentrations in Table 5.1 were factored by the ratio C_s (Treated/Untreated) to obtain the chloride content at the surface for treated concrete mixes.

Table 5.2: Surface chloride concentration (C_s/% by mass of binder) results

Mix no	Composition	w/b	C_s (Untreated)	C_s (Treated)	C_s (Treated/Untreated)
Mix 1	100% CEM I 52.5N	0.45	5.976	5.105	0.854
Mix 2	100% CEM I 52.5N	0.60	6.584	5.802	0.881
Mix 2 poor	100% CEM I 52.5N	0.60	4.272	2.203	0.516
Mix 3	70% CEM I/30% FA	0.45	5.428	2.434	0.448
Mix 4	70% CEM I/30% FA	0.60	6.390	1.157	0.181
Mix 4 poor	70% CEM I/30% FA	0.60	4.169	0.558	0.134
Mix 5	50% CEM I/50% GGCS	0.45	7.397	3.198	0.432
Mix 6	50% CEM I/50% GGCS	0.60	11.004	8.570	0.779
Mix 6 poor	50% CEM I/50% GGCS	0.60	5.798	1.644	0.284
Mix 7	100% CEM III/B 42.5N	0.45	4.859	4.329	0.891
Mix 8	100% CEM III/B 42.5N	0.60	9.348	4.715	0.504
Mix 8 poor	100% CEM III/B 42.5N	0.60	5.581	0.994	0.178

Note: The surface chloride concentration results (C_S) for Mix 7 obtained by curve fitting was not used in the calculations. Instead the chloride concentration measured in the first 1 mm slice was taken as the surface chloride concentration.

5.3 Apparent chloride diffusion coefficient (D_a)

The apparent diffusion coefficients used in the service life predictions were obtained from the experimental testing (bulk diffusion tests – Section 4.5.1). This involved curve fitting the measured data points (chloride concentration (%)) and (depth (m)) in a solution to Fick's second law of diffusion to obtain the regression parameter (D_a/m^2s^{-1}). The results for the untreated and treated concrete mixes are summarised in Table 5.3.

Table 5.3: Apparent chloride diffusion coefficient results

			D_a (m^2/s)	
Mix no	**Composition**	**w/b**	**Untreated**	**Treated**
Mix 1	100% CEM I 52.5N	0.45	4.02E-12	1.09E-12
Mix 2	100% CEM I 52.5N	0.60	1.77E-11	9.66E-13
Mix 2 poor	100% CEM I 52.5N	0.60	6.62E-11	1.08E-12
Mix 3	70% CEM I/30% FA	0.45	6.16E-12	2.64E-13
Mix 4	70% CEM I/30% FA	0.60	1.66E-11	2.81E-12
Mix 4 poor	70% CEM I/30% FA	0.60	1.42E-08	1.28E-12
Mix 5	50% CEM I/50% GGCS	0.45	7.03E-13	1.03E-13
Mix 6	50% CEM I/50% GGCS	0.60	2.63E-12	6.30E-13
Mix 6 poor	50% CEM I/50% GGCS	0.60	5.42E-11	1.57E-12
Mix 7	100% CEM III/B 42.5N	0.45	1.35E-12	4.49E-14
Mix 8	100% CEM III/B 42.5N	0.60	1.99E-12	7.86E-13
Mix 8 poor	100% CEM III/B 42.5N	0.60	6.51E-11	2.87E-12

The time dependence of the diffusion coefficient D(t) (that considers the reduction in chloride diffusivity with time) can be described by Equation 5.1 (Ballim *et al.*, 2009).

$$D(t) = D_0 \left(\frac{t_0}{t}\right)^n \quad \text{.....(5.1)}$$

where,

D_0 – diffusion coefficient at a reference time t_0 (136 days – age at testing) t – time (s)

n – aging coefficient (reduction factor)

Table 5.4 shows the ageing coefficient for various binder types and exposure conditions. These values are based on extensive and long-term field and laboratory experimental data (Soutsos, 2010). Hence, for each concrete mix (Mix 1-8), the appropriate ageing coefficient was selected and incorporated into a mathematical solution to Fick's second law of diffusion (Section 5.5)

Table 5.4: Ageing coefficients (n) for various binders and exposure classes (adapted from Soutsos, 2010 and Van der Wegen *et al.*, 2012)

Concrete type	Tidal/splash zone (XS3)	Atmospheric zone (XS1)
CEM I	0.40	0.60
CEM I with 30% FA	0.70	0.80
CEM I with 50% GGCS	0.45	0.65
CEM III/B (70% GGBS)	0.50	0.70

Note: The ageing coefficient (n) can theoretically be affected by hydrophobic impregnation of concrete, however to simplify the service life predictions, the same n value was used for untreated and treated concrete.

5.4 Chloride threshold value

This threshold value is defined as the critical chloride concentration at the rebar depth that causes depassivation of the reinforcement. The critical chloride content is a function of several interconnected factors such as the properties of the steel-concrete interface, pore solution chemistry, electrochemical potential of the steel reinforcement, amount of oxygen available and the cover depth and quality (Bertolini *et al.*, 2013). Hence, each concrete mix has a unique chloride threshold value. Hydrophobic impregnation of concrete can also theoretically affect the critical chloride threshold. However, to simplify the service life predictions, a reference value of 0.4% by mass of binder was used for all concrete mixes (Costa & Appleton, 1999, Frederiksen, 2000).

5.5 Prediction of service life

As discussed in Section 2.5.3, chloride ingress in concrete can be modelled using a mathematical solution to Fick's second law of diffusion. The expression used is given in Equation 5.2 and incorporates the time dependence of the apparent chloride diffusion coefficient. The model is similar to the DuraCrete model (Polder & Rooij, 2005; Van der Wegen *et al.*, 2012). A constant chloride surface concentration was used as specified in Section 5.2.

$$C(x,t) = C_s - (C_s - C_i) \cdot erf\left(\frac{x}{\sqrt{4D_a\left(\frac{t_0}{t}\right)^n t}}\right) \quad \text{(5.2)}$$

where,

C (x,t) – chloride concentration at depth x (m) at time t (s)

C_s – surface chloride concentration (%)

C_i – initial chloride content (%)

D_a – apparent chloride diffusion coefficient (m^2/s) at reference time (t_0 – 136 days/11750400 s)

t – time (s)

x – cover depth (m)

n – ageing coefficient

Hence by fixing the chloride concentration at depth (x/m) and time (t/s) to the chloride threshold (C_{cr} = 0.4% by mass of binder), initial chloride content to 0% by mass of binder, Equation 5.2 was rearranged by making the cover depth (x/m) the subject of formula:

$$C_{cr} = C_s - C_s \cdot erf\left(\frac{x}{\sqrt{4D_a\left(\frac{t_0}{t}\right)^n t}}\right) \quad \text{(5.3)}$$

$$x = erf^{-1}\left(\frac{C_s - C_{cr}}{C_s}\right) \cdot \sqrt{4D_a\left(\frac{t_0}{t}\right)^n t} \quad \text{(5.4)}$$

Realistically, w/b 0.45 mixes would be prescribed in the extreme exposure conditions (tidal/splash zone/XS3). Conventional w/b 0.60 mixes could be used in the less severe exposure levels (atmospheric zone/XS1) even though it must be noted that prescriptive durability codes such as the BS EN 206 and ACI 357R-84 specify a maximum w/b of 0.50 and 0.40 respectively for the atmospheric zone (XS1). Hence, the w/b 0.45 and w/b 0.60 mixes were modelled for the tidal/splash zone (XS3) and atmospheric zone (XS1) respectively.

The appropriate surface chloride concentration (C_s (% by mass of binder)), apparent chloride diffusion coefficient (D_a (m^2/s)) and ageing coefficient (n) for each mix, as presented in Section 5.2 and 5.3, were incorporated in Equation 5.4 to obtain suitable expressions that describe the depth of the critical chloride content (0.4% by mass of binder) with time and hence allowed the service life prediction of the untreated and silane treated concrete mixes.

5.5.1 Untreated concrete

Table 5.5 shows the expressions obtained for each untreated concrete mix.

Table 5.5: Mathematical expressions for the penetration of the critical chloride threshold (0.4% by mass of binder) with time for untreated concrete

	w/b	Mix no	Composition	Expression (untreated)
Tidal/splash zone (XS3)	0.45	Mix 1	100% CEM I 52.5N	$x = erf^{-1}\left(\frac{4 - C_{cr}}{4}\right) \cdot \sqrt{4(4.02x10^{-12})\left(\frac{t_0}{t}\right)^{0.4} t}$
		Mix 3	70% CEM I/30% FA	$x = erf^{-1}\left(\frac{5 - C_{cr}}{5}\right) \cdot \sqrt{4(6.16x10^{-12})\left(\frac{t_0}{t}\right)^{0.7} t}$
		Mix 5	50% CEM I/50% GGCS	$x = erf^{-1}\left(\frac{6 - C_{cr}}{6}\right) \cdot \sqrt{4(7.03x10^{-13})\left(\frac{t_0}{t}\right)^{0.45} t}$
		Mix 7	100% CEM III/B 42.5N	$x = erf^{-1}\left(\frac{5 - C_{cr}}{5}\right) \cdot \sqrt{4(1.35x10^{-12})\left(\frac{t_0}{t}\right)^{0.5} t}$
Atmospheric zone (XS1)	0.60	Mix 2	100% CEM I 52.5N	$x = erf^{-1}\left(\frac{2 - C_{cr}}{2}\right) \cdot \sqrt{4(1.77x10^{-11})\left(\frac{t_0}{t}\right)^{0.6} t}$
		Mix 2 poor	100% CEM I 52.5N	$x = erf^{-1}\left(\frac{2 - C_{cr}}{2}\right) \cdot \sqrt{4(6.62x10^{-11})\left(\frac{t_0}{t}\right)^{0.6} t}$
		Mix 4	70% CEM I/30% FA	$x = erf^{-1}\left(\frac{2.5 - C_{cr}}{2.5}\right) \cdot \sqrt{4(1.66x10^{-11})\left(\frac{t_0}{t}\right)^{0.8} t}$
		Mix 4 poor	70% CEM I/30% FA	$x = erf^{-1}\left(\frac{2.5 - C_{cr}}{2.5}\right) \cdot \sqrt{4(1.42x10^{-8})\left(\frac{t_0}{t}\right)^{0.8} t}$
		Mix 6	50% CEM I/50% GGCS	$x = erf^{-1}\left(\frac{3 - C_{cr}}{3}\right) \cdot \sqrt{4(2.63x10^{-12})\left(\frac{t_0}{t}\right)^{0.65} t}$
		Mix 6 poor	50% CEM I/50% GGCS	$x = erf^{-1}\left(\frac{3 - C_{cr}}{3}\right) \cdot \sqrt{4(5.42x10^{-11})\left(\frac{t_0}{t}\right)^{0.65} t}$
		Mix 8	100% CEM III/B 42.5N	$x = erf^{-1}\left(\frac{2.5 - C_{cr}}{2.5}\right) \cdot \sqrt{4(1.99x10^{-12})\left(\frac{t_0}{t}\right)^{0.7} t}$
		Mix 8 poor	100% CEM III/B 42.5N	$x = erf^{-1}\left(\frac{2.5 - C_{cr}}{2.5}\right) \cdot \sqrt{4(6.51x10^{-11})\left(\frac{t_0}{t}\right)^{0.7} t}$

5.5.2 Treated concrete

Two approaches (assumptions) were initially considered to model chloride ingress in the treated concrete:

- **Approach 1** – The hydrophobic (silane) impregnation reduces both the surface chloride content (C_s) and the apparent chloride diffusion coefficient (D_a). This approach assumes that the diffusion of chlorides is slower within the silane treated layer (x) and hence considers the treated concrete as a two-layer material (Figure 5-1); the impregnated layer (x) with diffusion coefficient D_t and the rest of the unaffected (untreated) concrete with diffusion coefficient D_u. This approach is based on the work of Tanaka et al (2015). Hence, in the model the treated surface concentration (Section 5.2.2) and treated apparent diffusion coefficient (Section 5.3) were used. It must be noted that the data points within both the impregnated layer (x) and the

unaffected layer were used in the curve fitting process (Appendix G). Hence, the treated apparent chloride diffusion coefficients shown in Section 5.3 are a combination of D_t and D_u.

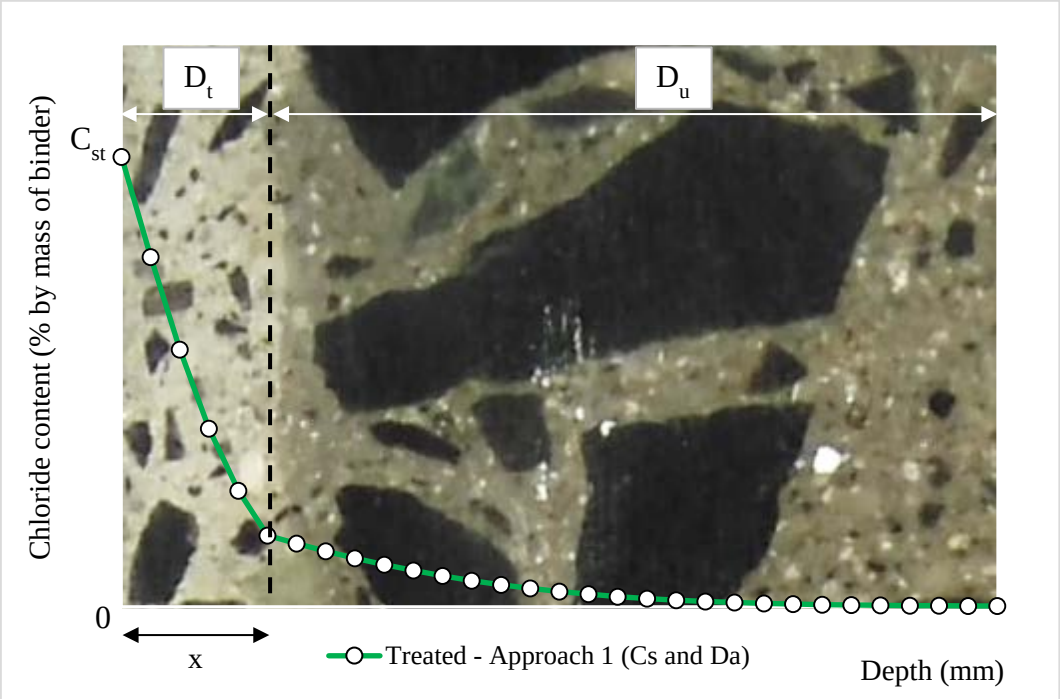

Figure 5-1: Treated concrete – Approach 1 (C_s and D_a)

- **Approach 2** – The hydrophobic (silane) impregnation decreases C_s only. This approach assumes that the chloride diffusion coefficient (D_a) is a material property and hence it is not affected by hydrophobic impregnation (Figure 5-2).

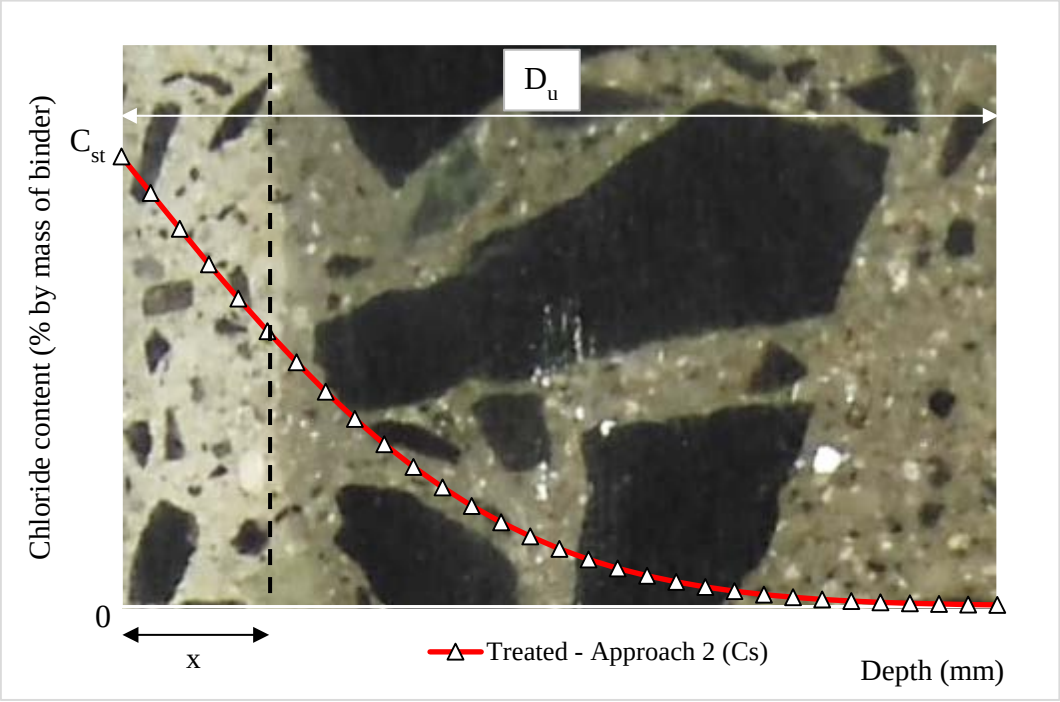

Figure 5-2: Treated concrete – Approach 2 (C_s)

This approach may be also valid for a situation where the penetration depth is very small. The treated surface concentrations (Section 5.2.2) and untreated apparent chloride diffusion coefficients (Section 5.3) were used. Figure 5-3 shows the chloride profiles (Mix 5) obtained using the two treated approaches relative to the untreated concrete.

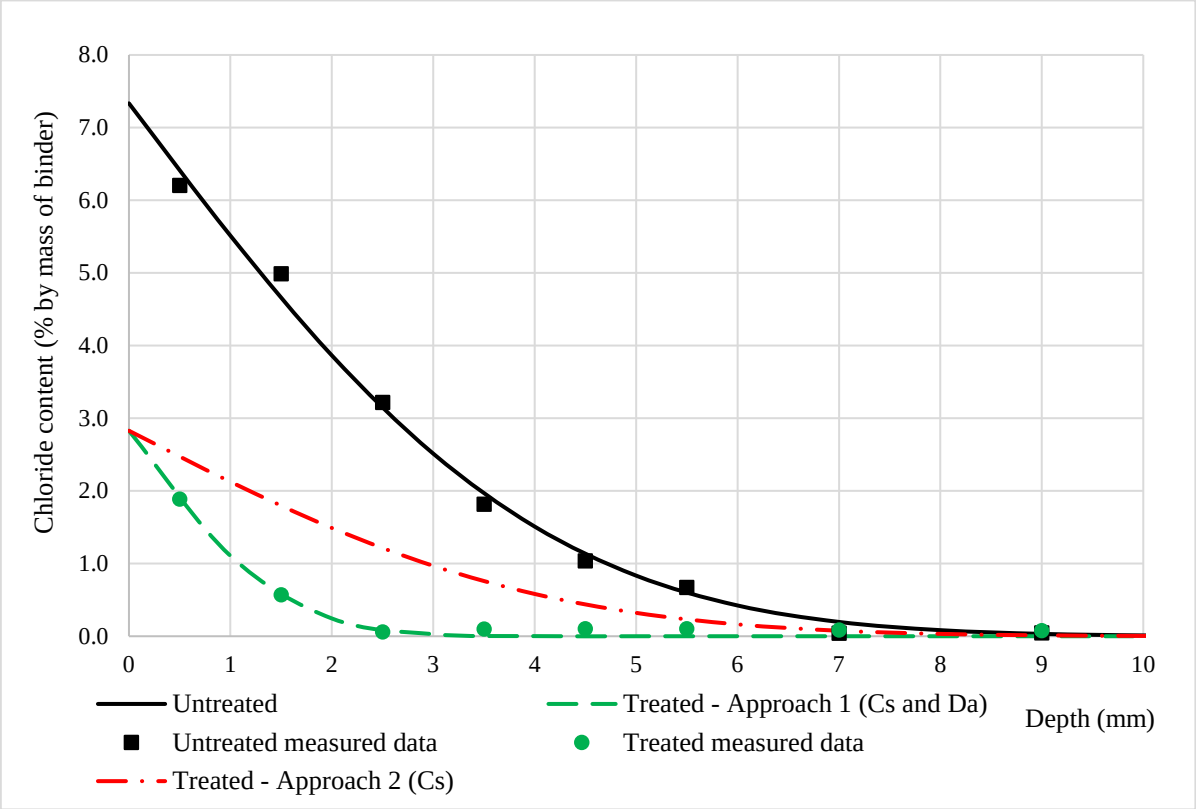

Figure 5-3: Illustration of the two treated approaches relative to the untreated concrete (Mix 5)

Table 5.6 and Table 5.7 show the equations for the treated concrete using the two respective approaches.

Table 5.6: Mathematical expressions for the penetration of the critical chloride threshold (0.4% by mass of binder) with time for treated concrete (Approach 1)

	w/b	Mix no	Composition	Expression (treated) – Approach 1
Tidal/splash zone (XS3)	0.45	Mix 1	100% CEM I 52.5N	$x = erf^{-1}\left(\frac{3.4 - C_{cr}}{3.4}\right) \cdot \sqrt{4(1.09x10^{-12})\left(\frac{t_0}{t}\right)^{0.4} t}$
		Mix 3	70% CEM I/30% FA	$x = erf^{-1}\left(\frac{2.3 - C_{cr}}{2.3}\right) \cdot \sqrt{4(2.64x10^{-13})\left(\frac{t_0}{t}\right)^{0.7} t}$
		Mix 5	50% CEM I/50% GGCS	$x = erf^{-1}\left(\frac{2.6 - C_{cr}}{2.6}\right) \cdot \sqrt{4(1.03x10^{-13})\left(\frac{t_0}{t}\right)^{0.45} t}$
		Mix 7	100% CEM III/B 42.5N	$x = erf^{-1}\left(\frac{4.6 - C_{cr}}{4.6}\right) \cdot \sqrt{4(4.49x10^{-14})\left(\frac{t_0}{t}\right)^{0.5} t}$

Atmospheric zone (XS1)	0.60	Mix 2	100% CEM I 52.5N	$x = erf^{-1}\left(\frac{1.8 - C_{cr}}{1.8}\right) \cdot \sqrt{4(9.66x10^{-13})\left(\frac{t_0}{t}\right)^{0.6} t}$
		Mix 2 poor	100% CEM I 52.5N	$x = erf^{-1}\left(\frac{1.03 - C_{cr}}{1.03}\right) \cdot \sqrt{4(1.08x10^{-12})\left(\frac{t_0}{t}\right)^{0.6} t}$
		Mix 4	70% CEM I/30% FA	$x = erf^{-1}\left(\frac{0.45 - C_{cr}}{0.45}\right) \cdot \sqrt{4(2.81x10^{-12})\left(\frac{t_0}{t}\right)^{0.8} t}$
		Mix 4 poor	70% CEM I/30% FA	$x = erf^{-1}\left(\frac{0.34 - C_{cr}}{0.34}\right) \cdot \sqrt{4(1.28x10^{-12})\left(\frac{t_0}{t}\right)^{0.8} t}$
		Mix 6	50% CEM I/50% GGCS	$x = erf^{-1}\left(\frac{2.3 - C_{cr}}{2.3}\right) \cdot \sqrt{4(6.30x10^{-13})\left(\frac{t_0}{t}\right)^{0.65} t}$
		Mix 6 poor	50% CEM I/50% GGCS	$x = erf^{-1}\left(\frac{0.9 - C_{cr}}{0.9}\right) \cdot \sqrt{4(1.57x10^{-12})\left(\frac{t_0}{t}\right)^{0.65} t}$
		Mix 8	100% CEM III/B 42.5N	$x = erf^{-1}\left(\frac{1.3 - C_{cr}}{1.3}\right) \cdot \sqrt{4(7.86x10^{-13})\left(\frac{t_0}{t}\right)^{0.7} t}$
		Mix 8 poor	100% CEM III/B 42.5N	$x = erf^{-1}\left(\frac{0.45 - C_{cr}}{0.45}\right) \cdot \sqrt{4(2.87x10^{-12})\left(\frac{t_0}{t}\right)^{0.7} t}$

Table 5.7: Mathematical expressions for the penetration of the critical chloride threshold (0.4% by mass of binder) with time for treated concrete (Approach 2)

	w/b	Mix no	Composition	Expression (treated) – Approach 2
Tidal/splash zone (XS3)	0.45	Mix 1	100% CEM I 52.5N	$x = erf^{-1}\left(\frac{3.4 - C_{cr}}{3.4}\right) \cdot \sqrt{4(4.02x10^{-12})\left(\frac{t_0}{t}\right)^{0.4} t}$
		Mix 3	70% CEM I/30% FA	$x = erf^{-1}\left(\frac{2.3 - C_{cr}}{2.3}\right) \cdot \sqrt{4(6.16x10^{-12})\left(\frac{t_0}{t}\right)^{0.7} t}$
		Mix 5	50% CEM I/50% GGCS	$x = erf^{-1}\left(\frac{2.6 - C_{cr}}{2.6}\right) \cdot \sqrt{4(7.03x10^{-13})\left(\frac{t_0}{t}\right)^{0.45} t}$
		Mix 7	100% CEM III/B 42.5N	$x = erf^{-1}\left(\frac{4.6 - C_{cr}}{4.6}\right) \cdot \sqrt{4(1.35x10^{-12})\left(\frac{t_0}{t}\right)^{0.5} t}$
Atmospheric zone (XS1)	0.60	Mix 2	100% CEM I 52.5N	$x = erf^{-1}\left(\frac{1.8 - C_{cr}}{1.8}\right) \cdot \sqrt{4(1.77x10^{-11})\left(\frac{t_0}{t}\right)^{0.6} t}$
		Mix 2 poor	100% CEM I 52.5N	$x = erf^{-1}\left(\frac{1.03 - C_{cr}}{1.03}\right) \cdot \sqrt{4(6.62x10^{-11})\left(\frac{t_0}{t}\right)^{0.6} t}$
		Mix 4	70% CEM I/30% FA	$x = erf^{-1}\left(\frac{0.45 - C_{cr}}{0.45}\right) \cdot \sqrt{4(1.66x10^{-11})\left(\frac{t_0}{t}\right)^{0.8} t}$
		Mix 4 poor	70% CEM I/30% FA	$x = erf^{-1}\left(\frac{0.34 - C_{cr}}{0.34}\right) \cdot \sqrt{4(1.42x10^{-8})\left(\frac{t_0}{t}\right)^{0.8} t}$
		Mix 6	50% CEM I/50% GGCS	$x = erf^{-1}\left(\frac{2.3 - C_{cr}}{2.3}\right) \cdot \sqrt{4(2.63x10^{-12})\left(\frac{t_0}{t}\right)^{0.65} t}$

		Mix 6 poor	50% CEM I/50% GGCS	$x = erf^{-1}\left(\frac{0.9 - C_{cr}}{0.9}\right) \cdot \sqrt{4(5.42x10^{-11})\left(\frac{t_0}{t}\right)^{0.65} t}$
		Mix 8	100% CEM III/B 42.5N	$x = erf^{-1}\left(\frac{1.3 - C_{cr}}{1.3}\right) \cdot \sqrt{4(1.99x10^{-12})\left(\frac{t_0}{t}\right)^{0.7} t}$
		Mix 8 poor	100% CEM III/B 42.5N	$x = erf^{-1}\left(\frac{0.45 - C_{cr}}{0.45}\right) \cdot \sqrt{4(6.51x10^{-11})\left(\frac{t_0}{t}\right)^{0.7} t}$

Figure 5-4 shows the predicted time to corrosion initiation (for specific cover depths) using the two approaches for Mix 5 (50% CEM I/50% GGCS, w/b 0.45) in the tidal/splash zone (XS3). Appendix I provides the results using the two approaches for the other mixes. From Figure 5-4, Approach 1 (assuming silane impregnation reduces both C_s and D_a) has the higher time to corrosion initiation for a particular cover depth compared to Approach 2 (assuming silane impregnation reduces C_s only).

Note: Both approaches depend on the durability of the hydrophobic impregnation. It is assumed that the water repellent product is reapplied (every 10-15 years) so that the protective measure is sustained.

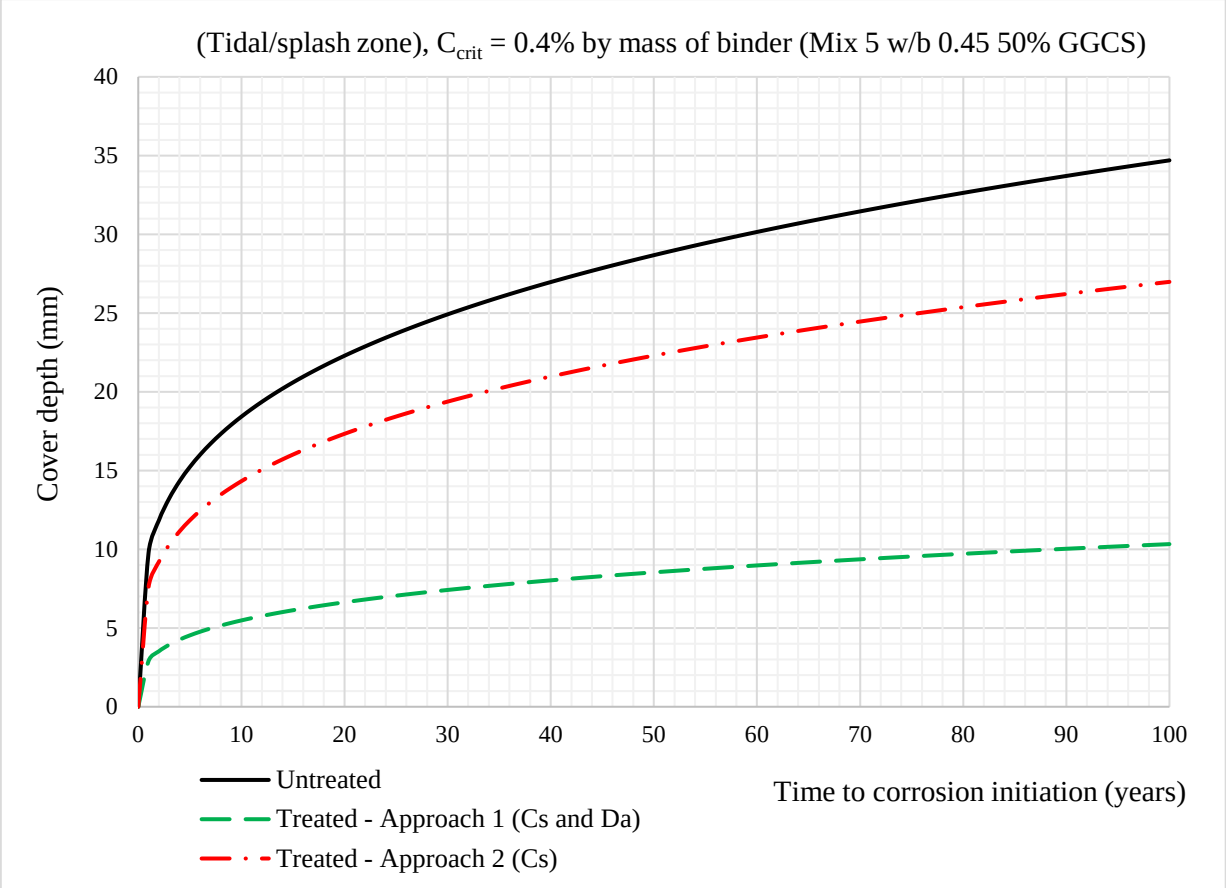

Figure 5-4: Time to corrosion initiation for Mix 5 using the two approaches

Figure 5-4 shows that a reduction in both surface chloride concentration (C_s) and apparent chloride diffusion coefficient (D_a) has more effect than a reduction in chloride surface concentration (C_s)

alone on the service life extension possible due to silane impregnation. From Figure 5-3, it can be noted that the measured (treated) data correlates best to Approach 1 (reduction in both C_s and D_a), otherwise the data points would follow a similar profile to the curve of Approach 2 (reduction in C_s only). Since silane impregnation reduces capillary absorption of water and dissolved chlorides, the supply of chlorides available to diffuse deeper into the concrete is limited. Hence, it can be assumed that silane impregnation reduces both the surface chloride concentration (C_s) and apparent chloride diffusion coefficient (D_a) (Tanaka *et al.*, 2015; Zhang *et al.*, 2017). Hence, Approach 1 was selected and used to predict the time to corrosion initiation for silane treated concrete.

5.5.3 Time to corrosion initiation graphs

Note: The graphs shown in Figure 5-5 to Figure 5-10 are based on the assumption that hydrophobic treatment is performed every 10-15 years (Section 2.8.4) so that the water repelling effectiveness is maintained with time.

Figure 5-5 and Figure 5-6 show the graphical representation of the penetration (mm) of the critical chloride concentration (0.4% by mass of binder) with time for (Mix 1/Mix 3) and (Mix 5/Mix 7) respectively in the tidal/splash zone. Considering the untreated concrete, it can be noted that rapid chloride penetration occurs within the first few years. Regardless of concrete quality, this rapid penetration within a short period further validates the use of large cover levels (50-60 mm) in the extreme marine environmental conditions (XS3). However, it must be emphasized that the rate of chloride ingress tends to attenuate with time, which can be explained by the reduction of the chloride diffusion coefficient due to ongoing hydration of the cementitious components (that reduces the capillary porosity over time) and chloride binding. This reduction in the rate of chloride ingress is more prominent in the blended mixes (Mix 3, Mix 5 and Mix 7). GGCS and GGBS can react with calcium hydroxide to form extra hydrated calcium silica hydrates in the cement paste matrix. These reactions lead to the densification of the concrete microstructure and reduction in porosity which overall decrease the penetrability to chloride ions (Siddique *et al.*, 2011).

Furthermore, as expected, an increase in cover depth (mm) extends the initiation period and overall service life of the concrete. Assuming the time to corrosion initiation is 50 years, cover depths of 70 mm, 44 mm, 29 mm and 34 mm are required for untreated Mix 1 (CEM I), Mix 3 (30% FA), Mix 5 (50% GGCS) and Mix 7 (CEM III/B) respectively. The results also highlight the superior performance of slag concretes and the poor chloride resistance of CEM I concrete. Similar results have been recorded in previous research undertaken by Mackechnie (2001). Considering the treated concrete results, it can be noted that rapid chloride penetration also occurs within the first few years, but to a much lesser extent compared to the untreated concrete. As time increases, the chloride threshold (0.4% by mass of binder) penetrates deeper into the treated concrete but the rate of ingress is reduced relative to the untreated concrete. The penetration rate also decreases with time most likely due to the time reduction of the overall porosity of the concrete. An increase in the cover depth extends the initiation period for reinforcement corrosion, and for 50 years time to corrosion initiation, the treated w/b 0.45 concrete mixes Mix 1 (CEM I), Mix 3 (30% FA), Mix 5 (50% GGCS) and Mix 7 (CEM III/B) require lower (theoretical) cover depths of 34 mm, 7 mm, 9 mm and 6 mm respectively.

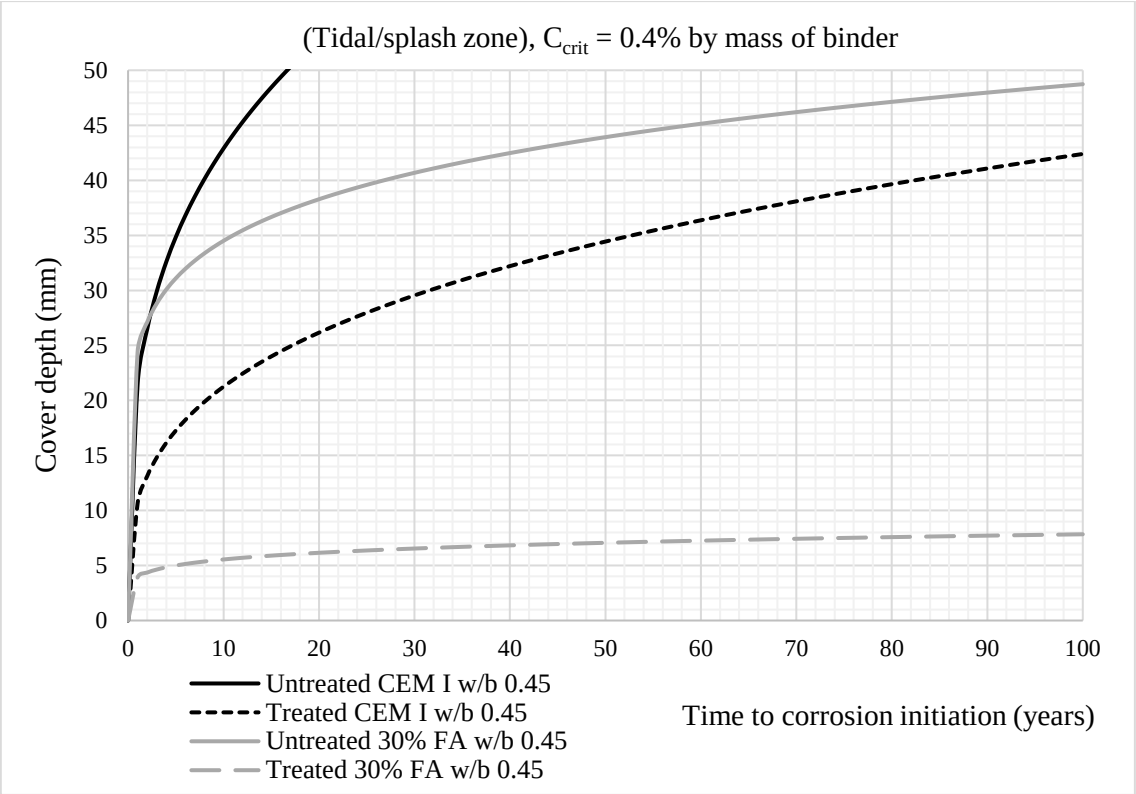

Figure 5-5: Time evolution of the critical chloride threshold for Mix 1 (100% CEM I – w/b 0.45) and Mix 3 (30% FA – w/b 0.45) in the tidal/splash zone

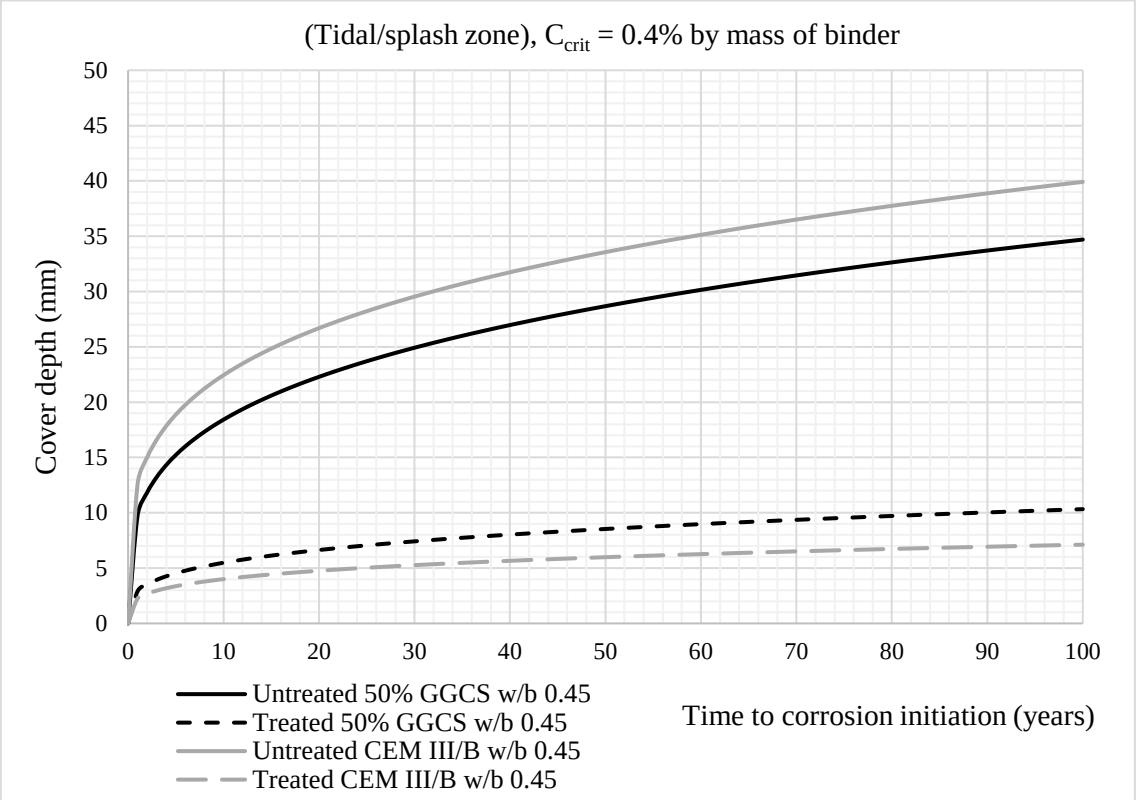

Figure 5-6: Time evolution of the critical chloride threshold for Mix 5 (50% GGCS – w/b 0.45) and Mix 7 (100% CEM III/B – w/b 0.45) in the tidal/splash zone

Figure 5-7 to Figure 5-10 show the penetration of the chloride threshold (0.4% by mass of binder) with time for the w/b 0.60 mixes (Mix 2, Mix 4, Mix 6 and Mix 8) and their respective poor-quality versions in the atmospheric zone (XS1). Similar to the w/b 0.45 mixes, ingress of chlorides occurs rapidly during the first few years followed by a gradual decrease in the rate of penetration with time. For a 50 years time to corrosion initiation, untreated concrete mixes Mix 2, Mix 4, Mix 6 and Mix 8 require cover levels of 70 mm, 45 mm, 28 mm and 20 mm respectively. Furthermore, considering the untreated poor-quality mixes, it can be noted that the critical chloride threshold for corrosion initiation (0.4% by mass of binder) is reached at depths 70-90 mm within only a few years, suggesting that large cover depths (>90 mm) are required to have any meaningful (useful) service life. However, in practice cover levels cannot be increased beyond certain limits (70-90 mm) due to mechanical and structural constraints. Hence, these (untreated) poor-quality mixes would be unsustainable and impractical to use from a concrete durability point of view.

From Figure 5-7 to Figure 5-10, considering the treated concrete mixes, to achieve 50-years time to corrosion initiation in the atmospheric zone (XS1), concrete mixes Mix 2, Mix 4, Mix 6 and Mix 8 hypothetically require smaller cover depths of 15 mm, 2 mm, 12 mm and 9 mm respectively. In theory, the treated poor-quality mixes (Mix 2 poor and Mix 6 poor) with cover depths of atleast 12 mm and 11 mm respectively, should ensure a time to corrosion initiation of 50-years in the atmospheric zone. No significant chloride penetration occurs during that period for Mix 4 poor and Mix 8 poor. The treated poor-quality mixes hence show better performance relative to their respective treated control mixes.

Note: In practice, a minimum cover depth is required for bond. Low of cover depths (<15 mm), even though treated with a water repellent (silane) product, are still sensitive to microcracking and carbonation which increase the risk of corrosion.

Tanaka et al (2015) used a similar methodology to quantify the service life extension possible using silane impregnation. The author showed that, assuming a critical chloride threshold of 0.38% by mass of cement, the service lives of untreated and silane treated concrete (Portland cement, w/b 0.50) with a cover of 50 mm in the atmospheric zone (C_s = 1.4% by mass of cement) was about 3 years and 20 years respectively. In this work, for the same cover of 50 mm, C_s = 2.0% by mass of cement and critical chloride threshold of 0.4% by mass of cement, untreated and treated Mix 2 (CEM I, w/b 0.60) have service lives of 9 and 100 years respectively. It must be noted that the time dependent reduction of the apparent chloride diffusion coefficient (Ballim *et al.*, 2009; Costa & Appleton, 1999) was considered in the calculations and therefore the service life extension through the use of silane impregnation is higher in this thesis. Furthermore, a higher amount of silane impregnation was used in this work (400 g/m^2) compared to Tanaka et al (2015) (200 g/m^2). Medeiros et al (2016) also investigated the service life extension of concrete (slag modified Portland cement, w/b 0.52) using surface treatments. However, the author made use of an accelerated diffusion (migration) test method to obtain the chloride diffusion coefficients for untreated and silane treated concrete. For a cover of 40 mm and assuming a chloride surface concentration (C_s) of 0.9% by mass of binder and a critical chloride threshold of 0.4% by mass of binder, the author found that service life of silane/siloxane treated concrete can be extended by 15%. In this work, for the same cover of 40 mm and chloride threshold and assuming C_s = 3%, the time to corrosion initiation for Mix 6 (50% CEM I/50% GGCS, w/b 0.60) can be extended by more than 100%.

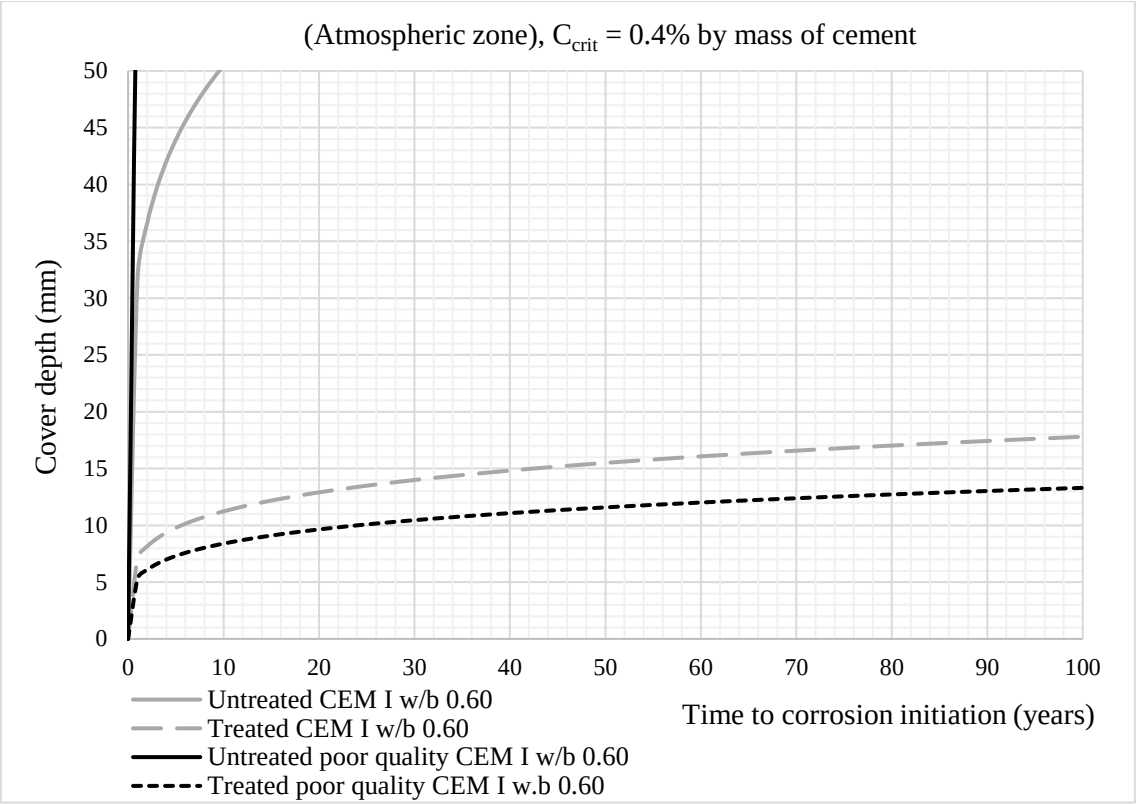

Figure 5-7: Time evolution of the critical chloride threshold for Mix 2 (100% CEM I – w/b 0.60) and Mix 2 poor (100% CEM I – w/b 0.60) in the atmospheric zone

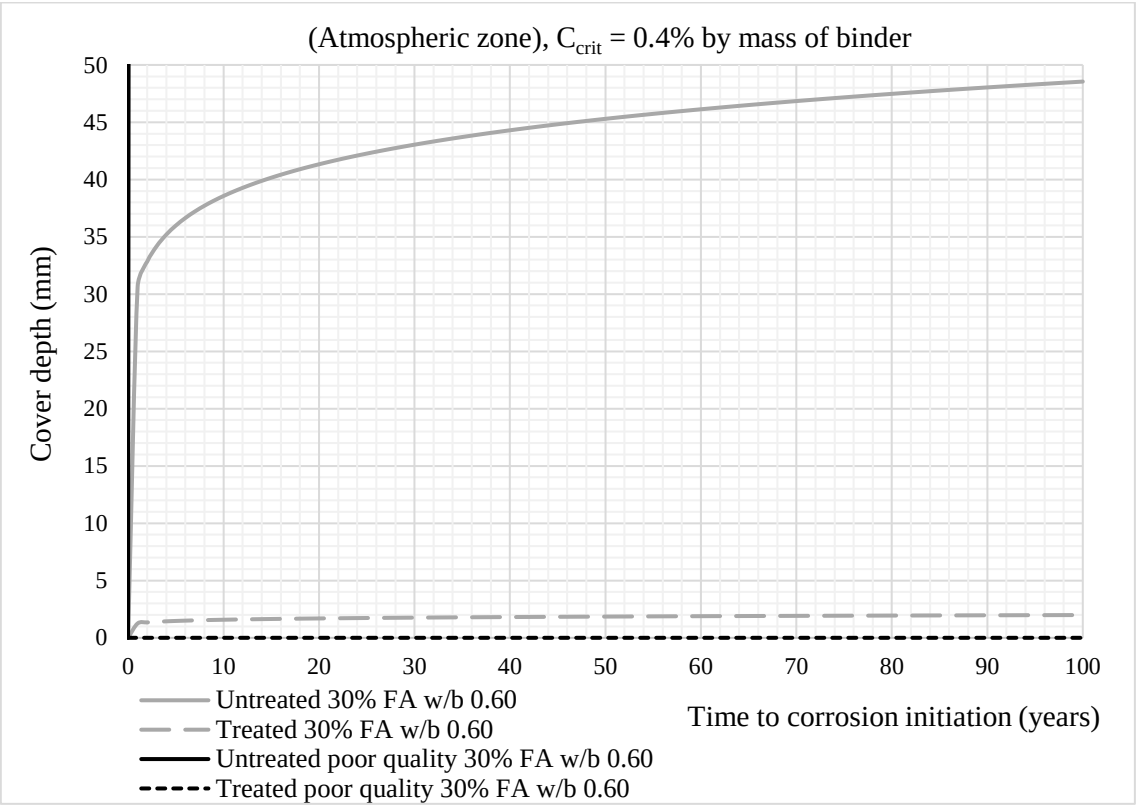

Figure 5-8: Time evolution of the critical chloride threshold for Mix 4 (30% FA – w/b 0.60) and Mix 4 poor (30% FA – w/b 0.60) in the atmospheric zone

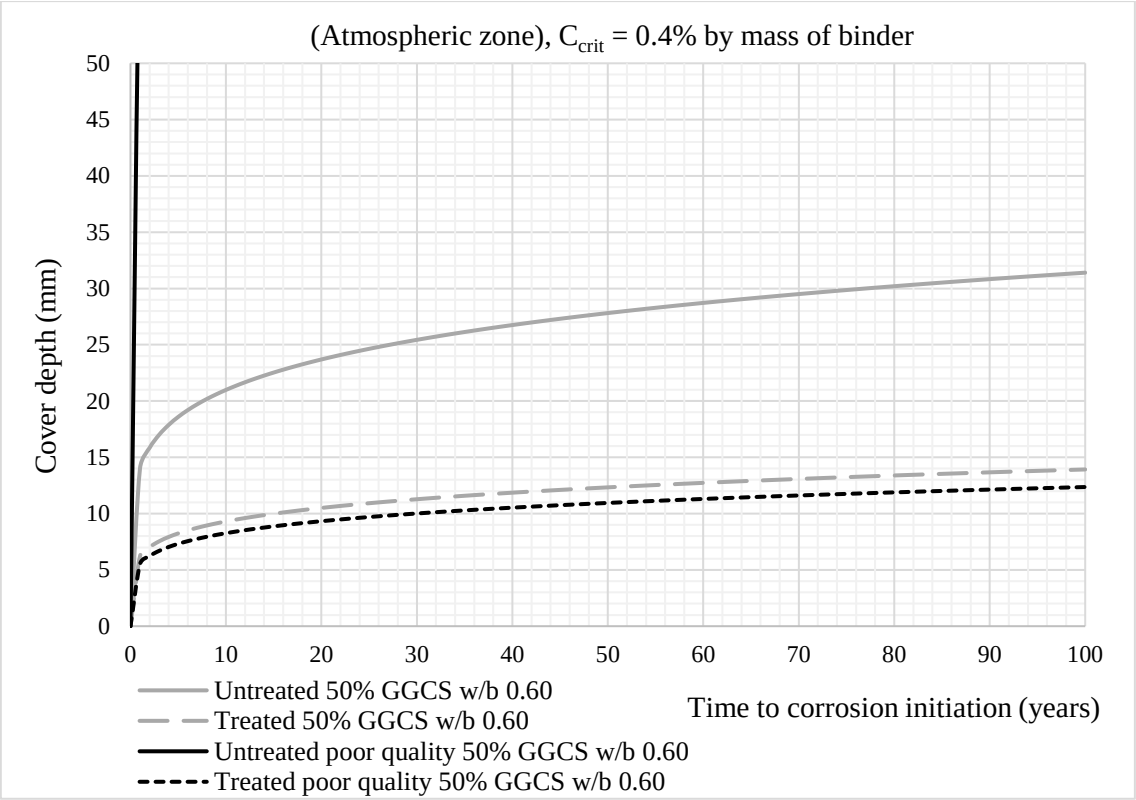

Figure 5-9: Time evolution of the critical chloride threshold for Mix 6 (50% GGCS – w/b 0.60) and Mix 6 poor (50% GGCS – w/b 0.60) in the atmospheric zone

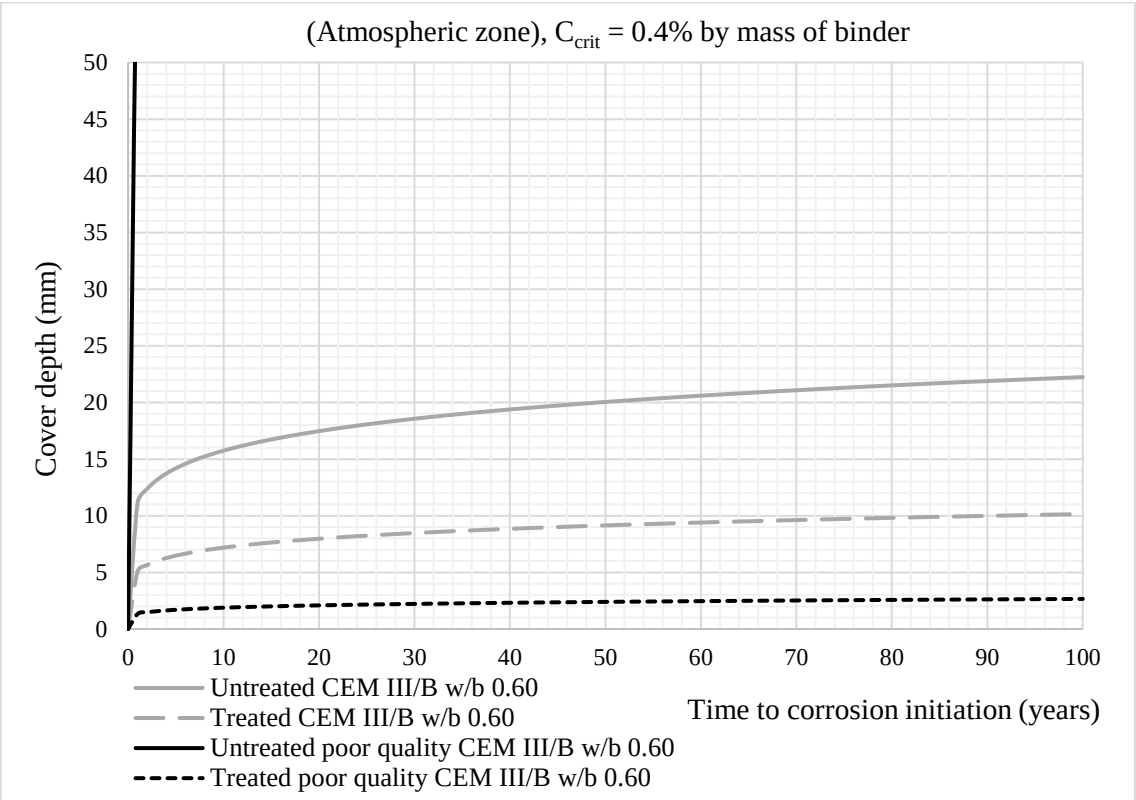

Figure 5-10: Time evolution of the critical chloride threshold for Mix 8 (100% CEM III/B – w/b 0.60) and Mix 8 poor (100% CEM III/B – w/b 0.60) in the atmospheric zone

5.6 Closure

This Chapter presented chloride ingress modelling into untreated and silane treated concrete. The chloride profiling data (obtained from the bulk diffusion test) was curve-fitted to a solution of Fick's second law of diffusion to obtain two regression parameters (surface chloride concentration/C_s) and (apparent chloride diffusion coefficient/D_a) for the untreated and treated concrete mixes. The short-term chloride ingress characteristics (C_s and D_a) measured in the bulk diffusion test were then used to predict long-term chloride ingress in concrete structures in the tidal/splash zone and atmospheric exposure zone, in order to quantify the effect of hydrophobic treatment on the durability of reinforced concrete structures in marine environments.

The apparent diffusion coefficients used in the predictions for the untreated and treated concrete were those obtained by curve fitting the chloride profiling data to a solution to Fick's second law of diffusion. The chloride surface concentrations (C_s/% of binder) used in the prediction of in-situ chloride ingress for the untreated concrete mixes were obtained from literature, based on measured data from marine concrete structures and field exposed specimens. The hydrophobic treatment had an effect on the chloride surface concentrations measured in the bulk diffusion test; generally, surface concentrations on treated samples were lower, compared to untreated samples made from the same concrete, as expected. It can therefore be assumed that the hydrophobic treatment also reduces C_s values in in-situ concrete structures. To account for this effect in the modelling of long-term chloride ingress in-situ, the surface concentrations (obtained from literature) were factored by the ratio (C_{st}/C_{su}) to calculate chloride surface contents for the treated concrete mixes, where C_{st} and C_{su} are the extrapolated surface chloride surface concentrations (% by mass of binder) for the treated and untreated concrete samples (obtained from curve fitting of experimental data) respectively. Hence, for the treated concrete, it was assumed that silane impregnation reduces both the surface chloride concentration (C_s) and apparent chloride diffusion coefficient (D_a).

Another solution to Fick's second law of diffusion was used to predict long term chloride ingress in untreated and silane treated concrete. This particular solution is similar to the one used by DuraCrete (2000) and incorporates the time dependence of the apparent chloride diffusion coefficient ($D_a(t)$). Hence, the appropriate surface chloride concentration (C_s), apparent chloride diffusion coefficient (D_a) and ageing coefficient (for each mix) were inserted into this solution. By determining the time taken for chloride concentration at the rebar level to reach a critical threshold (assumed to be 0.4% by mass of binder), the service life (time to corrosion initiation) of untreated and silane treated concrete was evaluated for specific cover depths.

6. Summary of results

6.1 Compressive strength

As expected, the water to binder ratio (w/b) had a major influence on the compressive strength of the concrete mixes; an increase in w/b correlated to a reduction in strength for all mixes. This was attributed to a weaker, more porous cement paste matrix and interfacial transition zone (ITZ). The compressive strength also increased with age as extended water curing provided the adequate conditions that promote cementing reactions (Mehta *et al.*, 2006). The use of supplementary cementitious materials (FA, GGCS, and GGBS) reduced the early age strength with the CEM I mixes showing the greatest strength gain due to a higher rate of hydration (Ramezanianpour, 2014). Relative to the CEM I mixes, the slag mixes (GGCS and GGBS) displayed similar compressive strength at 28 days while the FA mixes recorded lower strength values at all ages. Slags react slower than Portland cement to form the same hydration products, calcium silicates (C-S-H) leading to a reduction in early strength development but similar or higher strength is usually achieved in the long term (Nawy, 2008). FA usually reduces early age strength due to slower pozzolanic reactions that do not contribute to matrix densification but may increase the compressive strength in the long term. The poor-quality concrete mixes achieved significantly lower compressive strength at all ages relative to their respective control mixes. Since the concrete was exposed to relatively high temperature at early age, the moisture content in the capillaries was reduced. Hence, cementing (hydration) reactions were slowed down, leading to a reduction in strength development (Alexander & Beushausen, 2009; Thomas, 2013).

6.2 Durability Index

6.2.1 Cut surfaces

Durability Index tests (OPI, WSI and CCI) were performed on cut surfaces for mix characterisation purposes. All the main concrete mixes (Mix 1-8) achieved OPI values between 9.90 and 10.67, WSI values ranging from 4.2 to 7.8 mm/hr$^{0.5}$, and CCI values between 0.16 and 1.09 mS/cm. These results suggest that these mixes have sufficient resistance to carbonation, capillary absorption and chloride ingress respectively. The OPI and CCI values generally decreased and increased with a higher w/b ratio respectively and this was attributed to an increase in porosity of the cement paste microstructure and larger number of interconnections between the pores which act as channels of flow in the cement paste. This allowed greater permeation of oxygen gas and migration of chloride ions respectively. The effect of w/b on the WSI test was not clear due to the overlapping of the error bars. The effect of binder type on the OPI and WSI tests was not explicit due to similar results between mixes of the same w/b. In terms of the CCI test, for the same w/b ratio, the inclusion of GGCS and GGBS reduced the CCI values significantly. This was attributed to the ability of these supplementary cementitious materials to reduce the movement of chloride ions within the pore structure and thus increase the resistivity of the concrete under an externally applied potential difference. Furthermore, GGCS and GGBS can react with calcium hydroxide to form additional hydrated calcium silicate hydrates in the cement paste matrix. These reactions lead to the densifi-

cation of the concrete microstructure and a reduction in porosity which overall reduce the penetrability to chloride ions. The fly-ash mixes recorded similar CCI values relative to the CEM I mixes due to slower pozzolanic reactions that increase penetrability at relatively early age (Ramezanianpour, 2014; Siddique *et al.*, 2011).

The poor-quality mixes generally recorded lower OPI, higher WSI and CCI values and greater porosity compared to their respective control mixes, with atleast one Durability Index value falling within the following limits (OPI < 9.5, WSI > 10 mm/hr$^{0.5}$ and CCI > 1.50 mS/cm). This can be attributed to the insufficient curing (slower hydration reactions) that lead to the development of a relatively more porous cement paste matrix. The results suggest that these poor-quality mixes have low resistance to the ingress of deleterious agents such as chlorides and carbon dioxide gas (Mehta *et al.*, 2006; Alexander & Beushausen, 2009).

6.2.2 Uncut surfaces

Water Sorptivity Index (WSI) and Chloride Conductivity Index (CCI) tests were performed on uncut concrete discs to evaluate the influence of silane (hydrophobic) impregnation on the transport properties (sorptivity and conductivity) of the concrete mixes. According to the results, silane treated concrete recorded lower WSI and CCI values relative to the untreated concrete. Hydrophobic (silane) impregnation chemically modifies the near surface zone of the concrete and reduces the capillary uptake of water. Furthermore, as the silane molecules bond and cover the capillary walls, the latter become devoid of ionic electrical charges and polar molecules such as water are no longer attracted to the concrete surface (Tepfers, 2009; Raupach, 2014, Liu, 2017). Migration of chloride ions is also minimised as the capillary pores within the silane impregnated layer are less saturated relative to untreated concrete (Li, 2017; Poursaee, 2016). The results hence suggest that the transport properties (sorptivity and conductivity) of poor-quality concrete can be substantially improved through the application of silane impregnation. However, it must be emphasized that the resistance to capillary absorption and chloride migration is only increased within the impregnated layer and the rest of the concrete is still characterised as poor-quality.

6.3 Penetration depth

As expected, the silane penetration depth increased with a higher w/b ratio. This was attributed to the higher capillary porosity of the cement paste microstructure which allowed deeper penetration of the water repellent product (Johansson, 2006; Meier & Wittman, 2011). The effect of binder type for the w/b 0.60 mixes was unclear due to the overlapping of error bars but for the w/b 0.45 mixes, the inclusion of FA and GGBS (CEM III/B) increased and reduced the penetration depth respectively. Fly-ash usually increases the porosity of concrete at early age due to slower pozzolanic reactions that do not contribute to matrix densification while GGBS reduces capillary porosity by forming extra hydrated calcium silicate hydrates in the cement paste matrix (Ramezanianpour, 2014, Thomas, 2013).

The silane penetration depth was greater in the poor-quality concrete mixes. This can be related to the more porous cement paste microstructure that enables the product to penetrate deeper into the concrete. Moreover, as the concrete was exposed to high temperature at early age, the moisture content in the capillary pores was reduced compared to the control mixes. As the water

repellent agent enters the pore system mainly by capillary suction, a higher penetration depth is generally expected in less saturated (drier) concrete (Selander, 2010; Meier & Wittman, 2011). The silane penetration depth (mm) was also found to be highly related to the Oxygen Permeability Index (OPI/log-scale). This correlation was explained by the fact that the penetration depth of the product is a function of the overall quality (interconnectedness, tortuosity of the capillary pore structure) of the near surface concrete and the OPI test evaluates these properties.

6.4 Accelerated carbonation

The carbonation depth generally increased with a higher w/b ratio and the inclusion of supplementary cementitious materials (FA, GGCS and GGBS). An increase in w/b ratio contributed to a weaker and more porous cement paste microstructure with higher interconnectivity of the capillary pore structures which allowed higher diffusion of carbon dioxide gas. The use of cement extenders caused higher carbonation due to a reduction in calcium hydroxide (carbonatable material) content. For instance, fly-ash being a pozzolan, reacts slowly with calcium hydroxide liberated during the hydration of Portland cement. Slag is considered as a latent hydraulic binder which requires activation by lime to produce calcium silicate hydrates (C-S-H). Hence, the reactions of these supplementary cementitious materials decreased the calcium hydroxide content in the pore solution and reduced the resistance of the concrete to carbonation (Nawy, 2008; Soutsos, 2010, Thomas, 2013). Higher carbonation depths were obtained in the poor-quality mixes. This was attributed to insufficient curing (slower hydration reactions) that produced a relatively more porous cement paste matrix. The pores in the poor-quality concrete were also less saturated compared to the respective control mixes, and this further increased the diffusion rate of carbon dioxide (Alexander & Beushausen, 2009; Thomas, 2013; Poursaee, 2016).

No significant difference in carbonation depth was recorded between untreated and treated concrete for the w/b 0.45 and poor-quality mixes. The effect of silane impregnation was more apparent in the w/b 0.60 mixes, whereby the carbonation depth was reduced. This result was explained by the higher relative humidity (near the surface) in the treated concrete that reduced the diffusion of carbon dioxide.

6.5 Bulk diffusion

6.5.1 Uncracked concrete

The surface chloride concentration (C_s (% by mass of binder)) generally increased with a higher w/b ratio. The trend was less apparent in the CEM I and FA mixes. This result was attributed to a higher porosity of the cement paste matrix in the near surface zone. The influence of the binder type on the chloride surface concentration was unclear due to the overlapping of the error bars. The poor-quality mixes generally recorded lower surface chloride content relative to their respective control mixes. Silane treatment reduced the surface chloride concentration and the effect was more pronounced in the FA, GGCS, CEM III/B and poor-quality mixes. The apparent chloride diffusion coefficient (obtained by curve fitting the chloride profiling data points to a solution to Fick's second law of diffusion) decreased with a lower w/b and the use of slag. These results were

attributed to a reduction in capillary porosity with less interconnections between pores which otherwise act as channels of flow in the cement paste matrix. Slag in concrete can bind chlorides and hence reduce the chloride content in the pore solution. This results in a reduced chloride diffusion rate. The use of slag also contributes to pore size refinement and matrix densification over time which further reduce the penetrability to chlorides (Ramezanianpour, 2014; Siddique *et al.*, 2011). The poor-quality concrete showed higher apparent chloride diffusion coefficients relative to their respective control mixes and this result was explained by the significantly higher porosity and lower saturation of these concrete mixes which allowed a higher rate of chloride penetration and diffusion (Alexander & Beushausen, 2009; Poursaee, 2016).

The silane treated concrete had lower apparent chloride diffusion coefficients relative to the untreated concrete. As the chloride penetration and content is reduced within the near surface zone, the supply of chloride ions that can diffuse deeper into the concrete is smaller. Thus, the diffusion gradient is less steep in silane treated concrete. Diffusion of chlorides is also significantly slowed down as the capillary pores are less saturated in the silane impregnated (treated) concrete (Li, 2017, Zhang, 2017). A higher percentage reduction in chloride diffusion coefficient was observed in the poor-quality mixes and can be attributed to the higher penetration depth of the water repellent product.

6.5.2 Cracked concrete

Higher chloride content was measured in the cracked concrete samples at depths 50-60 mm compared to the uncracked samples. This was attributed to the fact that cracks provide localised and favourable paths for the ingress of deleterious agents (chlorides). As the salt solution penetrated deeper inside the concrete, the increased contact surface area allowed significantly higher diffusion of chlorides through the internal crack surface. In general, the chloride concentration decreased with increasing depth and this was explained by the decreasing crack width from the crack opening. Higher ingress of chlorides was noted in the 0.6 mm crack width compared to the 0.2 mm crack width specimens. The inclusion of slag (GGCS and GGBS) in the concrete reduced the penetration of chlorides in the cracked concrete samples while the fly-ash mix recorded similar chloride content relative to the CEM I mix. The results were explained by the chloride binding ability and slower pozzolanic reactions of slag and fly-ash respectively.

According to the results of the treated cracked concrete, the chloride content initially decreased with increasing depth and subsequently increased for all the mixes. Silane impregnation is a water repellent treatment and not a water proofing measure. Hence, treated cracked concrete has a lower efficiency under increased hydrostatic pressure. Nevertheless, the results suggest that the risk of reinforcement corrosion initiation in silane treated cracked concrete (up to a crack width of 0.6 mm) is reduced compared to the untreated cracked concrete, especially in slag concrete.

6.6 Moisture profiling

The moisture content of the near surface zone was significantly increased soon after silane treatment. This result was attributed to the condensation reactions that occur when the silane molecules react with the concrete substrate to form silicon resin. Water is released during this process which increases the relative humidity (Pan *et al.*, 2017). Higher moisture content was still observed after

16 weeks but the difference in relative humidity (near the surface) between silane treated and untreated concrete was reduced with time. This was related to the fact that the hydrophobic impregnation only lines the internal pore structure with silane molecules and hence does not hinder the movement of water vapour in and out of the concrete (Bertolini *et al.*, 2013).

6.7 Service life modelling

Note 1: The results presented assume that hydrophobic treatment is performed every 10-15 years (Section 2.8.4) so that the water repelling effectiveness is maintained with time.

Note 2: In practice, a minimum cover depth (safety margin) is required for bond. Low of cover depths (<15 mm), even though treated with a water repellent (silane) product, are still sensitive to microcracking and carbonation which can increase the risk of corrosion.

Rapid chloride penetration was predicted in the untreated normal (main) concrete mixes within the first few years, regardless of the concrete type. This further emphasized the use of sufficiently large cover depths (>30 mm), especially in the extreme (XS3) marine exposure conditions to have sufficient time before corrosion initiation. However, the rate of chloride ingress is reduced with time and this was attributed to the reduction of the chloride diffusion coefficient with time due to continuous cement hydration reactions that decrease capillary porosity. As expected, an increase in cover depth correlated to an increase in the time to corrosion initiation. Assuming the initiation period is 50 years, lower cover depths are required for the fly-ash and slag concretes relative to CEM I concrete. The critical chloride threshold (0.4% by mass of binder) was reached at depths of 70-90 mm within only a few years in the untreated poor-quality concrete mixes. These results indicated that relatively large cover depths (>90 mm) are necessary to have any meaningful time to corrosion initiation, suggesting that the untreated poor-quality concrete mixes were unsuitable from a durability perspective.

Chloride ingress also occurred rapidly in the treated normal and poor-quality concrete mixes. However, the depth to which the critical chloride threshold is reached after the first few years is limited to 5-10 mm. The critical chloride concentration front penetrates deeper in the treated concrete with time but at a lower rate compared to the untreated concrete. Hence, for the same time to corrosion initiation, the cover depths can be reduced in the treated concrete. It must be also noted that better performance is achieved in the treated poor-quality mixes compared to their respective control mixes which can be linked to the higher silane penetration depth.

Table 6.1 summarises the time to corrosion initiation (years) for different cover depths (20 mm, 30 mm, 40 mm and 50 mm). Hydrophobic (silane) impregnation can effectively increase the time to corrosion initiation regardless of the concrete quality (water to binder ratio (w/b), binder type, degree of curing). The increase in the initiation period due to silane treatment is more noticeable in the case of low cover depth (20 mm) compared to high cover depth (50 mm). The results also show that untreated w/b 0.60 concrete mixes, unless used with high cover depths (>40 mm) are not suitable for the marine environment (atmospheric zone) due to their low chloride ingress resistance.

Table 6.1: Time to corrosion initiation for different cover depths

Exposure class	Mix no	Time to corrosion initiation (years)							
		cover 20 mm		cover 30 mm		cover 40 mm		cover 50 mm	
		Un-treated	Treated	Un-treated	Treated	Un-treated	Treated	Un-treated	Treated
Tidal/ splash (XS3)	Mix 1	<1	8	3	30	8	79	17	>100
	Mix 3	<1	>100	4	>100	25	>100	>100	>100
	Mix 5	13	>100	56	>100	>100	>100	>100	>100
	Mix 7	6	>100	30	>100	96	>100	>100	>100
Atmos-pheric (XS1)	Mix 2	<1	>100	<1	>100	3	>100	10	>100
	Mix 2 poor	<1	>100	<1	>100	<1	>100	<1	>100
	Mix 4	<1	>100	<1	>100	13	>100	>100	>100
	Mix 4 poor	<1	>100	<1	>100	<1	>100	<1	>100
	Mix 6	7	>100	70	>100	>100	>100	>100	>100
	Mix 6 poor	<1	>100	<1	>100	<1	>100	<1	>100
	Mix 8	42	>100	>100	>100	>100	>100	>100	>100
	Mix 8 poor	<1	>100	<1	>100	<1	>100	<1	>100

7. Conclusions

This study aimed at quantifying the service life extension possible using hydrophobic (silane) impregnation. This work also involved evaluating the performance of silanes as a remedial measure to inadequate quantity and quality of cover concrete in newly constructed structures located in aggressive marine environments. The experimental test results on untreated and silane treated concrete were compared and analysed. The following section describes the main conclusions that can be drawn from the results of this investigation.

- As expected, the water to binder ratio (w/b) had a major influence on the strength and durability properties of the concrete mixes. For instance, lower w/b correlated to higher compressive strength and reduced overall penetrability. The inclusion of supplementary cementitious materials such as fly-ash and slag (GGCS and GGBS) also had a significant impact on strength and durability properties of the concrete mixes. The chloride ingress and carbonation resistance of the concrete mixes was increased and reduced respectively with the addition of these cement extenders.
- The poor-quality concrete mixes generally recorded lower OPI, greater WSI and CCI and higher porosity values compared to their respective control mixes, with at least one Durability Index value falling within the following limits (OPI < 9.5, WSI > 10 mm/hr$^{0.5}$ and CCI > 1.50 mS/cm). Higher carbonation rate and chloride ingress was recorded for the poor-quality mixes. The results hence highlighted the importance of good curing practice to produce durable concrete.
- The silane penetration depth was strongly dependent on the quality (porosity) and relative humidity of the near surface zone as deeper penetration was observed in the higher w/b and poor-quality (drier) concrete mixes. A high correlation was obtained between the silane penetration depth and OPI value, whereby a decrease in OPI resulted in an increase in penetration depth. This suggests that the OPI test represents an excellent method to estimate the potential silane penetration depth in concrete.
- Silane impregnation improved the transport properties (reduced sorptivity and conductivity) of both the main and poor-quality concrete mixes. The chloride surface concentration (C_s) and apparent chloride diffusion coefficient (D_a) were generally reduced for all treated concrete mixes. The effect of silane impregnation on carbonation was negligible in the w/b 0.45 mixes, while a slight decrease in carbonation depth was recorded in the w/b 0.60 mixes. This was attributed to the increase in relative humidity near the surface due to silane impregnation. Even though silane impregnation did not significantly improve the carbonation resistance of the concrete, in practice, treated concrete will have lower moisture content relative to untreated concrete, which all else equal, can potentially minimise corrosion rates. Further research is needed to investigate this assumption.
- Relative to the uncracked concrete mixes, deeper chloride penetration was observed in the cracked concrete. An increase in crack width also correlated to greater chloride ingress while the inclusion of slag generally reduced the chloride concentration deeper along the crack path.

The silane treated cracked concrete recorded lower chloride content and better performance was observed in the slag concrete mixes. The overall results indicate that risk of reinforcement corrosion initiation in cracks up to 0.6 mm can be minimised with silane impregnation.

- The model used to predict the service life (time to reinforcement corrosion initiation) of untreated and silane treated concrete was based on the error function solution to Fick's second law of diffusion. While it is based on several simplified assumptions, it remains one of the most widely used methods as it provides a reasonable estimate from an engineering standpoint. The time dependence of the apparent chloride diffusion coefficient (D_a) was considered and maximum surface chloride concentrations (C_s) found in practice were used to have realistic predictions. It must be noted that the modelling results presented in this work are based on short term testing under laboratory (controlled) environmental conditions. Further long term and field data is needed to improve the reliability of the model. A deterministic approach (based on main input values; 50% probability) was also used; hence the results should be regarded in the context of improving the durability of reinforced concrete structures rather than designing for durability (cover depths).
- The service life prediction results highlighted the importance of sufficient cover depths, especially in the extreme marine exposure class (XS3) and the superior performance of slag concrete compared to CEM I concrete. Rapid chloride penetration was predicted in the untreated poor-quality concrete within a short period, suggesting the need for unrealistic cover depths (>90 mm). Hence, these untreated poor-quality concrete mixes were inappropriate from a durability standpoint. However, lower rate of chloride ingress was predicted in all the silane treated concrete mixes and therefore for the same initiation period, smaller cover depths are required. In general, except for Mix 1 (CEM I w/b 0.45), all the treated concrete mixes theoretically require less than 30 mm cover for 50 years time to corrosion initiation in their respective exposure classes. However, it must be noted that in actual structures, a minimum cover depth (safety margin) is needed for bond and to minimise effects from microcracking and thermal shocks.
- In practice, the results of this thesis indicate that the time to corrosion initiation in reinforced concrete structures with insufficient cover depth and quality, (regardless of the binder type), can be effectively extended using silane impregnation, assuming proper surface preparation and application methods (regular maintenance and reapplication of the water repellent product). The time to corrosion initiation graphs presented in this work can be used to have an estimate of the service life of silane treated concrete for specific cover depths. This can ultimately help the various stakeholders to make informed decisions on the use of hydrophobic impregnation as a measure to extend the service life of newly constructed structures in the marine environment that failed to achieve necessary cover depth or quality.

8. Recommendations

In this study, the extent of experimental work was limited mainly by time availability. The scope of testing in certain instances might not have been sufficient to draw a final conclusion to the research topic. Additional detailed investigations need to be undertaken to obtain more comprehensive results and hence develop further understanding of the influence of silane impregnation on service life extension. The following are suggested to improve the outcome of this research topic and future related work:

- The bulk diffusion tests should be carried out over a longer period (1-2 years) to have more realistic chloride profiling data and therefore improve the reliability of the service life predictions. The long-term chloride penetration results could also be used to develop a full-probabilistic model for the service life prediction.
- Alternatively, silane treated and untreated concrete samples could be exposed to coastal environmental conditions (in the various exposure zones) for a sufficient amount of time. Hence, realistic surface chloride concentrations for the treated concrete can be obtained and incorporated into the model to obtain more accurate service life predictions.
- Literature provides mostly a qualitative assessment of how silanes function. Further research work should attempt to quantify how does silane impregnation modify the transport properties of concrete. For instance, the slower diffusion of chlorides within the treated concrete layer could be investigated by chloride profiling and curve fitting data within that impregnated layer. Larger silane consumption/application amounts (g/m^2) would be required to obtain the necessary penetration depth.
- The durability of the silane impregnation could be evaluated by performing a local survey of 10-20 years old silane treated concrete structures and measuring the residual silane penetration depth and resistance to capillary absorption.
- The performance of silane impregnation in cracked concrete should be assessed with salt water wetting and drying cycles over a longer period (1-2 years) to obtain more representative results.
- A cyclic wetting and drying procedure (using water) must be incorporated in the carbonation resistance and moisture profiling tests. Alternatively treated concrete samples could be preconditioned and exposed to outdoor environmental conditions (summer-winter cycles). This would give a better representation of the influence of silane impregnation on carbonation and moisture content in practice.

9. References

ACI 357R-84. 1997. *Guide for the Design and Construction of Fixed Offshore Concrete Structures.* American Concrete Institute.

Alexander, M., Bentur, A. & Mindess, S. 2017. *Durability of Concrete: Design and Construction.* CRC Press.

Alexander, M. 2016. *Marine Concrete Structures - Design, Durability and Performance.* Woodhead Publishing.

Alexander, M., Bertron, A. & De Belie, N. 2013. *Performance of cement-based materials in aggressive aqueous environments.* Springer.

Alexander *et al.,* 2012. Research Monograph No 9 – *Corrosion of steel in reinforced concrete: Influence of binder type, water/binder ratio, cover and cracking.* Concrete Materials and Structural Integrity Research Unit (CoMSIRU).

Alexander, M., Beushausen, H & Otieno, M. 2010. *Research report – Transport mechanisms in concrete, factors affecting corrosion of steel and assessment.* Concrete Materials and Structural Integrity Research Unit (CoMSIRU).

Alexander, M. G., Beushausen, H. & Otieno, M. B., 2012. *Corrosion of steel in reinforced concrete: Influence of binder type, water/binder ratio, cover and cracking.* Cape Town: University of Cape Town, Concrete Materials and Structural Integrity Research Unit, MSc Thesis.

Alexander, M. G., Jaufeerally, H & Mackechnie, J. R. 2003. *Structural and durability properties of concrete made with Corex slag.* Department of Civil Engineering. University of Cape Town; University of the Witwatersrand.

Alexander & Beushausen., 2009. *Fulton's concrete technology.* Cement & Concrete Institute.

Alexander, M. & Beushausen, H. 2008. *Performance-based durability testing, design and specification in South Africa: latest developments.* Excellence in Concrete Construction through Innovation. :429-434.

Alexander, M., Ballim, Y. & Stanish, K. 2008. *A framework for use of durability indexes in performance-based design and specifications for reinforced concrete structures.* Materials and Structures. 41(5):921-936.

Angelucci, M, Beushausen, H & Alexander, M.G. 2012. *Mix design optimisation – The influence of binder content on mechanical and durability properties of concrete.* Concrete Repair, Rehabilitation and Retrofitting III: 3rd International Conference on Concrete Repair, Rehabilitation and Retro-fitting, ICCRRR-3, 3-5 September 2012, Cape Town, South Africa. CRC Press.

Antons, U., Raupach, M. & Weichold, O. 2015. *Durability of Hydrophobic Treatments on Concrete.* Durability of Reinforced Concrete from Composition to Protection. Springer. 35-43.

ASTM C1556-04. 2004. *Standard Test Method for Determining the Apparent Chloride Diffusion Coefficient of Cementitious Mixtures by Bulk Diffusion.* ASTM International, USA.

ASTM C1152/C1152M-04. 2012. *Standard Test Method for Acid-Soluble Chloride in Mortar and Concrete.* ASTM International, USA.

Ballim, Y., Alexander, M., Beushausen, H. & Moyo, P. 2009. *Reflections on future needs in concrete durability research and development.*

Ballim, Y, Alexander, M & Beushausen, H. 2009. *'Durability of concrete',* in G Owens (ed.), Fulton's Concrete Technology, Cement and Concrete institute, Midrand.

Basheer, P.A.M. and Basheer, L. 1997. *Surface treatments for concrete: assessment methods and reported performance.* Construction and Building Materials, 11, 413–429.

Bertolini, L., Elsener, B., Pedeferri, P., Redaelli, E. & Polder, R.B. 2013. *Corrosion of steel in concrete: prevention, diagnosis, repair.* John Wiley & Sons.

Bertolini, L. 2008. *Steel corrosion and service life of reinforced concrete structures.* Structure and Infrastructure Engineering. 4(2):123-137.

Beushausen, H. & Luco, L.F. 2016. *Performance-Based Specifications and Control of Concrete Durability.* Springer.

Bijen, J. 2003. *Durability of engineering structures: design, repair and maintenance.* Elsevier.

Böhni, H. 2005. *Corrosion in reinforced concrete structures.* Elsevier.

Bofeldt, M. & Nyman, B. 2002. *Penetration depth of hydrophobic impregnating agents for concrete/Eindringtiefe von Hydrophobierungsmitteln in Beton.* Restoration of Buildings and Monuments. 8(2-3):217-232.

British Standards Institution (BSI). 2013. *BS EN 206 - Concrete: specification, performance, production and conformity.* British Standards Institution.

Burmeister, N. 2012. *Evaluation of Surface Treatments for RC Structures Failing to Meet South African Durability Index Requirements.* University of Cape Town (UCT).

Büttner, T. & Raupach, M. 2008. D*urability of hydrophobic treatments on concrete - results from laboratory tests.* 5th International Conference on Water Repellent Treatment of Building Materials. 329.

Christodoulou, C., Goodier, C.I., Austin, S.A., Webb, J. & Glass, G.K. 2013. *Long-term performance of surface impregnation of reinforced concrete structures with silane.* Construction and Building Materials. 48:708-716.

Costa, A. & Appleton, J. 1999. *Chloride penetration into concrete in marine environment—Part I: Main parameters affecting chloride penetration.* Materials and Structures. 32(4):252.

Costa, A. & Appleton, J. 1999. *Chloride penetration into concrete in marine environment-Part II: Prediction of long term chloride penetration.* Materials and Structures. 32(5):354-359.

Dai, J., Akira, Y., Wittmann, F., Yokota, H. & Zhang, P. 2010. *Water repellent surface impregnation for extension of service life of reinforced concrete structures in marine environments: the role of cracks.* Cement and Concrete Composites. 32(2):101-109.

Donadio, M., Schuerch, H., Marazzani, B. 2014. *Concrete durability improvement in the presence of chlorides using a silane based hydrophobic impregnating agents.* Hydrophobe VII 7th International Conference on Water Repellent Treatment and Protective Surface Technology for Building Materials. 85-93.

DuraCrete R17. 2000. DuraCrete Final Technical Report, Document BE95-1347/R17, May 2000, The European Union – Brite EuRam III, DuraCrete – *Probabilistic Performance based Durability Design of Concrete Structures, includes General Guidelines for Durability Design and Redesign*, Document BE95-1347/R15, February 2000, CUR, Gouda.

Dyer, T. 2014. *Concrete durability.* CRC Press.

ENCI. 2015. *MAASTRICHT CEM III/B 42,5 N-LH/SR Technical information.*

European Committee for Standardization. 2002. *Eurocode 2: design of concrete structures – Part 1: general rules and rules for buildings (European standard prEN1992-1-1).* CEN, Brussels, Belgium.

Frederiksen, J.M. 2000. *Chloride threshold values for service life design.* Testing and Modelling the Chloride Ingress into Concrete", Ed.C.Andrade and J.Kropp. :397-414.

Freitag, S. & Bruce, S. 2010. *The influence of surface treatments on the service lives of concrete bridges.* New Zealand Transport Agency.

Gardner, T.J. 2006. *Chloride Transport through Concrete and Implications for Rapid Chloride Testing.* University of Cape Town (UCT).

Gerdes, A. & Wittmann, F. 2001. *Requirements for the application of water repellent treatments in practice.* Surface Technology with Water Repellent Agents: Proceedings of Hydrophobe III. Third International Conference, Universität Hannover, Germany, September 25th and 26th, 2001. Aedificatio Verlag. 155.

Grantham, M.G. 2011. *Concrete Repair: A practical guide.* CRC Press.

Gu, C., Ye, G. & Sun, W. 2015. *A review of the chloride transport properties of cracked concrete: experiments and simulations.* Journal of Zhejiang University SCIENCE A. 16(2):81-92.

Guettala, A. & Abibsi, A. 2006. Corrosion degradation and repair of a concrete bridge. *Materials and Structures.* 39(4):471-478.

Hanaoka, D., Amino, T., Habuchi, T., Miyazato, S. & Tabata. S.2015. *A study on prediction method of chloride ion penetration into concrete with surface penetrants.* Life-Cycle of Structural Systems: Design, Assessment, Maintenance and Management. CRC Press.

Hua, X., van Breugel, K., Ye, G., Hoogenboom, P. & Houben, I.L. 2010. *Self-Healing of Engineered Cementitious Composites (ECC) in Concrete Repair System.*

Hunkeler, F. 1994. *'Grundlagen der Korrosion und der Potentialmessung bei Stahlbetonbauwerken'*, EVED/ASB, Bericht VSS 510.

Jiesheng, L., Faping, L., Xiang, H., XiaoFan, L. & Rongtang, Z. 2017. *Silane Treatment Effective for Concrete Durability.* Materials Performance. 56(4):39-43.

Johansson, A. 2006. *Impregnation of Concrete Structures: Transportation and Fixation of Moisture in Water Repellent Treated Concrete.* Doctoral dissertation, KTH.

Kanjee, J., Beushausen, H., Alexander, M. & Otieno, M. 2012. *Towards incorporating the influence of cracks in the durability index testing approach.* Concrete Repair, Rehabilitation and Retrofitting III: 3rd International Conference on Concrete Repair, Rehabilitation and Retrofitting, ICCRRR-3, 3-5 September 2012, Cape Town, South Africa. CRC Press. 144.

Kanjee, J. 2015. *Assessing the influence of crack width on the durability potential of cracked concrete using the Durability Index Approach.* University of Cape Town (UCT).

Li, K. 2017. *Durability Design of Concrete Structures: Phenomena, Modeling, and Practice.* John Wiley & Sons.

Liu, Y. 2017. *Silicone Dispersions.* CRC Press.

Lucquiaud, V., Courard, L., Gérard, O., Michel, F., Handy, M., Aggoun, S. & Cousture, A. 2014. *Evaluation of the durability of hydrophobic treatments on concrete architectural heritage.* Restoration of Buildings and Monuments. 20(6):395-404.

Luping, T., Nilsson, L. 1992. *Rapid determination of the chloride diffusivity in concrete by applying an electrical field.* ACI Mater. J., v.89, n.1, p. 49-53.

Luping, T., Nilsson, L. & Basheer, P. 2012. *Resistance of concrete to chloride ingress.* Spon Press, London and New York.

Mackechnie, J. & Alexander, M. 2002. *Durability predictions using early age durability index testing.* Proc. Ninth Durability and Building Materials Conference, Australian Corrosion Association, Brisbane, Australia.

Mackechnie, J.R. 2001. *Predictions of reinforced concrete durability in the marine environment.* University of Cape Town. ABC media, Epping.

Mays, G.C. 2002. *Durability of concrete structures: investigation, repair, protection.* CRC Press.

Medeiros, Marcelo Henrique Farias de, Pereira, E., Quarcioni, V.A. & Helene, Paulo Roberto do Lago. 2016. *Surface treatment systems for concrete in marine environment: Effect of concrete cover thickness.* REM-International Engineering Journal. 69(3):287-292.

Medeiros, M. & Helene, P. 2008. *Efficacy of surface hydrophobic agents in reducing water and chloride ion penetration in concrete.* Materials and Structures. 41(1):59-71.

Mehta, P.K. & Monteiro, P.J. 2006. *Concrete: microstructure, properties, and materials.* McGraw -Hill.

Meier, S. & Wittmann, F. 2011. *Water repellent surface impregnation of concrete: Guidelines and recommendations.* Proc. ASMES Intern. Workshop Basic Research on Concrete and Applications, Wittmann F. H. and Mercier O., Editors, Aedificatio Publishers Freiburg, Germany. 49.

Mindess, S., Young, J.F. & Darwin, D. 2003. *Concrete.* Prentice Hall.

Miyazato, S., Tanaka, H. 2015. *Influence of application method of surface penetrant materials on chloride attack.* Life-Cycle of Structural Systems: Design, Assessment, Maintenance and Management. CRC Press.

Moriconi, G., Tittarelli, F. & Corinaldesi, V. 2002. *Review of silicone-based hydrophobic treatment and admixtures for concrete.* Indian Concrete Journal. 76(10):637-642.

Nawy, E.G. 2008. *Concrete construction engineering handbook.* CRC press.

Nganga, G., Alexander, M. G., and Beushausen, H., 2013. *Practical implementation of the durability index performance-based design approach*, Construction and Building Materials, 45, 251–261.

Otieno, M., Alexander, M. & Beushausen, H. 2008. *Corrosion propagation in cracked and uncracked concrete.* Concrete Repair, Rehabilitation and Retrofitting II: 2nd International Conference on Concrete Repair, Rehabilitation and Retrofitting, ICCRRR-2, 24-26 November 2008, Cape Town, South Africa. CRC Press. 157.

Otieno, M., Alexander, M. & Beushausen, H. 2010. *Corrosion in cracked and uncracked concrete–influence of crack width, concrete quality and crack reopening.* Magazine of Concrete Research. 62(6):393-404.

Owens, G. 2013. *Fundamentals of concrete.* Cement and Concrete Institute.

Pacheco, J. & Polder, R. 2012. *Corrosion initiation and propagation in cracked concrete–a literature review.* In Advances in Modeling Concrete Service Life. Springer. 85-93.

Pan, X., Shi, Z., Shi, C., Ling, T. & Li, N. 2017. *A review on concrete surface treatment Part I: Types and mechanisms.* Construction and Building Materials. 132:578-590.

Parrott, L.J. 1988. *Moisture profiles in drying concrete.* British Cement Association, Advances in Cement Research Vol. 1. No. 3.

Polder, R.B., Borsje, H., and de Vries, J. 2000. *Corrosion protection of reinforcement by hydrophobic treatment of concrete, in Corrosion of Reinforcement in Concrete. Corrosion Mechanisms and Corrosion Protection,* The European Federation of Corrosion Publication number 31 (eds J. Mietz, R.B. Polder, and B. Elsener), The Institute of Materials, London, pp. 73–84.

Polder, R.B., Borsje, H., and de Vries, J. 2001. *Prevention of reinforcement corrosion by hydrophobic treatment of concrete.* Heron, 46 (4), 227–238.

Polder, R.B. & De Rooij, M.R. 2005. *Durability of marine concrete structures: field investigations and modelling.* Heron, 50 (3).

Polder, R.B., Nijland, T.G., and de Rooij. 2014. *Blast furnace slag cement concrete with high slag content (CEM III/B).* TNO.

Poursaee, A. 2016. *Corrosion of steel in concrete structures*. Woodhead publishing.

Poulsen, E. & Mejlbro, L. 2010. *Diffusion of chloride in concrete: theory and application.* CRC Press.

Pullar-Strecker, P. 2002. *Concrete Reinforcement Corrosion*—ICE Design and Practice Guide. Thomas Telford Publishing.

Ramezanianpour, A.A. 2014. *Cement Replacement Materials*. Springer.

Raupach, M. 2014. *Concrete Repair to EN 1504: Diagnosis, Design, Principles and Practice*. CRC Press.

Richardson, M. 2002. *Fundamentals of durable reinforced concrete.* Spon Press, London.

Salvoldi, B., Beushausen, H. & Alexander, M. 2015. *Oxygen permeability of concrete and its relation to carbonation.* Construction and Building Materials. 85:30-37.

Sarja, A. 2006. *Predictive and Optimised Life Cycle Management: Buildings and Infrastructure.* Routledge.

Schiessl, P. & Task Group Model Code for Service Life Design of Concrete Structures International Federation for Structural Concrete. 2006. *Model code for service life design.* fib, CEB-FIP.

Schueremans, L., Van Gemert, D., Friedel, M. & Giessler-Blank, S. 2008. *Durability of water repellents in a marine environment.* Proceedings of 5th International Conference on Water Repellent Treatment of Building Materials. Brussels, Belgium: *Aedificatio Publishers.* 357.

Selander, A. 2010. *Hydrophobic impregnation of concrete structures - Effect on Concrete Properties.* Royal Institute of Technology, Stockholm, Sweden.

South African National Roads Agency Limited (SANRAL). 2009. *Table 6000/1: Concrete Durability Specification Targets (Civil Engineering Structures only).* Available: http://www.nra.co.za/content/Table_60001_Concrete_Durability.pdf?Session_ID=61961b193ebe81e0cf281cef50fa4094. [2017, November 17].

South African Bureau of Standards (SABS). 2008. South African National Standard (SANS): *Sieve analysis, fines content and dust content of aggregates (SANS 201:2008).* Pretoria. SABS Standards Division.

South African Bureau of Standards (SABS). 2006. South African National Standard (SANS): *Concrete tests – Consistence of freshly mixed concrete - Slump test (SANS 5862-1:2006).* Pretoria. SABS Standards Division.

South African Bureau of Standards (SABS). 2006. South African National Standard (SANS): *Concrete tests — Compressive strength of hardened concrete (SANS 5863:2006).* Pretoria. SABS Standards Division.

South African Bureau of Standards (SABS). 2015. South African National Standard (SANS): *Civil engineering test methods Part CO3-1: Concrete durability index testing – Preparation of test specimens (SANS 3001-CO3:2015).* Pretoria. SABS Standards Division.

South African Bureau of Standards (SABS). 2015. South African National Standard (SANS): *Civil engineering test methods Part CO3-2: Concrete durability index testing – Oxygen permeability test (SANS 3001-CO3:2015).* Pretoria. SABS Standards Division.

South African Bureau of Standards (SABS). 2015. South African National Standard (SANS): *Civil engineering test methods Part CO3-3: Concrete durability index testing – Chloride conductivity test (SANS 3001-CO3:2015).* Pretoria. SABS Standards Division.

Soutsos, M. 2010. *Concrete durability: a practical guide to the design of durable concrete structures.* Thomas Telford Ltd.

Siddique, R. & Khan, M.I. 2011. *Supplementary cementing materials.* Springer Science & Business Media.

Sika. 2016. *New product showcase – SIKAGARD-706 THIXO*. Sika Canada Inc.

Sika. 2016. Product data sheet - *Sikagard®-706 Thixo: Silane based water repellent impregnation cream.* Sika Limited.

Sika. 2015. *Refurbishment Sika Technology and concepts for hydrophobic impregnation.* Sika Services AG, Zurich.

Stuart, M. 2013. *Concrete Deterioration.* PDHonline Course S155 (1 PDH).

Tanaka, H., Kurita, M. & Miyagawa, T. 2015. *Prediction of Chloride ion Penetration for Concrete Impregnated with Silane Water-repellent Material*. Life-Cycle of Structural Systems: Design, Assessment, Maintenance and Management. CRC Press.

Tepfers, R. 2009. *Some issues concerning concrete impregnation with silanes.* Politecnico di Milano.

Thomas, M. 2013. *Supplementary cementing materials in concrete.* CRC Press.

Tuutti, K. 1982. *Corrosion of Steel in Concrete.* Swedish Foundation for Concrete Research, Stockholm.

University of Cape Town (UCT). 2017. *Durability Index Testing Procedure Manual.* Department of Civil Engineering.

Van der Wegen, G., Polder, R.B. & Van Breugel, K. 2012. *Guideline for service life design of structural concrete–a performance based approach with regard to chloride induced corrosion.* Heron. 57(3):153-168.

Vassie, P.R. 1990. *Concrete coatings: do they reduce ongoing corrosion of reinforcing steel?,* in Corrosion of Reinforcement in Concrete (eds C.L. Page, K. Treadaway, and P. Bamforth), Elsevier, pp. 456–470.

Walraven, J. 2008. *Design for service life: how should it be implemented in future codes.* International Conference on Concrete Repair, Rehabilitation and Retrofitting, Proceedings ICCRRR. 3.

Wittmann, F., Guo, P. & Zhao, T. 2008. *Influence of cracks on the efficiency of surface impregnation of concrete.* Proceedings of the 5th International Conference on Water Repellent Treatment of Building Materials, Hydrophobe V, Brussels. 287.

Zhang, P., Shang, H., Hou, D., Guo, S. & Zhao, T. 2017. *The effect of water repellent surface impregnation on durability of cement-based materials.* Advances in Materials Science and Engineering.

Zhang, P., Li, P., Fan, H., Shang, H., Guo, S. & Zhao, T. 2017. *Carbonation of Water Repellent-Treated Concrete.* Advances in Materials Science and Engineering.

Zhang, J., McLoughlin, I. & Buenfeld, N. 1998. *Modelling of chloride diffusion into surface-treated concrete.* Cement and Concrete Composites. 20(4):253-261.

10. Appendices

APPENDIX A – Detailed compressive strength test results

Ref number	Mix 1
Composition	100% CEM I 52.5N
w/b	0.45
Cast date	12-Jul-17

Date: 15/07/17	Cube	Length (mm)	Breadth (mm)	Height (mm)	Mass (kg)	Load (kN)	Compressive strength (MPa)	Validity
Age: 3 days	**1**	100.00	100.00	103.03	2.440	520	52.0	OK
	2	100.00	100.00	103.75	2.455	522	52.2	
	3	100.00	100.00	101.53	2.435	536	53.6	
					Average	526	52.6	

Date: 19/07/17	Cube	Length (mm)	Breadth (mm)	Height (mm)	Mass (kg)	Load (kN)	Compressive strength (MPa)	Validity
Age: 7 days	**1**	100.00	100.00	103.82	2.475	620	62.0	OK
	2	100.00	100.00	100.06	2.435	602	60.2	
	3	100.00	100.00	101.92	2.460	606	60.6	
					Average	609	60.9	

Date: 09/08/17	Cube	Length (mm)	Breadth (mm)	Height (mm)	Mass (kg)	Load (kN)	Compressive strength (MPa)	Validity
Age: 28 days	**1**	100.00	100.00	101.61	2.449	660	66.0	OK
	2	100.00	100.00	101.27	2.439	642	64.2	
	3	100.00	100.00	101.80	2.445	700	70.0	
					Average	667	66.7	

Ref number	Mix 2
Composition	100% CEM I 52.5N
w/b	0.60
Cast date	13-Jul-17

Date: 16/07/17	**Cube**	**Length (mm)**	**Breadth (mm)**	**Height (mm)**	**Mass (kg)**	**Load (kN)**	**Compressive strength (MPa)**	**Validity**
Age: 3 days	**1**	100.00	100.00	101.20	2.420	362	36.2	OK
	2	100.00	100.00	101.11	2.395	363	36.3	
	3	100.00	100.00	100.62	2.440	358	35.8	
					Average	361	36.1	

Date: 20/07/17	**Cube**	**Length (mm)**	**Breadth (mm)**	**Height (mm)**	**Mass (kg)**	**Load (kN)**	**Compressive strength (MPa)**	**Validity**
Age: 7 days	**1**	100.00	100.00	100.97	2.440	439	43.9	OK
	2	100.00	100.00	100.40	2.445	420	42.0	
	3	100.00	100.00	100.57	2.420	440	44.0	
					Average	433	43.3	

Date: 10/08/17	**Cube**	**Length (mm)**	**Breadth (mm)**	**Height (mm)**	**Mass (kg)**	**Load (kN)**	**Compressive strength (MPa)**	**Validity**
Age: 28 days	**1**	100.00	100.00	102.28	2.478	464	46.4	OK
	2	100.00	100.00	100.99	2.442	474	47.4	
	3	100.00	100.00	102.35	2.475	492	49.2	
					Average	477	47.7	

Ref number	Mix 2 (poor quality)
Composition	100% CEM I 52.5N
w/b	0.60
Cast date	24-Sep-17

Date: 27/09/17	Cube	Length (mm)	Breadth (mm)	Height (mm)	Mass (kg)	Load (kN)	Compressive strength (MPa)	Validity
Age: 3 days	**1**	100.00	100.00	100.40	2.285	245	24.5	OK
	2	100.00	100.00	100.69	2.310	235	23.5	
	3	100.00	100.00	100.47	2.290	240	24.0	
					Average	240	24.0	

Date: 01/10/17	Cube	Length (mm)	Breadth (mm)	Height (mm)	Mass (kg)	Load (kN)	Compressive strength (MPa)	Validity
Age: 7 days	**1**	100.00	100.00	101.15	2.295	250	25.0	OK
	2	100.00	100.00	100.62	2.265	275	27.5	
	3	100.00	100.00	100.09	2.295	290	29.0	
					Average	272	27.2	

Date: 22/10/17	Cube	Length (mm)	Breadth (mm)	Height (mm)	Mass (kg)	Load (kN)	Compressive strength (MPa)	Validity
Age: 28 days	**1**	100.00	100.00	101.10	2.279	300	30.0	OK
	2	100.00	100.00	100.39	2.330	340	34.0	
	3	100.00	100.00	100.42	2.308	308	30.8	
					Average	316	31.6	

Ref number	Mix 3
Composition	70% CEM I/ 30% FA
w/b	0.45
Cast date	15-Jul-17

Date: 18/07/17	Cube	Length (mm)	Breadth (mm)	Height (mm)	Mass (kg)	Load (kN)	Compressive strength (MPa)	Validity
Age: 3 days	**1**	100.00	100.00	101.26	2.460	322	32.2	OK
	2	100.00	100.00	100.50	2.415	314	31.4	
	3	100.00	100.00	102.45	2.485	310	31.0	
					Average	315	31.5	

Date: 22/07/17	Cube	Length (mm)	Breadth (mm)	Height (mm)	Mass (kg)	Load (kN)	Compressive strength (MPa)	Validity
Age: 7 days	**1**	100.00	100.00	101.38	2.445	416	41.6	OK
	2	100.00	100.00	101.62	2.440	422	42.2	
	3	100.00	100.00	101.76	2.455	447	44.7	
					Average	428	42.8	

Date: 12/08/17	Cube	Length (mm)	Breadth (mm)	Height (mm)	Mass (kg)	Load (kN)	Compressive strength (MPa)	Validity
Age: 28 days	**1**	100.00	100.00	101.19	2.464	556	55.6	OK
	2	100.00	100.00	101.87	2.458	550	55.0	
	3	100.00	100.00	100.32	2.448	554	55.4	
					Average	553	55.3	

Ref number	Mix 4
Composition	70% CEM I/ 30% FA
w/b	0.60
Cast date	16-Jul-17

Date: 19/07/17	Cube	Length (mm)	Breadth (mm)	Height (mm)	Mass (kg)	Load (kN)	Compressive strength (MPa)	Validity
Age: 3 days	**1**	100.00	100.00	100.14	2.370	202	20.2	OK
	2	100.00	100.00	101.74	2.410	198	19.8	
	3	100.00	100.00	100.22	2.405	206	20.6	
					Average	202	20.2	

Date: 23/07/17	Cube	Length (mm)	Breadth (mm)	Height (mm)	Mass (kg)	Load (kN)	Compressive strength (MPa)	Validity
Age: 7 days	**1**	100.00	100.00	102.11	2.415	260	26.0	OK
	2	100.00	100.00	101.97	2.465	260	26.0	
	3	100.00	100.00	102.50	2.405	279	27.9	
					Average	266	26.6	

Date: 13/08/17	Cube	Length (mm)	Breadth (mm)	Height (mm)	Mass (kg)	Load (kN)	Compressive strength (MPa)	Validity
Age: 28 days	**1**	100.00	100.00	101.08	2.409	358	35.8	OK
	2	100.00	100.00	102.13	2.448	350	35.0	
	3	100.00	100.00	101.23	2.416	359	35.9	
					Average	356	35.6	

Ref number	Mix 4 (poor quality)
Composition	70% CEM I/ 30% FA
w/b	0.60
Cast date	17-Jul-17

Date: 20/07/17	Cube	Length (mm)	Breadth (mm)	Height (mm)	Mass (kg)	Load (kN)	Compressive strength (MPa)	Validity
Age: 3 days	**1**	100.00	100.00	102.27	2.360	174	17.4	OK
	2	100.00	100.00	101.31	2.330	166	16.6	
	3	100.00	100.00	100.86	2.350	174	17.4	
					Average	171	17.1	

Date: 24/07/17	Cube	Length (mm)	Breadth (mm)	Height (mm)	Mass (kg)	Load (kN)	Compressive strength (MPa)	Validity
Age: 7 days	**1**	100.00	100.00	101.82	2.380	210	21.0	OK
	2	100.00	100.00	100.96	2.340	206	20.6	
	3	100.00	100.00	102.25	2.370	212	21.2	
					Average	209	20.9	

Date: 14/08/17	Cube	Length (mm)	Breadth (mm)	Height (mm)	Mass (kg)	Load (kN)	Compressive strength (MPa)	Validity
Age: 28 days	**1**	100.00	100.00	101.41	2.340	240	24.0	OK
	2	100.00	100.00	100.72	2.305	242	24.2	
	3	100.00	100.00	101.14	2.308	250	25.0	
					Average	244	24.4	

Ref number	Mix 5
Composition	50% CEM I/ 50% GGCS
w/b	0.45
Cast date	18-Jul-17

Date:21/07/17	Cube	Length (mm)	Breadth (mm)	Height (mm)	Mass (kg)	Load (kN)	Compressive strength (MPa)	Validity
Age: 3 days	**1**	100.00	100.00	102.96	2.455	325	32.5	OK
	2	100.00	100.00	101.18	2.415	327	32.7	
	3	100.00	100.00	101.98	2.470	332	33.2	
					Average	328	32.8	

Date: 25/07/17	Cube	Length (mm)	Breadth (mm)	Height (mm)	Mass (kg)	Load (kN)	Compressive strength (MPa)	Validity
Age: 7 days	**1**	100.00	100.00	101.63	2.430	479	47.9	OK
	2	100.00	100.00	101.91	2.425	472	47.2	
	3	100.00	100.00	101.53	2.445	509	50.9	
					Average	487	48.7	

Date: 15/08/17	Cube	Length (mm)	Breadth (mm)	Height (mm)	Mass (kg)	Load (kN)	Compressive strength (MPa)	Validity
Age: 28 days	**1**	100.00	100.00	100.90	2.405	632	63.2	OK
	2	100.00	100.00	100.78	2.408	614	61.4	
	3	100.00	100.00	101.63	2.440	646	64.6	
					Average	631	63.1	

Ref number	Mix 6
Composition	50% CEM I/ 50% GGCS
w/b	0.60
Cast date	19-Jul-17

Date: 22/07/17	Cube	Length (mm)	Breadth (mm)	Height (mm)	Mass (kg)	Load (kN)	Compressive strength (MPa)	Validity
Age: 3 days	**1**	100.00	100.00	101.76	2.450	200	20.0	OK
	2	100.00	100.00	101.54	2.435	202	20.2	
	3	100.00	100.00	100.87	2.440	200	20.0	
					Average	201	20.1	

Date: 26/07/17	Cube	Length (mm)	Breadth (mm)	Height (mm)	Mass (kg)	Load (kN)	Compressive strength (MPa)	Validity
Age: 7 days	**1**	100.00	100.00	100.79	2.330	349	34.9	OK
	2	100.00	100.00	100.17	2.405	355	35.5	
	3	100.00	100.00	101.88	2.455	356	35.6	
					Average	353	35.3	

Date: 16/08/17	Cube	Length (mm)	Breadth (mm)	Height (mm)	Mass (kg)	Load (kN)	Compressive strength (MPa)	Validity
Age: 28 days	**1**	100.00	100.00	101.58	2.405	488	48.8	OK
	2	100.00	100.00	100.50	2.424	506	50.6	
	3	100.00	100.00	101.10	2.428	483	48.3	
					Average	492	49.2	

Ref number	Mix 6 (poor quality)
Composition	50% CEM I/ 50% GGCS
w/b	0.60
Cast date	20-Jul-17

Date: 23/07/17	Cube	Length (mm)	Breadth (mm)	Height (mm)	Mass (kg)	Load (kN)	Compressive strength (MPa)	Validity
Age: 3 days	**1**	100.00	100.00	102.71	2.320	158	15.8	OK
	2	100.00	100.00	101.10	2.335	164	16.4	
	3	100.00	100.00	102.05	2.350	166	16.6	
					Average	163	16.3	

Date: 27/07/17	Cube	Length (mm)	Breadth (mm)	Height (mm)	Mass (kg)	Load (kN)	Compressive strength (MPa)	Validity
Age: 7 days	**1**	100.00	100.00	101.66	2.325	214	21.4	OK
	2	100.00	100.00	102.82	2.365	222	22.2	
	3	100.00	100.00	101.93	2.330	212	21.2	
					Average	216	21.6	

Date: 17/08/17	Cube	Length (mm)	Breadth (mm)	Height (mm)	Mass (kg)	Load (kN)	Compressive strength (MPa)	Validity
Age: 28 days	**1**	100.00	100.00	102.26	2.320	260	26.0	OK
	2	100.00	100.00	101.31	2.305	260	26.0	
	3	100.00	100.00	102.32	2.325	265	26.5	
					Average	262	26.2	

Ref number	Mix 7
Composition	CEM III/B 42.5N
w/b	0.45
Cast date	21-Jul-17

Date: 24/07/17	Cube	Length (mm)	Breadth (mm)	Height (mm)	Mass (kg)	Load (kN)	Compressive strength (MPa)	Validity
Age: 3 days	**1**	100.00	100.00	102.26	2.440	254	25.4	OK
	2	100.00	100.00	102.96	2.440	266	26.6	
	3	100.00	100.00	102.77	2.455	260	26.0	
					Average	260	26.0	

Date: 28/07/17	Cube	Length (mm)	Breadth (mm)	Height (mm)	Mass (kg)	Load (kN)	Compressive strength (MPa)	Validity
Age: 7 days	**1**	100.00	100.00	102.13	2.455	417	41.7	OK
	2	100.00	100.00	101.80	2.450	435	43.5	
	3	100.00	100.00	102.31	2.465	419	41.9	
					Average	424	42.4	

Date: 18/08/17	Cube	Length (mm)	Breadth (mm)	Height (mm)	Mass (kg)	Load (kN)	Compressive strength (MPa)	Validity
Age: 28 days	**1**	100.00	100.00	101.79	2.468	572	57.2	OK
	2	100.00	100.00	102.19	2.488	610	61.0	
	3	100.00	100.00	102.15	2.452	574	57.4	
					Average	585	58.5	

Ref number	Mix 8
Composition	CEM III/B 42.5N
w/b	0.60
Cast date	22-Jul-17

Date: 25/07/17	Cube	Length (mm)	Breadth (mm)	Height (mm)	Mass (kg)	Load (kN)	Compressive strength (MPa)	Validity
Age: 3 days	**1**	100.00	100.00	102.62	2.430	139	13.9	OK
	2	100.00	100.00	101.74	2.410	140	14.0	
	3	100.00	100.00	102.11	2.440	139	13.9	
					Average	139	13.9	

Date: 29/07/17	Cube	Length (mm)	Breadth (mm)	Height (mm)	Mass (kg)	Load (kN)	Compressive strength (MPa)	Validity
Age: 7 days	**1**	100.00	100.00	100.85	2.410	305	30.5	OK
	2	100.00	100.00	102.37	2.445	300	30.0	
	3	100.00	100.00	102.28	2.405	305	30.5	
					Average	303	30.3	

Date: 19/08/17	Cube	Length (mm)	Breadth (mm)	Height (mm)	Mass (kg)	Load (kN)	Compressive strength (MPa)	Validity
Age: 28 days	**1**	100.00	100.00	101.40	2.448	464	46.4	OK
	2	100.00	100.00	102.35	2.430	438	43.8	
	3	100.00	100.00	101.36	2.435	460	46.0	
					Average	454	45.4	

Ref number	Mix 8 (poor quality)
Composition	CEM III/B 42.5N
w/b	0.60
Cast date	02-Oct-17

Date: 05/10/17	Cube	Length (mm)	Breadth (mm)	Height (mm)	Mass (kg)	Load (kN)	Compressive strength (MPa)	Validity
Age: 3 days	**1**	100.00	100.00	101.95	2.310	120	12.0	OK
	2	100.00	100.00	102.69	2.375	109	10.9	
	3	100.00	100.00	101.83	2.350	110	11.0	
					Average	113	11.3	

Date: 09/10/17	Cube	Length (mm)	Breadth (mm)	Height (mm)	Mass (kg)	Load (kN)	Compressive strength (MPa)	Validity
Age: 7 days	**1**	100.00	100.00	100.64	2.340	214	21.4	OK
	2	100.00	100.00	101.41	2.325	208	20.8	
	3	100.00	100.00	101.95	2.335	210	21.0	
					Average	211	21.1	

Date: 30/10/17	Cube	Length (mm)	Breadth (mm)	Height (mm)	Mass (kg)	Load (kN)	Compressive strength (MPa)	Validity
Age: 28 days	**1**	100.00	100.00	101.58	2.330	280	28.0	OK
	2	100.00	100.00	100.45	2.325	270	27.0	
	3	100.00	100.00	101.64	2.335	275	27.5	
					Average	275	27.5	

APPENDIX B – Detailed Durability Index (DI) test results

Table B.1: Detailed Oxygen Permeability Index test results (cut surfaces)

OPI	Mix 1	Mix 2	Mix 2 poor	Mix 3	Mix 4	Mix 4 poor	Mix 5	Mix 6	Mix 6 poor	Mix 7	Mix 8	Mix 8 poor
Log scale	100% CEM I 52.5N	100% CEM I 52.5N	100% CEM I 52.5N	70% CEM I/ 30% FA	70% CEM I/ 30% FA	70% CEM I/ 30% FA	50% CEM I/ 50% GGCS	50% CEM I/ 50% GGCS	50% CEM I/ 50% GGCS	100% CEM III/B 42.5N	100% CEM III/B 42.5N	100% CEM III/B 42.5N
w/b	0.45	0.60	0.60	0.45	0.60	0.60	0.45	0.60	0.60	0.45	0.60	0.60
1	10.49	10.01	10.00	9.92	10.03	9.49	10.41	10.06	9.37	10.67	10.40	9.59
2	10.50	9.86	9.99	10.04	10.11	9.44	10.48	9.71	9.04	10.60	10.13	9.55
3	10.61	9.94	9.92	9.98	10.07	9.43	10.14	9.78	9.15	10.58	10.33	9.52
4	10.57	9.99	9.75	10.08	9.94	9.44	10.32	10.04	9.33	10.83	10.40	9.51
Mean	10.54	9.95	9.91	10.00	10.04	9.45	10.34	9.90	9.22	10.67	10.32	9.54

Table B.2.1: Detailed Water Sorptivity Index test results (cut surfaces)

WSI	Mix 1		Mix 2		Mix 2 (poor quality)		Mix 3		Mix 4		Mix 4 (poor quality)	
	100% CEM I 52.5N		100% CEM I 52.5N		100% CEM I		70% CEM I/ 30% FA		70% CEM I/ 30% FA		70% CEM I/ 30% FA	
w/b	0.45		0.60		0.60		0.45		0.60		0.60	
	Sorptivity ($mm/hr^{0.5}$)	Porosity (%)	Sorptivity ($mm/hr^{0.5}$)	Porosity (%)	Sorptivity ($mm/hr^{0.5}$)	Porosity (%)	Sorptivity ($mm/hr^{0.5}$)	Porosity (%)	Sorptivity ($mm/hr^{0.5}$)	Porosity (%)	Sorptivity ($mm/hr^{0.5}$)	Porosity (%)
1	5.9	9.0	7.5	12.2	6.9	11.6	9.2	8.9	8.8	10.9	15.1	12.7
2	6.0	9.5	7.0	11.2	6.5	12.9	7.4	9.6	6.6	10.9	13.1	12.4
3	5.5	8.7	6.8	12.3	8.0	12.6	9.5	10.1	7.1	10.4	14.0	12.8
4	5.4	8.6	6.1	11.7	6.1	12.0	8.3	9.4	7.4	11.2	13.6	13.2
Mean	5.7	9.0	6.8	11.9	6.9	12.3	7.8	9.5	7.5	10.9	13.9	12.8

Table B.2.2: Detailed Water Sorptivity Index test results (cut surfaces)

WSI	Mix 5		Mix 6		Mix 6 (poor quality)		Mix 7		Mix 8		Mix 8 (poor quality)	
	50% CEM I/ 50% GGCS		50% CEM I/ 50% GGCS		50% CEM I/ 50% GGCS		CEM III/B 42.5N		CEM III/B 42.5N		CEM III/B 42.5N	
w/b	0.45		0.60		0.60		0.45		0.60		0.60	
	Sorptivity ($mm/hr^{0.5}$)	Porosity (%)	Sorptivity ($mm/hr^{0.5}$)	Porosity (%)	Sorptivity ($mm/hr^{0.5}$)	Porosity (%)	Sorptivity ($mm/hr^{0.5}$)	Porosity (%)	Sorptivity ($mm/hr^{0.5}$)	Porosity (%)	Sorptivity ($mm/hr^{0.5}$)	Porosity (%)
1	3.1	7.5	5.6	8.7	11.1	12.7	7.1	6.9	6.4	9.2	11.2	14.4
2	4.7	6.6	5.6	8.4	10.1	12.0	6.9	7.9	8.4	10.2	13.0	15.4
3	4.6	7.4	6.6	8.4	12.5	11.6	7.4	8.1	7.3	10.3	12.1	14.2
4	4.6	7.9	4.4	9.9	9.4	11.9	7.2	7.7	6.6	9.4	13.1	13.5
Mean	4.2	7.3	5.5	8.8	10.8	12.0	7.1	7.7	7.2	9.8	12.4	14.4

Table B.3.1: Detailed Chloride Conductivity Index test results (cut surfaces)

CCI	Mix 1		Mix 2		Mix 2 (poor quality)		Mix 3		Mix 4		Mix 4 (poor quality)	
	100% CEM I 52.5N		100% CEM I 52.5N		100% CEM I 52.5N		70% CEM I/ 30% FA		70% CEM I/ 30% FA		70% CEM I/ 30% FA	
w/b	0.45		0.60		0.60		0.45		0.60		0.60	
	Conduc-tivity (mS/cm)	Porosity (%)	Conduc-tivity (mS/cm)	Porosity (%)	Conduc-tivity (mS/cm)	Porosity (%)	Conduc-tivity (mS/cm)	Porosity (%)	Conduc-tivity (mS/cm)	Porosity (%)	Conduc-tivity (mS/cm)	Porosity (%)
1	0.53	3.58	1.05	4.08	1.56	4.71	0.75	3.70	0.92	4.14	2.17	5.15
2	0.53	3.49	1.24	4.40	1.51	4.88	0.78	4.16	0.97	4.07	2.15	4.99
3	0.69	4.55	1.00	3.98	1.54	4.74	0.57	3.28	1.06	4.22	1.95	4.69
4	0.56	3.62	1.07	4.15	1.93	4.91	0.54	3.28	0.98	4.10	2.01	4.53
Mean	0.58	3.81	1.09	4.15	1.63	4.81	0.66	3.60	0.98	4.13	2.07	4.84

Table B.3.2: Detailed Chloride Conductivity Index test results (cut surfaces)

CCI	Mix 5		Mix 6		Mix 6 (poor quality)		Mix 7		Mix 8		Mix 8 (poor quality)	
	50% CEM I/ 50% GGCS		50% CEM I/ 50% GGCS		50% CEM I/ 50% GGCS		CEM III/B 42.5N		CEM III/B 42.5N		CEM III/B 42.5N	
w/b	0.45		0.60		0.60		0.45		0.60		0.60	
	Conduc-tivity (mS/cm)	Porosity (%)	Conduc-tivity (mS/cm)	Porosity (%)	Conduc-tivity (mS/cm)	Porosity (%)	Conduc-tivity (mS/cm)	Porosity (%)	Conduc-tivity (mS/cm)	Porosity (%)	Conduc-tivity (mS/cm)	Porosity (%)
1	0.16	2.78	0.26	3.49	0.76	4.88	0.14	2.78	0.26	3.90	1.42	5.57
2	0.15	2.92	0.21	3.23	0.90	5.23	0.18	3.01	0.30	3.76	1.10	5.46
3	0.16	2.80	0.27	3.38	0.84	4.85	0.17	2.88	0.32	3.89	1.31	6.20
4	0.16	2.71	0.25	3.34	0.71	5.11	0.18	3.11	0.25	3.75	1.34	5.55
Mean	0.16	2.80	0.25	3.36	0.80	5.02	0.16	2.94	0.28	3.83	1.29	5.69

Table B.4.1: Detailed Water Sorptivity Index test results (uncut surfaces)

WSI	Mix 1		Mix 2		Mix 2 (poor quality)		Mix 3		Mix 4		Mix 4 (poor quality)	
mm/hr$^{0.5}$	100% CEM I 52.5N		100% CEM I 52.5N		100% CEM I		70% CEM I/ 30% FA		70% CEM I/ 30% FA		70% CEM I/ 30% FA	
w/b	0.45		0.60		0.60		0.45		0.60		0.60	
	Untreated	Treated	Untreated	Treated	Untreated	Treated	Untreated	Treated	Untreated	Treated	Untreated	Treated
1	7.4	1.2	7.7	0.8	9.0	0.9	8.2	0.7	9.9	0.8	14.4	1.6
2	5.6	0.9	8.6	0.8	8.1	0.6	7.4	0.6	9.6	1.0	13.1	1.2
3	8.3	0.9	10.1	1.2	8.0	0.5	9.1	0.8	9.1	0.9	15.0	1.2
4	6.6	0.6	9.9	0.9	8.8	0.8	8.2	0.7	9.6	0.7	17.9	1.2
Mean	7.0	0.9	9.1	0.9	8.5	0.7	8.2	0.7	9.5	0.9	15.1	1.3

Table B.4.2: Detailed Water Sorptivity Index test results (uncut surfaces)

WSI	Mix 5		Mix 6		Mix 6 (poor quality)		Mix 7		Mix 8		Mix 8 (poor quality)	
mm/hr$^{0.5}$	50% CEM I/ 50% GGCS		50% CEM I/ 50% GGCS		50% CEM I/ 50% GGCS		CEM III/B 42.5N		CEM III/B 42.5N		CEM III/B 42.5N	
w/b	0.45		0.60		0.60		0.45		0.60		0.60	
	Untreated	Treated	Untreated	Treated	Untreated	Treated	Un-treated	Treated	Un-treated	Treated	Un-treated	Treated
1	5.3	1.2	7.4	1.3	9.6	1.2	8.6	1.0	8.6	1.1	12.0	1.8
2	4.9	1.7	6.7	1.4	11.8	1.5	8.1	1.0	6.1	1.3	13.0	1.6
3	7.4	1.9	8.9	1.5	12.6	1.6	8.0	1.6	7.8	1.4	12.1	1.7
4	5.7	1.1	6.7	1.1	15.3	1.7	8.3	1.0	8.2	0.9	13.1	1.2
Mean	5.8	1.5	7.4	1.3	12.3	1.5	8.2	1.1	7.7	1.2	12.6	1.6

Table B.5.1: Detailed Chloride Conductivity Index test results (uncut surfaces)

CCI	Mix 1		Mix 2		Mix 2 (poor quality)		Mix 3		Mix 4		Mix 4 (poor quality)	
mS/cm	100% CEM I 52.5N		100% CEM I 52.5N		100% CEM I 52.5N		70% CEM I/ 30% FA		70% CEM I/ 30% FA		70% CEM I/ 30% FA	
w/b	0.45		0.60		0.60		0.45		0.60		0.60	
	Untreated	Treated	Untreated	Treated	Untreated	Treated	Untreated	Treated	Untreated	Treated	Untreated	Treated
1	0.48	0.16	1.06	0.34	1.66	0.32	0.73	0.25	1.01	0.30	1.65	0.20
2	0.44	0.34	1.11	0.26	1.57	0.24	1.00	0.23	1.12	0.18	1.89	0.15
3	0.44	0.27	1.02	0.44	1.45	0.22	0.67	0.21	0.96	0.31	1.83	0.15
4	0.43	0.27	1.19	0.28	1.56	0.26	0.64	0.19	1.39	0.24	1.74	0.29
Mean	0.45	0.26	1.09	0.33	1.56	0.26	0.76	0.22	1.12	0.26	1.78	0.20

Table B.5.2: Detailed Chloride Conductivity Index test results (uncut surfaces)

CCI	Mix 5		Mix 6		Mix 6 (poor quality)		Mix 7		Mix 8		Mix 8 (poor quality)	
mS/cm	50% CEM I/ 50% GGCS		50% CEM I/ 50% GGCS		50% CEM I/ 50% GGCS		CEM III/B 42.5N		CEM III/B 42.5N		CEM III/B 42.5N	
w/b	0.45		0.60		0.60		0.45		0.60		0.60	
	Untreated	Treated	Untreated	Treated	Untreated	Treated	Untreated	Treated	Untreated	Treated	Untreated	Treated
1	0.16	0.12	0.32	0.20	1.13	0.20	0.24	0.13	0.49	0.25	2.00	0.65
2	0.14	0.08	0.36	0.22	0.81	0.37	0.19	0.12	0.43	0.20	1.73	0.73
3	0.17	0.11	0.33	0.28	0.80	0.29	0.22	0.13	0.38	0.28	1.81	0.75
4	0.17	0.11	0.34	0.23	0.78	0.29	0.17	0.15	0.44	0.27	1.75	0.47
Mean	0.16	0.10	0.34	0.23	0.88	0.29	0.20	0.13	0.43	0.25	1.82	0.65

APPENDIX C – Detailed silane penetration depth test results

Table C.1: Detailed silane penetration depth test results

Mix number	Composition	w/b	Penetration depth (mm)						Average (mm)
Mix 1	100% CEM I 52.5N	0.45	5.80	5.71	5.21	5.67	4.27	4.45	5.19
Mix 2	100% CEM I 52.5N	0.60	6.69	8.38	6.42	7.80	7.69	8.42	7.57
Mix 2 poor	100% CEM I 52.5N	0.60	7.76	8.11	7.82	8.29	7.26	8.87	8.02
Mix 3	70% CEM I/30% FA	0.45	7.59	6.13	6.99	6.25	6.70	6.48	6.69
Mix 4	70% CEM I/30% FA	0.60	7.02	8.04	7.84	6.19	7.40	7.38	7.31
Mix 4 poor	70% CEM I/30% FA	0.60	7.94	8.86	8.50	8.68	9.44	8.89	8.72
Mix 5	50% CEM I/50% GGCS	0.45	5.42	6.01	5.63	5.34	5.48	5.36	5.54
Mix 6	50% CEM I/50% GGCS	0.60	7.90	7.70	6.00	6.30	7.00	6.30	6.87
Mix 6 poor	50% CEM I/50% GGCS	0.60	10.00	9.60	9.50	10.20	9.90	10.10	9.88
Mix 7	100% CEM III/B 42.5N	0.45	3.70	3.92	3.80	2.87	3.63	2.99	3.49
Mix 8	100% CEM III/B 42.5N	0.60	4.69	4.43	5.73	4.76	5.46	5.22	5.05
Mix 8 Poor	100% CEM III/B 42.5N	0.60	7.26	7.75	6.82	8.12	8.42	8.10	7.75

APPENDIX D – Detailed accelerated carbonation test results

Table D.1: Accelerated carbonation test results (16 weeks)

Carbonation depth	Mix 1		Mix 2		Mix 2 (poor quality)		Mix 3		Mix 4		Mix 4 (poor quality)	
mm	100% CEM I 52.5N		100% CEM I 52.5N		100% CEM I 52.5N		70% CEM I/ 30% FA		70% CEM I/ 30% FA		70% CEM I/ 30% FA	
w/b	0.45		0.60		0.60		0.45		0.60		0.60	
	Untreated	Treated	Untreated	Treated	Untreated	Treated	Untreated	Treated	Untreated	Treated	Untreated	Treated
1	7.17	7.17	13.37	10.54	14.37	15.16	11.03	10.37	17.25	14.91	26.28	24.99
2	6.72	6.84	13.50	12.74	16.63	16.34	10.64	9.65	16.64	12.78	27.09	25.35
3	7.70	7.47	10.86	10.92	16.64	13.22	13.24	12.24	16.42	14.43	24.62	26.77
4	7.28	6.14	11.55	9.86	15.96	14.64	11.97	9.41	16.25	14.42	27.16	28.02
5	8.45	6.76	13.50	11.03	18.57	15.36	11.57	12.04	16.80	13.17	25.98	25.49
6	8.64	7.23	10.90	8.34	17.84	14.54	10.97	10.95	16.15	16.47	28.05	23.88
7	7.59	6.80	11.33	10.29	15.47	13.86	11.05	9.96	16.73	15.34	26.74	27.92
8	7.65	6.12	10.71	10.59	16.46	16.44	12.05	10.71	16.63	14.09	25.32	26.00
Average	7.65	6.82	11.97	10.54	16.49	14.95	11.57	10.67	16.61	14.45	26.41	26.05

Carbona-tion depth	Mix 5		Mix 6		Mix 6 (poor quality)		Mix 7		Mix 8		Mix 8 (poor quality)	
mm	50% CEM I/ 50% GGCS		50% CEM I/ 50% GGCS		50% CEM I/ 50% GGCS		100% CEM III/B 42.5N		100% CEM III/B 42.5N		100% CEM III/B 42.5N	
w/b	0.45		0.60		0.60		0.45		0.60		0.60	
	Untreated	Treated	Untreated	Treated	Untreated	Treated	Un-treated	Treated	Untreated	Treated	Untreated	Treated
1	9.42	9.48	14.86	10.29	29.40	33.11	12.95	11.29	20.43	17.17	47.27	41.30
2	9.81	8.54	13.27	10.67	29.87	30.08	11.35	10.26	19.52	17.76	44.86	44.52
3	12.00	10.16	14.84	11.23	33.32	30.33	15.45	10.99	18.91	16.20	42.77	43.92
4	9.99	6.75	14.00	11.40	33.60	31.52	14.51	12.06	19.62	17.56	43.62	47.82
5	7.88	9.13	15.69	12.26	33.24	28.24	14.52	12.62	19.19	18.13	45.10	41.59
6	8.28	8.12	13.62	13.07	29.52	27.04	14.20	12.48	22.43	16.66	42.18	43.95
7	10.50	10.40	14.00	12.66	31.73	29.72	11.08	14.07	19.29	17.02	43.01	43.03
8	10.05	6.55	13.95	14.49	33.35	33.44	12.34	13.37	19.49	15.02	41.90	41.79
Average	9.74	8.64	14.28	12.01	31.75	30.44	13.30	12.14	19.86	16.94	43.84	43.49

APPENDIX E – Bulk diffusion test results (uncracked concrete)

Table E.1: Chloride profiling results (uncracked concrete – Mix 1 and Mix 3)

w/b 0.45		Chloride content (% by mass of binder)			
		Mix 1 (100% CEM I 52.5N)		Mix 3 (70% CEM I/30% FA)	
Depth (mm)	Average depth (mm)	Untreated	Treated	Untreated	Treated
0-2	1	5.758	3.987	4.783	1.454
2-4	3	3.766	1.681	4.055	0.226
4-6	5	2.402	0.952	3.037	0.180
6-8	7	2.124	0.567	2.244	0.232
8-10	9	1.495	0.314	1.720	0.209
10-15	12.5	1.071	0.168	0.691	0.080
15-20	17.5	0.284	0.100	0.260	0.232
20-25	22.5	0.026	0.073	0.265	0.062
25-30	27.5	0.000	0.061	0.085	0.022

Table E.2: Chloride profiling results (uncracked concrete – Mix 5 and Mix 7)

w/b 0.45		Chloride content (% by mass of binder)			
		Mix 5 (50% CEM I/50% GGCS)		Mix 7 (100% CEM III/B 42.5N)	
Depth (mm)	Average depth (mm)	Untreated	Treated	Untreated	Treated
0-1	0.5	6.202	1.889	4.859	4.457
1-2	1.5	4.986	0.569	5.300	0.103
2-3	2.5	3.218	0.057	4.018	0.067
3-4	3.5	1.817	0.098	2.547	0.095
4-5	4.5	1.034	0.101	1.747	0.077
5-6	5.5	0.669	0.100	1.166	0.082
6-8	7	0.039	0.084	0.057	0.084
8-10	9	0.045	0.076	0.047	0.055
10-15	12.5	0.112	0.049	0.061	0.068
15-20	17.5	0.098	0.064	0.074	0.086

Table E.3: Chloride profiling results (uncracked concrete – Mix 2, Mix 2 poor, Mix 4 and Mix 4 poor)

w/b 0.60		Chloride content (% by mass of binder)							
		Mix 2 (100% CEM I 52.5N)		Mix 2 poor (100% CEM I 52.5N)		Mix 4 (70% CEM I/30% FA)		Mix 4 poor (70% CEM I/30% FA)	
Depth (mm)	Average depth (mm)	Untreated	Treated	Untreated	Treated	Untreated	Treated	Untreated	Treated
0-5	2.5	6.544	2.828	4.090	1.138	5.661	0.789	4.327	0.310
5-10	7.5	2.726	0.302	2.922	0.111	3.883	0.247	3.798	0.038
10-15	12.5	2.804	0.054	3.078	0.042	2.369	0.054	4.168	0.000
15-20	17.5	1.865	0.043	2.864	0.000	1.657	0.000	4.022	0.000
20-25	22.5	1.182	0.000	1.924	0.000	1.053	0.000	3.822	0.000
25-30	27.5	0.885	0.000	1.528	0.000	0.534	0.000	3.779	0.000
30-35	32.5	0.488	0.000	1.134	0.000	0.194	0.000	3.956	0.000
35-40	37.5	0.261	0.010	0.671	0.000	0.019	0.000	3.774	0.000

Table E.4: Chloride profiling results (uncracked concrete – Mix 6, Mix 6 poor, Mix 8 and Mix 8 poor)

w/b 0.60		Chloride content (% by mass of binder)							
		Mix 6 (50% CEM I/50% GGCS)		Mix 6 poor (50% CEM I/50% GGCS)		Mix 8 (100% CEM III/B 42.5N)		Mix 8 poor (100% CEM III/B 42.5N)	
Depth (mm)	Average depth (mm)	Untreated	Treated	Untreated	Treated	Untreated	Treated	Untreated	Treated
0-5	2.5	7.130	3.366	5.158	0.886	5.655	2.069	6.578	0.700
5-10	7.5	1.972	0.088	4.214	0.108	1.238	0.101	2.757	0.160
10-15	12.5	0.498	0.174	4.240	0.081	0.398	0.061	3.596	0.144
15-20	17.5	0.172	0.066	3.253	0.153	0.073	0.074	3.052	0.113
20-25	22.5	0.111	0.097	2.714	0.000	0.053	0.063	2.711	0.166
25-30	27.5	0.071	0.089	1.877	0.000	0.076	0.000	2.328	0.084
30-35	32.5	0.071	0.000	1.028	0.000	0.087	0.000	1.706	0.000
35-40	37.5	0.055	0.000	0.409	0.000	0.072	0.000	1.161	0.000

APPENDIX F – Bulk diffusion test results (cracked concrete)

Table F.1: Chloride profiling results (cracked concrete – Mix 2 and Mix 4)

w/b 0.60		Chloride content (% by mass of binder)							
		Mix 2 (100% CEM I 52.5N)				Mix 4 (70% CEM I/30% FA)			
		0.2 mm		0.6 mm		0.2 mm		0.6 mm	
Depth (mm)	Average depth (mm)	Untreated	Treated	Untreated	Treated	Untreated	Treated	Untreated	Treated
0-10	5	3.124	2.463	3.473	1.844	3.561	1.422	3.899	0.905
10-20	15	2.723	1.005	3.504	0.577	2.978	0.541	3.376	0.384
20-30	25	2.407	0.722	2.893	0.917	2.945	0.560	2.990	0.832
30-40	35	2.232	0.780	2.611	1.175	2.536	1.114	2.429	0.940
40-50	45	2.234	1.053	2.786	1.673	2.628	1.153	2.399	0.902
50-60	55	1.967	1.717	2.625	2.100	1.992	1.453	2.410	1.388

Table F.2: Chloride profiling results (cracked concrete – Mix 6 and Mix 8)

w/b 0.60		Chloride content (% by mass of binder)							
		Mix 6 (50% CEM I/50% GGCS)				Mix 8 (100% CEM III/B 42.5N)			
		0.2 mm		0.6 mm		0.2 mm		0.6 mm	
Depth (mm)	Average depth (mm)	Untreated	Treated	Untreated	Treated	Untreated	Treated	Untreated	Treated
0-5	2.5	4.118	2.986	4.339	2.205	4.051	0.866	4.517	0.130
5-10	7.5	2.589	0.199	3.147	0.249	2.734	0.056	2.900	0.049
10-15	12.5	1.234	0.549	2.075	0.063	1.542	0.047	1.700	0.067
15-20	17.5	1.256	0.281	1.726	0.053	1.265	0.050	1.448	0.072
20-25	22.5	0.805	0.478	1.579	0.622	1.182	0.070	1.239	0.083
25-30	27.5	0.817	0.341	1.310	0.664	1.081	0.068	1.226	0.058
30-35	32.5	0.762	0.199	1.217	0.065	0.902	0.055	1.317	0.066
35-40	37.5	0.892	0.474	1.382	0.726	0.826	0.089	0.913	0.074
40-45	42.5	0.726	0.505	1.425	0.460	1.010	0.162	1.245	0.063
45-50	47.5	0.778	0.735	1.507	0.688	0.935	0.094	1.126	0.082
50-60	55	0.906	0.637	1.475	0.843	0.886	0.304	1.191	0.064

APPENDIX G – Curve fitting results

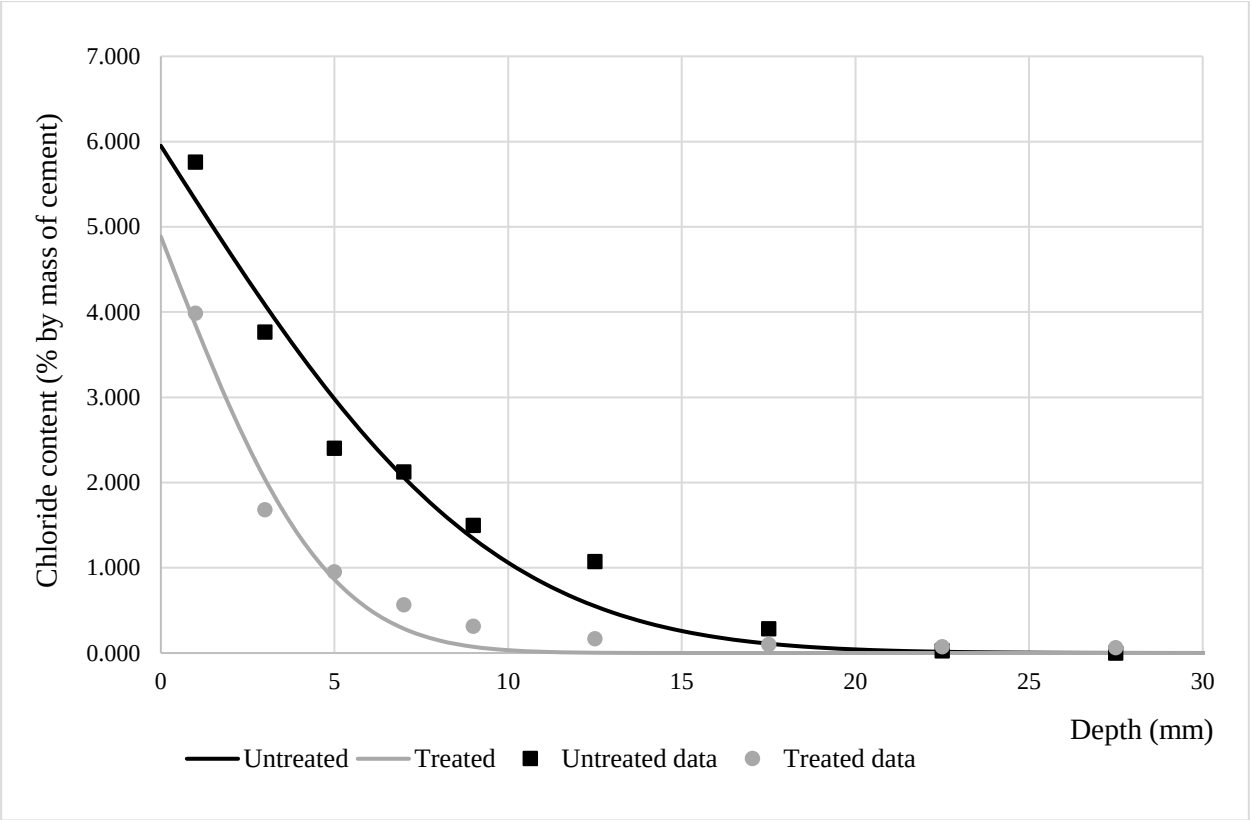

Figure G-1: Chloride profile after curve fitting (Mix 1 – CEM I 52.5N w/b 0.45)

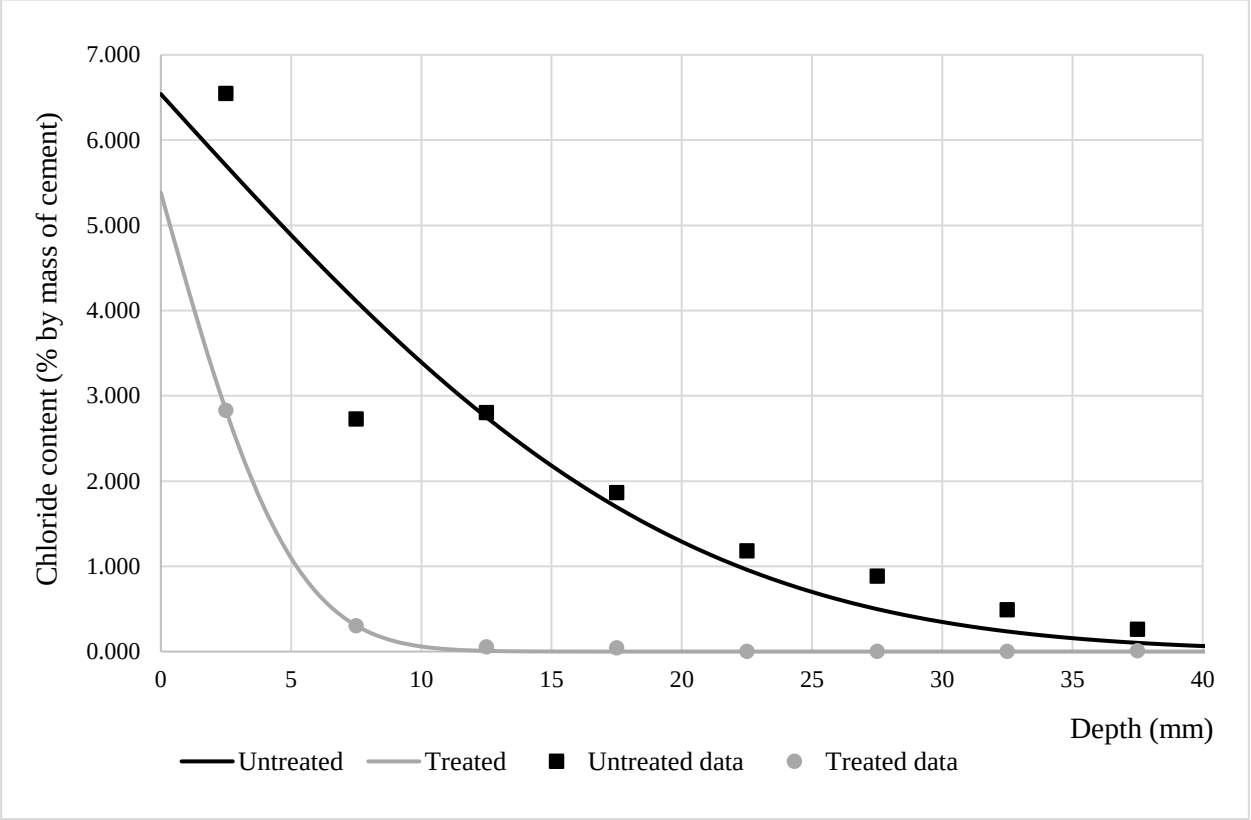

Figure G-2: Chloride profiling after curve fitting (Mix 2 – CEM I 52.5N w/b 0.60)

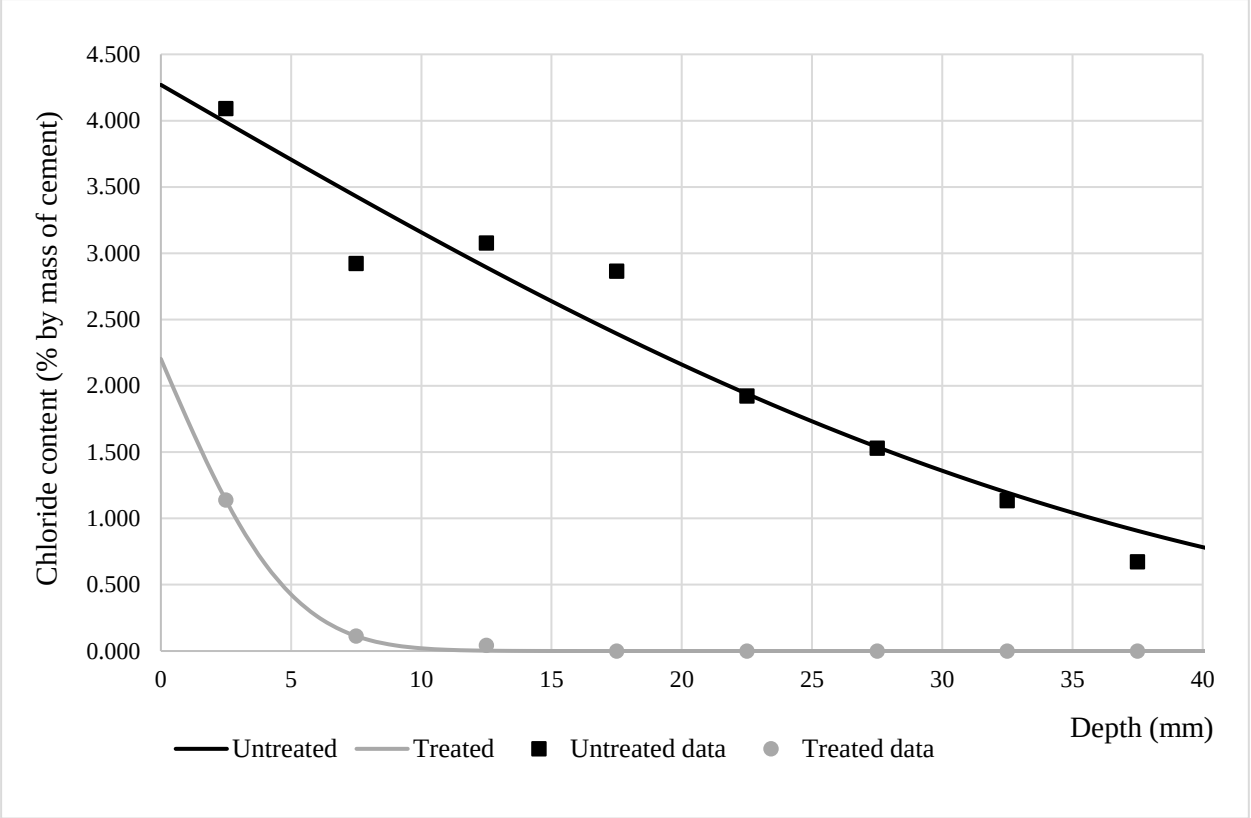

Figure G-3: Chloride profile after curve fitting (Mix 2 poor – CEM I 52.5N w/b 0.60)

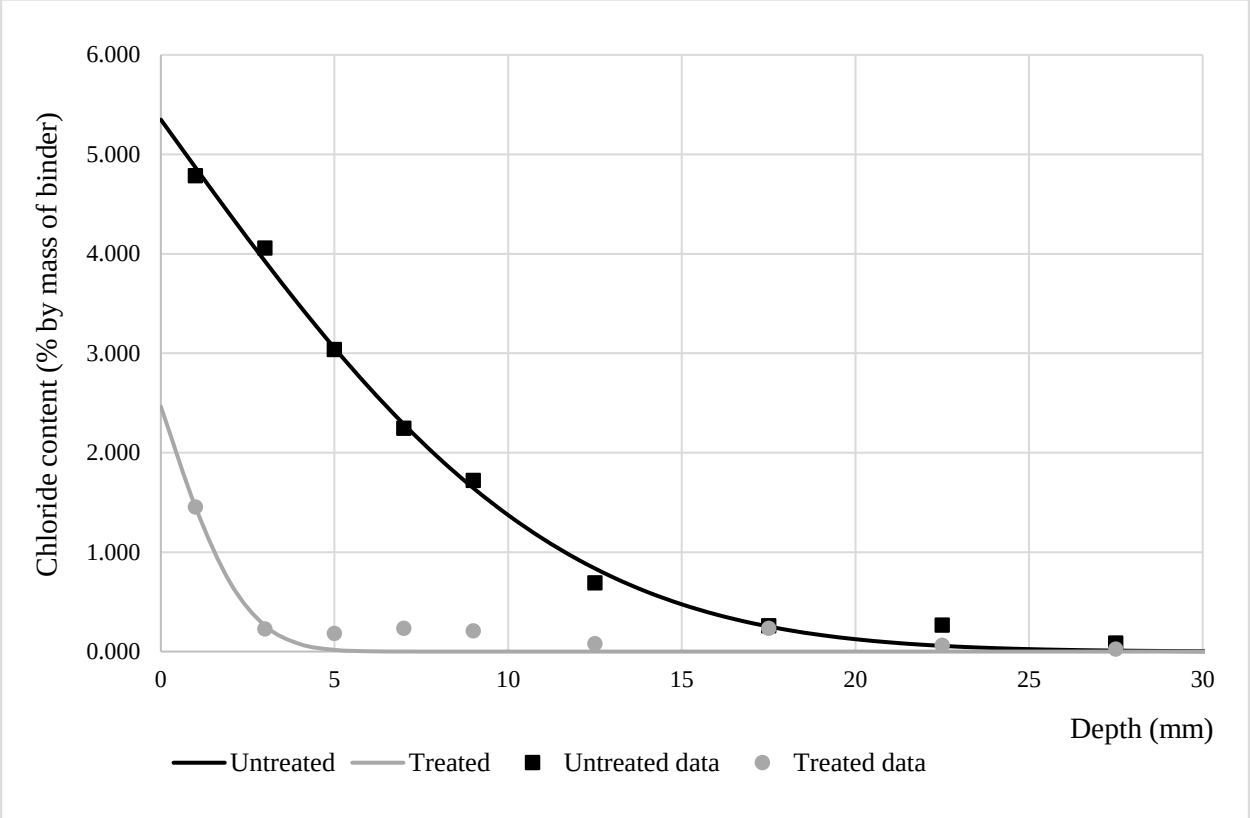

Figure G-4: Chloride profile after curve fitting (Mix 3 – 30% FA w/b 0.45)

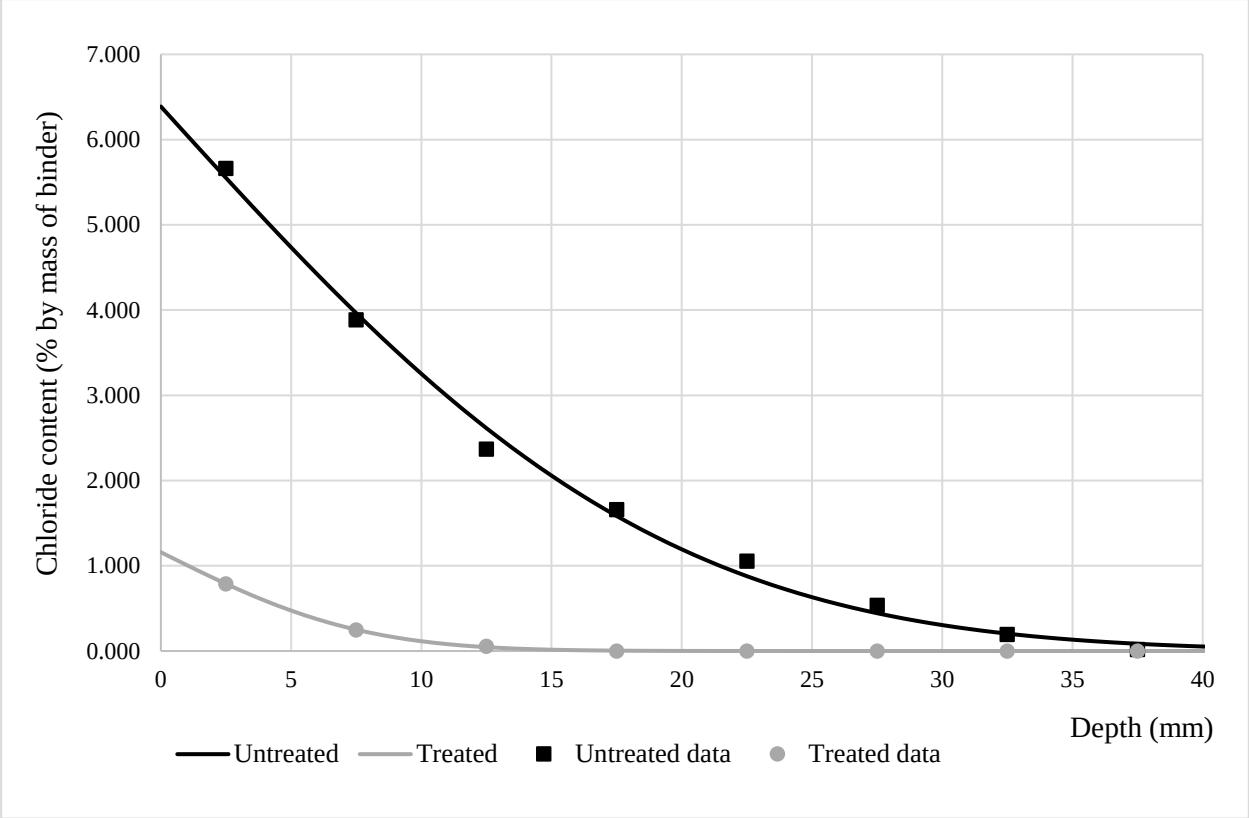

Figure G-5: Chloride profile after curve fitting (Mix 4 – 30% FA w/b 0.60)

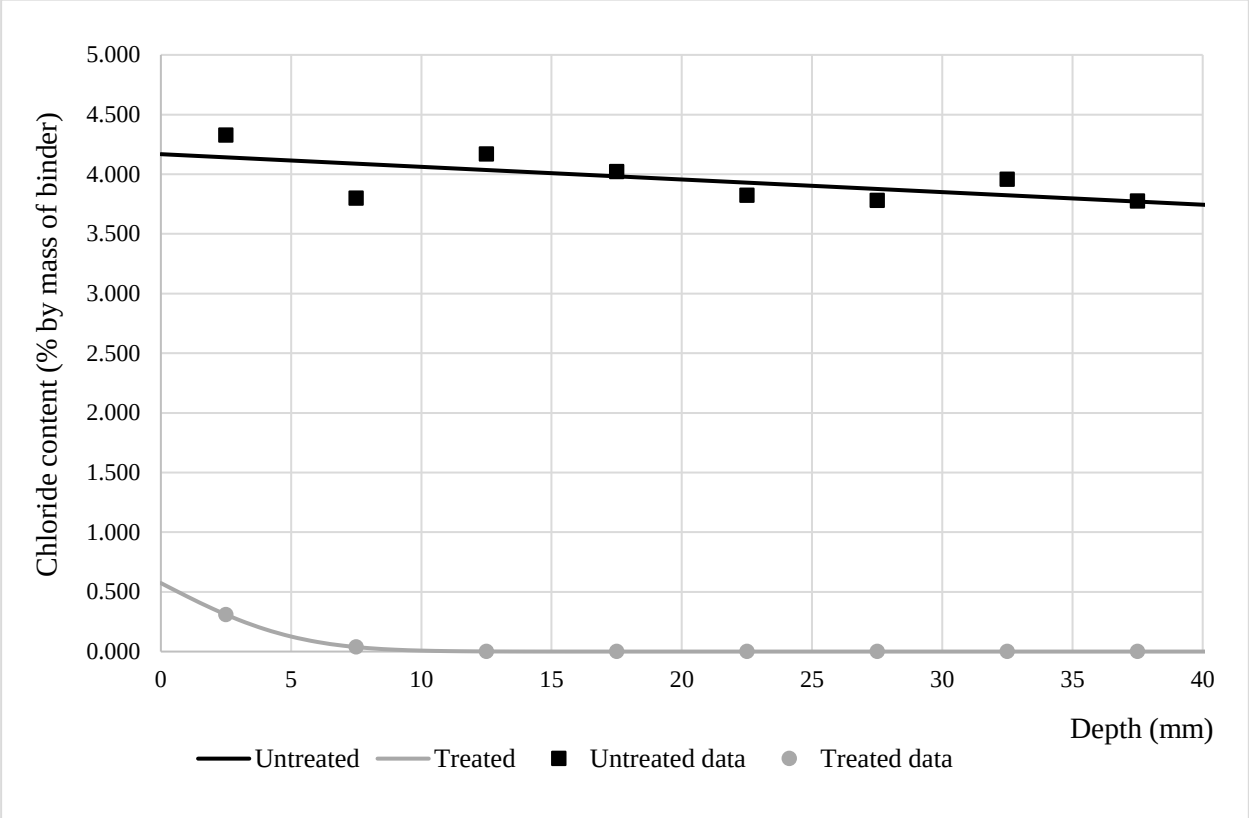

Figure G-6: Chloride profile after curve fitting (Mix 4 poor – 30% FA w/b 0.60)

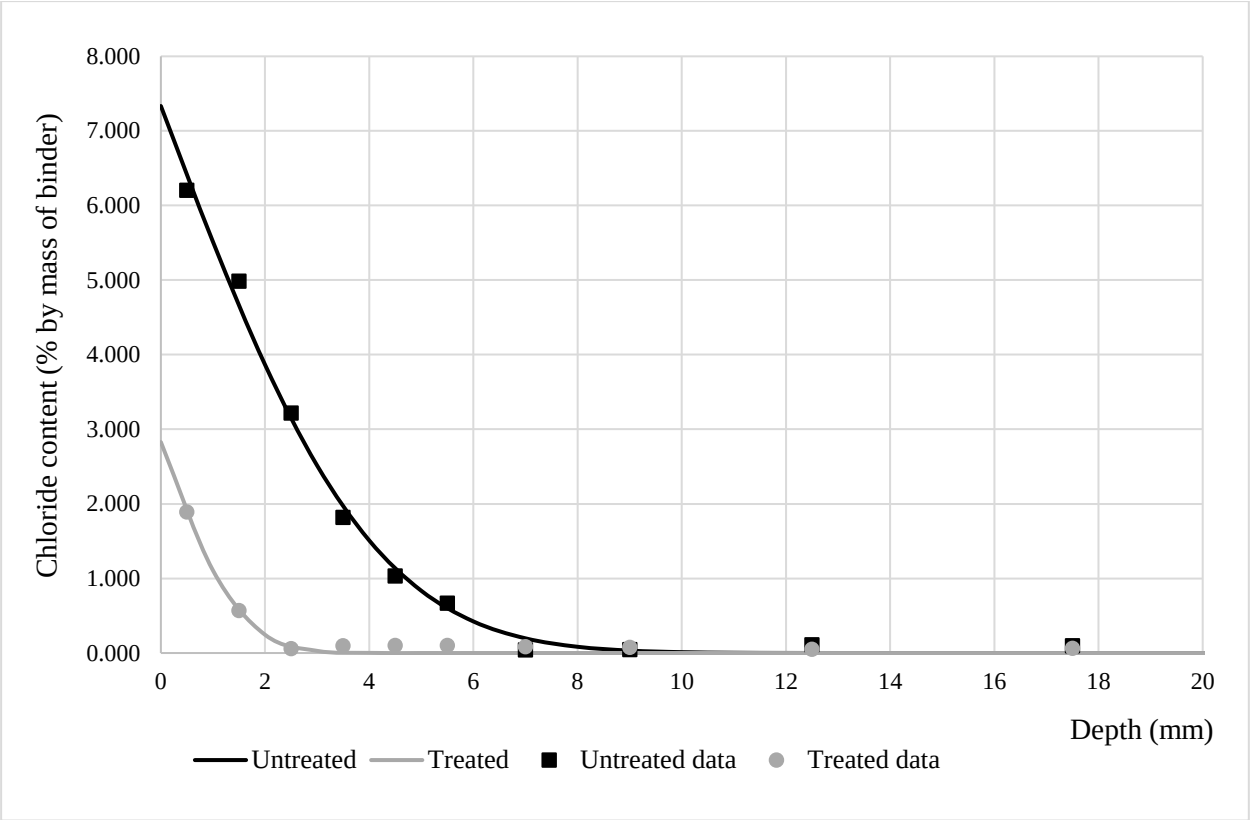

Figure G-7: Chloride profile after curve fitting (Mix 5 – 50% GGCS w/b 0.45)

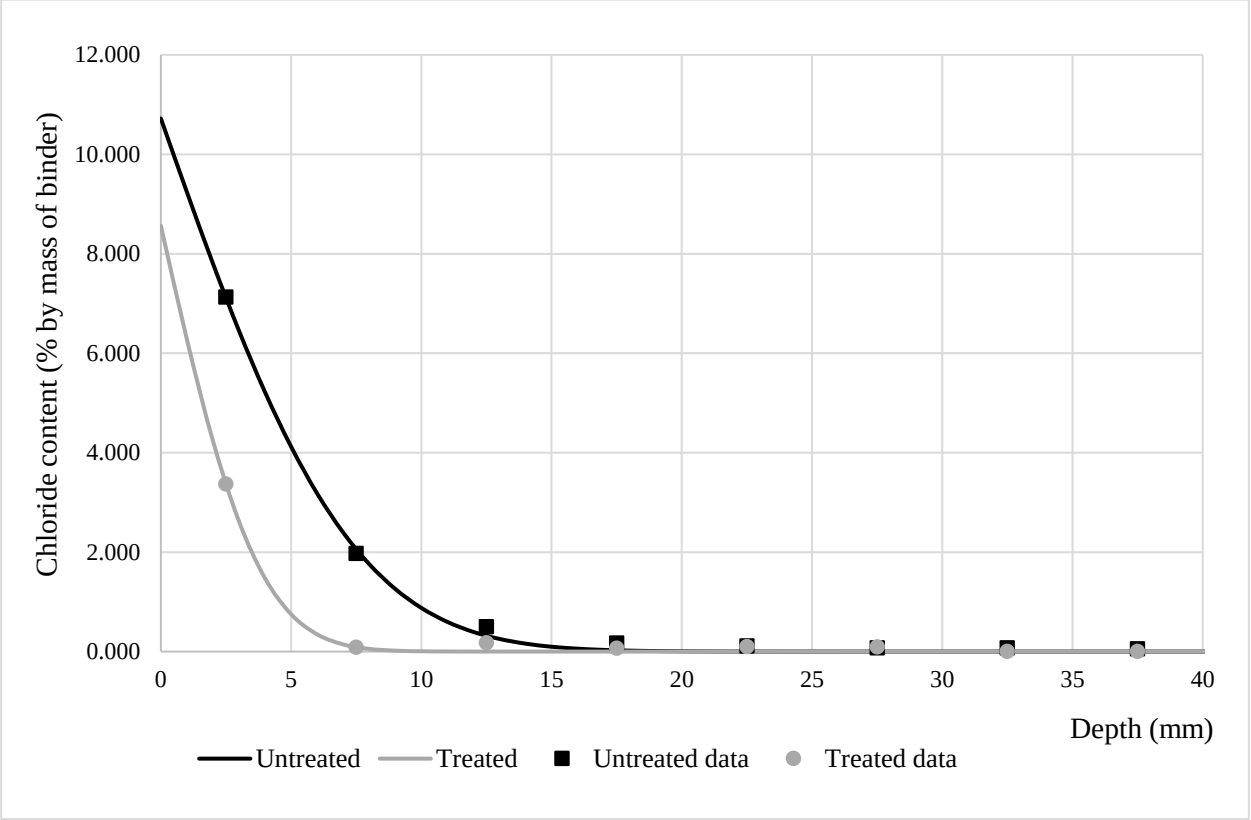

Figure G-8: Chloride profile after curve fitting (Mix 6 – 50% GGCS w/b 0.60)

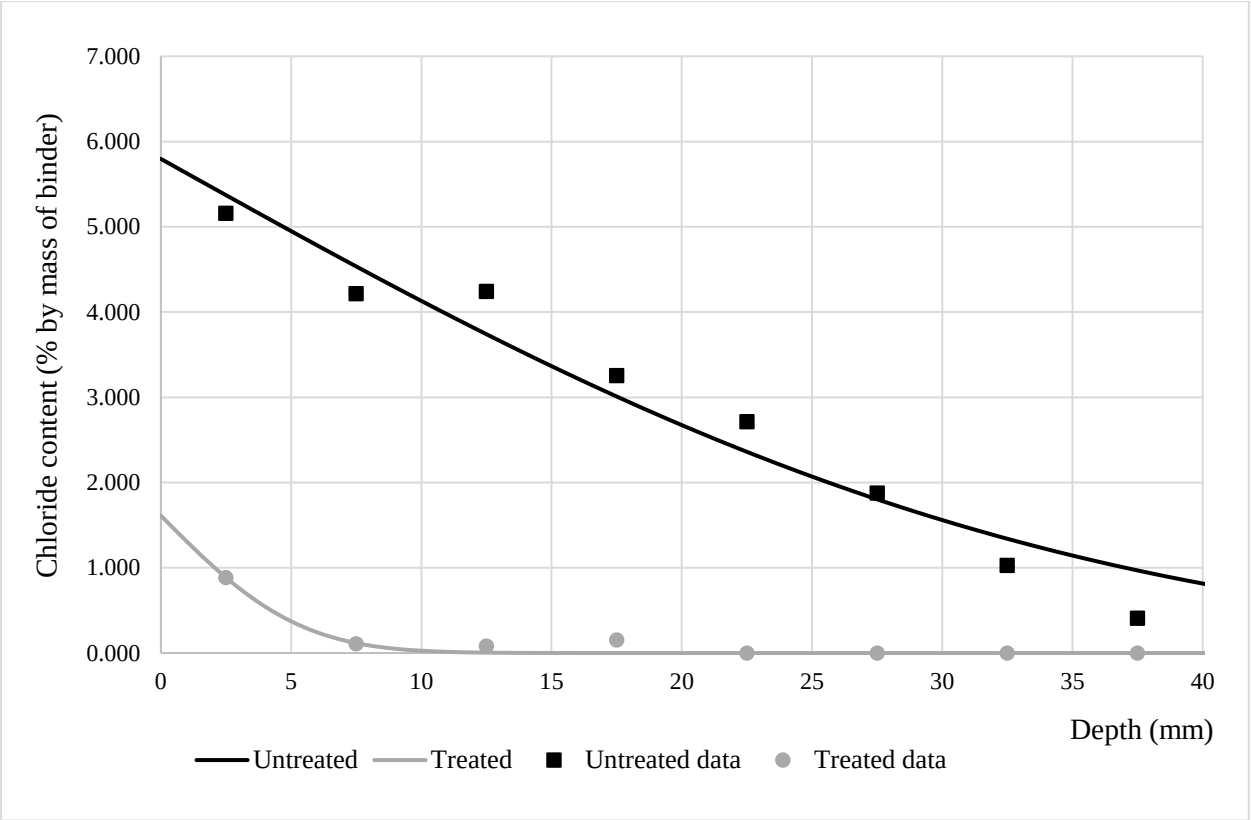

Figure G-9: Chloride profile after curve fitting (Mix 6 poor – 50% GGCS w/b 0.60)

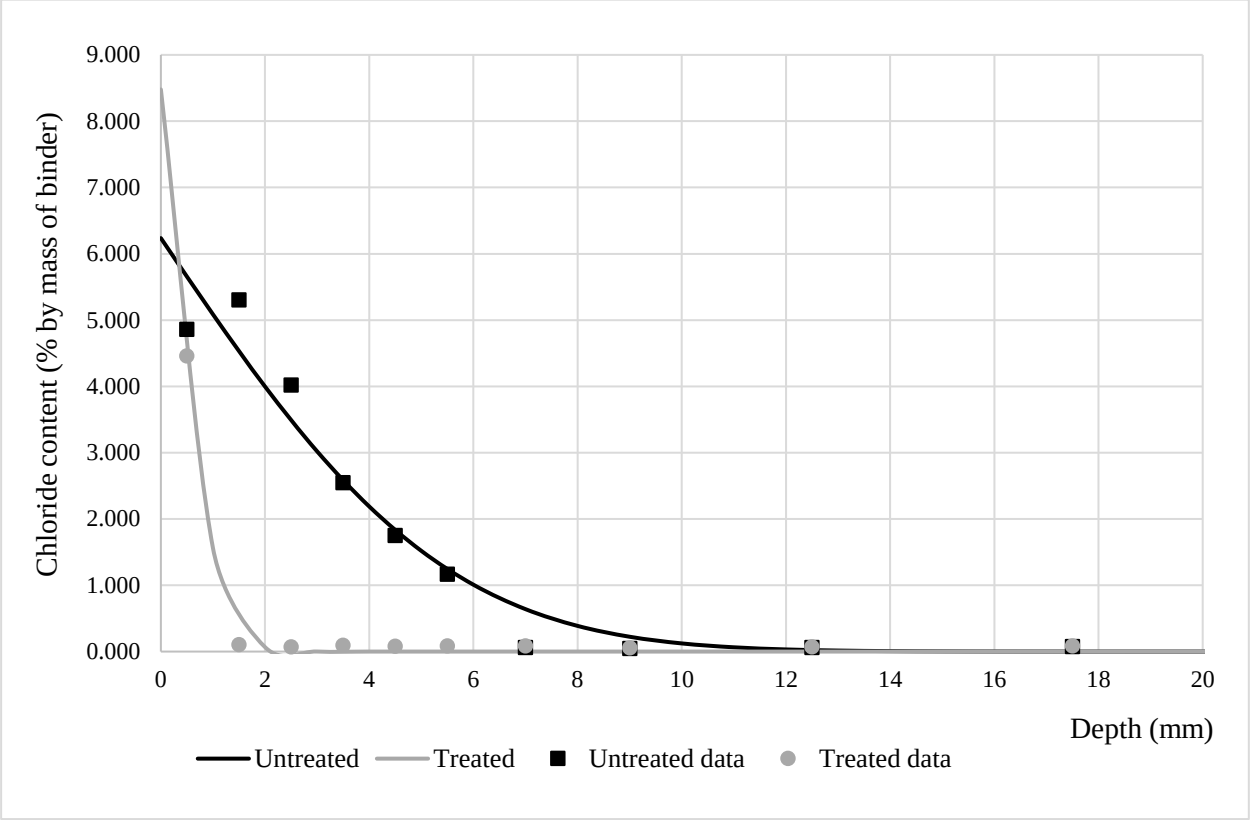

Figure G-10: Chloride profile after curve fitting (Mix 7 – CEM III/B 42.5N w/b 0.45)

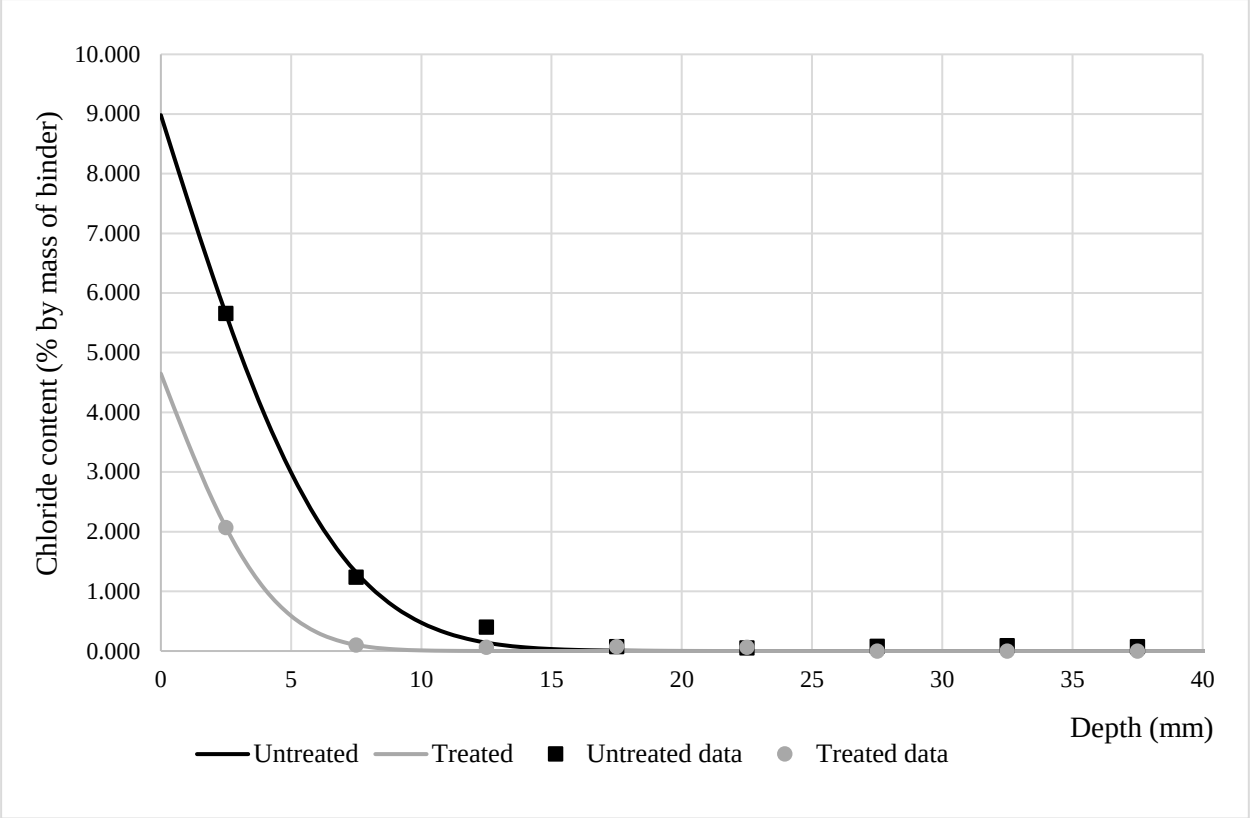

Figure G-11: Chloride profile after curve fitting (Mix 8 – CEM III/B 42.5N w/b 0.60)

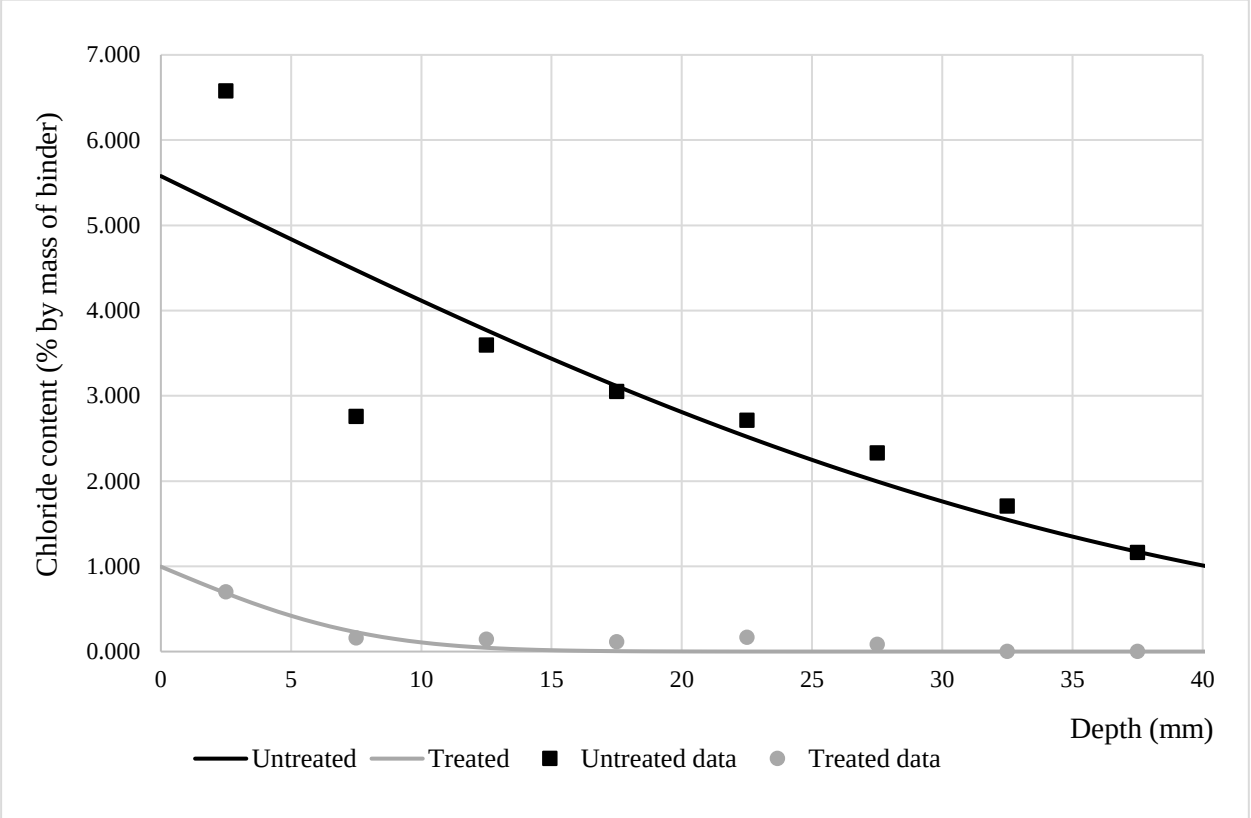

Figure G-12: Chloride profile after curve fitting (Mix 8 poor – CEM III/B 42.5N w/b 0.60)

Table G.1.1: Chloride surface concentration (C_s/%) obtained by curve fitting of data points

Chloride surface concentration (C_s)	Mix 1		Mix 2		Mix 2 (poor quality)		Mix 3		Mix 4		Mix 4 (poor quality)	
%	100% CEM I 52.5N		100% CEM I 52.5N		100% CEM I 52.5N		70% PC/ 30% FA		70% PC/ 30% FA		70% PC/ 30% FA	
w/b	0.45		0.60		0.60		0.45		0.60		0.60	
	Untreated	Treated	Untreated	Treated	Untreated	Treated	Untreated	Treated	Untreated	Treated	Untreated	Treated
1	5.257	5.793	4.725	7.552	4.265	2.167	4.472	2.891	5.355	2.055	4.051	0.441
2	7.174	5.005	7.514	5.303	4.900	1.960	4.493	2.281	7.348	0.623	4.265	0.798
3	5.498	4.518	7.514	4.552	3.652	2.481	7.320	2.131	6.467	0.793	4.190	0.434
Average	5.976	5.105	6.584	5.802	4.272	2.203	5.428	2.434	6.390	1.157	4.169	0.558

Table G.1.2: Chloride surface concentration (C_s/%) obtained by curve fitting of data points

Chloride surface concentration (C_s)	Mix 5		Mix 6		Mix 6 (poor quality)		Mix 7		Mix 8		Mix 8 (poor quality)	
%	50% PC/ 50% GGCS		50% PC/ 50% GGCS		50% PC/ 50% GGCS		100% CEM III/B 42.5N		100% CEM III/B 42.5N		100% CEM III/B 42.5N	
w/b	0.45		0.60		0.60		0.45		0.60		0.60	
	Untreated	Treated	Untreated	Treated	Untreated	Treated	Untreated	Treated	Untreated	Treated	Untreated	Treated
1	7.522	4.223	7.651	9.550	5.585	0.710	6.114	8.170	8.318	5.836	5.485	0.977
2	8.098	2.351	12.680	10.480	5.772	1.219	6.720	8.024	11.120	5.402	5.415	1.019
3	6.572	3.021	12.680	5.679	6.037	3.003	6.008	8.017	8.606	2.907	5.843	0.985
Average	7.397	3.198	11.004	8.570	5.798	1.644	6.281	8.070	9.348	4.715	5.581	0.994

Table G.2.1: Apparent chloride diffusion coefficients (D_a/m^2s^{-1}) obtained by curve fitting of data points

Apparent diffusion coefficients (D_a)	Mix 1		Mix 2		Mix 2 (poor quality)		Mix 3		Mix 4		Mix 4 (poor quality)	
m^2/s	100% CEM I 52.5N		100% CEM I 52.5N		100% CEM I 52.5N		70% PC/ 30% FA		70% PC/ 30% FA		70% PC/ 30% FA	
w/b	0.45		0.60		0.60		0.45		0.60		0.60	
	Untreated	Treated	Untreated	Treated	Untreated	Treated	Untreated	Treated	Untreated	Treated	Untreated	Treated
1	3.17E-12	3.49E-13	2.15E-11	1.55E-12	6.24E-11	1.09E-12	7.71E-12	2.26E-13	1.74E-11	2.52E-12	2.39E-08	1.34E-12
2	3.71E-12	1.50E-12	1.58E-11	6.07E-13	6.11E-11	1.12E-12	7.24E-12	3.47E-13	1.69E-11	3.27E-12	2.22E-09	1.04E-12
3	5.17E-12	1.42E-12	1.58E-11	7.41E-13	7.51E-11	1.03E-12	3.53E-12	2.20E-13	1.54E-11	2.63E-12	1.65E-08	1.45E-12
Average	4.02E-12	1.09E-12	1.77E-11	9.66E-13	6.62E-11	1.08E-12	6.16E-12	2.64E-13	1.66E-11	2.81E-12	1.42E-08	1.28E-12

Table G.2.2: Apparent chloride diffusion coefficients (D_a/m^2s^{-1}) obtained by curve fitting of data points

Apparent diffusion coefficients (D_a)	Mix 5		Mix 6		Mix 6 (poor quality)		Mix 7		Mix 8		Mix 8 (poor quality)	
m^2/s	50% PC/ 50% GGCS		50% PC/ 50% GGCS		50% PC/ 50% GGCS		100% CEM III/B 42.5N		100% CEM III/B 42.5N		100% CEM III/B 42.5N	
w/b	0.45		0.60		0.60		0.45		0.60		0.60	
	Untreated	Treated	Untreated	Treated	Untreated	Treated	Untreated	Treated	Untreated	Treated	Untreated	Treated
1	7.55E-13	3.10E-14	4.22E-12	6.67E-13	6.51E-11	2.48E-12	1.22E-12	4.49E-14	2.29E-12	6.38E-13	7.11E-11	2.19E-12
2	8.37E-13	1.64E-13	1.83E-12	5.94E-13	5.11E-11	1.23E-12	1.05E-12	4.55E-14	1.02E-12	8.32E-13	6.75E-11	3.68E-12
3	5.16E-13	1.14E-13	1.83E-12	6.28E-13	4.64E-11	1.01E-12	1.77E-12	4.42E-14	2.66E-12	8.89E-13	5.66E-11	2.75E-12
Average	7.03E-13	1.03E-13	2.63E-12	6.30E-13	5.42E-11	1.57E-12	1.35E-12	4.49E-14	1.99E-12	7.86E-13	6.51E-11	2.87E-12

APPENDIX H – Detailed moisture profiling results

Table H.1: Moisture profiling results (1 day after silane treatment)

After 1 day @ 63 ± 2% RH		Untreated		Treated	
%RH	Depth (mm)	1	2	1	2
Mix 2	4	78.34	76.70	93.87	91.95
	50	92.05	92.50	94.54	93.81
	80	95.42	95.27	95.61	94.48
Mix 4	4	77.37	81.26	95.08	94.93
	50	95.01	97.60	97.06	97.64
	80	97.32	98.62	98.69	98.36
Mix 6	4	73.39	77.91	88.56	85.10
	50	92.29	93.53	91.58	91.44
	80	93.62	93.67	92.57	92.40

Table H.2: Moisture profiling results (after 16 weeks @ 63 ± 2% RH)

After 16 weeks @ 63 ± 2% RH		Untreated		Treated	
%RH	Depth (mm)	1	2	1	2
Mix 2	4	67.68	70.34	77.48	76.15
	50	79.75	81.29	84.72	84.03
	80	83.29	83.67	85.88	85.85
Mix 4	4	64.00	68.90	72.70	72.83
	50	83.87	85.96	86.57	86.60
	80	89.84	90.51	88.53	89.35
Mix 6	4	62.72	65.00	69.62	70.60
	50	81.68	82.38	83.90	82.69
	80	84.95	84.80	83.92	85.51

APPENDIX I – Time to corrosion initiation graphs

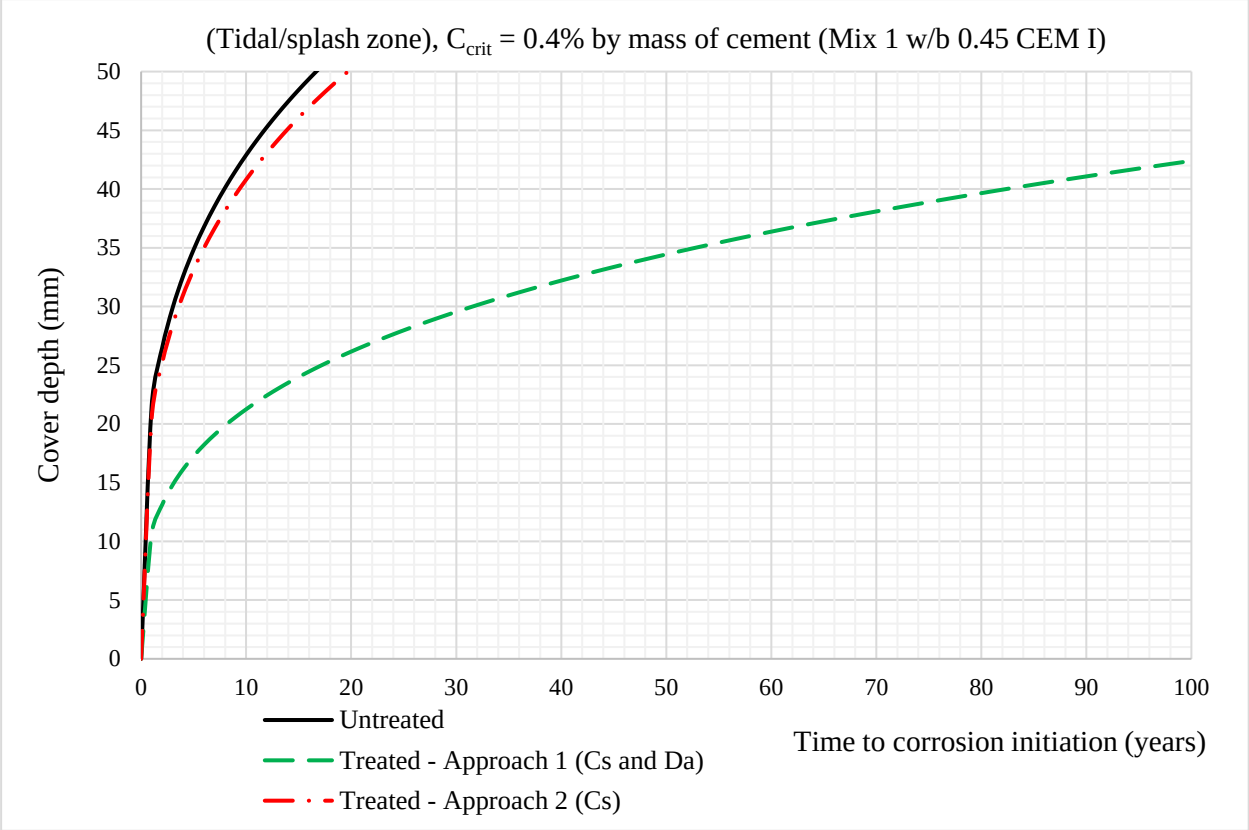

Figure I-1: Time evolution of the critical chloride threshold for Mix 1 (CEM I w/b 0.45)

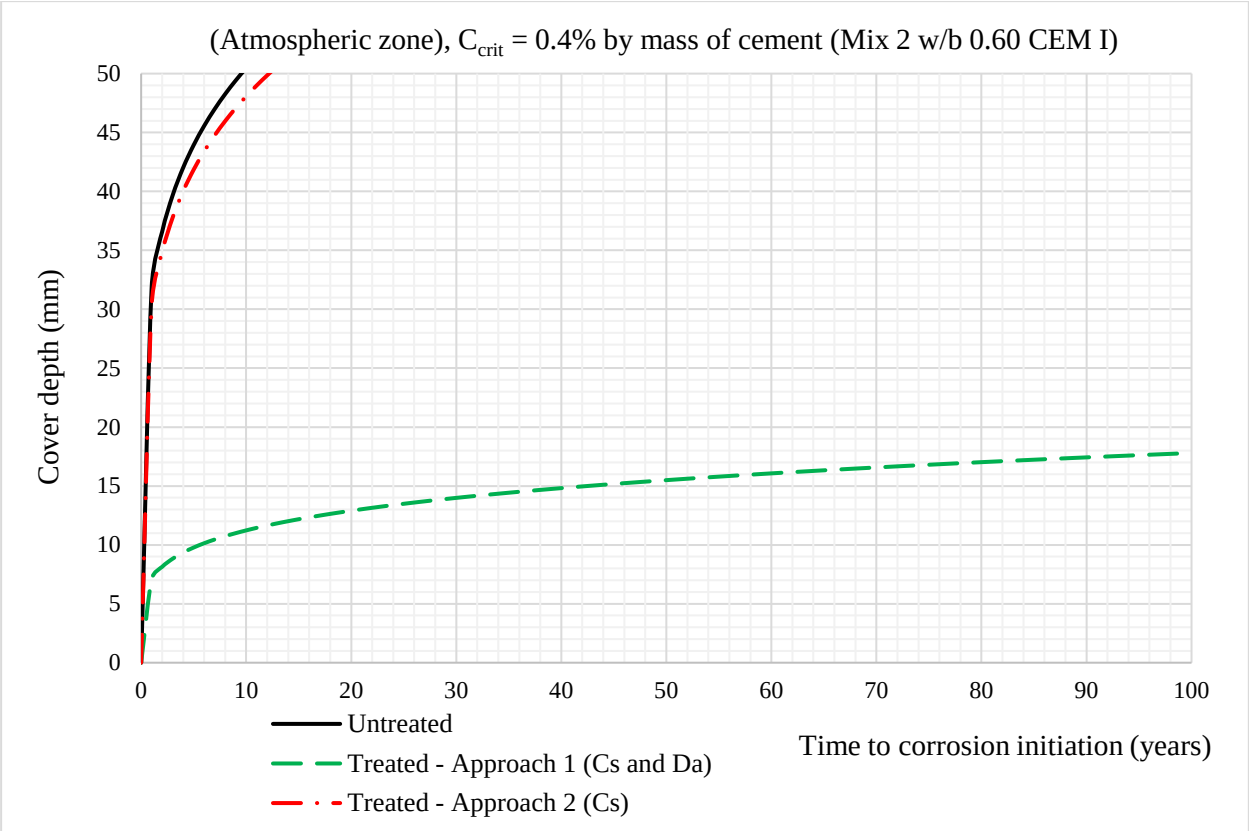

Figure I-2: Time evolution of the critical chloride threshold for Mix 2 (CEM I w/b 0.60)

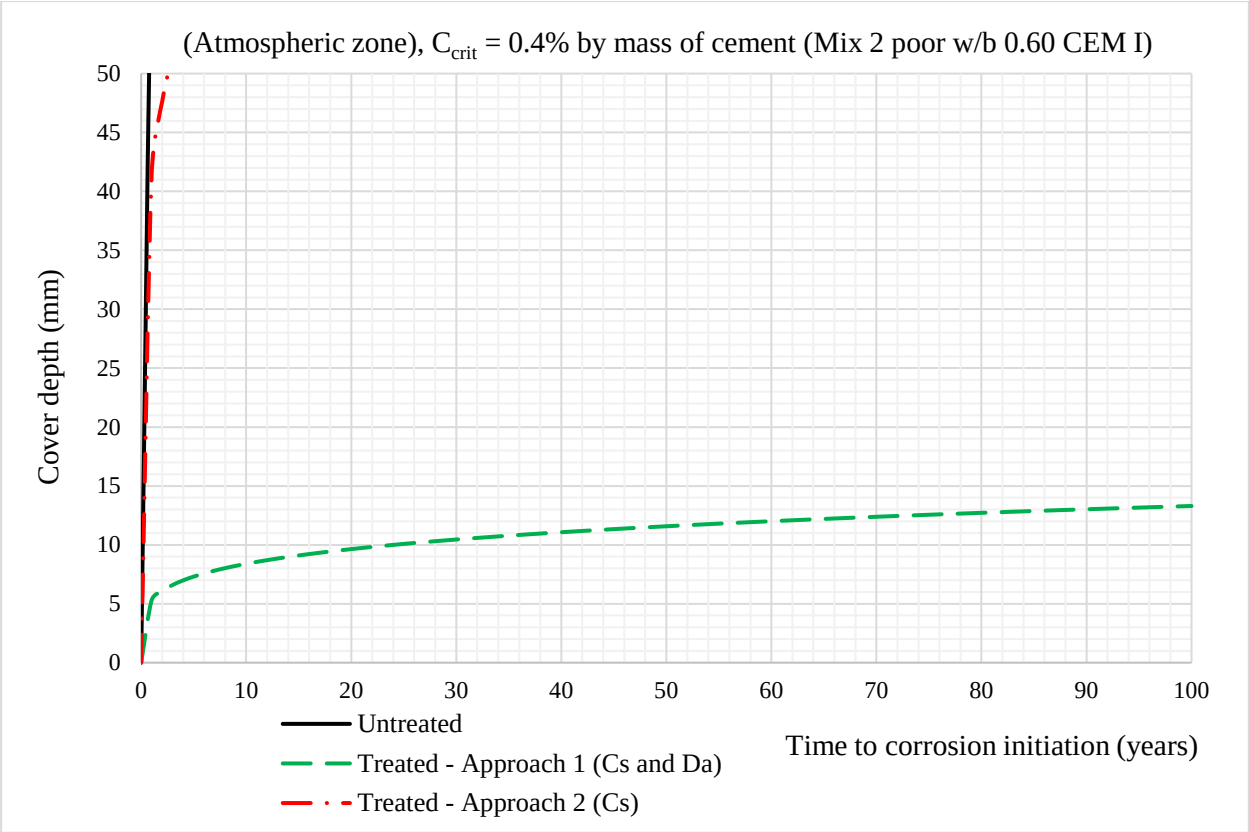

Figure I-3: Time evolution of the critical chloride threshold for Mix 2 poor (CEM I w/b 0.60)

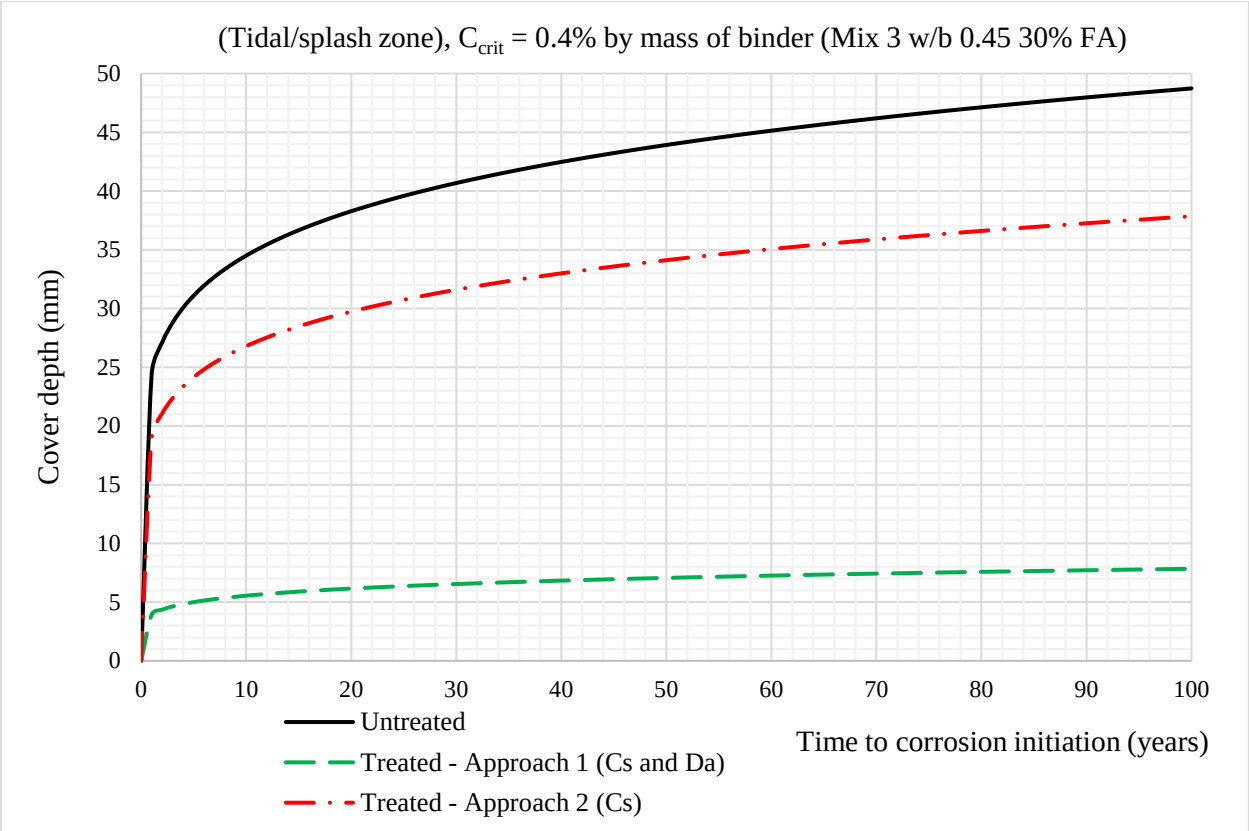

Figure I-4: Time evolution of the critical chloride threshold for Mix 3 (30% FA w/b 0.45)

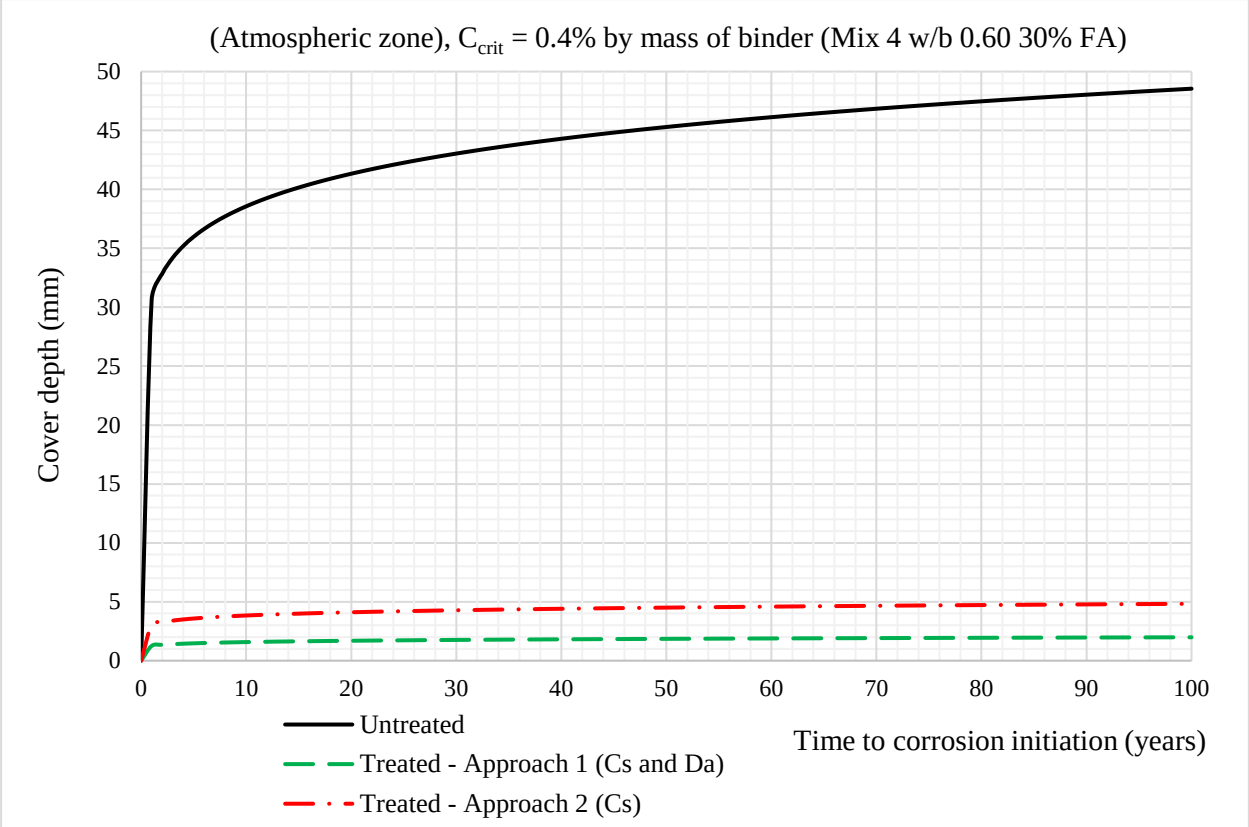

Figure I-5: Time evolution of the critical chloride threshold for Mix 4 (30% FA w/b 0.60)

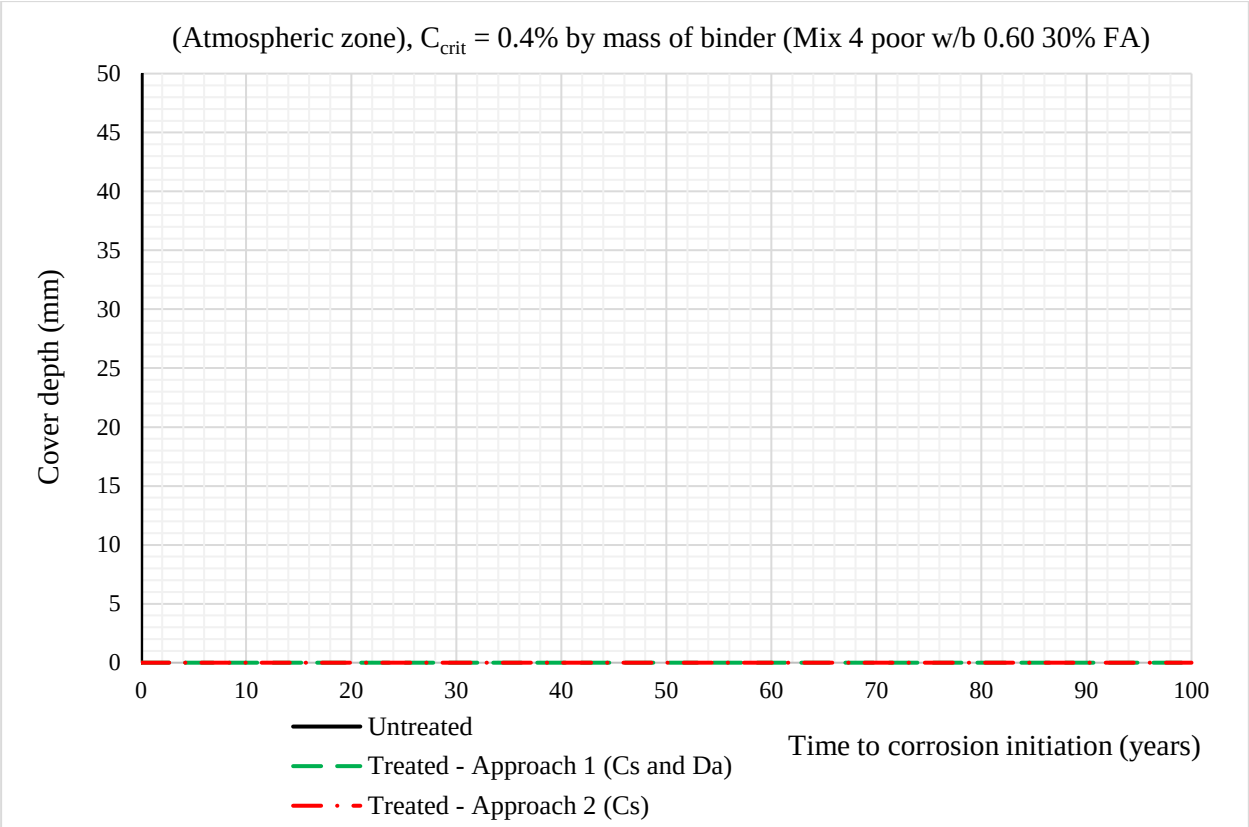

Figure I-6: Time evolution of the critical chloride threshold for Mix 4 poor (30% FA w/b 0.60)

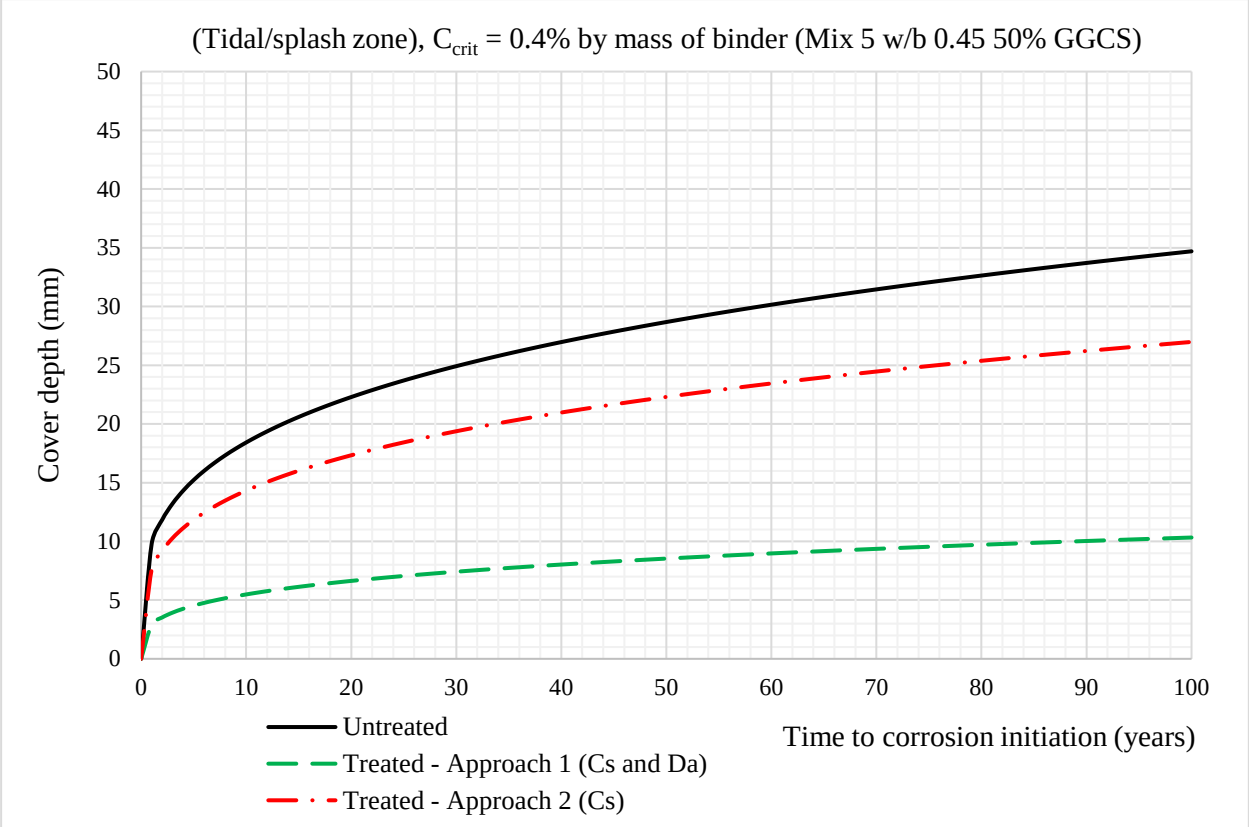

Figure I-7: Time evolution of the critical chloride threshold for Mix 5 (50% GGCS w/b 0.45)

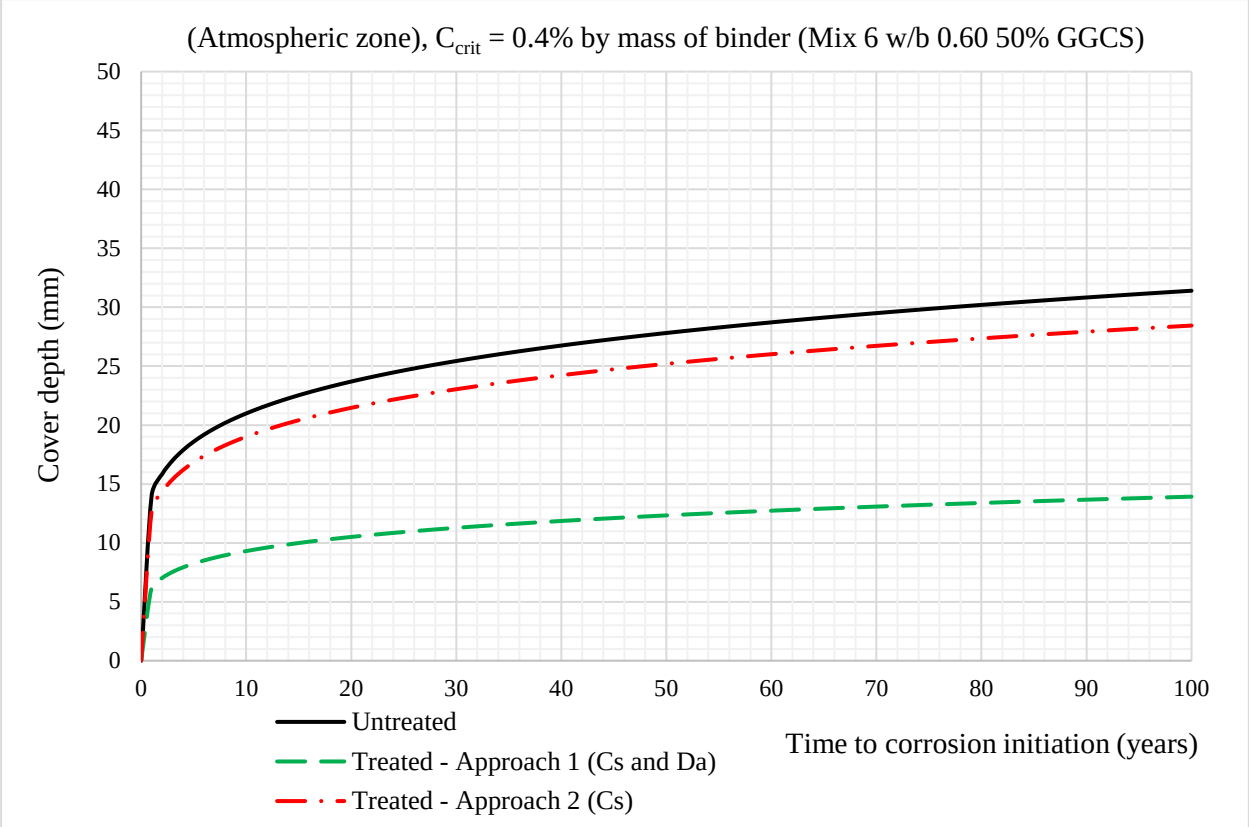

Figure I-8: Time evolution of the critical chloride threshold for Mix 6 (50% GGCS w/b 0.60)

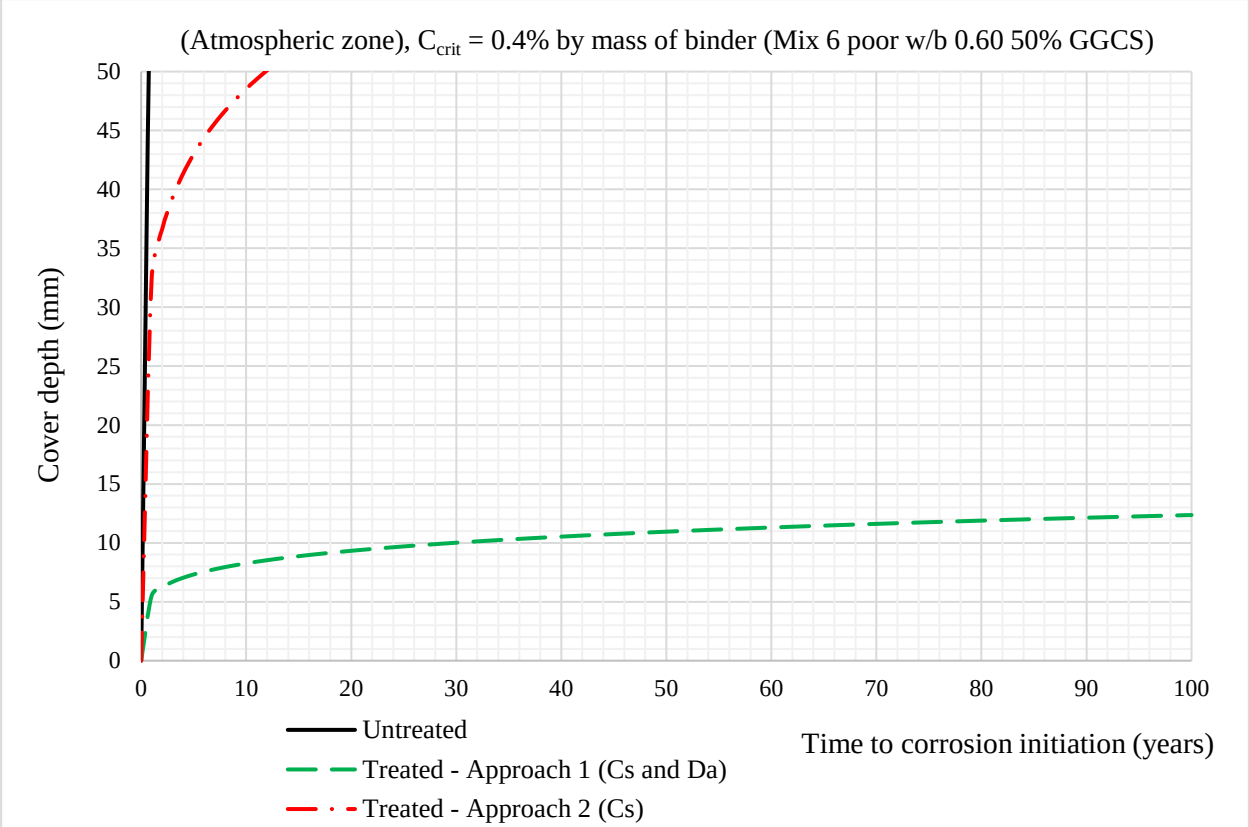

Figure I-9: Time evolution of the critical chloride threshold for Mix 6 poor (50% GGCS w/b 0.60)

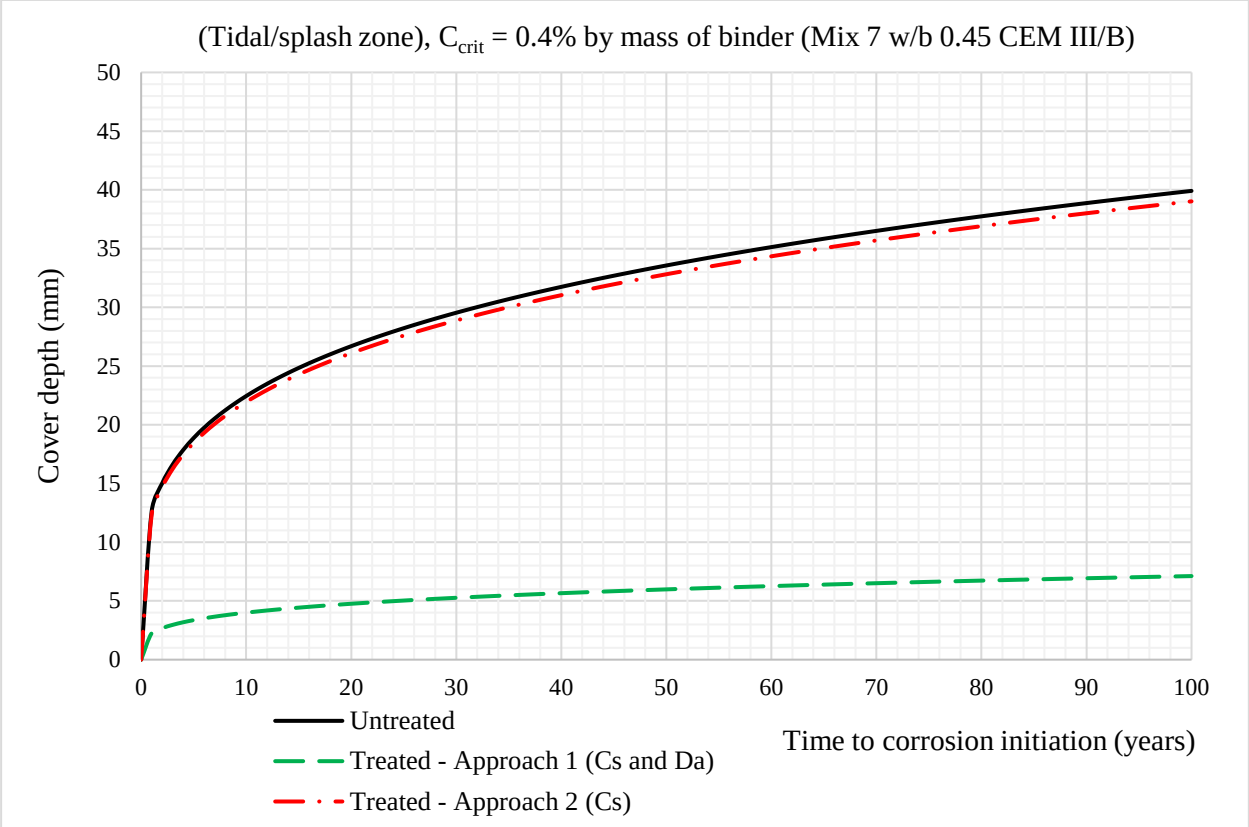

Figure I-10: Time evolution of the critical chloride threshold for Mix 7 (CEM III/B w/b 0.45)

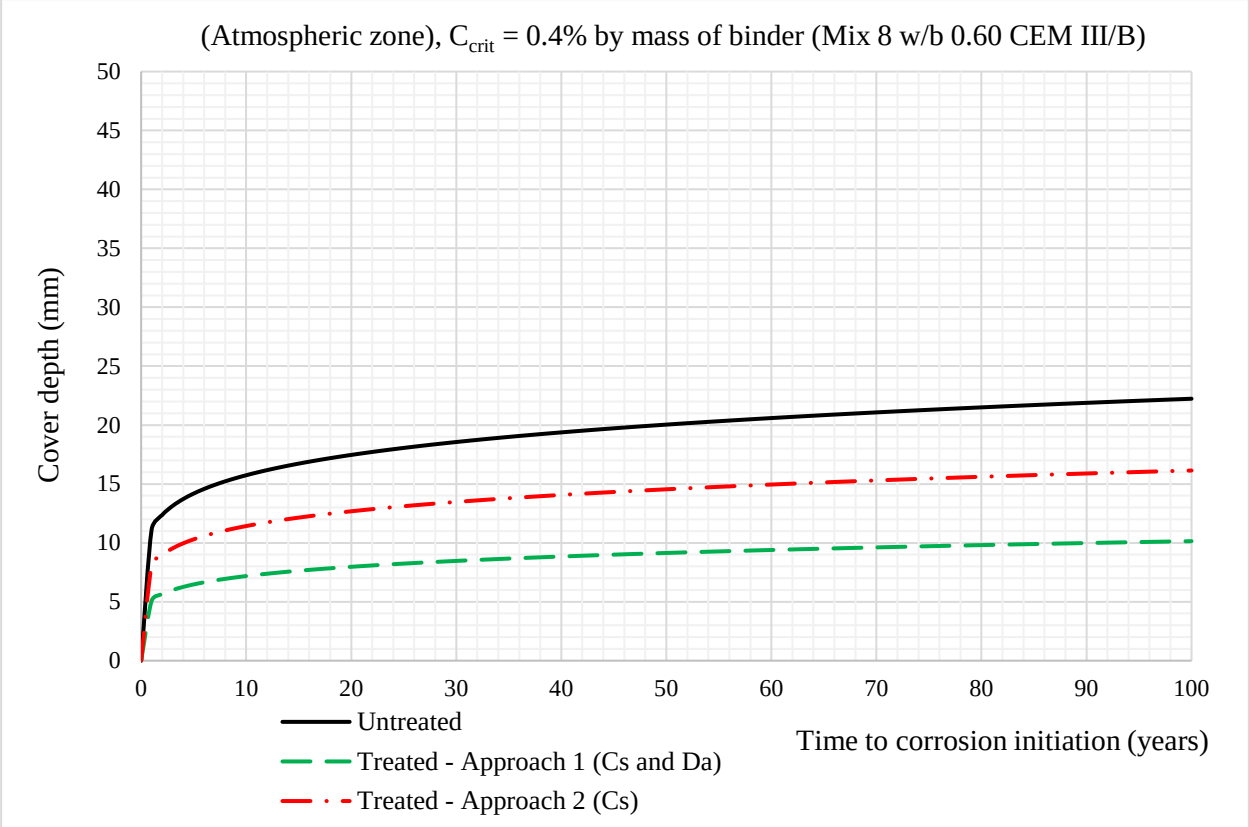

Figure I-11: Time evolution of the critical chloride threshold for Mix 8 (CEM III/B w/b 0.60)

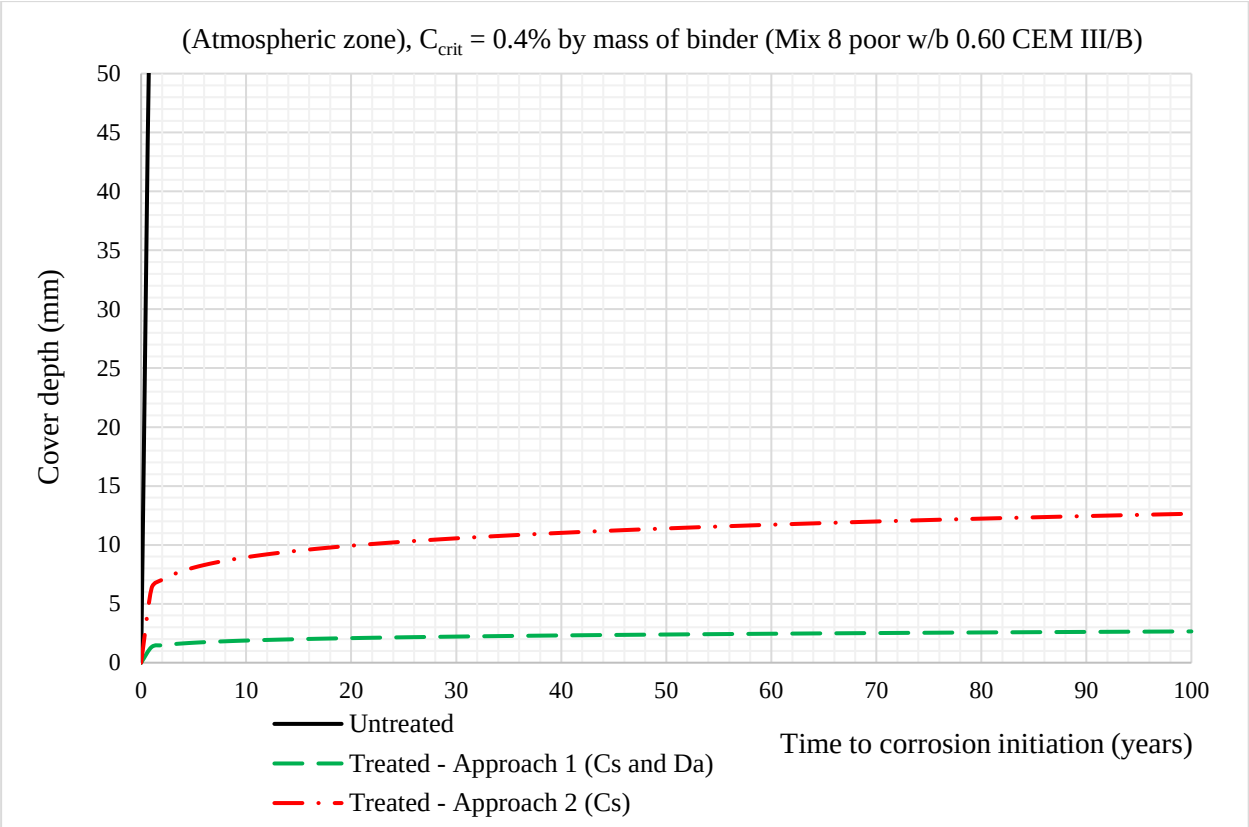

Figure I-12: Time evolution of the critical chloride threshold for Mix 8 poor (CEM III/B w/b 0.60)

APPENDIX J – SANRAL microenvironments definitions

Table J.1: SANRAL microenvironment definitions for carbonation induced corrosion (adapted from SANRAL Table 6000/1, 2009)

Microenvironment designation	Description	Condition of exposure	Description of exposure
XC1a	Low humidity (<50%); exterior concrete sheltered from moisture, arid areas; interior concrete	Mild	Inland dry areas – arid to semi-arid, Karoo etc. Very low (<40%) to low humidity (40% - 50%). Concrete surfaces not in contact with ground, protected against wetting.
XC1b	Permanently wet or damp		All areas with access to external or environmental moisture saturated conditions (RH >95%). Concrete surfaces above ground level kept permanently moist by exposure to water; concrete that never appreciably dries. Concrete surfaces below ground such as piles and buried foundations or abutments kept permanently damp.
XC2	Wet, rarely dry	Moderate	All areas with access to external or environmental moisture. Concrete surfaces above ground level kept mostly in moist condition by exposure to water; concrete may occasionally dry for appreciable periods such as when tanks are emptied.
XC3	Moderate humidity (50-80%), Exterior concrete sheltered from rain in non-arid areas		Near-coastal areas with no chlorides; moist inland areas; adjacent to dams, lakes, major rivers. Moderate humidity (50% to 80%), moist climate. Exterior concrete surfaces in moist areas or adjacent to major water bodies, permanently sheltered from rain or direct surface moisture.
XC4	Cyclic wetting and drying	Severe	All areas with access to external or environmental moisture; arid areas excluded, Moderate humidity (50% to 80%), moist climate. Concrete surfaces exposed to rain or alternately wet and dry conditions.

Table J.2: SANRAL microenvironment definitions for chloride induced corrosion (adapted from SANRAL Table 6000/1, 2009)

Microenvironment designation	Description	Condition of exposure	Description of exposure
XS1	Exposed to airborne salt but not in direct contact with seawater or inland saline waters	Very severe	Proven presence of chlorides; generally < 1km from sea, and coastal river valleys (where chlorides are present) and estuaries, or the presence of chlorides proven by experience or testing. This will include inland salt pans or groundwater carrying salts.
XS2a	Permanently submerged in sea (or saline waters)	Severe	Permanently (or substantially) submerged: in the sea (without heavy wave action); in coastal saline estuaries and rivers; in any aggressive saline waters. Concrete surfaces exposed to heavily polluted industrial waters; permanently or substantially submerged or permanently wet saline conditions (generally oxygen starved area approximately 1-1, 5m below spring type level)
XS2b	XS2a + exposed to abrasion	Extreme	As above, but with heavy wave action; in any aggressive saline waters where abrasion occurs.
XS3a	Tidal, splash and spray zones	Extreme	Sea or saline estuaries and rivers. But not permanently submerged; tidal zone; and in a spray or splash zone. Surfaces exposed to aggressive saline waters, including heavily polluted industrial waters, without being permanently wet.
XS3b	XS3a + exposed to abrasion		As above, but with heavy wave action or where abrasion or erosion can occur.

APPENDIX K – Aggregate sieve analysis

Table K.1: Sieve analysis (dune sand)

Dune sand						
Sieve Size (mm)	**Mass of Sieve (g)**	**Mass of Sieve & Aggregate (g)**	**Mass retained (g)**	**Percentage aggregate retained (%)**	**Cumulative percentage aggregate retained (%)**	**Cumulative percentage aggregate passing (%)**
4.75	657.89	657.89	0.00	0.0	0.0	100.0
2.36	412.94	412.95	0.01	0.0	0.0	100.0
1.18	350.22	354.51	4.29	0.4	0.4	99.6
0.600	519.94	791.78	271.84	27.2	27.6	72.4
0.425	500.85	748.23	247.38	24.7	52.3	47.7
0.300	280.93	519.97	239.04	23.9	76.3	23.7
0.150	473.26	698.23	224.97	22.5	98.7	1.3
0.075	463.19	474.87	11.68	1.2	99.9	0.1
PAN	446.19	447.03	0.84	0.1	100.0	0.0

Table K.2: Sieve analysis (crusher sand)

Crusher sand						
Sieve Size (mm)	**Mass of Sieve (g)**	**Mass of Sieve & Aggregate (g)**	**Mass retained (g)**	**Percentage aggregate retained (%)**	**Cumulative percentage aggregate retained (%)**	**Cumulative percentage aggregate passing (%)**
4.75	657.86	676.35	18.49	1.8	1.8	98.2
2.36	413.05	695.86	282.81	28.3	30.1	69.9
1.18	350.38	548.01	197.63	19.8	49.9	50.1
0.600	520.12	677.10	156.98	15.7	65.6	34.4
0.425	500.88	554.94	54.06	5.4	71.0	29.0
0.300	281.05	323.06	42.01	4.2	75.2	24.8
0.150	473.32	546.80	73.48	7.3	82.5	17.5
0.075	463.22	568.27	105.05	10.5	93.0	7.0
PAN	446.23	515.42	69.19	6.9	100.0	0.0

Table K.3: Sieve analysis (50 dune sand/50 crusher sand)

50 Dune sand / 50 Crusher sand						
Sieve Size (mm)	**Mass of Sieve (g)**	**Mass of Sieve & Aggregate (g)**	**Mass retained (g)**	**Percentage aggregate retained (%)**	**Cumulative percentage aggregate retained (%)**	**Cumulative percentage aggregate passing (%)**
4.75	657.83	671.68	13.85	1.4	1.4	98.6
2.36	412.92	571.52	158.60	15.9	17.2	82.8
1.18	350.23	464.04	113.81	11.4	28.6	71.4
0.600	519.90	741.21	221.31	22.1	50.8	49.2
0.425	500.89	658.74	157.85	15.8	66.5	33.5
0.300	280.94	412.18	131.24	13.1	79.7	20.3
0.150	473.26	613.38	140.12	14.0	93.7	6.3
0.075	463.16	503.83	40.67	4.1	97.7	2.3
PAN	446.18	468.54	22.36	2.2	100.0	0.0

Table K.4: Sieve analysis (19 mm greywacke stone)

19 mm greywacke						
Sieve Size (mm)	**Mass of Sieve (g)**	**Mass of Sieve & Aggregate (g)**	**Mass retained (g)**	**Percentage aggregate retained (%)**	**Cumulative percentage aggregate retained (%)**	**Cumulative percentage aggregate passing (%)**
26.5	1630	1630	0	0.0	0.0	100.0
19	1505	1735	230	7.7	7.7	92.3
13.2	1360	2795	1435	47.9	55.6	44.4
9.5	1415	2310	895	29.9	85.5	14.5
6.7	1470	1720	250	8.3	93.8	6.2
4.75	1605	1665	60	2.0	95.8	4.2
PAN	1390	1515	125	4.2	100.0	0.0

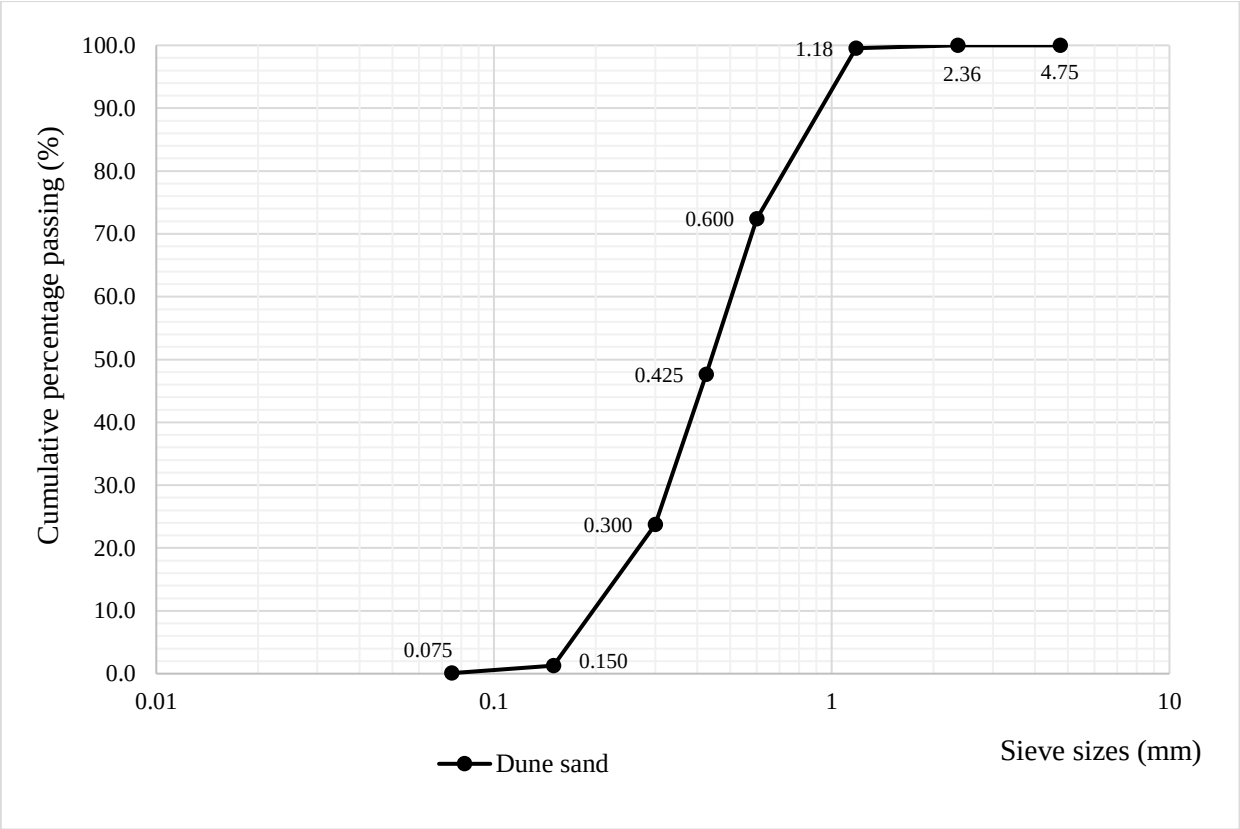

Figure K-1: Grading curve (Dune sand)

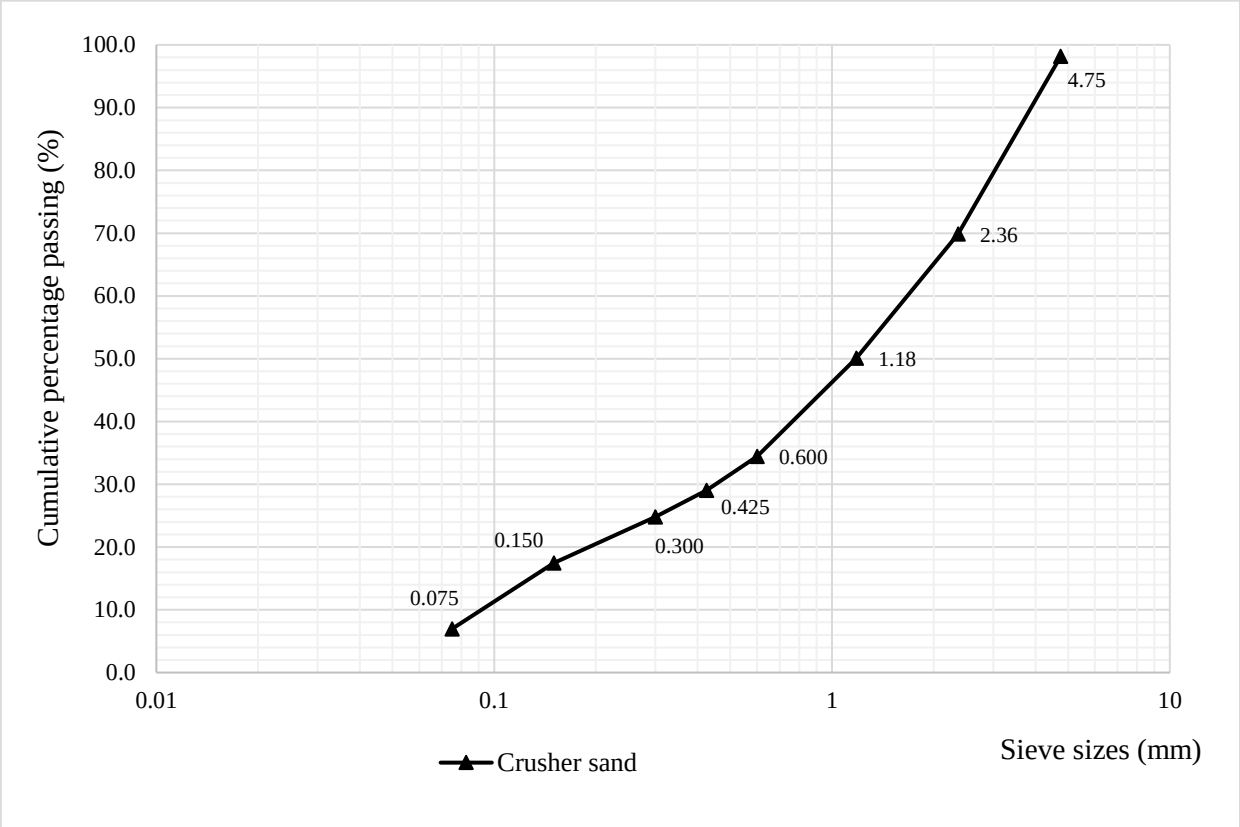

Figure K-2: Grading curve (Crusher sand)

APPENDIX L – Assessment of ethics form

Application for Approval of Ethics in Research (EiR) Projects
Faculty of Engineering and the Built Environment, University of Cape Town

APPLICATION FORM

Please Note:
Any person planning to undertake research in the Faculty of Engineering and the Built Environment (EBE) at the University of Cape Town is required to complete this form **before** collecting or analysing data.The objective of submitting this application *prior* to embarking on research is to ensure that the highest ethical standards in research, conducted under the auspices of the EBE Faculty, are met. Please ensure that you have read, and understood the **EBE Ethics in Research Handbook**(available from the UCT EBE, Research Ethics website) prior to completing this application form: http://www.ebe.uct.ac.za/usr/ebe/research/ethics.pdf

APPLICANT'S DETAILS		
Name of principal researcher, student or external applicant		Haris Sohawon
Department		Civil Engineering
Preferred email address of applicant:		shwhar001@myuct.ac.za
If a Student	Your Degree: e.g., MSc, PhD, etc.,	MSc Civil Structural Engineering
	Name of Supervisor (if supervised):	Professor Hans Beushausen
If this is a researchcontract, indicate the source of funding/sponsorship		CoMSIRU
Project Title		Service life extension of reinforced concrete structures in marine environments using surface treatments

I hereby undertake to carry out my research in such a way that:

- there is no apparent legal objection to the nature or the method of research; and
- the research will not compromise staff or students or the other responsibilities of the University;
- the stated objective will be achieved, and the findings will have a high degree of validity;
- limitations and alternative interpretations will be considered;
- the findings could be subject to peer review and publicly available; and
- I will comply with the conventions of copyright and avoid any practice that would constitute plagiarism.

SIGNED BY	Full name	Signature	Date
Principal Researcher/ Student/External applicant	Haris Sohawon		11.10.16

APPLICATION APPROVED BY	Full name	Signature	Date
Supervisor (where applicable)	Professor Hans Beushausen		11.10.16
HOD (or delegated nominee) Final authority for all applicants who have answered NO to all questions in Section1; and for all Undergraduateresearch (Including Honours).	M Vanderschuren		31/10/16
Chair : Faculty EIR Committee For applicants other than undergraduate students who have answered YES to any of the above questions.			